



**BERGISCHE
UNIVERSITÄT
WUPPERTAL**

**Functionalized biochars (im)mobilize potentially toxic elements under dynamic redox
conditions in paddy soil and regulate the yield and quality of rice**

**Dissertation
for the acquisition
of the academic title “Dr.-Ing.”**

submitted to the
Faculty of Architecture and Civil Engineering
Bergische Universität Wuppertal

by

Xing Yang
from Anyang, China

Wuppertal 2022



**BERGISCHE
UNIVERSITÄT
WUPPERTAL**

**Functionalized biochars (im)mobilize potentially toxic elements under dynamic redox
conditions in paddy soil and regulate the yield and quality of rice**

Dissertation
zur Erlangung eines Doktorgrades
(Dr.-Ing.)

in der
Fakultät für Architektur und Bauingenieurwesen
der
Bergischen Universität Wuppertal

vorgelegt von
Xing Yang
aus Anyang, China

Wuppertal 2022

“对搞科学的人来说，勤奋就是成功之母”

——茅以升

“For those who engage in science, diligence is the mother of success”

——**Yisheng Mao**

Table of Contents

Dedication.....	1
Acknowledgements	2
Preface and Declaration	6
Abstract	9
Kurzfassung	11
List of Figures	14
List of Tables	18
CHAPTER 1: Introduction.....	20
1.1 Research background.....	21
1.1.1 Contamination of paddy soils with potentially toxic elements	21
1.1.2 Biochar application in remediation of PTE-contaminated soils	23
1.1.3 Silicon-rich amendments	25
1.1.4 Phosphorus-rich amendments.....	26
1.1.5 Iron-rich amendments.....	26
1.2 Key research questions	28
1.3 Research objectives	28
1.4 Methodologies	29
1.4.1 Incubation experiments (Part/Research question 1)	29
1.4.2 Mechanism elucidation (Part/Research question 2)	30
1.4.3 Pot experiments (Part/Research question 3).....	31
1.5 Technical route	32
1.6 References	33
CHAPTER 2: Effects of Pig Carcass-Derived Phosphorus-Rich Biochar on Arsenic Mobilization under Fluctuating Controlled Redox Conditions in Paddy Soil	40
Abstract	41
2.1 Introduction	42
2.2 Materials and methods.....	44
2.2.1 Soil collection and properties	44
2.2.2 Biochar preparation and characterization	44
2.2.3 Redox experiment using an automated biogeochemical microcosm (MC) experiment	45
2.2.4 Sampling and analysis	46
2.2.5 Data processing and statistical analysis.....	47

2.3 Results	47
2.3.1 Effect of PB application on Eh and pH	47
2.3.2 The concentration of dissolved As in the soil solution	48
2.3.3 The concentrations of Fe, Mn, Cl ⁻ , SO ₄ ²⁻ , DOC and SUVA in the soil solution	49
2.3.4 The speciation of As in soil samples by XANES analysis	51
2.4 Discussion	53
2.4.1 Dynamics of Eh and pH	53
2.4.2 Alterations of Eh-dependent controlling factors.....	54
2.4.3 As mobilization	57
2.5 Conclusions	61
2.6 Acknowledgements.....	61
2.7 References	61
CHAPTER 3: Effects of Iron-Impregnated Green Waste Biochar on Arsenic Mobilization under Fluctuating Controlled Redox Conditions in Paddy Soil	66
Abstract	67
3.1 Introduction	68
3.2 Materials and methods.....	70
3.2.1 Collection and characterization of the studied soil.....	70
3.2.2 Biochar production and characterization.....	71
3.2.3 Pre-incubation of the non- and biochar-treated soils.....	71
3.2.4 Microcosm experiment.....	72
3.2.5 XANES analysis.....	73
3.2.6. Quality assurance and statistical analysis	73
3.3 Results and discussion.....	74
3.3.1 Characteristics of biochars: impact of modification.....	74
3.3.2 Arsenic mobilization as affected by the biochar-induced alterations of Eh and pH.....	76
3.3.3 Arsenic mobilization as affected by the biochar-induced changes in Fe (hydro)oxides.....	82
3.3.4 Arsenic mobilization as affected by the biochar-induced changes in DOC.....	87
3.3.5 Arsenic mobilization as affected by the biochar-induced changes in SO ₄ ²⁻	88
3.4 Conclusions	89
3.5 Acknowledgements.....	90
3.6 References	91
CHAPTER 4: Effects of Phosphorus- and Iron-Rich Biochars on Cadmium and Lead Mobilization under Fluctuating Controlled Redox Conditions in Paddy Soil	96

Abstract	97
4.1 Introduction	98
4.2 Materials and methods.....	100
4.2.1 Soil collection and characterization.....	100
4.2.2 Biochar preparation and methods of characterization	100
4.2.3 Biochar characteristics	101
4.2.4 Pre-incubation of soil	102
4.2.5 Redox experiment set up	103
4.2.6 Quality control and statistical analysis	104
4.3 Results and discussion.....	105
4.3.1 Eh and pH.....	105
4.3.2 Redox-induced changes in pH, Fe, Mn, DOC, and S affect the mobilization of Cd and Pb	107
4.3.3 Effect of biochar application on the redox-induced mobilization of Cd and Pb.....	111
4.4 Conclusions	118
4.5 Acknowledgements.....	118
4.6 References	119
CHAPTER 5: Influences of Iron-Modified Phosphorus- and Silicon-Rich Biochars on Arsenic, Cadmium, and Lead Accumulation in Rice and Microbial Activities in Paddy Soil	124
Abstract	125
5.1 Introduction	126
5.2 Materials and methods.....	128
5.2.1 Soil collection and characterization.....	128
5.2.2 Preparation of functionalized biochars	128
5.2.3 Experimental design	128
5.2.4 Plant harvesting, soil collection and chemical analyses	130
5.2.5 Data processing and quality control	131
5.3 Results	132
5.3.1 Characteristics of the functionalized biochars.....	132
5.3.2 Plant growth and grain yield	132
5.3.3 Potential availability and plant accumulation of PTEs.....	133
5.3.4 Soil enzyme activities.....	135
5.4 Discussion	135
5.4.1 Effect of functionalized biochars on the potential availability of PTEs in soils and their accumulation in rice plants	135

5.4.2 Effect of functionalized biochars on soil enzyme activities	141
5.4.3 Effect of functionalized biochars on plant growth.....	143
5.5 Conclusions	145
5.6 Acknowledgments	145
5.7 References	146
CHAPTER 6: Influences of the Iron-Modified Phosphorus-Rich Biochar on Rice Yield, Arsenic and Lead Redistribution, and Bacterial Community Structure in Paddy Soil	150
Abstract	151
6.1 Introduction	152
6.2 Materials and methods.....	154
6.2.1 Soil and biochar preparation.....	154
6.2.2 Rice cultivation experiment.....	155
6.2.3 Fractionation of As and Pb	156
6.2.4 DNA extraction and high-throughput sequencing	156
6.2.5 Data processing and statistical analysis.....	157
6.3 Results and discussion.....	157
6.3.1 Soil pH, organic carbon content and nutrient availability	157
6.3.2 Redistribution of As and Pb.....	161
6.3.3 Bacterial community structure	166
6.3.4 Rice yield and accumulation of As and Pb	171
6.4 Conclusions	174
6.5 Acknowledgments	174
6.6 References	175
CHAPTER 7: Summary and Outlook	180
7.1 Summary	181
7.2 Outlook.....	186
Appendix A.....	188
Appendix B.....	193
Appendix C.....	196
Appendix D.....	201
Appendix E.....	205
List of Publications (During Ph.D. Study).....	209
Curriculum Vitae.....	212

Dedication

This dissertation is dedicated to my mother Qiuying Ma and father Yanjun Yang. As a son of Chinese farmer parents, I was taught since I was a small child that the easiest way to get a better life is to study hard. Even though they still do not understand what I am doing or what degree I am getting, they still show me unconditional support and never-ending love. This project is also dedicated to my late grandfather Xiaoshan Yang, who passed away in 2015. They have always been the true inspiration in my life.

Acknowledgements

Four years ago, when I got the offer to begin my doctoral study in Germany, I had no ideas about the journey I would start nor the richness and depth of knowledge I would gain as a result of this journey. I would not be who and where I am today without the help, encouragement, support, and love of numerous colleagues, friends and family members. I owe a tremendous debt of gratitude to so many people who were instrumental to the completion of this incredible journey.

First and foremost, I would like to express my sincerest gratitude to my supervisor, Prof. Jörg Rinklebe, the Head of the Laboratory and Head of the Team Soil- and Groundwater-Management at University of Wuppertal, for his gracious guidance and continuous support during my doctoral studies. Despite his busy schedule, he was always very responsive and easy to contact. He was always readily available to provide clear explanations to some key concepts whenever the need arose. I have been very lucky and honored to work in his lab and be supervised by him and have learned tremendously from him. I appreciate the constant words of encouragement and the enduring faith he had in me. He always told me, “Xing, please don’t put too much pressure on yourself, you are on a good track and you will make it!” The invaluable experience working with him will benefit me throughout my entire life.

I owe my heartfelt gratitude to my co-supervisor, Prof. Hailong Wang (from Foshan University), who taught me the essential academic skills and provided me the opportunity to take my first step into the world of soil science. I began my study as a postgraduate student under Prof. Wang’s supervision at Zhejiang A & F University since 2012. Over the past decade, he has played a vital role in my career and personal growth. Prof. Wang has been the most supporting person and role model in science to me. He is one of the main reasons that motivated me to enter the doctoral program. I am grateful to him not only for his exceptional and professional supervision but also for his major contribution to the development of my character as a young scientist. I will cherish all the tremendous efforts he made in my scientific career development.

I would also like to express a special thanks to Prof. Sabry M. Shaheen for his selfless advice and support throughout my journey in Wuppertal. He has been always hard-working and helpful to others. I consider him to be a primary example of what a great scientist should be, and I will strive to become a scientist of his same caliber. I sincerely appreciate his valuable recommendations and encouragement and the hours he has dedicated to reviewing my drafts. Prof. Shaheen has been extremely helpful and supportive during my doctoral studies and I am lucky to have worked with him. He has offered guidance, advice, critique, praise, support, admonishment,

patience, motivation, laughter, and ear to listen, as well as quiet conversation. He is more than an advisor (I consider him as my “third supervisor”); he is a friend.

My lovely colleagues, Dr. Tatiane Medeiros Melo, M.Sc. Felizitas Boie, M.Sc. Marina Schauerte, M.Sc. Viraj Gunarathne, and Dr. Albert Kobina Mensah (Ruhr-Universität Bochum), thanks for the meaningful ways they contributed to my nice journey in Wuppertal, for making the lab life even more fun, and for being such good friends in and outside of the office and lab. My commitment to this journey has been continually fueled by words of encouragement and support from these guys. Tatiane’s kindness is one of a kind. I thank her for treating me like a little brother of hers and showing so much care and support to me, especially at a time when I needed it the most. Her husband, Mr. Janis Kasper, is also a nice guy who has been jokingly searched for Chinese girls and encouraged me to go straight over and chat them up on our trips to the Black Forest and Heidelberg. Feli was always a friendly listener to me, including during my rants about experiments or the doctoral experiences. I really enjoyed the scientific conversations with her. She was always so “sporty” and definitely an avid cyclist; unfortunately, I was hardly influenced although she often encouraged me to do some sports instead of sitting in the office all day long. Marina, a friend in need, has been super supportive and has helped me handle a lot of troubles in these years. She has been my private barber during the COVID-19 pandemic time; it was funny to get my hair cut in the office. Her lovely boyfriend, Mr. Denis Tischkov, who became a good Bruder to me, thus I sportively called Marina my “sister-in-law”. I really appreciate the laughter, hugs, and words of encouragement from both of them. Viraj was always so kind to me and actually he is such a kind-hearted person who is friendly with everyone. As his motherland Sri Lanka is a geographical neighbor of China, we called each other “my neighbor”. I will miss working, talking, laughing, and hanging out with my neighbor. My thanks also go to Kobina (Albert likes us to call him by his middle name) for being a fantastic friend and working partner, our brief conversations about science were always inspirational and encouraging.

I would especially like to thank Mr. Christoph Kinder, Ms. Lisa Duchscherer, Mr. Marko Roschkowski, Mr. Yazid B. Hwaiti, Mr. Marvin Hinzmann, Mr. Ilya Mironov, Ms. Yen-Lin Cho, as well as Ms. Nadine Gersdorf, who have become lifelong friends I will always appreciate, and whose friendship and encouragement I hold dear. Chris, Herr Kinder (as kind as his name), was the first German brother I got from the lab, who accompanied me on my first day in the lab and brought me the first German beer (Flensburger), but I wondered for a long time why it was not his favorite brand (Kölsch) afterwards, when I got to know more about him. I guess then later, probably he knew from the beginning that I dislike “water”. Lisa is a friend who shared a lot of German history and culture with me (especially on our trip to Berlin), making me more adapted and more German. She taught me a German

word of “Schnitte”, which became one of our biggest jokes that brought us much joy and laughter. It was always wonderful to visit her tranquil village full of idyllic scenery, and I will not forget her friendly Papa, Mr. Wolfgang Duchscherer, and their cute dog, Frida. My Italian Bruder Marko, a handsome guy who was always dressed appropriately. I was surprised that he seemed to know every single corner and every single person in the whole city. With him, we could always enjoy delicious Italian food and fancy Italian wine. Yazid, my brother from different parents, a smart guy who can speak Arabic, English, German, Portuguese, Spanish, and a little Russian. He is probably a real human being who is half angel half demon, but I saw more of his angelic side as a true friend. Although he is seven years younger than me, he acted as an elder brother in many situations to listen to my complains and then to offer feedback, which was highly appreciated. The glove box made Marvin and I good friends, our conversations during sampling, centrifugation, and filtration, from scientific to mundane were interesting and valuable to me. Marvin is talented at composing music; he could have been a musician instead of an engineer. About carnival, I will remember the song “Mama Lauda”, the first “Bratwurst”, the “shark” who always got lost, and the “hunter” who lost his binoculars, “Now, I like Germany...”. Ilya, a Russian guy who was always complaining and always had a question to ask. Well...there were also good memories of course, he earnestly told me YOLO and urged me to be better to myself while I was hesitating to buy a box of chocolate; he silently brought me a jar of honey because he thought it was good for my gastritis. He got a chance to start a Ph.D. journey in China, probably we will celebrate the next Chinese New Year in China, well... without arm-breaking. Yen-Lin was the only one I could speak Chinese to in the lab at the post-pandemic period. She is an easy-going girl and always poised even in difficult moments. Importantly, she reminded me that health always comes first in our life and she also encouraged me go to the gymnasium regularly. I had few friends outside the lab during my stay in Wuppertal, Nadine, the brown lawyer has been a really good one. The legendary experiences and stories from her encouraged and inspired me a lot, when I felt down, depressed, and even exhausted from my doctoral studies, especially during the COVID-19 pandemic period. She is such a shiny and happy person, just like the meaning of her name, HOPE. It was so exciting and funny when I was driving her car, she seemed more nervous than I was while she was sitting on the passenger seat. Guys, our many talks and outings were the power I needed to recharge my batteries and continue full-steam on my work. They really made my life in Wuppertal enjoyable and memorable. Many thanks for all the stories, fun, and laughter we shared together. I will cherish these memories, conversations, and friendships for the rest of my life.

I would also like to thank Dr. Jianxu Wang, Dr. Ying Xing and their adorable son, Zirui Wang, for their help and friendship, especially at the very beginning of this journey when I just arrived in Wuppertal. I want to thank Jianxu

for his infinite support in my experimental design and implementation, who has primarily trained and educated me in microcosm system that I used for studies in Chapters 2-4. I also thank Prof. Shan-Li Wang (National Taiwan University) and his students for their assistance and advice concerning XANES analysis. Without their generosity, I would not have been able to complete Chapters 2-3.

I also want to acknowledge Mr. Claus Vandenhirtz and Mr. Kail Matuszak for their technical support in the lab. Especially, during my stay in Wuppertal, Claus provided a lot of care and love to me; he is my “uncle” in the office (as he has the same age as my parents), and my “God” in the lab (as he knows everything in the lab). I will remember my best uncle in Germany, he is a brilliant beer drinker who has already tasted more than three thousand different brands of beer from all over the world.

To all the people I have had the pleasure of working alongside in the lab, my gratitude goes to M.Sc. Marvin Hinzmann, M.Sc. Ilya Mironov, and M.Sc. Alan Nicol, the long hours in the lab for microcosm experiments (Chapters 2-4) were greatly shortened by their company. I would also like to extend my gratitude to M.Sc. Ergang Wen, M.Sc. He Pan, and M.Sc. Zhinan Dai in China (Zhejiang A & F University), for their assistance in the implementation of the pot experiments (Chapters 5-6). It was also my pleasure to work with those visiting scientists who had a short stay in our lab in Wuppertal. My appreciation goes to Dr. Yi Yang (The Education University of Hong Kong), M.Sc. Katerina Mitzia (Czech University of Life Sciences Prague), Dr. Shuai Zhang (China Agricultural University), Dr. Pavani Dulanja Dissanayake (Korea University), Dr. Muhammad Mahroz Hussain (University of Agriculture Faisalabad), and Ms. Larisa Vujnovic.

Last but not least, I am sincerely grateful to my beloved parents for the huge sacrifices they made, as well as their boundless love, unconditional support, and continuous encouragement, which kept inspiring me even though we were thousands of kilometers apart. I would like to thank my incredible little sister, Min Yang, for taking care of our parents for me in these years I have been absent. I never told them all, but they have always been my greatest inspiration in life. I cannot flourish without all of them backing me up. I hope they are proud of me at the moment. Finally, I also want to take this opportunity to thank all my relatives and friends who played a role in the successful completion of this wonderful journey.

Preface and Declaration

This thesis has been completed based on the National Natural Science Foundation of China (Grant No. 21876027), “Effect of pristine and nano zerovalent iron-modified biochars on the transformation of heavy metals in soils under various redox conditions”. The Ph.D. project was sponsored by the Doctoral Training Program between University of Wuppertal, Germany and Foshan University, China. The experimental results from the thesis (Chapters 2-6) are presented in five research articles either published or submitted to peer-reviewed journals. This presentation gives an advantage that each chapter can be easily read and understood independently. Complete and continuous reading is also possible, given the logical succession of chapters leading to an overall understanding of the objectives and conclusions.

Chapter 2

Yang, X., Hinzmann, M., Pan, H., Wang, J., Bolan, N., Tsang, D.C.W., Ok, Y.S., Wang, S.L., Shaheen, S.M., Wang, H., Rinklebe, J., 2022. Pig carcass-derived biochar caused contradictory effects on arsenic mobilization in a contaminated paddy soil under fluctuating controlled redox conditions. *Journal of Hazardous Materials* 421, 126647. <https://doi.org/10.1016/j.jhazmat.2021.126647>

Credit authorship contribution statement:

Xing Yang: conducting the experiment, investigation, data collection and analysis, writing the original draft, writing corrections according to the advices of the co-authors. **Marvin Hinzmann:** performing the experiment, data collection, treatment of samples, methodology. **He Pan:** soil-sampling, treatment of samples. **Jianxu Wang:** accurateness of data analysis, scientific advice concerning XANES analysis, correction and editing. **Nanthi Bolan:** review, correction and editing. **Daniel C.W. Tsang:** review, correction and editing. **Yong Sik Ok:** review, correction and editing. **Shan-Li Wang:** accurateness of data analysis, scientific advice concerning XANES analysis, correction and editing. **Sabry M. Shaheen:** accurateness of calculations, correction, writing and editing. **Hailong Wang:** concept, supervision, correction and editing. **Jörg Rinklebe:** research idea, scientific and experimental concept, close experimental guidance, experimental, laboratory, technical and analytical facilities, supervision, correction and editing.

Chapter 3

Yang, X., Shaheen, S.M., Wang, J., Hou, D., Ok, Y.S., Wang, S.L., Wang, H., Rinklebe, J., 2022. Elucidating the redox-driven dynamic interactions between arsenic and iron-impregnated biochar in a paddy soil using geochemical and spectroscopic techniques. *Journal of Hazardous Materials* 422, 126808.

<https://doi.org/10.1016/j.jhazmat.2021.126808>

Credit authorship contribution statement:

Xing Yang: conducting the experiment, investigation, data processing, creating the figures and tables, writing the original draft, writing corrections according to the advices of the co-authors and reviewers. **Sabry M. Shaheen:** accurateness of calculations, correction, writing – review and editing. **Jianxu Wang:** accurateness of data analysis, correction and editing. **Deyi Hou:** writing – review and editing, correction. **Yong Sik Ok:** writing – review & editing, correction. **Shan-Li Wang:** accurateness of data analysis, scientific advice concerning XANES analysis, correction and editing. **Hailong Wang:** concept, supervision, correction and editing. **Jörg Rinklebe:** research idea, scientific and experimental concept, close experimental guidance, experimental, laboratory, technical and analytical facilities, supervision, correction and editing.

Chapter 4

Yang, X., Pan, H., Shaheen, S.M., Wang, H., Rinklebe, J., 2021. Immobilization of cadmium and lead using phosphorus-rich animal-derived and iron-modified plant-derived biochars under dynamic redox conditions in a paddy soil. *Environment International* 156, 106628. <https://doi.org/10.1016/j.envint.2021.106628>

Credit authorship contribution statement:

Xing Yang: conducting the experiment, investigation, data processing, creating the figures and tables, writing the original draft, writing corrections according to the advices of the co-authors and reviewers. **He Pan:** performing the pre-incubation experiment, treatment of soil samples. **Sabry M. Shaheen:** accurateness of calculations, correction, writing – review & editing. **Hailong Wang:** concept, supervision, correction and editing. **Jörg Rinklebe:** research idea, scientific and experimental concept, close experimental guidance, experimental, laboratory, technical and analytical facilities, supervision, correction and editing.

Chapter 5

Yang, X., Wen, E., Ge, C., El-Naggar, A., Wang, S., Kwon, E.E., Song, H., Shaheen, S.M., Wang, H., Rinklebe, J. Iron-modified phosphorus- and silicon-based biochars exhibited various influences on arsenic, cadmium and lead accumulation in rice and enzyme activities in a paddy soil. Ready for being submitted to *Journal of Cleaner Production*.

Credit authorship contribution statement:

Xing Yang: conducting the experiment, laboratory analyses, data processing, creating the figures and tables, writing the original draft, writing corrections according to the advices of the co-authors. **Ergang Wen:** pot

experiment management, laboratory analyses. **Chengjun Ge:** proofreading, review and editing. **El-Naggar Ali:** accurateness of data analysis, correction and editing. **Shengsen Wang:** writing – review and editing. **Eilhann E. Kwon:** writing – review and editing. **Hocheol Song:** correction, review and editing. **Sabry M. Shaheen:** accurateness of calculations, correction, writing – review and editing. **Hailong Wang:** scientific and experimental concept, supervision, correction and editing. **Jörg Rinklebe:** supervision, correction and editing.

Chapter 6

Yang, X., Dai, Z., Ge, C., Bolan, N., Tsang, D.C.W., Song, H., Hou, D., Shaheen, S.M., Wang, H., Rinklebe, J. Multiple-functionalized biochar enhances rice yield via regulating arsenic and lead redistribution and bacterial community structure in soils under different hydrological conditions. Ready for being submitted to *Environmental International*.

Credit authorship contribution statement:

Xing Yang: conducting the experiment, laboratory analyses, data processing, creating the figures and tables, writing the original draft, writing corrections according to the advices of the co-authors. **Zhinan Dai:** laboratory analyses. **Chengjun Ge:** proofreading, review and editing. **Nanthi Bolan:** correction and editing. **Daniel C.W. Tsang:** writing-review and editing. **Hocheol Song:** correction, review and editing. **Deyi Hou:** writing – review and editing. **Sabry M. Shaheen:** correction, writing – review and editing. **Hailong Wang:** scientific and experimental concept, supervision, correction and editing. **Jörg Rinklebe:** supervision, correction and editing.

Abstract

Contamination of paddy soils with potentially toxic elements (PTEs), such as arsenic (As), cadmium (Cd), and lead (Pb) has become a serious agricultural, environmental, and public health problem worldwide. These elements can be readily taken up by rice plant and eventually accumulated in rice grain, thus posing a severe risk to human health through the food chain. It is imperative to discover an effective way to lessen human exposure to these PTEs. Simultaneously minimizing As, Cd, and Pb uptake by rice is challenging since these elements are strongly affected by soil redox conditions. In this study, the feasibility of using phosphorus (P)-, silicon (Si)-, and iron (Fe)-rich functionalized biochars derived from pyrolysis of pig carcasses, rice husks, and loading with Fe materials, respectively, for the remediation of paddy soils contaminated with As, Cd, and Pb was elucidated through conducting microcosm incubation and pot experiments. The objectives were to (1) investigate the effects of different functionalized biochars on the mobilization and speciation of PTEs under different redox conditions in a contaminated paddy soil, (2) elucidate the mechanisms of the transformation of PTEs as affected by application of functionalized biochars and change in redox conditions, and (3) assess the impacts of functionalized biochars on soil physicochemical and microbial properties, plant growth, PTE bioavailability, as well as interactions between PTEs, microorganisms, and functionalized biochars in the soil-rice plant interface.

Based on the microcosm experiments (Chapters 2-4), it was found that the application of the P-rich biochar could immobilize Cd by 8-19%, compared to the non-treated control, which could be due to the formation of stable Cd-sulfides under reducing condition, while due to the increased pH under oxidizing conditions. In addition, application of the P-rich biochar was more effective on immobilizing Pb than other biochars, especially under reducing conditions with $E_h < 0$ mV, due to the formation of insoluble Pb-phosphates. Compared to the control, application of the P-rich biochar decreased the concentration of dissolved As at $E_h = +100$ and $+200$ mV by 38.7 and 35.4%, respectively, due to the co-precipitation of As with Fe-Mn oxides and the complexation between As and the aromatic compounds. However, it increased the concentration of dissolved As by 13.5% at $E_h = -300$ mV, through promoting reduction and decomposition of As-bearing Fe minerals, and increased the dissolved As by 317.6% at $E_h = +250$ mV, due to the associated increase of pH. Application of the Fe-modified green waste biochar decreased the concentrations of dissolved Cd by 31-59% under varying redox conditions, which was mainly due to the redox interactions between Cd and the applied Fe, including re-sorption and co-precipitation. The Fe-modified green waste biochar immobilized Pb at $E_h < -300$ mV; however, it mobilized Pb at $E_h > -200$ mV, especially at $E_h = +100$ mV, due to the declined pH at this point. Modification of the green waste biochar

with Fe materials enhanced its capability on As (im)mobilization under different redox conditions. At Eh = -300 mV, application of the Fe-modified biochar reduced the concentration of dissolved As by 71.8%, compared to the control, due to the decrease of pH. Under oxidizing conditions, the Fe-modified biochar was effective on decreasing the concentration of dissolved As, which could be due to the co-precipitation and complexation with exogenous Fe materials. The Fe-rich biochar was more effective on immobilizing As and Cd than Pb, whereas the P-rich biochar was more effective on immobilizing Cd and Pb, in particular Pb, than As.

The pot experiments (Chapters 5-6) showed that the Si-rich rice husk biochar decreased the concentration of As in rice grain by 59.4%, whereas it had no significant impacts on grain-Cd and grain-Pb, compared to the control. Although the Fe-modified Si-rich biochar significantly promoted plant growth, increased rice yield (by 38.6%), it elevated Cd and Pb accumulation in rice grain, thus posing a relatively high environmental risk. Compared to the control, application of the P-rich pig carcass biochar enhanced soil enzyme activities, and reduced grain-Pb by 60.1% (to 0.12 mg kg⁻¹), under continuously flooded conditions, whereas it promoted the accumulation of As in rice grain under both irrigation regimes. The Fe-modified P-rich biochar increased the rice yield by 47.4 and 19.6%, respectively, under continuously and intermittently flooded conditions, due to the improved soil nutrient availability and the enhanced microbial activities. Under intermittently flooded conditions, application of the Fe-modified P-rich biochar reduced the concentration of As in rice grain by 12.2%, while increased the concentrations of Cd and Pb, compared to the control. Meanwhile, the concentrations of grain-Pb increased by 2.9 and 6.6 times, respectively, compared to the controls under continuously and intermittently flooded conditions. Thus, the Fe-modified Si-rich rice husk and P-rich pig carcass biochars could be used to remediate paddy soils contaminated with As, while the P-rich biochar could also be a promising strategy to remediate the Pb-contaminated paddy soils and limit Pb accumulation in rice.

In conclusion, application of the P-rich pig carcass biochar could be a promising way for immobilizing Cd and Pb, in particular Pb in paddy soils; the raw and Fe-rich green waste biochars had higher ability in immobilizing Cd (under both reducing and oxidizing conditions) and As (under reducing conditions); the Si-rich rice husk biochar could be a suitable amendment for ameliorating soil quality and improving the quality and yield of rice when As is the only concern in soils. Overall, none of the tested functionalized biochars could reach an appropriate effectiveness on a simultaneous mitigation of multi-PTEs in the paddy soil. Future studies are warranted to select suitable feedstocks for producing functionalized biochars, optimize practical techniques for biochar modification, and investigate the suitable application manners and dosages of functionalized biochars to achieve simultaneous immobilization of multiple-elements in contaminated soils.

Kurzfassung

Die Kontaminierung von Reisböden mit potentiell toxischen Elementen (PTEs), wie Arsen (As), Cadmium (Cd) und Blei (Pb) ist zu einem ernstzunehmenden Problem der Landwirtschaft, Umwelt und dem Gesundheitswesen weltweit geworden. Diese Elemente können leicht von Reispflanzen aufgenommen werden, sich in deren Reiskörnern akkumulieren und gelangen so in die anthropogene Nahrungskette. Dies birgt ein großes Risiko für die menschliche Gesundheit. Es ist daher unerlässlich einen effizienten Weg zu finden, um die Exposition des Menschen gegenüber diesen PTEs zu minimieren. Gleichzeitig ist es eine Herausforderung die Aufnahme von As, Cd und Pb in die Reispflanze zu verringern, da diese Elemente stark von den Redoxbedingungen im Boden beeinflusst werden. In dieser Studie wurde die Machbarkeit der Verwendung von phosphor (P)-, silizium (Si)- und eisen (Fe)-reichen, funktionalisierten Biokohlen, welche aus der Pyrolyse von Schweinekadavern oder Reishülsen stammen und teilweise mit Fe-Materialien geladen sind, für die Sanierung von mit As, Cd und Pb kontaminierten Reisböden, durch die Durchführung von Mikrokosmeninkubations- und Topfexperimenten, untersucht. Die Ziele waren (1) die Effekte verschiedener funktionalisierter Biokohle auf die Mobilisierung und Spezierung der PTEs unter verschiedenen Redoxbedingungen in kontaminiertem Reisboden zu untersuchen, (2) die Mechanismen der Transformation, der durch die Anwendung funktionalisierter Biokohle und der Veränderung der Redoxbedingungen affizierten PTEs zu erläutern und (3) die Auswirkungen funktionalisierter Biokohle auf die physikalischen, chemischen und mikrobiellen Eigenschaften des Bodens, das Pflanzenwachstum, die Bioverfügbarkeit sowie die Interaktionen zwischen PTEs, Mikroorganismen und funktionalisierter Biokohle an der Boden-Reispflanze-Schnittstelle zu bewerten.

Basierend auf den Mikrokosmeninkubationsexperimenten (Kapitel 2-4), wurde festgestellt, dass die Anwendung P-reicher Biokohle Cd im Vergleich zur unbehandelten Kontrolle um 8-19 % immobilisieren konnte, was auf die Bildung stabiler Cd-Sulfide unter reduzierenden Bedingungen zurückführen sein könnte, während unter oxidierenden Bedingungen der erhöhte pH-Wert maßgebend war. Zusätzlich war die Anwendung P-reicher Biokohle aufgrund der Bildung unlöslicher Pb-phosphate insbesondere unter reduzierenden Bedingungen mit $E_h < 0$ mV effizienter in der Immobilisierung von Pb als andere Biokohlen. Im Vergleich zu der Kontrolle verringerte die Anwendung der P-reichen Biokohle die Konzentration von gelöstem As bei $E_h = +100$ und $+200$ mV um jeweils 38,7 und 35,4 %, was auf die Mitfällung von As mit Fe-/Mn-Oxiden und die Komplexbildung zwischen As und den aromatischen Verbindungen zurückzuführen

ist; dennoch steigerte die P-reiche Biokohle die Konzentration von gelöstem As um 13,5 % bei Eh = -300 mV. Des Weiteren wurde durch die Förderung der Reduzierung und Zersetzung As-haltiger Fe-Mineralien die Konzentration von gelöstem As um 317,6 % bei Eh = +250 mV erhöht, was auf den damit verbundenen Anstieg des pH-Wertes zurückzuführen ist. Die Anwendung der Fe-modifizierten Grünabfall-Biokohle unter verschiedenen Redoxbedingungen senkte die Konzentration von gelöstem Cd um 31-59 %, was hauptsächlich aufgrund der Redox-Wechselwirkungen zwischen Cd und dem angewandten Fe, inklusive Resorption und Mitfällung, erfolgte. Die Fe-modifizierte Grünabfall-Biokohle immobilisierte Pb bei Eh < -300 mV; jedoch mobilisierte sie Pb bei Eh > -200 mV, besonders bei Eh = +100 mV, aufgrund des an diesem Punkt gefallen pH-Wertes. Die Modifikation der Grünabfall-Biokohle mit Fe-Materialien verbesserte ihre Fähigkeit der (Im)Mobilisation von As unter verschiedenen Redoxbedingungen. Bei Eh = -300 mV reduzierte die Anwendung Fe-modifizierter Biokohle, aufgrund des gesunkenen pH-Wertes, die Konzentration von gelöstem As um 71,8 % im Vergleich zu der Kontrolle. Unter oxidierenden Bedingungen war die Fe-modifizierte Biokohle effektiv in der Senkung der Konzentration von gelöstem As, was an der Mitfällung und Komplexbildung mit Fe-Materialien liegen könnte. Die Fe-reiche Biokohle war effektiver bei der Immobilisierung von As und Cd als bei Pb, wobei die P-reiche Biokohle effektiver bei der Immobilisierung von Cd und insbesondere von Pb als von As war. Die Topfexperimente (Kapitel 5-6) zeigten, dass die Si-reiche Reishülsen-Biokohle die Konzentration von As in Reiskörnern um 59,4 % verringern konnte, wobei sie im Vergleich zur Kontrolle keine großen Auswirkungen auf Cd- und Pb-Konzentrationen in den Reiskörnern hatte. Obwohl Fe-modifizierte Si-reiche Biokohle das Pflanzenwachstum erheblich unterstützte (mit einem erhöhten Reisertrag von 38,6 %), erhöhte sie die Akkumulation von Cd und Pb im Reiskorn und stellt somit ein relativ hohes Umweltrisiko dar. Im Vergleich zur Kontrolle verbesserte die Anwendung von P-reicher Schweinekadaver-Biokohle die Aktivität der Bodenenzyme und reduzierte die Pb-Konzentration im Reiskorn unter durchgehend gefluteten Bedingungen um 60,1 % (0,12 mg kg⁻¹), wobei sie die Akkumulation von As im Reiskorn in beiden Bewässerungsregimen steigerte. Die Fe-modifizierte, P-reiche Biokohle erhöhte den Reisertrag aufgrund der verbesserten Verfügbarkeit von Nährstoffen im Boden und einer erhöhten mikrobiellen Aktivitäten unter kontinuierlichen und intermittierenden Flutungsbedingungen um 47,4 bzw. 19,6 %. Unter intermittierenden Flutungsbedingungen reduzierte die Anwendung von Fe-modifizierter, P-reicher Biokohle die Konzentration von As im Reiskorn um 12,2 %, wobei die Konzentrationen von Cd und Pb im Vergleich zur Kontrolle zunahm. Währenddessen stiegen die Konzentrationen von Pb im Reiskorn unter kontinuierlichen und intermittierenden Flutungsbedingungen um

das 2,9- bzw. 6,6-fache im Vergleich zu der Kontrolle. Somit könnten Fe-modifizierte, Si-reiche Reishülsen- und Schweinekadaver-Biokohlen benutzt werden, um mit As kontaminierten Reisboden zu sanieren, während die P-reiche Biokohle eine vielversprechende Strategie für die Sanierung von Pb-kontaminiertem Reisboden darstellen und Ansammlungen von Pb in der Reispflanze senken könnte.

Zusammenfassend könnte die Anwendung der P-reichen Schweinekadaver-Biokohle ein vielversprechender Weg für die Immobilisierung von Cd und insbesondere von Pb in Reisböden sein; die rohe und die Fe-reiche Grünabfall-Biokohlen hatten eine höhere Fähigkeit Cd (unter reduzierenden und oxidierenden Bedingungen) und As (unter reduzierenden Bedingungen) zu immobilisieren; die Si-reiche Reishülsen-Biokohle könnte eine geeignete Ergänzung zur Verbesserung der Bodenqualität sein und die Qualität sowie den Ertrag des Reis verbessern sofern As das einzige Problem des Bodens darstellt. Insgesamt konnte keine der getesteten funktionalisierten Biokohlen eine angemessene Wirksamkeit bei gleichzeitiger Minderung von multi-PTEs Kontaminationen im Reisboden erreichen. Zukünftige Studien sind notwendig, um geeignete Ausgangsmaterialien für die Herstellung funktionalisierter Biokohle auszuwählen, praktische Techniken zur Modifikation von Biokohle zu optimieren und die geeigneten Anwendungsmethoden und Dosierungen von funktionalisierter Biokohle zu untersuchen, um eine gleichzeitige Immobilisierung mehrerer Elemente in kontaminierten Böden erreichen zu können.

List of Figures

Figure 1-1 A schematic of human health hazards posed by different PTEs.	22
Figure 1-2 Favorable biochar characteristics and the postulated mechanisms of biochar interactions with cationic PTEs.	24
Figure 1-3 A schematic of the proposed functionalized biochar and its postulated mechanisms for multi-PTE immobilization.	28
Figure 1-4 Photos of the MC system used for incubation experiments.	30
Figure 1-5 Photos of the synchrotron-based Beamlines TLS 17C1 and TPS 44A1.	31
Figure 1-6 Photos of the rice cultivation pot experiments.	32
Figure 2-1 Sequential extraction of As in the control and biochar-treated soils.	44
Figure 2-2 The scanning electron microscope results (SEM, a), energy dispersive X-ray spectrometry (EDS, b), X-ray diffraction (XRD, c), Fourier transform infrared spectra (FTIR, d), X-ray photoelectron spectra (XPS-C1s, e), and Raman spectra (f) of pig biochar.	45
Figure 2-3 The concentrations of dissolved As, Fe, Mn, Cl ⁻ , SO ₄ ²⁻ , dissolved organic carbon (DOC), and specific UV absorbance (SUVA) in the control and pig biochar-treated soils under different redox conditions.	49
Figure 2-4 Dynamics of redox potential and pH in each microcosm with control (1~4) and pig biochar-treated soil (5~8).	50
Figure 2-5 Linear combination fitting (LCF) results of As K-edge XANES spectra of soils collected from different redox conditions.	52
Figure 2-6 First derivative Fe K-edge XANES spectra of standard materials and soils collected from different redox conditions.	53
Figure 2-7 Distribution of sampling points on the As-Eh-pH diagram (Takeno, 2005).....	58
Figure 2-8 Factor analysis of the control and pig biochar-treated soils.	60
Figure 3-1 Effect of biochar application on soil pH (a), organic carbon (b, OC) and NH ₄ H ₂ PO ₄ -extractable As (c) after pre-incubation. Control: non-treated soil; Raw Biochar: raw biochar-treated soil; Fe-impregnated Biochar: Fe-impregnated biochar-treated soil.	70
Figure 3-2 Effect of raw and Fe-impregnated biochar application on the geochemical fractions of As in soils after pre-incubation.....	71
Figure 3-3 Biogeochemical microcosm setup.....	74

Figure 3-4 The scanning electron microscope (SEM) images of the raw (a) and Fe-impregnated biochar(b); SEM-EDX K α map of Fe in the Fe-impregnated biochar(c); Fourier transform infrared spectra of the raw and Fe-impregnated biochar (d); and the energy dispersive X-ray patterns of the raw biochar (e) and Fe-impregnated biochar (f).	76
Figure 3-5 Effect of raw and Fe-impregnated biochars on the concentration of dissolved As and governing factors under dynamic and pre-defined redox conditions.	78
Figure 3-6 Dynamics of Eh and pH in each microcosm of control (1~4), raw biochar treatment (5~8) and Fe-impregnated biochar treatment (9~12). Control: non-treated soil; Raw Biochar: raw biochar-treated soil; Fe-impregnated Biochar: Fe-impregnated biochar-treated soil.	79
Figure 3-7 First derivative Fe K-edge XANES spectra of soils collected under pre-defined redox conditions against reference materials.	83
Figure 3-8 Linear combination fitting results of As K-edge XANES spectra of soils collected under pre-defined redox conditions (a), and the relatively proportions of different representative As species in soils (b).	84
Figure 3-9 First derivative As K-edge XANES spectra of reference materials and soil samples collected from different redox conditions. Control: non-treated soil; RBC: raw biochar-treated soil; FeBC: Fe-impregnated biochar-treated soil.	86
Figure 4-1 Scanning electron microscope images (SEM, A-C) and SEM-EDX K α maps (D-F) of biochars. ...	101
Figure 4-2 Energy dispersive X-ray patterns (A: P-rich biochar; B: raw biochar; C: Fe-rich biochar) and Fourier transform infrared spectra (D) of biochars.	102
Figure 4-3 Effect of pre-defined Eh conditions on the concentration of dissolved Cd and Pb, as well as concentration of dissolved Fe, Mn and Fe ²⁺ , DOC, SO ₄ ²⁻ in control and biochar-treated soils.	105
Figure 4-4 Dynamics of redox potential and pH in the microcosms with biochar-treated soils (each MC).	107
Figure 4-5 Correlation coefficients between the concentration of dissolved Cd, Pb and other measured geochemical factors (n=144).	108
Figure 4-6 Effect of biochar application on the pH of the pre-incubated soils.	109
Figure 4-7 Factor analysis of the concentration of dissolved Cd, Pb and other measured geochemical factors (all treatments).	110
Figure 4-8 Effect of biochar application on the geochemical fractions of Cd and Pb in the pre-incubated soils.	111
Figure 4-9 Effect of biochar application on the concentrations of Cd, Pb, Fe, Mn, Fe ²⁺ , DOC and SO ₄ ²⁻ in soil	

solutions collected from the redox experiment. (Different letters indicate significant differences between treatments in each sampling.)	112
Figure 4-10 Factor analysis of the dissolved Cd, Pb and other measured geochemical factors in control soil(A) and soils treated with P-rich biochar (B), raw biochar (C) and Fe-rich biochar (D) (The solid and dotted ellipses with the same color represent the same cluster).	113
Figure 4-11 Effect of biochar application on the organic carbon content, concentrations of Olsen P and potential available Fe in the pre-incubated soils.....	115
Figure 4-12 Canonical discriminant analysis of dissolved Cd, Pb and other measured geochemical factors.....	117
Figure 5-1 Fourier transform infrared (FTIR) spectra of different functionalized biochars.	129
Figure 5-2 The scanning electron microscope (SEM) images and the energy dispersive X-ray (EDX) patterns of functionalized biochars.....	131
Figure 5-3 Effect of functionalized biochars on plant growth and grain yield.	133
Figure 5-4 Effect of functionalized biochars on the availability of As, Cd, Pb, and their accumulation in rice grain and straw.....	134
Figure 5-5 Pearson's correlation coefficients among different parameters.....	136
Figure 5-6 Effect of functionalized biochars on organic carbon content and concentrations of available nutrients in the soil.	137
Figure 5-7 Effect of functionalized biochars on soil pH.....	139
Figure 5-8 Redundancy analysis (RDA) between enzyme activities and environmental factors (soil pH, organic carbon, and available nutrients and PTEs).....	142
Figure 5-9 Principal analysis (PCA) among rice plant growth parameters and soil pH, organic carbon, and available nutrients and PTEs.	144
Figure 6-1 The scanning electron microscope (SEM) images and the energy dispersive X-ray patterns (EDS) of biochars.....	154
Figure 6-2 Fourier transform infrared (FTIR) spectra of both biochars.	156
Figure 6-3 Pearson's correlation matrix of various parameters as affected by water management regimes.....	160
Figure 6-4 As (a) and Pb (b) fractions in soils as affected by biochar application and water management regime.	162
Figure 6-5 Pearson's correlation matrix of various parameters as affected by biochar application (a: control + PBC treatments; b: control + FePBC treatments).	165

Figure 6-6 Relative abundance of top 10 bacterial phyla in soils as affected by biochar application and water management regime (a) and their principal component analysis (PCA) (b)..... 167

Figure 6-7 Redundancy analysis (RDA) between environmental factors and soil bacterial communities at the phyla level. 169

Figure 6-8 Hierarchical clustering dendrogram and heat map based on the relative abundance of bacterial communities at the genus level. 171

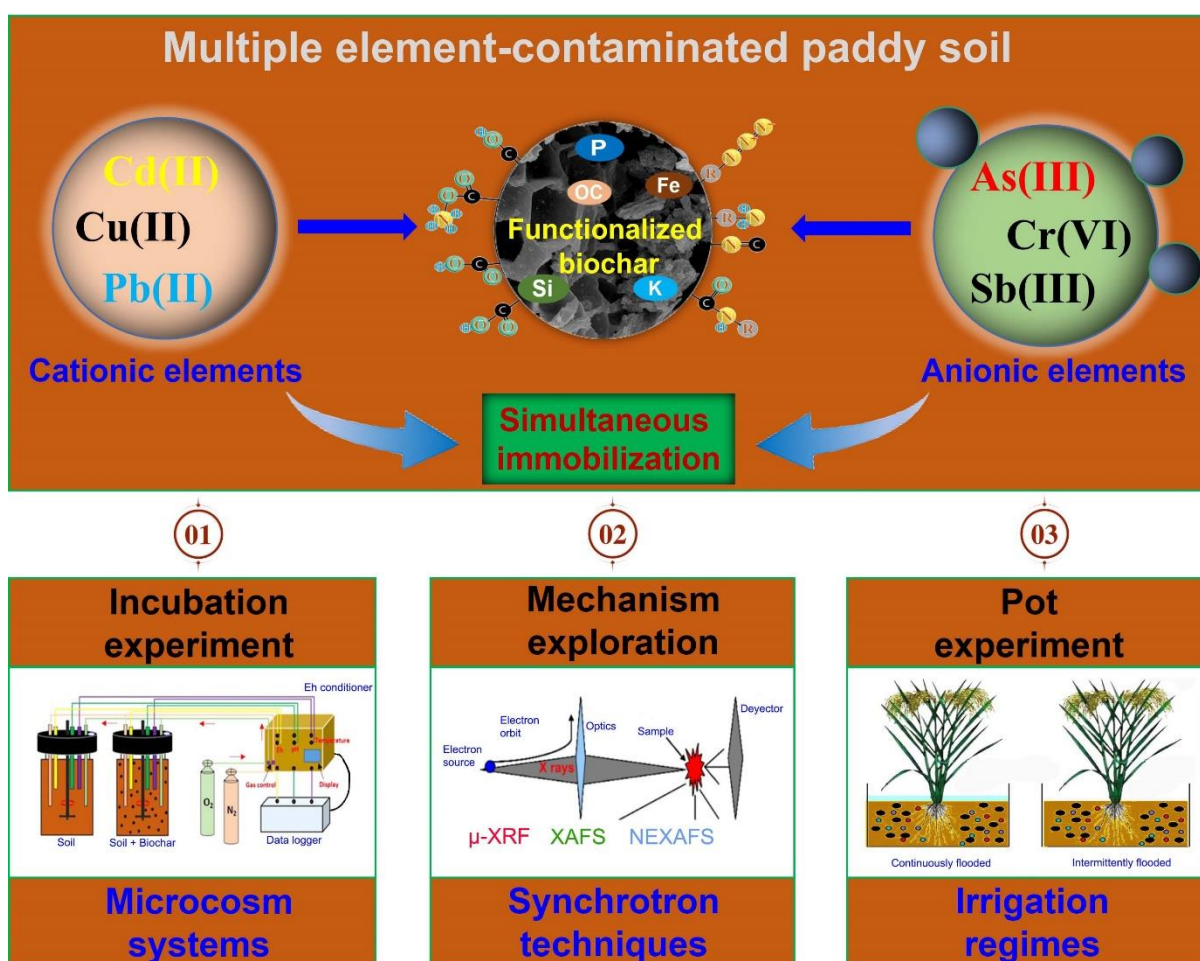
Figure 6-9 Rice grain yield and concentrations of As and Pb in rice grains as affected by biochar application and water management regime. 172

List of Tables

Table 2-1 Physicochemical properties of the tested pig biochar	46
Table 2-2 Variation of As concentration and potential affecting factors in the soil solutions as well as Eh and pH in the control and soil pig biochar-treated soils.	48
Table 2-3 Impact of pig biochar on the changes (%) of the dissolved As in the treated soil as compared to the control.....	50
Table 2-4 Linear combination fitting (LCF) results of As K-edge XANES spectra of soil samples collected at different redox windows.	52
Table 2-5 Pearson's correlations between As and controlling factors including Eh, Fe, Mn, dissolved organic carbon (DOC), specific UV absorbance (SUVA), Cl ⁻ and SO ₄ ²⁻ in the control and pig biochar-treated soils (n=32).	55
Table 3-1 Selected physicochemical properties of the tested soil.	70
Table 3-2 Properties of the tested raw and Fe-impregnated biochars.	72
Table 3-3 Eight-step modified sequential extraction procedures.	75
Table 3-4 Variation of Eh, pH and concentrations of As, Fe, Fe ²⁺ , SO ₄ ²⁻ and DOC in the control and biochar treatments.	77
Table 3-5 Correlation coefficients between As concentration and potential affecting factors.	80
Table 3-6 Average values (mean values of 4 replicates) of As dissolved concentrations and the induced changes (%) in the biochar-treated soils as compared to the control.....	81
Table 3-7 Linear combination fitting (LCF) results of As K-edge XANES spectra of soil samples collected from different redox conditions and bulk soil.	85
Table 4-1 Properties of used P-rich, raw and Fe-rich biochars.	100
Table 4-2 Variation of concentration of Eh, dissolved Cd and Pb and measured governing factors in the slurry of soil treated with different biochars (four replicates).	106
Table 4-3 Impact of biochars on the changes (%) of the mobilization Cd and Pb in the treated soil as compared to the control.....	114
Table 5-1 Physicochemical properties of functionalized biochars.	129
Table 5-2 Analytical methods of various enzyme activities.....	130
Table 5-3 Enzyme activities in non- and functionalized biochar-treated soils (mean ± standard error, n = 4). ..	135

Table 5-4 Effect of functionalized biochars on uptake of K, P and N in rice grain and straw, and iron plaque content on rice root.....	138
Table 6-1 Physicochemical properties of the studied biochars.	155
Table 6-2 Soil pH, organic carbon content and available nutrient in soils as affected by biochar application and water management regime. (mean \pm standard error, n = 4).	158
Table 6-3 Distribution of different fractions of As and Pb in soils as affected by biochar application and water regime.....	163
Table 6-4 Relative abundance of bacterial phyla in soils as affected by biochar application and water regime.	168
Table 6-5 Relative abundance of bacterial genus in soils as affected by biochar application and water regime.	173

CHAPTER 1: Introduction



1.1 Research background

1.1.1 Contamination of paddy soils with potentially toxic elements

Soil contamination with potentially toxic elements (PTEs) such as heavy metals and metalloids is an alarming global environmental problem because of its adverse effects on human health and the entire biosphere (Khanam *et al.*, 2020; Palansooriya *et al.*, 2020; Liu *et al.*, 2022). These PTEs are often transported into soils through geogenic sources and anthropogenic activities, including mining and smelting, agricultural inputs, sewage irrigation and sewage sludge application, fossil fuel combustion, and waste dumping (Mu *et al.*, 2019; He *et al.*, 2020). More than 10 million contaminated soil sites have been recognized globally and more than half of these sites have been contaminated by PTEs (Natasha *et al.*, 2021). The European Environmental Agency (EEA) reported that more than 342,000 highly PTE-contaminated sites have been found in EEA member countries (EEA, 2011). In addition, approximately 10^6 ha of land in the USA and Europe has been contaminated by PTEs (Lewandowski *et al.*, 2006). In these PTEs, arsenic (As), cadmium (Cd), and lead (Pb) are three typical ones that have been ranked, respectively, the first, seventh, and second as hazardous substances by the Agency for Toxic Substance and Disease Registry (ATSDR, 2019). Based on an intensive Chinese national survey, 2.7%, 7.0%, and 1.5% of the surveyed sites exceeded the regulatory limit of As, Cd, and Pb, respectively, based on the Soil Environmental Quality Risk Control Standard for Soil Contamination of Agricultural Land (MEE, 2018), ranked at the third, first, and sixth positions in the eight monitored inorganic pollutants (MEE and MNR, 2014).

Rice (*Oryza sativa* L.) is one of the most important cereals and is a foremost staple food for more than half of the global population, particularly in Asia, where more than 90% of the global rice is produced and consumed (Mu *et al.*, 2019; Shaheen *et al.*, 2022a). Rice plants exhibit a high ability to accumulate PTEs, which is a common dietary source for PTE exposure, posing a severe risk to the production of rice and human health via the food chain (Rong *et al.*, 2019). In China, rapid growing industrialization and urbanization have resulted in accelerated contamination of paddy soils with PTEs over the last three decades (Ali *et al.*, 2020). PTEs including As, Cd, Hg, Pb, and Se are ubiquitously found in rice paddy soils. These elements could be absorbed by rice roots and then transferred to different plant organs, although these elements are not known to be essentially needed for optimum plant growth (Khanam *et al.*, 2020). Widespread contamination of these PTEs in paddy soils has caused substantial intake and accumulation of PTEs in the food chain, thereby leading to a series of adverse impacts on human health (Ali *et al.*, 2020; Sharma *et al.*, 2021). A schematic of human health hazards posed by different PTEs (As, Cd, chromium (Cr), copper (Cu), mercury (Hg), nickel (Ni), Pb, and zinc (Zn)) is shown in Figure 1-1.

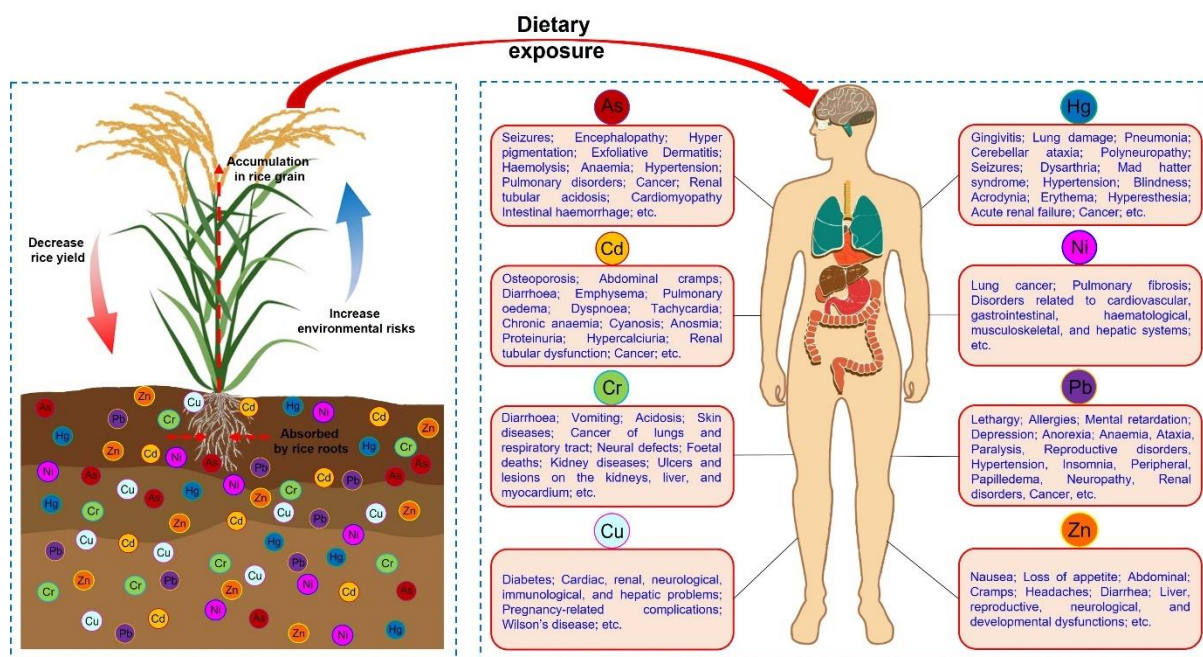


Figure 1-1 A schematic of human health hazards posed by different PTEs.

In general, paddy soils are periodically flooded with a fluctuation of redox potential (Eh) (Yang *et al.*, 2022a), which is known to significantly affect the mobilization and bioavailability of PTEs (Rinklebe *et al.*, 2016a; Zhang and Furman, 2021). In China, a considerable part of the paddy soils is co-contaminated with various PTEs, rather than single-metal contamination (Li *et al.*, 2020). Among those PTEs, As and Cd can be readily absorbed and transferred in rice plant, and eventually accumulate in rice grain (Zhao *et al.*, 2015; Palansooriya *et al.*, 2020; Zhao, 2020). In addition to As and Cd, there is a considerable likelihood that Pb can be absorbed by rice plant and accumulate in rice grain, thus causing risks to human health through dietary exposure (Williams *et al.*, 2009). A survey of rice grain collected from multi-element contaminated paddy fields in Hunan Province, China, demonstrated that 50, 65, and 34% of the samples exceeded the national permissible values of As, Cd, and Pb, respectively (Zhao *et al.*, 2015). Therefore, mitigating the bioavailability and toxicity of multi-PTEs (e.g., As, Cd, and Pb) in paddy soils has become an urgent need for food safety and human health. The Eh in paddy soil is deemed as one of the most important factors that affects the bioavailability and mobility of As in paddy soils (Yang *et al.*, 2022b). In general, water management of paddy soils could be an effective agronomic practice to regulate As bioavailability, while the effect on Cd and Pb being opposite to that on As, due to their contrasting biogeochemical behaviors as compared with As (Arao *et al.*, 2009; Zhao, 2020). Thus, simultaneously immobilize those elements, especially under different redox conditions, is complex and challenging. In addition, a report issued by The Ministry of Land and Resource of China indicated that the arable land per capita in China is less than half of the world average value, thus conservation of the precious resource from contamination and

degradation has been placed a high priority by the Chinese government (Zhao *et al.*, 2015). Large sums of public funding have also been promised for the remediation of contaminated soils. In this context, the urgent task is to develop effective soil remediation technologies for simultaneous alleviating the bioavailability of PTEs in paddy soils and controlling their uptake by rice plants to maintain cleaner rice production and food security. In the past decade, biochar has been widely used for the remediation of soils contaminated with organic and inorganic contaminants (Yang *et al.*, 2016; Palansooriya *et al.*, 2019; Azeem *et al.*, 2021b; Nie *et al.*, 2021; Shaheen *et al.*, 2022b), due to its potential economic, agronomic, and environmental benefits (Natasha *et al.*, 2021; Shaheen *et al.*, 2021; Liu *et al.*, 2022).

1.1.2 Biochar application in remediation of PTE-contaminated soils

Biochar is a carbonaceous material produced from a range of agricultural and forestry biomass wastes in an oxygen-limited environment (Joseph *et al.*, 2021). As a low-cost and eco-friendly product with high adsorption capacity and favorable physicochemical properties, such as large specific surface area, highly porous structure, and abundant oxygen-containing functional groups (Figure 1-2), biochar has been frequently used as a soil amendment for immobilization of PTEs, regulating soil physical, chemical, and biological properties and functions (Xu *et al.*, 2019; Gholami *et al.*, 2020; El-Naggar *et al.*, 2021). For instance, a field-scale study conducted by Nie *et al.* (2018) found that the application of sugarcane bagasse-derived biochar significantly enhanced soil microbial activities, improved soil fertility, decreased the availability of Cd, copper (Cu), and Pb in soil, thus reducing their accumulation in the edible part of pak choi, and eventually promoting plant growth and yield. A pot experiment was carried out by Lu *et al.* (2017), where they found that the addition of both bamboo and rice straw biochars declined the heavy metal concentration in the pore water, and promoted the transformation of heavy metals (i.e., Cd, Cu, Pb, and Zn) from mobile fractions to relatively stable fractions, thereby minimizing the uptake of those heavy metals by *Sedum plumbizincicola* (Lu *et al.*, 2014). In an incubation experiment under different redox conditions, Yang *et al.* (2021) found that the application of the pig carcass-derived biochar could more effectively immobilize Pb than Cd, in particular under reducing conditions. However, previous studies indicated that biochar is a promising amendment in mitigating the bioavailability and toxicity of cationic PTEs (e.g., Cd and Pb) in soils, mainly through physisorption, liming effect, ion exchange, precipitation, and complexation, etc. (He *et al.*, 2019; Joseph *et al.*, 2021; Shaheen *et al.*, 2022b), which are summarized in Figure 1-2.

However, previous studies reported that the capability of raw/pristine biochar application on the removal and immobilization of anionic PTEs was limited, primarily due to its negatively-charged surface and alkalinity (Kumar

et al., 2020; Shaheen *et al.*, 2021). For example, Van Vinh *et al.* (2014) found that the application of the raw pine cone-derived biochar promoted the desorption of As through increasing the pH. Chen *et al.* (2021) concluded that the electrostatic repulsion between $\text{Sb}(\text{OH})_4^-$ and negatively-charged surface of the green waste biochar could be responsible for the decline of Sb(III) sorption on the biochar. Thus, it is of critical importance to enhance the effectiveness of biochar on the immobilization of multiple elements in paddy soils, in particular those have been contaminated with both cationic (e.g., Cd and Pb) and anionic elements (e.g., As) (Pan *et al.*, 2021; Wen *et al.*, 2021), in order to achieve a simultaneous immobilization of both types of elements.

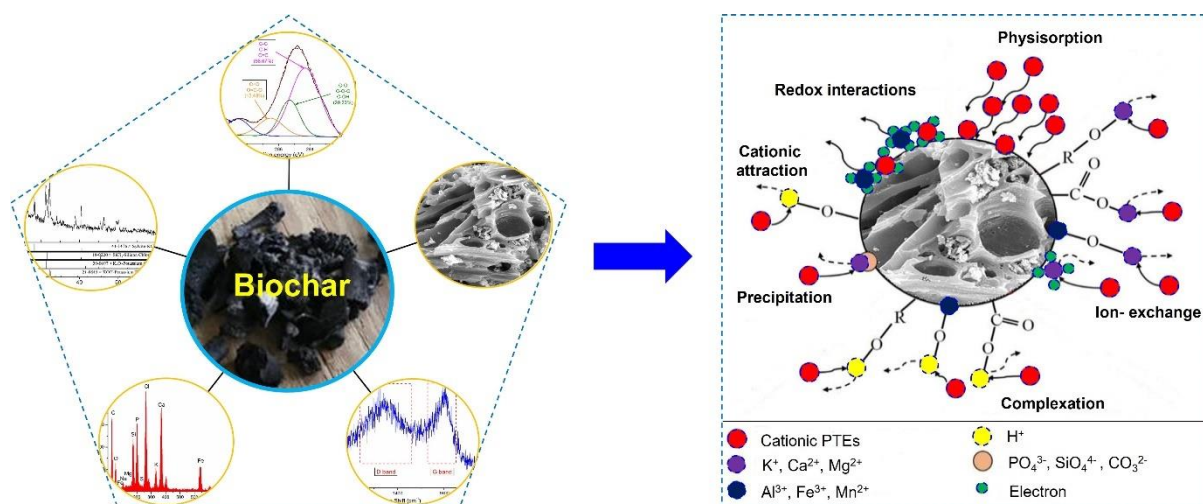


Figure 1-2 Favorable biochar characteristics and the postulated mechanisms of biochar interactions with cationic PTEs.

Functionalize biochar could be obtained by selecting superior biomass or loading other organic or inorganic materials for remediation of multi-PTE contaminated paddy soils (Xiao *et al.*, 2018; Wang *et al.*, 2019; Liu *et al.*, 2022). It has been proven that the pyrolysis condition and feedstock type are the two most important factors that determine the basic physicochemical characteristics of biochar, such as pH, cation exchange capacity, porous structure, surface area, and elemental composition (Gong *et al.*, 2022). Therefore, the functions of biochar could be specifically designed through screening precursors, i.e., different feedstocks can be exploited to produce biochars for different purposes (Xiao *et al.*, 2018). For instance, biochars derived from wood-based feedstocks generally have relatively high surface area; straw-based materials generate biochars have high cationic exchange capacity; manure- and animal-originated biochar gave relatively high content of N and P (Ippolito *et al.*, 2020; Joseph *et al.*, 2021). The mineral elements presented in biochar are considered as the fundamental building blocks, which experience various physicochemical processes during pyrolysis (Xiao *et al.*, 2018). The content of nonvolatile or hard-volatile mineral elements, such as silicon (Si), phosphorus (P), potassium (K), calcium (Ca)

Magnesium (Mg), iron (Fe), and manganese (Mn), could be condensed during pyrolysis (at certain temperatures), thus leading to an enrichment of these elements in biochars. For instance, P-rich materials, such as poultry litter (Mierzwa-Hersztek *et al.*, 2016), cow dung (Guo *et al.*, 2013), and animal carcasses (Yang *et al.*, 2017), and Si-rich biomass, such as rice, wheat, barley, and maize straw (Herath *et al.*, 2020; Wang *et al.*, 2020), could be utilized for the production of P- and Si-rich biochars (Limmer *et al.*, 2018; Yang *et al.*, 2022a). Additionally, modification of biochar with metal elements, such as aluminum (Al) (Wang and Wang, 2019), bismuth (Bi) (Zhu *et al.*, 2019), cerium (Ce) (Dong *et al.*, 2020), Cu (Zhong *et al.*, 2020), lanthanum (La) (Wang *et al.*, 2018), Mg (Zheng *et al.*, 2020), Fe (Shaheen *et al.*, 2022b), Mn (Shaheen *et al.*, 2021), through loading of those metal oxides and metal salts. In these materials, Fe-rich compounds have been widely used for the modification of biochar, especially for the purpose of immobilizing As in aquatic and soil systems (Yin *et al.*, 2017; Islam *et al.*, 2021; Wen *et al.*, 2021).

1.1.3 Silicon-rich amendments

Silicon is a vital mineral element for soil-plant interactions, which is not considered to be essential, yet confers high benefits to plant growth because of its ability to alleviate abiotic and biotic stresses (e.g., PTEs) in the soil-plant system (Wang *et al.*, 2019). Moreover, application of Si fertilizers and/or Si-rich soil amendments is a cost-effective agronomic practice for preventing the adverse effects of PTEs, promoting plant growth, and alleviating the accumulation of PTEs in rice plants (Sohail *et al.*, 2020; Xiao *et al.*, 2021). Recently, Si-rich materials and/or Si fertilizers have been amended to contaminated soils to alleviate As, Cd, and Pb toxicity and reduce their mobility and bioavailability (Seyfferth *et al.*, 2019; Sohail *et al.*, 2020; Wei *et al.*, 2021). Increasing Si can alleviate As uptake because 1) the main form of Si in flooded paddy soils is silicic acid (H_4SiO_4^0 , $\text{pK}_a = 9.8$), which is chemically similar to arsenite (H_3AsO_3^0 , $\text{pK}_a = 9.2$); 2) H_3AsO_3^0 and H_4SiO_4^0 share the same transport pathway (Lsi1 and Lsi2) in rice plants (Limmer *et al.*, 2018). Therefore, the increase of soluble Si in soil solution can downregulate Si transporter expression, thus minimizing As uptake through competition of transporters (Teasley *et al.*, 2017). In addition, Si fertilizers and Si-rich materials have been reported to reduce the Cd transport in apoplast and symplast of plant tissues (Cui *et al.*, 2017; Ji *et al.*, 2017). Silicon deposited in the cell walls promotes binding of Cd on the cell surface. This process affects the further Cd translocation into cells (Shi *et al.*, 2005; Cui *et al.*, 2017). Moreover, polysilicic acids and silica sol can adsorb Cd, thus reducing its apoplectic flow (Pan *et al.*, 2019). Previous studies on Pb immobilization using Si amendments showed that Si-rich materials are also effective on immobilizing Pb in contaminated soils (Zhao *et al.*, 2017). Gu *et al.* (2011) demonstrated that the addition of Si-rich fly ash and steel slag significantly reduced the accumulation of Pb in rice grains. **Therefore, it was hypothesized that biochars derived from Si-rich feedstocks, such as rice straw and husk biochars, might**

be a promising source of Si for remediation of paddy soils co-contaminated with As, Cd, and Pb.

1.1.4 Phosphorus-rich amendments

Phosphorus is not only an essential nutrient for plant and microbe growth (Xiao *et al.*, 2018), but also an effective material for the immobilization of PTEs (especially Cd and Pb) in soils, due to the formation of stable phosphate precipitates and complexes (Zhang *et al.*, 2020). P-rich materials have been used for immobilizing Pb in soils since soluble phosphate (PO_4^{3-}) could transform labile Pb into stable compounds such as $\text{Pb}_5(\text{PO}_4)_3\text{OH}$ and $\text{Pb}_5(\text{PO}_4)_3\text{Cl}$ (Bolan *et al.*, 2003; Chen *et al.*, 2022). For example, Gao *et al.* (2019) reported that the application of P-containing amendments enhanced the removal of Pb(II) from aqueous solution. In addition, application of P-containing materials could also be a promising approach for the immobilization of Cd. For instance, Sneddon *et al.* (2006) found that the application of the P-containing bone meal amendments can immobilize Cd through adsorption or formation of less soluble Cd-carbonates or mixed Ca-Cd-phosphates. In addition, both As and P belong to periodic group 15, and arsenate (AsO_4^{3-}) and phosphate (PO_4^{3-}) are considered as chemical analogues, due to their similar chemical speciation, indicating that they can substitute for each other in chemical reactions (Strawn, 2018). Due to their chemical similarity, PO_4^{3-} shared the same transporters (OsPT1, OsPT4, and OsPT8) with As(V) to rice roots, thus the elevated concentration of PO_4^{3-} may inhibit the uptake of As by rice plants (Bolan *et al.*, 2015; Zhao and Wang, 2019). Recently, several studies have paid attention on using P-rich biochar for the remediation of soils contaminated with PTEs. For instance, Yang *et al.* (2021) found that the biochar derived from pig carcasses was a promising soil amendment for alleviating the release of Pb in soils. Competition between phosphate and arsenate (As(V)) for the binding sites on soil particles, due to their chemical similarities, has been well-documented in the literature (Seyfferth and Fendorf, 2012). Azeem *et al.* (2021a) indicated that the application of P-rich materials can immobilize Cd through the formation of insoluble $\text{Cd}_3(\text{PO}_4)_2$ and Ca-Cd phosphates. **Therefore, it was hypothesized that the application of P-rich biochar would improve soil fertility, promote rice plant growth, and simultaneously diminish the assimilation of multi-PTEs in rice.**

1.1.5 Iron-rich amendments

Previous studies showed that Fe-containing materials, such as Fe (hydro)oxides, Fe sulfides, nano zero-valent Fe and goethite have been used for the modification of biochar to improve its effectiveness on immobilization of PTEs (Bian *et al.*, 2018; Rajendran *et al.*, 2019). In particular, iron is an essential element that affects the fate of As in soils (Wu *et al.*, 2018; Han *et al.*, 2019), where seasonal redox alteration may trigger the reversible reductive dissolution and oxidative precipitation of Fe (hydro)oxides, thereby affecting the mobilization and speciation of As (Aeppli *et al.*, 2019; Amen *et al.*, 2020; Shi *et al.*, 2020). Fe materials are effective on removal of PTEs from

aquatic and soil systems, but it has the disadvantages of being prone to agglomeration, passivation, poor transportability and high cost (Wen *et al.*, 2021). The loading of those Fe materials onto biochar could take the merits of both Fe and biochar to achieve an ideal effectiveness on the immobilization of PTEs. Recently, Fe-based biochars have been frequently produced and used for remediation of soils contaminated with PTEs. For example, Kashif Irshad *et al.* (2020) found that the incorporation of the goethite-modified biochar was more effective on decreasing Cd mobilization than the raw biochar. Yu *et al.* (2020) reported that application of *Pennisetum sinense Roxb* and coffee grounds biochars coupled with the iron fertilizer significantly decreased the exchangeable and reducible Cd and Pb in a contaminated soil. Wen *et al.* (2021) indicated that the modification of green waste biochar using FeCl₃ enhanced its ability for reducing the uptake of As by rice plants. Zhu *et al.* (2020) produced an α -FeOOH modified-wheat straw biochar (α -FeOOH@BC) and the adsorption experiments demonstrated that α -FeOOH@BC was a promising material for simultaneous removal of Cd(II) and As(III) from aqueous solutions, and the maximum adsorption capacities for Cd(II) and As(III) were 63 and 78 mg g⁻¹, respectively. However, to the best of our knowledge, there are still uncertainties in the effects of Fe-modified Si- and P-rich biochars on the bioavailability of PTEs and their accumulation in rice. **Therefore, it was hypothesized that the Fe-modified Si-rich or P-rich functionalized biochars would synthesize the advanced functions of different materials, thereby regulating soil properties and fertility, in turn promoting rice plant growth, reducing PTE mobility and bioavailability, and eventually ameliorating the accumulation of PTEs in rice grain.** A schematic of this multiple functionalized biochar and its postulated mechanisms for PTE immobilization are depicted in Figure 1-3.

In addition, as aforementioned (section 1.1.1), the mobilization, transformation, speciation, and bioavailability of PTEs might be affected by the fluctuating redox potential (Eh) in paddy soils. **Overall, it was hypothesized that the application of different functionalized (Si-, P-, and Fe-rich) biochars would cause significant changes in soil Eh and the redox-induced soil biogeochemical processes, thus affecting the mobilization, transformation, speciation, and bioavailability of PTEs (i.e., As, Cd, and Pb) in paddy soils.** Therefore, it was essential to understand the geochemical behaviors of these elements in paddy soils, so that their mobilization, bioavailability, and eco-toxicity can be better predicted in response to changing redox conditions. In addition, the impact of different functionalized biochars on the mobilization, bioavailability, transformation and speciation of As, Cd, and Pb in paddy soils under flooding conditions with different redox conditions is still not clear. Furthermore, the effects of different functionalized biochars on soil physicochemical and microbial properties, nutrient availability, PTE toxicity during rice cultivation, and in turn on rice growth, eventually on the rice yield

and quality need to be clarified.

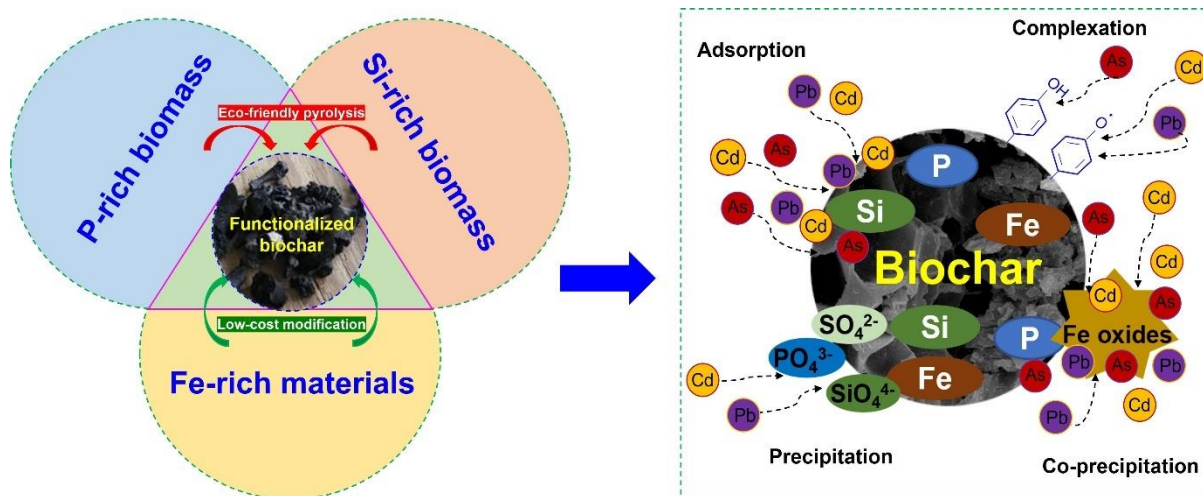


Figure 1-3 A schematic of the proposed functionalized biochar and its postulated mechanisms for multi-PTE immobilization.

1.2 Key research questions

Based on the above-mentioned hypotheses and knowledge gaps, it is therefore important to build a novel understanding of the following research questions:

- (1) Can functionalized biochars affect the release dynamics and biogeochemical behaviors of As, Cd and Pb under dynamic redox conditions in paddy soil?
- (2) How do functionalized biochars affect the biogeochemical processes and redox reactions while they are incorporated into the contaminated soils, and how do they affect the transformation and biogeochemical fractionation of As, Cd and Pb under fluctuating redox conditions?
- (3) Are functionalized biochars able to regulate the physicochemical and microbial properties of paddy soils, growth of rice plants (*Oryza sativa*), as well as the biogeochemical behaviors of As, Cd, and Pb in the soil-plant interface and their uptake by rice plants and translocation from the roots to stems and leaves, and then edible grain under different irrigation regimes (simulation of different redox conditions)?

1.3 Research objectives

Part 1: Impact of the application of different functionalized biochars on the mobilization, transformation, speciation, and potential availability of As, Cd, and Pb under systematic changed redox conditions in a contaminated paddy soil (Research question 1).

In this part, the impact of redox fluctuation on the mobilization and transformation of As, Cd, and Pb was investigated via conducting redox incubation experiments. The interactions between these PTEs and the

controlling factors, such as pH, the concentration and composition of DOC, concentrations of dissolved Fe, Mn, as well as anions (e.g., SO_4^{2-} , Cl^- , PO_4^{3-} , etc.) were also studied.

Part 2: Elucidating the mechanisms of the transformation and species of As, Cd, and Pb as affected by application of functionalized biochars and changes in the redox conditions in the paddy soil (Research question 2).

In this part, both sequential extraction method and synchrotron-based X-ray absorption near edge spectroscopic (XANES) techniques were used for the species of As and redistribution (binding forms) of these PTEs in selected sediment (soil) samples collected from the incubation experiments conducted in part (1), and then the underlying mechanisms were elucidated.

Part 3: Effects of different functionalized biochars on the soil properties, soil fertility, rice growth and yield, and the bioavailability of As, Cd, and Pb in paddy soils, as well as the interactions between these PTEs, microorganisms, and functionalized biochars in the soil-rice plant interface, and the accumulation of these PTEs in rice grain. (Research question 3)

In this part, rice cultivation pot trails with different water management regimes (i.e., continuously flooded and intermittently flooded) were conducted to practically investigate the impact of the functionalized biochars on the bioavailability and ecotoxicity of As, Cd, and Pb, and their accumulation in rice grain. The physicochemical and biological properties (e.g., organic carbon content, nutrient bioavailability, enzyme activity, and microbial community structure), plant growth parameters, bioavailability of these PTEs, as well as their concentrations in different rice organs were analyzed.

1.4 Methodologies

1.4.1 Incubation experiments (Part/Research question 1)

An automated biogeochemical microcosm (MC) system was used to simulate the flooding of the contaminated paddy soils under laboratory conditions (Figure 1-4). The main advantages of this system are: 1) the redox conditions can be defined accurately, 2) the redox conditions can be maintained and altered automatically by purging with either oxygen or nitrogen, and 3) the reaction condition in the MC system is homogenized by constant stirring (Rinklebe *et al.*, 2016b; Shaheen *et al.*, 2016). More technical details of this system were described by Yu and Rinklebe (Yu and Rinklebe, 2011).

The soil slurry was sampled minimum 48 h after reaching each new Eh-window (target windows = -400, -300, -200, -100, 0, +100, +200, and +300 mV, respectively). At each sampling point, approximately 85 mL of slurry was taken from each vessel, and then centrifuged at 5,000 rpm for 15 min. Thereafter, the samples were

immediately transferred to an anaerobic glove box (Don Whitley Scientific, Shipley, UK) to pass through a 0.45- μm membrane filter (Whatman Inc., Maidstone, UK). Afterwards, sub-samples of the filtrate were used for the analyses of the concentrations of As, Cd, and Pb, as well as the controlling factors such as dissolved organic carbon (DOC), specific UV absorbance (SUVA), iron (Fe), manganese (Mn), ferrous iron (Fe^{2+}), sulfide (S^{2-}), chlorite (Cl^-), and sulfate (SO_4^{2-}). In the meantime, the selected samples of the remained soil-sediments after centrifugation were freeze-dried and prepared as wax pellets for XANES analyses in Part 2. The entire procedure was carried out in an anaerobic chamber.



Figure 1-4 Photos of the MC system used for incubation experiments.

1.4.2 Mechanism elucidation (Part/Research question 2)

The species of As and Fe in the solid phase (soil samples) collected after centrifugation (sampled under Eh = -300, 0 and +250 mV conditions) were analyzed using As/Fe K-edge X-ray absorption near edge structure (XANES) spectroscopy at the National Synchrotron Radiation Research Center (NSRRC) in Taiwan, ROC (Figure 1-5). The spectra were collected in fluorescence mode, using a Soller-slits Lytle detector in an energy range of 11,667-12,867 eV for As, and 6,912-7,912 eV for Fe, respectively. Spectral analysis was conducted using Athena software (Ravel and Newville, 2005). The energy scale was calibrated using gold (Au) foil for As (calibration energy = 11,919 eV) and Fe foil for Fe (calibration energy = 7712 eV), respectively. After normalization, principal component analysis (PCA) was subsequently performed to extract the major components in all spectra. Thereafter, the linear combination fitting (LCF) of As K-edge XANES spectra was conducted to determine the species of As according to the method reported by Yang *et al.* (2020). The fit quality was evaluated based on the R value, and the best LCF result with smallest R value was used. The oxidation states of Fe in soils can be fairly estimated by Fe K-edge XANES (Prietzl *et al.*, 2007). However, it is difficult to quantify specific Fe species in soils using Fe

K-edge XANES, because of the complexity of Fe compounds caused by soil weathering and pedogenesis. Thus, FeO and Alpha-Fe₂O₃ were selected as the representative Fe(II) and Fe(III) reference minerals, respectively, to estimate the oxidation states of Fe in the soil samples collected from different redox conditions (Paul *et al.*, 2020).



Figure 1-5 Photos of the synchrotron-based Beamlines TLS 17C1 and TPS 44A1.

1.4.3 Pot experiments (Part/Research question 3)

Pot experiments were conducted using an As, Cd and Pb co-contaminated paddy soil, which treated with different types of functionalized biochars at an application rate of 3 wt.%. The dose is selected based on the findings in our previous studies (Yang *et al.*, 2016; Lu *et al.*, 2017; Chen *et al.*, 2020). The pots were irrigated with different amount of deionized water to control different hydrological management regimes (i.e., continuously flooded & intermittently flooded) (Figure 1-6). For the continuously flooded treatment, the pots were irrigated daily until the soil moisture reached nearly saturated, and then were continuously flooded until 10 days before the harvest. For the intermittently flooded treatment, the pots were re-flooded when small cracks are present on the surface soil. After harvest, the rice growth parameters, such as plant height, straw biomass, number of panicles, and grain yield were measured. The concentrations of nutrients (e.g., N, P, and K) and PTEs (e.g., As, Cd, and Pb) in rice straw and grain were extracted and determined using ICP-OES. The soil samples were collected, air-dried, and then passed through a 2-mm sieve for the analyses of the basic soil properties, nutrient availability, as well as the available and geochemical fractions of PTEs. The ecotoxicological effect of PTEs on the soil enzyme activities and microbial community structure was analyzed.

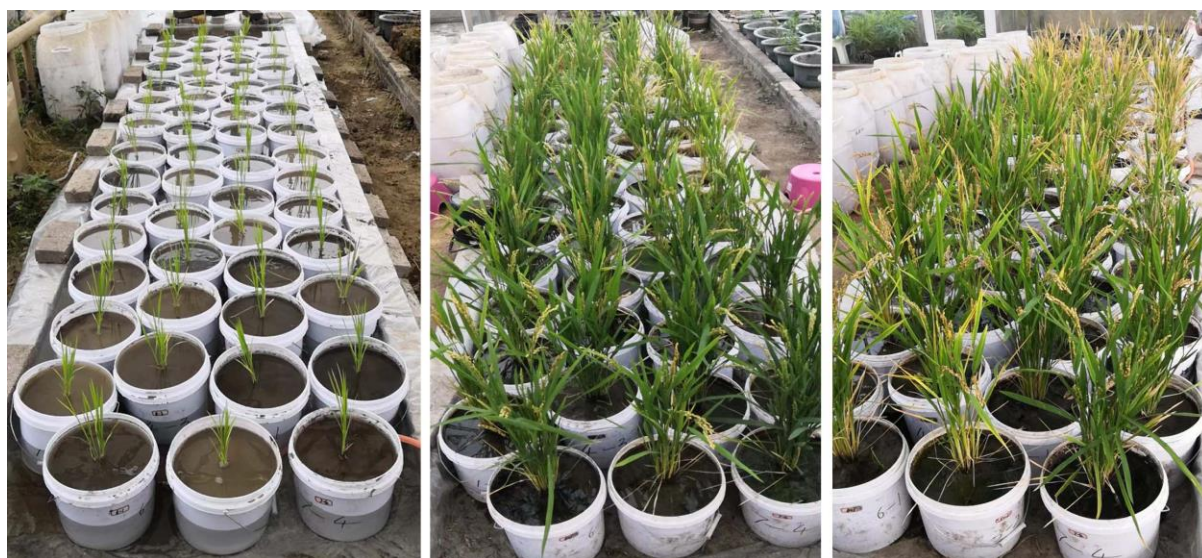
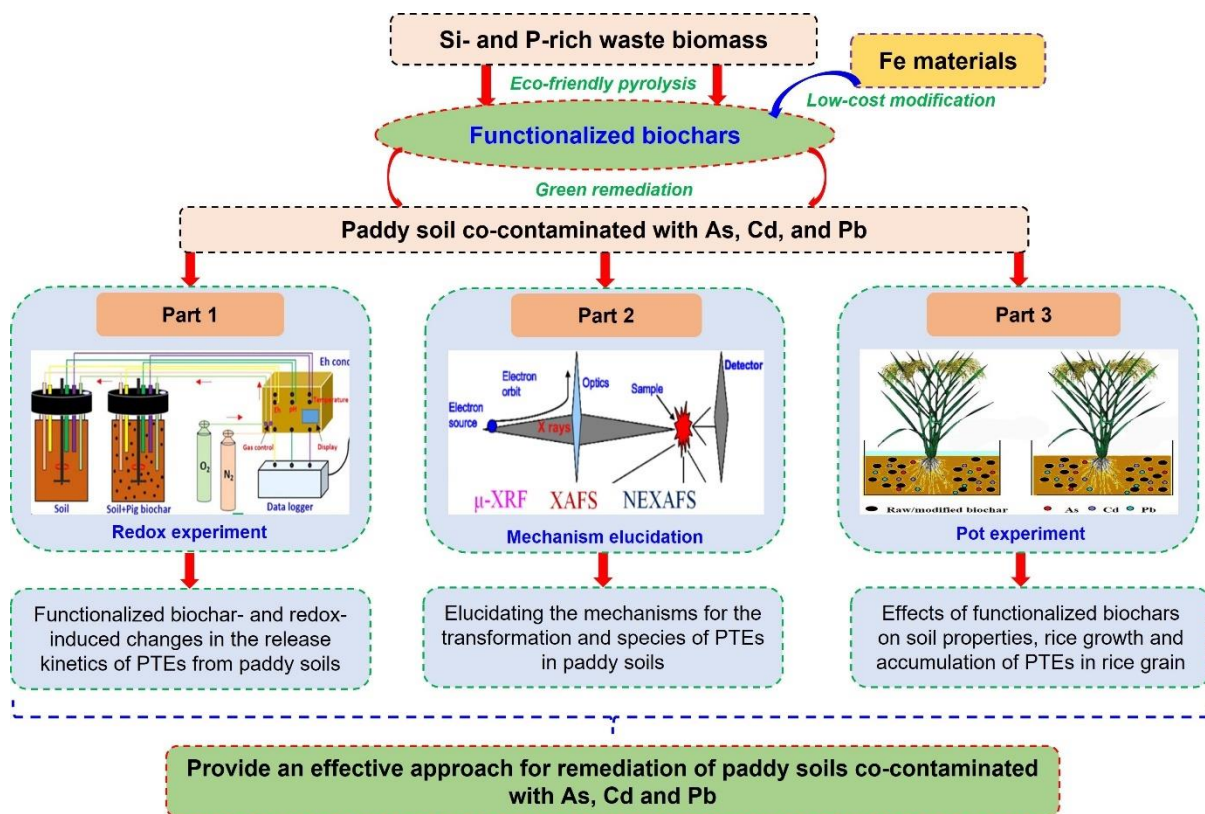


Figure 1-6 Photos of the rice cultivation pot experiments.

1.5 Technical route



1.6 References

- Aeppli, M., Vranic, S., Kaegi, R., Kretzschmar, R., Brown, A.R., Voegelin, A., Hofstetter, T.B., Sander, M., 2019. Decreases in iron oxide reducibility during microbial reductive dissolution and transformation of ferrihydrite. *Environ. Sci. Technol.* 53, 8736-8746. <https://doi.org/10.1021/acs.est.9b01299>
- Ali, W., Mao, K., Zhang, H., Junaid, M., Xu, N., Rasool, A., Feng, X., Yang, Z., 2020. Comprehensive review of the basic chemical behaviours, sources, processes, and endpoints of trace element contamination in paddy soil-rice systems in rice-growing countries. *J. Hazard. Mater.* 397, 122720. <https://doi.org/10.1016/j.jhazmat.2020.122720>
- Amen, R., Bashir, H., Bibi, I., Shaheen, S.M., Niazi, N.K., Shahid, M., Hussain, M.M., Antoniadis, V., Shakoor, M.B., Al-Solaimani, S.G., Wang, H., Bundschuh, J., Rinklebe, J., 2020. A critical review on arsenic removal from water using biochar-based sorbents: The significance of modification and redox reactions. *Chem. Eng. J.* 396, 125195. <https://doi.org/10.1016/j.cej.2020.125195>
- Arao, T., Kawasaki, A., Baba, K., Mori, S., Matsumoto, S., 2009. Effects of water management on cadmium and arsenic accumulation and dimethylarsinic acid concentrations in Japanese rice. *Environ. Sci. Technol.* 43, 9361-9367. <https://doi.org/10.1021/es9022738>
- ATSDR's substance priority list., Available from: <https://www.atsdr.cdc.gov/spl/index.html#2019spl>.
- Azeem, M., Ali, A., Soundari, P.G., Li, Y., Abdelrahman, H., Latif, A., Li R., Basta, N., Li, G., Shaheen, S.M., Rinklebe, J., Zhang, Z., 2021. Bone-derived biochar improved soil quality and reduced Cd and Zn phytoavailability in a multi-metal contaminated mining soil. *Environ. Pollut.* 116800. <https://doi.org/10.1016/j.envpol.2021.116800>
- Azeem, M., Shaheen, S.M., Ali, A., Jeyasundar, P., Latif, A., Abdelrahman, H., Li, R., Almazroui, M., Niazi, N.K., Sarmah, A.K., Li, G., Rinklebe, J., Zhu, Y.G., Zhang, Z., 2021b. Removal of potentially toxic elements from contaminated soil and water using bone char compared to plant- and bone-derived biochars: A review. *J. Hazard. Mater.* 427, 128131. <https://doi.org/10.1016/j.jhazmat.2021.128131>
- Bian, P., Zhang, J., Zhang, C., Huang, H., Rong, Q., Wu, H., Li, X., Xu, M., Liu, Y., Ren, S., 2018. Effects of silk-worm excrement biochar combined with different iron-based materials on the speciation of cadmium and lead in soil. *Appl. Sci.* 8, 1999. <https://doi.org/10.3390/app8101999>
- Bolan, N., Mahimairaja, S., Kunhikrishnan, A., Seshadri, B., Thangarajan, R., 2015. Bioavailability and ecotoxicity of arsenic species in solution culture and soil system: implications to remediation. *Environ. Sci. Pollut. Res.* 22, 8866-8875. <https://doi.org/10.1007/s11356-013-1827-2>
- Bolan, N. S., Adriano, D. C., Naidu, R., 2003. Role of phosphorus in (im)mobilization and bioavailability of heavy metals in the soil-plant system. *Rev. Environ. Contam. Toxicol.* 177, 1-44. https://doi.org/10.1007/0-387-21725-8_1
- Chen, H., Feng, Y., Yang, X., Yang, B., Sarkar, B., Bolan, N., Meng, J., Wu, F., Wong, J.W.C., Chen, W., Wang, H., 2022. Assessing simultaneous immobilization of lead and improvement of phosphorus availability through application of phosphorus-rich biochar in a contaminated soil: A pot experiment. *Chemosphere* 296, 133891. <https://doi.org/10.1016/j.chemosphere.2022.133891>
- Chen, H., Gao, Y., El-Naggar, A., Niazi, N.K., Sun, C., Shaheen, S.M., Hou, D., Yang, X., Tang, Z., Liu, Z., Hou, H., Chen, W., Rinklebe, J., Pohorely, M., Wang, H., 2021. Enhanced sorption of trivalent antimony by chitosan-loaded biochar in aqueous solutions: Characterization, performance and mechanisms. *J. Hazard. Mater.* 425, 127971. <https://doi.org/10.1016/j.jhazmat.2021.127971>
- Chen, H., Yang, X., Wang, H., Sarkar, B., Shaheen, S. M., Gielen, G., Bolan, N., Guo, J., Che, L., Sun, H., Rinklebe, J., 2020. Animal carcass- and wood-derived biochars improved nutrient bioavailability, enzyme activity, and plant growth in metal-phthalic acid ester co-contaminated soils: A trial for reclamation and improvement of

- degraded soils. *J. Environ. Manage.* 261, 110246. <https://doi.org/10.1016/j.jenvman.2020.110246>
- Cui, J., Liu, T., Li, F., Yi, J., Liu, C., Yu, H., 2017. Silica nanoparticles alleviate cadmium toxicity in rice cells: Mechanisms and size effects. *Environ. Pollut.* 228, 363-369. <https://doi.org/10.1016/j.envpol.2017.05.014>
- Dong, C.-D., Chen, C.-W., Nguyen, T.-B., Huang, C.P., Hung, C.-M., 2020. Degradation of phthalate esters in marine sediments by persulfate over Fe–Ce/biochar composites. *Chem. Eng. J.* 384, 123301. <https://doi.org/10.1016/j.cej.2019.123301>
- EEA. (2011). Progress in management of contaminated sites. European Environment Agency. <https://www.eea.europa.eu/data-and-maps/indicators/progress-in-managementof-contaminated-sites-3/assessment>
- El-Naggar, A., Chang, S.X., Cai, Y., Lee, Y.H., Wang, J., Wang, S.L., Ryu, C., Rinklebe, J., Sik Ok, Y., 2021. Mechanistic insights into the (im)mobilization of arsenic, cadmium, lead, and zinc in a multi-contaminated soil treated with different biochars. *Environ. Int.* 156, 106638. <https://doi.org/10.1016/j.envint.2021.106638>
- Gao, R., Fu, Q., Hu, H., Wang, Q., Liu, Y., Zhu, J., 2019. Highly-effective removal of Pb by co-pyrolysis biochar derived from rape straw and orthophosphate. *J. Hazard. Mater.* 371, 191-197. <https://doi.org/10.1016/j.jhazmat.2019.02.079>
- Gholami, L., Rahimi, G., Khademi Jolgeh Nezhad, A., 2020. Effect of thiourea-modified biochar on adsorption and fractionation of cadmium and lead in contaminated acidic soil. *Int. J. Phytoremediation* 22, 468-481. <https://doi.org/10.1080/15226514.2019.1678108>
- Gong, H., Zhao, L., Rui, X., Hu, J., Zhu, N., 2022. A review of pristine and modified biochar immobilizing typical heavy metals in soil: Applications and challenges. *J. Hazard. Mater.* 432, 128668. <https://doi.org/10.1016/j.jhazmat.2022.128668>
- Gu, H.H., Qiu, H., Tian, T., Zhan, S.S., Deng, T.H., Chaney, R.L., Wang, S.Z., Tang, Y.T., Morel, J.L., Qiu, R.L., 2011. Mitigation effects of silicon rich amendments on heavy metal accumulation in rice (*Oryza sativa* L.) planted on multi-metal contaminated acidic soil. *Chemosphere* 83, 1234-1240. <https://doi.org/10.1016/j.chemosphere.2011.03.014>
- Guo, Y., Tang, H., Li, G., Xie, D., 2013. Effects of Cow Dung Biochar Amendment on Adsorption and Leaching of Nutrient from an Acid Yellow Soil Irrigated with Biogas Slurry. *Water Air Soil Pollut.* 225. <https://doi.org/10.1007/s11270-013-1820-x>
- Han, Y. S., Park, J. H., Kim, S. J., Jeong, H. Y., Ahn, J. S., 2019. Redox transformation of soil minerals and arsenic in arsenic-contaminated soil under cycling redox conditions. *J. Hazard. Mater.* 378, 120745. <https://doi.org/10.1016/j.jhazmat.2019.120745>
- He, H., Xiao, Q., Yuan, M., Huang, R., Sun, X., Wang, X., Zhao, H., 2020. Effects of steel slag amendments on accumulation of cadmium and arsenic by rice (*Oryza sativa*) in a historically contaminated paddy field. *Environ. Sci Pollut. Res.* 27, 40001-40008. <https://doi.org/10.1007/s11356-020-10028-3>
- He, L., Zhong, H., Liu, G., Dai, Z., Brookes, P.C., Xu, J., 2019. Remediation of heavy metal contaminated soils by biochar: Mechanisms, potential risks and applications in China. *Environ. Pollut.* 252, 846-855. <https://doi.org/10.1016/j.envpol.2019.05.151>
- Herath, I., Zhao, F.J., Bundschuh, J., Wang, P., Wang, J., Ok, Y.S., Palansooriya, K.N., Vithanage, M., 2020. Microbe mediated immobilization of arsenic in the rice rhizosphere after incorporation of silica impregnated biochar composites. *J. Hazard. Mater.* 398, 123096. <https://doi.org/10.1016/j.jhazmat.2020.123096>
- Ippolito, J.A., Cui, L., Kammann, C., Wrage-Mönnig, N., Estavillo, J.M., Fuertes-Mendizabal, T., Cayuela, M.L., Sigua, G., Novak, J., Spokas, K., Borchard, N., 2020. Feedstock choice, pyrolysis temperature and type influence biochar characteristics: a comprehensive meta-data analysis review. *Biochar* 2, 421-438. <https://doi.org/10.1007/s42773-020-00067-x>

- Islam, M.S., Magid, A., Chen, Y., Weng, L., Ma, J., Arafat, M.Y., Khan, Z.H., Li, Y., 2021. Effect of calcium and iron-enriched biochar on arsenic and cadmium accumulation from soil to rice paddy tissues. *Sci. Total Environ.* 785, 147163. <https://doi.org/10.1016/j.scitotenv.2021.147163>
- Ji, X., Liu, S., Juan, H., Bocharnikova, E.A., Matichenkov, V.V., 2017. Effect of silicon fertilizers on cadmium in rice (*Oryza sativa*) tissue at tillering stage. *Environ. Sci. Pollut. Res.* 24, 10740-10748. <https://doi.org/10.1007/s11356-017-8730-1>
- Joseph, S., Cowie, A.L., Van Zwieten, L., Bolan, N., Budai, A., Buss, W., Cayuela, M.L., Graber, E.R., Ippolito, J.A., Kuzyakov, Y., Luo, Y., Ok, Y.S., Palansooriya, K.N., Shepherd, J., Stephens, S., Weng, Z., Lehmann, J., 2021. How biochar works, and when it doesn't: A review of mechanisms controlling soil and plant responses to biochar. *Glob. Change Biol. Bioenergy* 13, 1731-1764. <https://doi.org/10.1111/gcbb.12885>
- Kashif Irshad, M., Chen, C., Noman, A., Ibrahim, M., Adeel, M., Shang, J., 2020. Goethite-modified biochar restricts the mobility and transfer of cadmium in soil-rice system. *Chemosphere* 242, 125152. <https://doi.org/10.1016/j.chemosphere.2019.125152>
- Khanam, R., Kumar, A., Nayak, A.K., Shahid, M., Tripathi, R., Vijayakumar, S., Bhaduri, D., Kumar, U., Mohanty, S., Panneerselvam, P., Chatterjee, D., Satapathy, B.S., Pathak, H., 2020. Metal(loid)s (As, Hg, Se, Pb and Cd) in paddy soil: Bioavailability and potential risk to human health. *Sci. Total Environ.* 699, 134330. <https://doi.org/10.1016/j.scitotenv.2019.134330>
- Kumar, M., Xiong, X., Wan, Z., Sun, Y., Tsang, D.C.W., Gupta, J., Gao, B., Cao, X., Tang, J., Ok, Y.S., 2020. Ball milling as a mechanochemical technology for fabrication of novel biochar nanomaterials. *Bioresour. Technol.* 312, 123613. <https://doi.org/10.1016/j.biortech.2020.123613>
- Lewandowski, I., Weger, J., Van Hooijdonk, A., Havlicekova, K., Van Dam, J., Faaij, A., 2006. The potential biomass for energy production in the Czech Republic. *Biomass Bioenerg.* 30, 405-421. <https://doi.org/10.1016/j.biombioe.2005.11.020>
- Li, Z., Wang, L., Wu, J., Xu, Y., Wang, F., Tang, X., Xu, J., Ok, Y.S., Meng, J., Liu, X., 2020. Zeolite-supported nanoscale zero-valent iron for immobilization of cadmium, lead, and arsenic in farmland soils: Encapsulation mechanisms and indigenous microbial responses. *Environ. Pollut.* 260, 114098. <https://doi.org/10.1016/j.envpol.2020.114098>
- Limmer, M.A., Mann, J., Amaral, D.C., Vargas, R., Seyfferth, A.L., 2018. Silicon-rich amendments in rice paddies: Effects on arsenic uptake and biogeochemistry. *Sci. Total Environ.* 624, 1360-1368. <https://doi.org/10.1016/j.scitotenv.2017.12.207>
- Liu, M., Almatrafi, E., Zhang, Y., Xu, P., Song, B., Zhou, C., Zeng, G., Zhu, Y., 2022. A critical review of biochar-based materials for the remediation of heavy metal contaminated environment: Applications and practical evaluations. *Sci. Total Environ.* 806, 150531. <https://doi.org/10.1016/j.scitotenv.2021.150531>
- Lu, K., Yang, X., Gielen, G., Bolan, N., Ok, Y.S., Niazi, N.K., Xu, S., Yuan, G., Chen, X., Zhang, X., Liu, D., Song, Z., Liu, X., Wang, H., 2017. Effect of bamboo and rice straw biochars on the mobility and redistribution of heavy metals (Cd, Cu, Pb and Zn) in contaminated soil. *J. Environ. Manage.* 186, 285-292. <https://doi.org/10.1016/j.jenvman.2016.05.068>
- Lu, K., Yang, X., Shen, J., Robinson, B., Huang, H., Liu, D., Bolan, N., Pei, J., Wang, H., 2014. Effect of bamboo and rice straw biochars on the bioavailability of Cd, Cu, Pb and Zn to *Sedum plumbizincicola*. *Agric. Ecosyst. Environ.* 191, 124-132. <https://doi.org/10.1016/j.agee.2014.04.010>
- MEE, C., 2018. Soil Environmental Quality Risk Control Standard for Soil Contamination of Agricultural Land.
- MEE, C., MNR, C., 2014. The Report on the National Soil Contamination Survey. http://www.mlr.gov.cn/xwdt/jrxw/201404/t20140417_1312998.htm.
- Mierzwa-Hersztek, M., Gondek, K., Baran, A., 2016. Effect of poultry litter biochar on soil enzymatic activity,

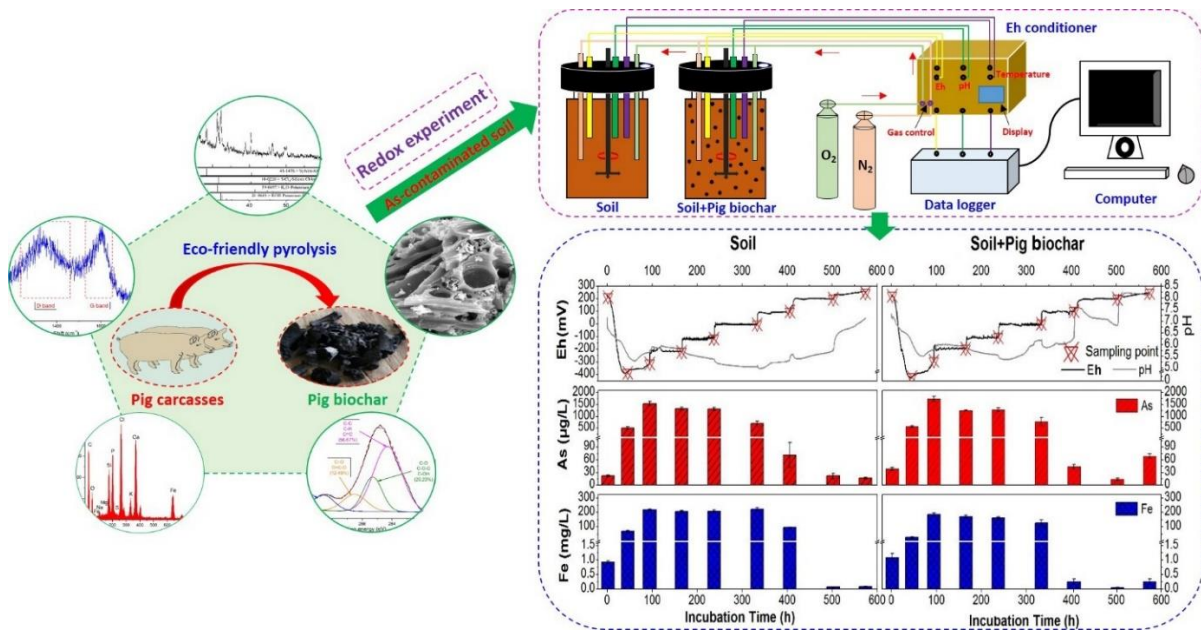
- ecotoxicity and plant growth. *Appl. Soil Ecol.* 105, 144-150. <https://doi.org/10.1016/j.apsoil.2016.04.006>
- Mu, T., Wu, T., Zhou, T., Li, Z., Ouyang, Y., Jiang, J., Zhu, D., Hou, J., Wang, Z., Luo, Y., Christie, P., Wu, L., 2019. Geographical variation in arsenic, cadmium, and lead of soils and rice in the major rice producing regions of China. *Sci Total Environ* 677, 373-381. <https://doi.org/10.1016/j.scitotenv.2019.04.337>
- Natasha, N., Shahid, M., Khalid, S., Bibi, I., Naeem, M.A., Niazi, N.K., Tack, F.M.G., Ippolito, J.A., Rinklebe, J., 2021. Influence of biochar on trace element uptake, toxicity and detoxification in plants and associated health risks: A critical review. *Crit. Rev. Environ. Sci. Technol.*, 1-41. <https://doi.org/10.1080/10643389.2021.1894064>
- Nie, C., Yang, X., Niazi, N.K., Xu, X., Wen, Y., Rinklebe, J., Ok, Y.S., Xu, S., Wang, H., 2018. Impact of sugarcane bagasse-derived biochar on heavy metal availability and microbial activity: A field study. *Chemosphere* 200, 274-282. <https://doi.org/10.1016/j.chemosphere.2018.02.134>
- Nie, T., Yang, X., Chen, H., Müller K., Shaheen, S. M., Rinklebe, J., Song, H., Xu, S., Wu, F., Wang, H., 2021. Effect of biochar aging and co-existence of diethyl phthalate on the mono-sorption of cadmium and zinc to biochar-treated soils. *J. Hazard. Mater.* 408, 124850. <https://doi.org/10.1016/j.jhazmat.2020.124850>
- Palansooriya, K.N., Shaheen, S.M., Chen, S.S., Tsang D.C.W., Hashimoto, Y., Hou, D., Bolan, N.S., Rinklebe, J., Ok, Y.S., 2020. Soil amendments for immobilization of potentially toxic elements in contaminated soils: A critical review. *Environ. Int.* 134, 105046. <https://doi.org/10.1016/j.envint.2019.105046>
- Palansooriya, K.N., Wong, J.T.F., Hashimoto, Y., Huang, L., Rinklebe, J., Chang, S.X., Bolan, N., Wang, H., Ok, Y.S., 2019. Response of microbial communities to biochar-amended soils: a critical review. *Biochar* 1, 3-22. <https://doi.org/10.1007/s42773-019-00009-2>
- Pan, D., Liu, C., Yu, H., Li, F., 2019. A paddy field study of arsenic and cadmium pollution control by using iron-modified biochar and silica sol together. *Environ. Sci. Pollut. Res.* 26, 24979-24987. <https://doi.org/10.1007/s11356-019-05381-x>
- Pan, H., Yang, X., Chen, H., Sarkar, B., Bolan, N., Shaheen, S. M., Wu, F., Che, L., Ma, Y., Rinklebe, J., Wang, H., 2021. Pristine and iron-engineered animal- and plant-derived biochars enhanced bacterial abundance and immobilized arsenic and lead in a contaminated soil. *Sci. Total Environ.* 763, 144218. <https://doi.org/10.1016/j.scitotenv.2020.144218>
- Paul, R., Sarkar, C., Yan, Y., Trinh, Q. T., Rao, B. S., Pao, C. W., Lee, J. F., Liu, W., Mondal, J., 2020. Porous-Organic-Polymer-Triggered Advancement of Sustainable Magnetic Efficient Catalyst for Chemoselective Hydrogenation of Cinnamaldehyde. *ChemCatChem* 12, 3687-3704. <https://doi.org/10.1002/cctc.202000072>
- Prietzl, J., Thieme, J., Eusterhues, K., Eichert, D., 2007. Iron speciation in soils and soil aggregates by synchrotron-based X-ray microspectroscopy (XANES, μ -XANES). *Eur. J. Soil Sci.* 58, 1027-1041. <https://doi.org/10.1111/j.1365-2389.2006.00882.x>
- Rajendran, M., Shi, L., Wu, C., Li, W., An, W., Liu, Z., Xue, S., 2019. Effect of sulfur and sulfur-iron modified biochar on cadmium availability and transfer in the soil-rice system. *Chemosphere* 222, 314-322. <https://doi.org/10.1016/j.chemosphere.2019.01.149>
- Ravel, B., Newville, M., 2005. ATHENA, ARTEMIS, HEPHAESTUS: data analysis for X-ray absorption spectroscopy using IFEFFIT. *J. Synchrotron Radiat.* 12, 537-541. <https://doi.org/10.1107/S0909049505012719>
- Rinklebe, J., Shaheen, S.M., Frohne, T., 2016a. Amendment of biochar reduces the release of toxic elements under dynamic redox conditions in a contaminated floodplain soil. *Chemosphere* 142, 41-47. <https://doi.org/10.1016/j.chemosphere.2015.03.067>
- Rinklebe, J., Shaheen, S.M., Yu, K.W., 2016b. Release of As, Ba, Cd, Cu, Pb, and Sr under pre-definite redox conditions in different rice paddy soils originating from the USA and Asia. *Geoderma* 270, 21-32.

- <https://doi.org/10.1016/j.geoderma.2015.10.011>
- Rong, Q., Zhong, K., Li, F., Huang, H., Li, C., Nong, X., Zhang, C., 2019. Combined effect of ferrous ion and biochar on cadmium and arsenic accumulation in rice. *Appl. Sci.* 10, 300. <https://doi.org/10.3390/app10010300>
- Seyfferth, A.L., Amaral, D., Limmer, M.A., Guilherme, L.R.G., 2019. Combined impacts of Si-rich rice residues and flooding extent on grain As and Cd in rice. *Environ. Int.* 128, 301-309. <https://doi.org/10.1016/j.envint.2019.04.060>
- Seyfferth, A.L., Fendorf, S., 2012. Silicate mineral impacts on the uptake and storage of arsenic and plant nutrients in rice (*Oryza sativa* L.). *Environ. Sci. Technol.* 46, 13176-13183. <https://doi.org/10.1021/es3025337>
- Shaheen, S.M., Antoniadis, V., Kwon, E., Song, H., Wang, S.L., Hseu, Z.Y., Rinklebe, J., 2020. Soil contamination by potentially toxic elements and the associated human health risk in geo- and anthropogenic contaminated soils: A case study from the temperate region (Germany) and the arid region (Egypt). *Environ. Pollut.* 262. <https://doi.org/10.1016/j.envpol.2020.114312>
- Shaheen, S.M., Mosa, A., Natasha, Abdelrahman, H., Niazi, N.K., Antoniadis, V., Shahid, M., Song, H., Kwon, E.E., Rinklebe, J., 2022b. Removal of toxic elements from aqueous environments using nano zero-valent iron- and iron oxide-modified biochar: a review. *Biochar* 4, 24. <https://doi.org/10.1007/s42773-022-00149-y>
- Shaheen, S.M., Natasha, Mosa, A., El-Naggar, A., Faysal Hossain, M., Abdelrahman, H., Khan Niazi, N., Shahid, M., Zhang, T., Fai Tsang, Y., Trakal, L., Wang, S., Rinklebe, J., 2021. Manganese oxide-modified biochar: production, characterization and applications for the removal of pollutants from aqueous environments - a review. *Bioresour. Technol.* 346, 126581. <https://doi.org/10.1016/j.biortech.2021.126581>
- Shaheen, S.M., Rinklebe, J., Frohne, T., White, J.R., DeLaune, R.D., 2014. Biogeochemical Factors Governing Cobalt, Nickel, Selenium, and Vanadium Dynamics in Periodically Flooded Egyptian North Nile Delta Rice Soils. *Soil Sci. Soc. Am. J.* 78, 1065-1078. <https://doi.org/10.2136/sssaj2013.10.0441>
- Sharma, S., Kaur, I., Nagpal, A.K., 2021. Contamination of rice crop with potentially toxic elements and associated human health risks--a review. *Environ. Sci. Pollut. Res.* 28, 12282-12299. <https://doi.org/10.1007/s11356-020-11696-x>
- Shi, X., Zhang, C., Wang, H., Zhang, F., 2005. Effect of Si on the distribution of Cd in rice seedlings. *Plant Soil* 272, 53-60. <https://doi.org/10.1007/s11104-004-3920-2>
- Shi, Z., Hu, S., Lin, J., Liu, T., Li, X., Li, F., 2020. Quantifying microbially mediated kinetics of ferrihydrite transformation and arsenic reduction: role of the arsenate-reducing gene expression pattern. *Environ. Sci. Technol.* 54 (11), 6621-6631. <https://doi.org/10.1021/acs.est.9b07137>
- Sneddon, I.R., Orueetxebarria, M., Hodson, M.E., Schofield, P.F., Valsami-Jones, E., 2006. Use of bone meal amendments to immobilise Pb, Zn and Cd in soil: A leaching column study. *Environ. Pollut.* 144, 816-825. <https://doi.org/10.1016/j.envpol.2006.02.008>
- Sohail, M.I., Zia Ur Rehman, M., Rizwan, M., Yousaf, B., Ali, S., Anwar Ul Haq, M., Anayat, A., Waris, A.A., 2020. Efficiency of various silicon rich amendments on growth and cadmium accumulation in field grown cereals and health risk assessment. *Chemosphere* 244, 125481. <https://doi.org/10.1016/j.chemosphere.2019.125481>
- Strawn, D.G., 2018. Review of interactions between phosphorus and arsenic in soils from four case studies. *Geochem Trans* 19, 10. <https://doi.org/10.1186/s12932-018-0055-6>
- Teasley, W.A., Limmer, M.A., Seyfferth, A.L., 2017. How Rice (*Oryza sativa* L.) Responds to Elevated As under Different Si-Rich Soil Amendments. *Environ. Sci. Technol.* 51, 10335-10343. <https://doi.org/10.1021/acs.est.7b01740>
- Van Vinh, N., Zafar, M., Behera, S. K., Park, H. S., 2014. Arsenic(III) removal from aqueous solution by raw and

- zinc-loaded pine cone biochar: equilibrium, kinetics, and thermodynamics studies. *Int. J. Environ. Sci. Technol.* 12, 1283-1294. <https://doi.org/10.1007/s13762-014-0507-1>
- Williams, P.N., Lei, M., Sun, G., Huang, Q., Lu, Y., Deacon, C., Meharg, A.A., Zhu, Y., 2009. Occurrence and Partitioning of Cadmium, Arsenic and Lead in Mine Impacted Paddy Rice: Hunan, China. *Environmental Science & Technology* 43, 637-642. <https://doi.org/10.1021/es802412r>
- Wang, J., Wang, S., 2019. Preparation, modification and environmental application of biochar: A review. *J. Clean. Prod.* 227, 1002-1022. <https://doi.org/10.1016/j.jclepro.2019.04.282>
- Wang, L., Wang, J., Wang, Z., He, C., Lyu, W., Yan, W., Yang, L., 2018. Enhanced antimonate (Sb(V)) removal from aqueous solution by La-doped magnetic biochars. *Chem. Eng. J.* 354, 623-632. <https://doi.org/10.1016/j.cej.2018.08.074>
- Wang, Y., Xiao, X., Xu, Y., Chen, B., 2019. Environmental Effects of Silicon within Biochar (Sichar) and Carbon-Silicon Coupling Mechanisms: A Critical Review. *Environ. Sci. Technol.* 53, 13570-13582. <https://doi.org/10.1021/acs.est.9b03607>
- Wang, Y., Zhang, K., Lu, L., Xiao, X., Chen, B., 2020. Novel insights into effects of silicon-rich biochar (Sichar) amendment on cadmium uptake, translocation and accumulation in rice plants. *Environ. Pollut.* 265, 114772. <https://doi.org/10.1016/j.envpol.2020.114772>
- Wei, X., Zhang, P., Zhan, Q., Hong, L., Bocharnikova, E., Matichenkov, V., 2021. Regulation of As and Cd accumulation in rice by simultaneous application of lime or gypsum with Si-rich materials. *Environ. Sci. Pollut. Res.* 28, 7271-7280. <https://doi.org/10.1007/s11356-020-11053-y>
- Wen, E., Yang, X., Chen, H., Shaheen, S. M., Sarkar, B., Xu, S., Song, H., Liang, Y., Rinklebe, J., Hou, D., Li, Y., Wu, F., Pohorelý, M., Wong, J. W. C., Wang, H., 2021. Iron-modified biochar and water management regime-induced changes in plant growth, enzyme activities, and phytoavailability of arsenic, cadmium and lead in a paddy soil. *J. Hazard. Mater.* 124344. <https://doi.org/10.1016/j.jhazmat.2020.124344>
- Wu, S., Fang, G., Wang, D., Jaisi, D.P., Cui, P., Wang, R., Wang, Y., Wang, L., Sherman, D.M., Zhou, D., 2018b. Fate of As(III) and As(V) during microbial reduction of arsenic-bearing ferrihydrite facilitated by activated carbon. *ACS Earth Space Chem.* 2, 878-887. <https://doi.org/10.1021/acsearthspacechem.8b00058>
- Xiao, X., Chen, B., Chen, Z., Zhu, L., Schnoor, J.L., 2018. Insight into multiple and multilevel structures of biochars and their potential environmental applications: A critical review. *Environ. Sci. Technol.* 52, 5027-5047. <https://doi.org/10.1021/acs.est.7b06487>
- Xiao, Z., Peng, M., Mei, Y., Tan, L., Liang, Y., 2021. Effect of organosilicone and mineral silicon fertilizers on chemical forms of cadmium and lead in soil and their accumulation in rice. *Environ. Pollut.* 283, 117107. <https://doi.org/10.1016/j.envpol.2021.117107>
- Xu, M., Gao, P., Yang, Z., Su, L., Wu, J., Yang, G., Zhang, X., Ma, J., Peng, H., Xiao, Y., 2019. Biochar impacts on phosphorus cycling in rice ecosystem. *Chemosphere* 225, 311-319. <https://doi.org/10.1016/j.chemosphere.2019.03.069>
- Yang, P.-T., Hashimoto, Y., Wu, W.-J., Huang, J.-H., Chiang, P.-N., Wang, S.-L., 2020a. Effects of long-term paddy rice cultivation on soil arsenic speciation. *J. Environ. Manage.* 254, 109768. <https://doi.org/10.1016/j.jenvman.2019.109768>
- Yang, X., Hinzmann, M., Pan, H., Wang, J., Bolan, N., Tsang, D.C.W., Ok, Y.S., Wang, S.-L., Shaheen, S.M., Wang, H., Rinklebe, J., 2022a. Pig carcass-derived biochar caused contradictory effects on arsenic mobilization in a contaminated paddy soil under fluctuating controlled redox conditions. *J. Hazard. Mater.* 421, 126647. <https://doi.org/10.1016/j.jhazmat.2021.126647>
- Yang, X., Liu, J., McGroutner, K., Huang, H., Lu, K., Guo, X., He, L., Lin, X., Che, L., Ye, Z., Wang, H., 2016. Effect of biochar on the extractability of heavy metals (Cd, Cu, Pb, and Zn) and enzyme activity in soil.

- Environ. Sci. Pollut. Res. 23, 974-984. <https://doi.org/10.1007/s11356-015-4233-0>
- Yang, X., Lu, K., Mcgrouter, K., Lei, C., Hu, G., Wang, Q., Liu, X., Shen, L., Huang, H., Ye, Z., Wang, H., 2017. Bioavailability of Cd and Zn in soils treated with biochars derived from tobacco stalk and dead pigs. *J. Soil. Sediment.* 17, 751-762. <https://doi.org/10.1007/s11368-015-1326-9>
- Yang, X., Pan, H., Shaheen, S.M., Wang, H., Rinklebe, J., 2021a. Immobilization of cadmium and lead using phosphorus-rich animal-derived and iron-modified plant-derived biochars under dynamic redox conditions in a paddy soil. *Environ. Int.* 156, 106628. <https://doi.org/10.1016/j.envint.2021.106628>
- Yang, X., Shaheen, S.M., Wang, J., Hou, D., Ok, Y.S., Wang, S.L., Wang, H., Rinklebe, J., 2022b. Elucidating the redox-driven dynamic interactions between arsenic and iron-impregnated biochar in a paddy soil using geochemical and spectroscopic techniques. *J. Hazard. Mater.* 422, 126808. <https://doi.org/10.1016/j.jhazmat.2021.126808>
- Yin, D., Wang, X., Peng, B., Tan, C., Ma, L.Q., 2017. Effect of biochar and Fe-biochar on Cd and As mobility and transfer in soil-rice system. *Chemosphere* 186, 928-937. <https://doi.org/10.1016/j.chemosphere.2017.07.126>
- Yu, B., Li, D., Wang, Y., He, H., Li, H., Chen, G., 2020. The compound effects of biochar and iron on watercress in a Cd/Pb-contaminated soil. *Environ. Sci. Pollut. Res.* 27, 6312-6325. <https://doi.org/10.1007/s11356-019-07353-7>
- Yu, K., Rinklebe, J., 2011. Advancement in soil microcosm apparatus for biogeochemical research. *Ecol. Eng.* 37, 2071-2075. <https://doi.org/10.1016/j.ecoleng.2011.08.017>
- Zhang, H., Shao, J., Zhang, S., Zhang, X., Chen, H., 2020. Effect of phosphorus-modified biochars on immobilization of Cu (II), Cd (II), and As (V) in paddy soil. *J. Hazard. Mater.* 390, 121349. <https://doi.org/10.1016/j.jhazmat.2019.121349>
- Zhang, Z., Furman, A., 2021. Soil redox dynamics under dynamic hydrologic regimes - A review. *Sci. Total Environ.* 763, 143026. <https://doi.org/10.1016/j.scitotenv.2020.143026>
- Zhao, F.-J., 2020. Strategies to manage the risk of heavy metal(loid) contamination in agricultural soils. *Front. Agr. Sci. Eng.* 7, 333-338. <https://doi.org/10.15302/J-FASE-2020335>
- Zhao, F.-J., Wang, P., 2019. Arsenic and cadmium accumulation in rice and mitigation strategies. *Plant Soil* 446, 1-21. <https://doi.org/10.1007/s11104-019-04374-6>
- Zhao, F.J., Ma, Y., Zhu, Y.G., Tang, Z., McGrath, S.P., 2015. Soil contamination in China: current status and mitigation strategies. *Environ. Sci. Technol.* 49, 750-759. <https://doi.org/10.1021/es5047099>
- Zhao, M., Liu, Y., Li, H., Cai, Y., Wang, M.K., Chen, Y., Xie, T., Wang, G., 2017. Effects and mechanisms of meta-sodium silicate amendments on lead uptake and accumulation by rice. *Environ. Sci. Pollut. Res.* 24, 21700-21709. <https://doi.org/10.1007/s11356-017-9746-2>
- Zheng, Y., Wan, Y., Chen, J., Chen, H., Gao, B., 2020. MgO modified biochar produced through ball milling: A dual-functional adsorbent for removal of different contaminants. *Chemosphere* 243, 125344. <https://doi.org/10.1016/j.chemosphere.2019.125344>
- Zhong, Q., Lin, Q., Huang, R., Fu, H., Zhang, X., Luo, H., Xiao, R., 2020. Oxidative degradation of tetracycline using persulfate activated by N and Cu codoped biochar. *Chem. Eng. J.* 380. <https://doi.org/10.1016/j.cej.2019.122608>
- Zhu, N., Qiao, J., Yan, T., 2019. Arsenic immobilization through regulated ferrolysis in paddy field amendment with bismuth impregnated biochar. *Sci Total Environ* 648, 993-1001. <https://doi.org/10.1016/j.scitotenv.2018.08.200>
- Zhu, S., Qu, T., Irshad, M.K., Shang, J., 2020. Simultaneous removal of Cd(II) and As(III) from co-contaminated aqueous solution by α -FeOOH modified biochar. *Biochar* 2, 81-92. <https://doi.org/10.1007/s42773-020-00040-8>

CHAPTER 2: Effects of Pig Carcass-Derived Phosphorus-Rich Biochar on Arsenic Mobilization under Fluctuating Controlled Redox Conditions in Paddy Soil ¹



¹ Adapted from Yang, X., Hinzmann, M., Pan, H., Wang, J., Bolan, N., Tsang, D.C.W., Ok, Y.S., Wang, S.L., Shaheen, S.M., Wang, H., Rinklebe, J., 2022. Pig carcass-derived biochar caused contradictory effects on arsenic mobilization in a contaminated paddy soil under fluctuating controlled redox conditions. *Journal of Hazardous Materials* 421, 126647.

A supplementary data is provided in Appendix A.

Abstract

Contamination of paddy soils by the hazardous arsenic (As) is of great concern for human health the environment. The impact of animal-derived biochar on As mobilization under fluctuating redox conditions in paddy soils has not been studied. Consequently, we investigated the effects of pig carcass-derived biochar (PB) on As (im)mobilization in a contaminated paddy soil under controlled redox potential (Eh) using a biogeochemical microcosm-setup. The addition of PB decreased the concentration of dissolved As at Eh = +100 and +200 mV by 38.7% and 35.4%, respectively (compared to the control), due to the co-precipitation of As with Fe-Mn oxides and the complexation between As and the aromatic organic molecules. However, PB increased As mobilization at Eh= -300 mV by 13.5%, due to promoting reduction and decomposition of As-bearing Fe minerals (e.g., ferrihydrite-As, Fe-humic-As) and facilitating As mobilization as indicated by the As K-edge XANES. PB increased As mobilization at Eh= +250 mV by 317.6%, due to the associated increase of pH. We conclude that As mobilization in PB-treated paddy soils is highly controlled by Eh. PB can be used to reduce the risk of As under moderately reducing conditions, but it may increase the risk under strongly reducing and oxidizing conditions.

Keywords: Hazardous metal(loid); Paddy soil contamination; Redox condition; Soil remediation; Biochar

2.1 Introduction

Arsenic (As) is a ubiquitous hazardous metalloid that can eventually threaten the soil ecosystem and human health through food chain (Antoniadis *et al.*, 2017; Zhu *et al.*, 2017; Rinklebe *et al.*, 2019). Arsenic has been considered as a proverbial carcinogen (Niazi *et al.*, 2018) which may cause several diseases such as cardiovascular disease, infertility, diabetes, neurological problems and skin lesions (Li *et al.*, 2018; Antoniadis *et al.*, 2019). Contamination of arable land including paddy fields with As by geogenic source and anthropogenic activities, including the application of phosphate fertilizers, pesticides, herbicides, as well as mining, smelting and other industrial activities (Wu *et al.*, 2018; Shaheen *et al.*, 2020), is a severe problem due to its toxic and non-degradable nature (Bessa *et al.*, 2020; Palansooriya *et al.*, 2020). Rice (*Oryza sativa* L.) is one of the most widely consumed staple food for more than half of the population worldwide (Kim *et al.*, 2018). Arsenic can be easily taken up by rice plant, leading to adverse impacts on human health via daily diet (Li *et al.*, 2018; Antoniadis *et al.*, 2019). Therefore, mitigating human dietary exposure to As by decreasing As mobility and bioavailability in paddy soil is an urgent requirement for the global food safety and the sustainable development of agriculture.

Biochar as a soil amendment has attracted considerable attention due to its potentially agronomic, environmental and economic benefits (Shaheen *et al.*, 2019; Bandara *et al.*, 2020). Extensive efforts have been made on how biochar might improve carbon sequestration, enhance soil fertility, promote plant growth, and mitigate soil contamination (e.g., Rinklebe *et al.*, 2016a; Yang *et al.*, 2016; Nie *et al.*, 2018), based on its favorable properties such as having rich carbon content, presence of various functional groups, highly porous structure and large surface area (Yuan *et al.*, 2017; Shaheen *et al.*, 2019). Recently, biochar amendment has been exploited as a potential technology for remediation of paddy soils contaminated with As (Wang *et al.*, 2017; Wu *et al.*, 2018; Pan *et al.*, 2021). For example, Khan *et al.* (2013) indicated that the sewage sludge biochar was able to decrease the bioavailability of As by 38% in a paddy soil. Wu *et al.* (2018) found that biochar modified with Fe-oxyhydroxy sulfate could effectively reduce the mobile fractions of As in paddy soils. However, several studies reported that the mobilization of As from paddy soils was undesirably facilitated due to the incorporation of biochar (e.g., Vithanage *et al.*, 2017; Frick *et al.*, 2019).

Generally, paddy soils are periodically flooded with a fluctuation of redox potentials (Eh) during the rice growing period (Wang *et al.*, 2017). It is commonly accepted that the mobilization of As in paddy soils mainly depend on the Eh and Eh-induced alterations of geochemical factors such as pH, solubility of iron (Fe) and manganese (Mn), the concentrations of dissolved organic carbon (DOC) and inorganic anions (e.g., Cl⁻ and SO₄²⁻) (e.g., El-Naggar *et al.*, 2019; Shaheen *et al.*, 2019). Although partly explored, the impact of biochar on the mobilization of As in

soils under different redox conditions have been reported by Rinklebe *et al.* (2016a) and El-Naggar *et al.* (2019), whereas both studies focused mainly on the mobilization of multi-elements from different soils rather than paddy soils. To our understanding, less information has been given to the specific effect of pig carcass-derived biochar (pig biochar) on As im(mobilization) in contaminated paddy soils under dynamic redox conditions.

In China, approximately 20 million of dead pig carcasses are generated each year (Chen *et al.*, 2019). This huge hazardous number of dead pigs causes serious environmental concerns because of improper disposal (Yang *et al.*, 2017). Novel approaches for disposing dead pigs are urgently needed to solve this intractable problem. Previously, biochar derived from dead pigs has been used to remediate soils contaminated with heavy metals and organic pollutants (Chen *et al.*, 2019; Nie *et al.*, 2021), reduce nitrogen leaching loss (Feng *et al.*, 2020), improve soil fertility (Chen *et al.*, 2020) and promote plant growth (Yang *et al.*, 2017). As an animal-derived biochar, pig biochar (PB) has high alkalinity and aromaticity, abundant functional groups and high phosphorus content (Yang *et al.*, 2017; Chen *et al.*, 2020; Pan *et al.*, 2021). Therefore, we hypothesize that the application of PB may affect variously the mobilization of As in paddy soils under different redox conditions. The application of PB may inhibit the mobilization of As from paddy soils through changing Eh and Eh-induced biochemical processes such as chemistry of Fe and Mn, cycling of organic carbon due to its electron transfer ability (e.g., through complexation under reducing conditions and co-precipitation under oxidizing conditions). On the other hand, PB may promote the mobilization of As via changing soil pH or altering the ionic exchange capacity of paddy soils due to its high alkalinity and high phosphorus content (e.g., through competitive adsorption).

To fill the above mentioned knowledge gap and test our scientific hypotheses, we aimed here to (1) quantify the impact of PB on the mobilization of As in a contaminated paddy soil under fluctuating redox conditions using a unique biogeochemical microcosm-setup, (2) examine the PB-induced changes in the speciation of As in the solid phase under reducing and oxidizing conditions, (3) determine the alterations of different parameters which govern the behavior of As, such as soil pH, Fe-Mn oxides, and the composition of DOC caused by the change in redox conditions and the addition of PB, and (4) evaluate the feasibility of using PB as an amendment for remediation of As-contaminated paddy soils in response to redox changes.

2.2 Materials and methods

2.2.1 Soil collection and properties

The soil used in this study was taken from the top 20 cm of a paddy field near a mining site in Shangyu City, Zhejiang Province, China (29°59' N, 120°46' E). The bulk soil was mixed, air-dried, ground, and passed through a 3-mm sieve after removing debris and characterized according to the procedure of Lu (2000). The soil contains 33% of sand, 46% of silt and 21% of clay. The soil was acidic with a pH of 5.8. The electrical conductivity, cation exchange capacity and organic carbon content of the soil were 0.05 dS/m, 13.4 cmol/kg and 1.3%, respectively. The total content of Fe and Mn was 32.1 and 0.9 g/kg, respectively. The total content of As in the soil was 141.3 mg/kg which exceeds the maximum allowable As content of 30 mg/kg in acidic paddy soils (pH < 6.5), as defined in the Soil Environmental Quality Risk Control Standard for *Soil Contamination of Agricultural Land* (GB15618-2018) (Ministry of Ecology and Environment of China, 2018). The sequential extraction of As geochemical fractions in the pre-incubated soils were determined according to a method described by Zeien and Brümmer (1989) and modified by Beiyuan *et al.* (2017) and El-Naggar *et al.* (2019) (Figure 2-1; *Appendix A*). The detailed design is provided in *Appendix A*.

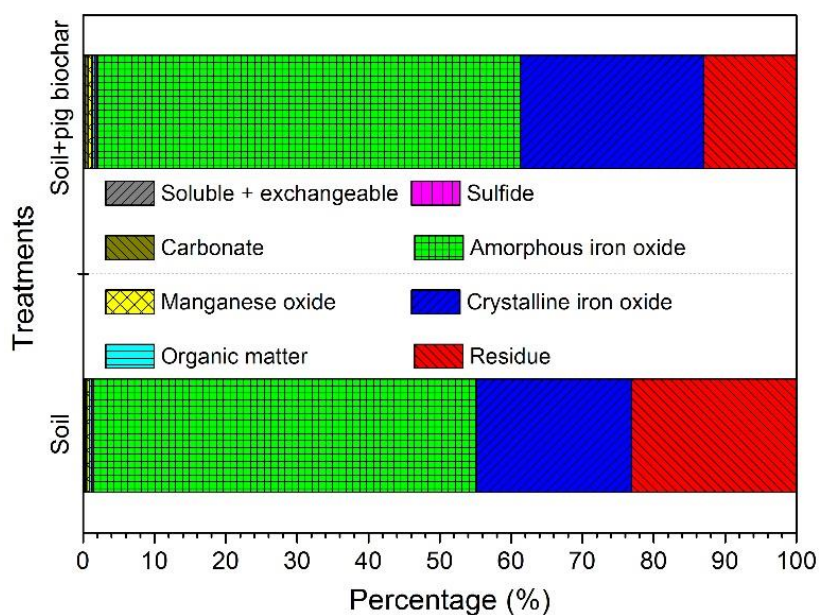


Figure 2-1 Sequential extraction of As in the control and biochar-treated soils.

2.2.2 Biochar preparation and characterization

The pig carcasses-derived biochar (pig biochar: PB) was produced via pyrolyzing dead pig bodies at a final temperature of 650°C for approximately 2 h using a batch pyrolysis facility according to the description of the local producer (Zhejiang Eco Environmental Technology Co., Ltd.). The biochar was processed by crushing and

sieving through a 2-mm sieve, and thereafter was characterized. The physicochemical analyses of PB were performed according to International Biochar Initiative (2015) protocols. The physicochemical properties of the tested PB are shown in Table 2-1. Furthermore, various spectroscopic techniques including the scanning electron microscope images (SEM), energy dispersive X-ray spectrometry (EDS), X-ray diffraction (XRD), Fourier transform infrared spectra (FTIR), X-ray photoelectron spectroscopy (XPS) and Raman spectroscopy (see details in Appendix A) were used for the surface characteristics of PB (Figure 2-2).

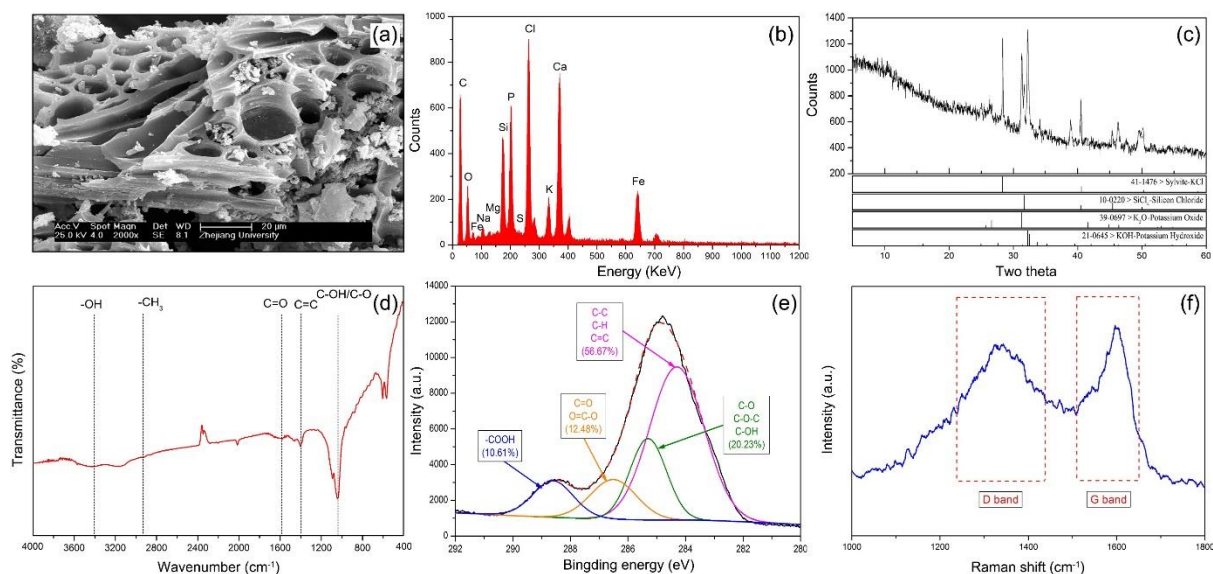


Figure 2-2 The scanning electron microscope results (SEM, a), energy dispersive X-ray spectrometry (EDS, b), X-ray diffraction (XRD, c), Fourier transform infrared spectra (FTIR, d), X-ray photoelectron spectra (XPS-C1s, e), and Raman spectra (f) of pig biochar.

2.2.3 Redox experiment using an automated biogeochemical microcosm (MC) experiment

A 30-day pre-incubation experiment was carried out to allow a proper stabilization and aging of biochar after application into the soil, more details about the pre-incubation experiment were published in our previous study (Pan *et al.*, 2021). After the pre-incubation, the incubated soils were aged for 90 days at the laboratory conditions. An advanced automated biogeochemical MC system was exploited to control the redox conditions of the non-treated (control) and PB-treated soils. The main advantages of this system are: 1) the redox conditions can be defined accurately, 2) the redox conditions can be maintained and altered automatically by flushing with either oxygen or nitrogen, and 3) the reaction condition in the microcosm is homogenized by constant stirring (Rinklebe *et al.*, 2016b; Shaheen *et al.*, 2016). All technical details of this system were described by Frohne *et al.* (2011) and Yu and Rinklebe (2011). In the current study, eight independent MCs were employed for the control and PB-treated soils. The microcosm experiment was conducted in four independent replicates using 210 g of the control

and PB-treated soils and 1680 mL of tap water at a ratio of 1 g of soils: 8 mL of tap water. Simultaneously 5 g of glucose and 10 g of rice straw were added to the control and PB-treated soils as an additional source of organic carbon for microorganisms. All materials were enclosed together in the microcosm glass vessel with an air-tight cover. The mixture was stirred continually during the microcosm experiment (574 h). A data logger coupled with a computer was used for recording the redox and pH values from each MC in every 10 min. The redox potential inside the closed systems was set from -400 to +300 mV by automatically purging with either nitrogen or oxygen (synthetic air). More details are provided in *Appendix A*.

Table 2-1 Physicochemical properties of the tested pig biochar.

Properties	Units	Values
pH (H ₂ O)	--	10.6
Electrical conductivity	(mS/cm)	2.0
Total C	(%)	30.8
Total N	(%)	2.1
Total H	(%)	1.3
Total S	(%)	0.2
Total P	(%)	8.1
Cation exchange capacity	(cmol/kg)	4.7
Surface area	(m ² /g)	18.4
Surface alkalinity	(cmol/kg)	245.7
Volatile content	(%)	17.1
Ash content	(%)	49.9
Total As	(mg/kg)	1dl

1dl: lower than detection limit.

2.2.4 Sampling and analysis

Nine soil slurry samplings from the microcosm system were conducted during the entire experiment, therein the 1st (initial) sampling was done 2 h after starting of the experiment, the 2nd to 9th samplings were done minimum 48 h after the stepwise target windows of redox values, -400, -300, -200, -100, 0, +100, +200 and +250 mV, respectively, were reached (the expected value of +300 mV could not be reached). The values of Eh and pH for the MCs were recorded every 10 min in a data logger. The Eh values were measured by a 3 M silver-silver chloride (Ag/AgCl) reference electrode (EMC 33). These values were not normalized according to the standard hydrogen electrode, aiming to present the actual redox potential in the system. The slurry samples were taken from each bottle before changing to the next redox window. The collected slurry samples were filtrated through a 0.45- μ m membrane filter after centrifuged at 5000 rpm for 15 min. Afterwards, the filtrate was divided as different sub-samples for the measurement of dissolved As, as well as other parameters such as the concentrations of dissolved

Fe, Mn, dissolved organic carbon (DOC), chloride (Cl⁻), sulfate (SO₄²⁻) and specific UV absorbance (SUVA). More details on the analytical methods and sampling preparation procedures are provided in *Appendix A*.

The species of As and Fe in the solid phase after centrifugation (collected from -300 mV, 0 mV and +250 mV conditions) were analyzed using As/Fe K-edge X-ray absorption near edge structure (XANES) spectroscopy in the National Synchrotron Radiation Research Center (NSRRC) in Taiwan, ROC. The spectra were collected in fluorescence mode, using a Soller-slits Lytle detector in an energy range of 11,667 to 12,867 eV for As, and 6,912 to 7,912 eV for Fe, respectively. Spectral analysis was conducted using Athena software (Ravel and Newville, 2005). The energy scale was calibrated using gold foil for As (calibration energy = 11,919.0 eV) and Fe foil for Fe (calibration energy = 7,712.0 eV) as standards, respectively. After normalization, principal component analysis (PCA) was subsequently performed to extract the major components in all spectra. Then, the linear combination fitting (LCF) of As XANES spectra was conducted to determine the species of As in the samples according to the method reported by Yang *et al.* (2020). The fit quality was evaluated based on the R value, and the best LCF result with smallest R value was used. The oxidation states of Fe in soils can be fairly estimated by Fe K-edge XANES (Prietzl *et al.*, 2007). However, it is difficult to quantify specific Fe species in soils using Fe K-edge XANES because of the complexity of Fe compounds caused by soil weathering and pedogenesis. Thus, FeO and Alpha-Fe₂O₃ were selected as the representative Fe(II) and Fe(III) reference minerals, respectively, to estimate the oxidation states of Fe in the soils collected from different redox conditions (Paul *et al.*, 2020).

2.2.5 Data processing and statistical analysis

The minimum, maximum and average values of Eh and pH from all the results (Eh_{all} and pH_{all}) recorded by data loggers were counted and calculated. According to Rinklebe *et al.* (2016a), the mean values of Eh and pH for 6 h (Eh_{6h} and pH_{6h}) prior to sampling were calculated for statistics. A SPSS 18.0 statistical package program (SPSS Institute, USA) was used to perform statistical analysis of the data. The correlations between Eh_{6h}, the concentration of As and other controlling parameters were analyzed based on the Pearson's correlation coefficients ($P < 0.05$). Factor analysis was run for exploring the intricate internal relationships and associations among different parameters.

2.3 Results

2.3.1 Effect of PB application on Eh and pH

The temporal course of the average values of Eh and pH in the soil suspension and sampling points are presented in Figure 2-3, and the values of the four replicates of each treatment are presented in Figure 2-4. The descriptive

analyses of the Eh and pH values are given in Table 2-2. The application of PB caused a wider redox range (Eh_{6h}: -420 to +247 mV) as compared to the control (Eh_{6h}: -386 to +248 mV; Table 2-2), indicating the importance of PB for mediating the redox conditions of soil. After flooding in the redox experiment, the pH of both control and PB-treated soils decreased rapidly in the first 50 h; then, increased gradually with the increase of Eh (Figure 2-3). The pH_{all} ranged from 4.32 to 7.64 and pH_{6h} ranged from 4.97 to 7.11 in the control. In the PB treatment, the pH_{all} ranged from 5.14 to 8.86 and pH_{6h} ranged from 5.51 to 8.10 (Table 2-2). The application of PB increased the pH values, especially under reducing conditions.

Table 2-2 Variation of As concentration and potential affecting factors in the soil solutions as well as Eh and pH in the control and soil pig biochar-treated soils.

Parameter	Unit	Soil				Soil + Pig biochar			
		n	Minimum	Maximum	Mean	n	Minimum	Maximum	Mean
Eh _{all}	mV	13,778	-464.81	293.24	-13.23	13,764	-456.84	278.37	-15.16
Eh _{6h}	mV	36	-386.36	248.03	-34.78	36	-419.88	247.49	-30.88
pH _{all}	-	13,775	4.32	7.64	5.58	13,777	5.14	8.86	6.39
pH _{6h}	-	36	4.97	7.11	5.76	36	5.51	8.10	6.45
As	µg/L	32	3.40	1756	640.92	32	9.90	1946	603.03
Fe	mg/L	32	0.05	240.06	110.09	32	0.03	211.33	77.07
Mn	mg/L	32	0.94	35.20	19.27	32	0.14	28.09	12.90
Cl ⁻	mg/L	32	64.46	128.13	98.23	32	83.94	128.52	105.78
SO ₄ ²⁻	mg/L	32	13.19	38.26	27.78	32	7.98	38.46	25.80
DOC	mg/L	32	46.55	826.43	510.97	32	52.04	837.17	431.67
SUVA	L/cm/mg	32	0.18	2.48	0.70	32	0.20	2.71	1.04

2.3.2 The concentration of dissolved As in the soil solution

At the beginning of the experiment (2 h after flooding), the concentrations of dissolved As were 22.0 and 30.9 µg/L, respectively, in the control and PB treatment (Figure 2-3; Table 2-3), whereas they dramatically increased to 502.5 and 566.8 µg/L, respectively, after 50 h of incubation. After approximately 100 h of incubation, the concentrations of dissolved As further increased to 1,535.8 and 1,742.5 µg/L, respectively. The increase of dissolved As was accompanied by the decline of Eh and pH caused by flooding. An increase of the concentration of dissolved As was noticed when the Eh increased from -400 to -300 mV. In general, the behaviors of As were basically similar in the control and PB treatment under reducing conditions. However, the application of PB had limited effect on the mobilization of As under moderately reducing conditions (Eh = -200 to 0 mV), a slight decrease was found under -200 to -100 mV, whereas a slight increase was noticed under 0 mV (Figure 2-3). In comparison to the control, application of PB decreased the concentration of dissolved As by 38.7% at Eh = +100

mV and by 35.4% at Eh = +200 mV, respectively (Table 2-3). Interestingly, the concentration of dissolved As increased by 317% under oxidizing conditions (Eh = +250 mV), compared to the control. Under highly reducing conditions (Eh = -300 mV), the concentration of dissolved As in the PB treatment increased by 13.5%, compared to the control.

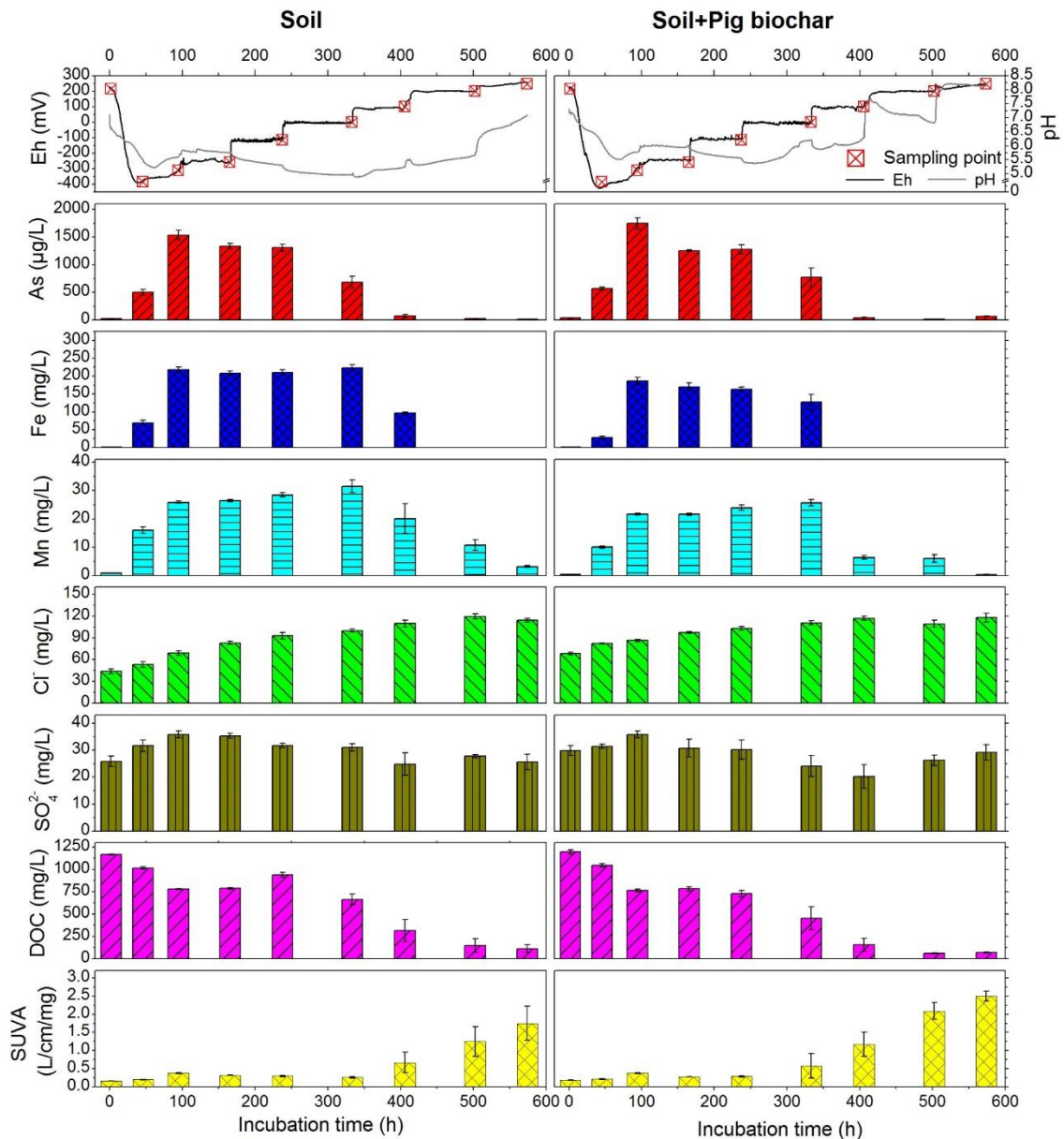


Figure 2-3 The concentrations of dissolved As, Fe, Mn, Cl⁻, SO₄²⁻, dissolved organic carbon (DOC), and specific UV absorbance (SUVA) in the control and pig biochar-treated soils under different redox conditions.

2.3.3 The concentrations of Fe, Mn, Cl⁻, SO₄²⁻, DOC and SUVA in the soil solution

Lower concentrations of dissolved Fe and Mn were observed in the PB treatment than in the control (Figure 2-3, Table 2-2). In the control, the dissolved Fe and Mn decreased sharply when the Eh increased from 0 to +100 mV

(approximately 500 h of incubation), whereas a dramatic decrease of both elements was found in the biochar treatment when the Eh increased from -100 to 0 mV (approximately 400 h of incubation), implying that the application of PB could accelerate the immobilization of Fe and Mn, particularly under moderately reducing conditions.

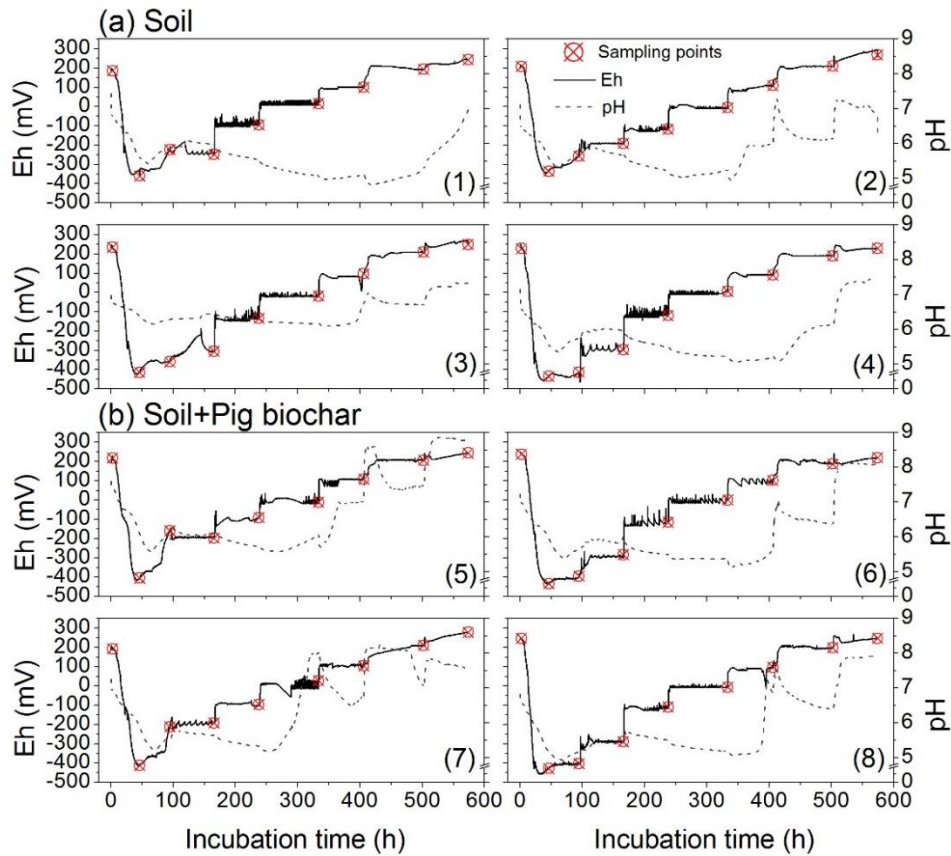


Figure 2-4 Dynamics of redox potential and pH in each microcosm with control (1~4) and pig biochar-treated soil (5~8).

Table 2-3 Impact of pig biochar on the changes (%) in the dissolved As in the treated soil as compared to the control

Targeted Eh (mV)	Concentration of dissolved As ($\mu\text{g L}^{-1}$)		Change in As (%) compared to the control
	Soil	Soil + Pig biochar	
Initial sampling	22.0	38.9	76.4
-400	502.5	566.8	12.8
-300	1,535.8	1,742.5	13.5
-200	1,332.0	1,253.3	-5.9
-100	1,307.3	1,277.3	-2.3
0	686.2	770.1	12.2
+100	71.1	43.6	-38.7
+200	21.6	13.9	-35.4
+300	16.5	68.9	317.6

The concentration of Cl^- increased with increasing Eh, whereas the concentration of SO_4^{2-} showed a large variation with the change in Eh (Figure 2-3). For both anions, similar trends were noticed in the control and PB treatment. The application of PB significantly increased the concentration of Cl^- , averagely by approximately 7.7%, but had no obvious influence on the concentration of SO_4^{2-} , which may be related to the difference in their indigenous concentrations in PB (Figure 2-2).

The highest concentration of DOC was observed in the initial samples (Figure 2-3). Thereafter, the concentrations of DOC remained relatively constant in a range from 750 to 1000 mg/L under reducing conditions (Eh = -400 ~ -100 mV). Under oxidizing conditions (Eh = 0 ~ +100 mV), the concentration of DOC decreased rapidly. An opposite trend was found for the specific ultraviolet absorbance (SUVA), which is a parameter for estimating the dissolved aromatic carbon compounds and it could act as an indicator for the composition of DOC in soil solutions (Shaheen *et al.*, 2016). The SUVA values ranged between 0.18 and 2.48 in the control and between 0.20 and 2.71 in the biochar treatment, respectively (Table 2-2). With the application of PB, the concentrations of DOC slightly decreased, whereas the values of SUVA increased, indicating that the addition of PB may change the content and compositions of organic carbon in soils.

2.3.4 The speciation of As in soil samples by XANES analysis

The LCF results for As K-edge XANES spectra of soil samples collected under highly reducing (-300 mV), moderately reducing (0 mV) and oxidizing (+250 mV) conditions (Figure 2-5; Table 2-4) showed that the best fit was obtained with three reference compounds, including As(V)-sorbed ferrihydrite (ferrihydrite-As(V)), As(III)-sorbed ferrihydrite (ferrihydrite-As(III)) and As(III)-sorbed ferric iron complexes of humic substances (Fe-humic-As(III)). These results revealed that As in soils was mainly associated with Fe minerals (e.g., ferrihydrite), which agreed with the sequential extraction results, where the As was predominantly bound to the amorphous and crystalline Fe oxides (Figure 2-1). The detection of Fe-humic-As(III) indicated the presence of As-bearing organic compounds, as LCF results could be suitable for distinguishing between Fe oxyhydroxides and Fe organic compounds (Prietzl *et al.*, 2007). Moreover, Mikutta and Kretzschmar (2011) have indicated the formation of a ternary complex between As oxyanions and Fe humic substances and clarified the feasibility of using XAS to distinguish between As-sorbed ferrihydrite and As-bound Fe-humic substances. The first derivative XANES spectra of Fe (Figure 2-6) illustrated that the predominant oxidation states of Fe in all soils were Fe(III), such as Fe(III) (hydro)oxides (e.g., ferrihydrite, goethite, hematite, lepidocrocite) and Fe(III) organic compounds (e.g., Fe(III) citrate, Fe(III) oxalate, Fe(III) humic substances). However, a discrimination among these Fe(III) (hydro)oxides and Fe(III) organic compounds is challenging, as the spectra of these minerals are similar (Prietzl

et al., 2007). Thus, the detected As-sorbed ferrihydrite and Fe-humic-As(III) could not be interpreted as the actual presence of such phases in the soils, but those with a similar configuration on soil minerals. Meanwhile, the association of As with other minerals (e.g., Al hydrous oxides, Fe sulfides) cannot be ruled out due to the detection limit of XAS for As species (Yang *et al.*, 2020). In this study, the compounds of ferrihydrite-As(V), ferrihydrite-As(III) and Fe-humic-As(III) obtained from the best fit were defined as the representative As phases.

Table 2-4 Linear combination fitting (LCF) results of As K-edge XANES spectra of soil samples collected at different redox windows.

Soil samples	Sampling conditions	As components (%)			R-factor
		Ferrihydrite-As(V)	Ferrihydrite-As(III)	Fe-humic-As(III)	
Soil	-300 mV	68.9	--	31.1	0.010
	0 mV	55.5	42.7	1.8	0.010
	+250 mV	65.3	33.0	1.7	0.013
Soil + Pig biochar	-300 mV	63.7	34.2	2.1	0.010
	0 mV	57.6	32.8	9.6	0.010
	+250 mV	70.3	29.7	--	0.013

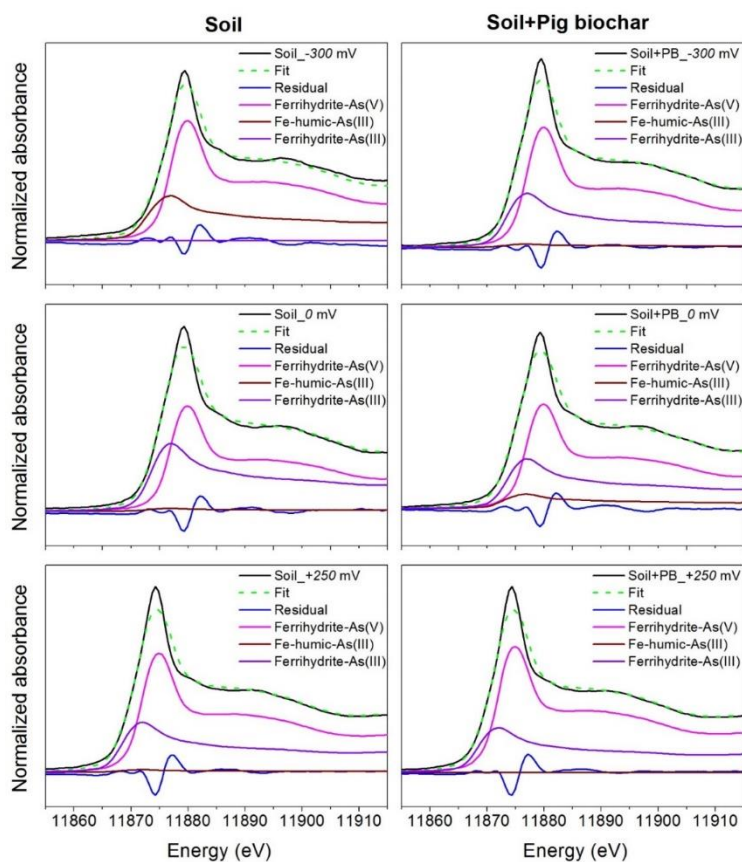


Figure 2-5 Linear combination fitting (LCF) results of As K-edge XANES spectra of soils collected from different redox conditions.

The spectra and LCF results of As K-edge XANES showed a distinct variation of As species among soils collected from different redox conditions. Under highly reducing conditions ($E_h = -300$ mV), ferrihydrite-As(V) was the predominant phase in both control and PB-treated soils, and accounted for 68.9 and 63.7%, respectively. The Fe-humic-As(III) was the secondary phase in the control (31.1%), whereas ferrihydrite-As(III) was the secondary phase in the biochar-treated soil (34.2%). In the soil samples collected from moderately reducing conditions ($E_h = 0$ mV), the relative proportion of ferrihydrite-As(V) accounted for 55.5 and 57.6%, respectively, in the control and PB treatment. Interestingly, when the E_h was changed from highly reducing to moderately reducing conditions, the relative proportion of ferrihydrite-As(III) increased to 42.7% in the control, but no noticeable change was observed in the PB treatment. Under oxidizing conditions ($E_h = +250$ mV), the relative proportion of ferrihydrite-As(V) increased, whereas the proportion of ferrihydrite-As(III) decreased in both soils, compared to the soils sampled under moderately reducing conditions ($E_h = 0$ mV).

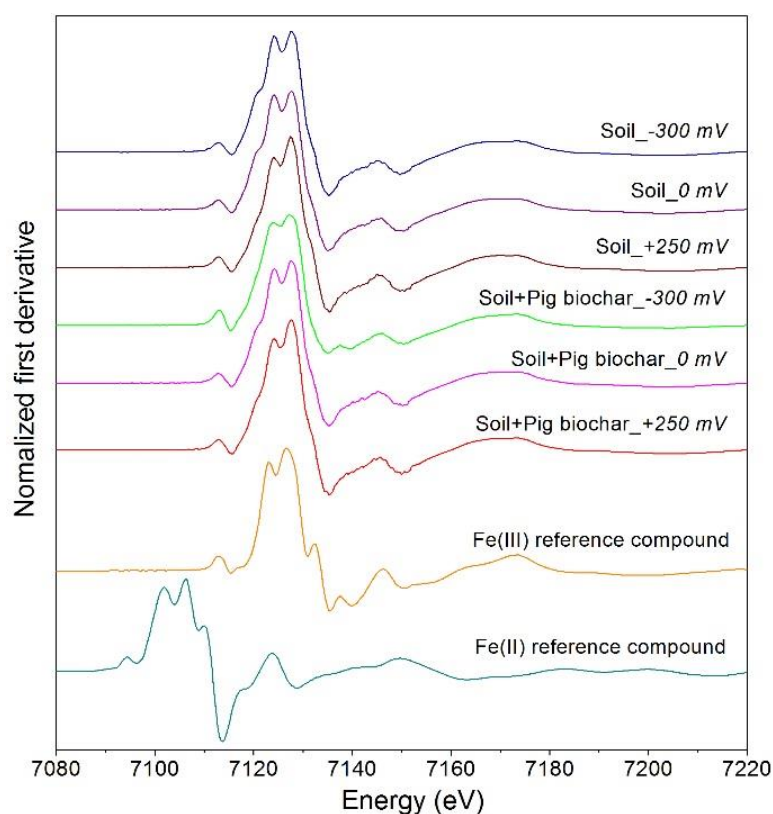


Figure 2-6 First derivative Fe K-edge XANES spectra of standard materials and soils collected from different redox conditions.

2.4 Discussion

2.4.1 Dynamics of E_h and pH

Generally, an increase of E_h in the acidic flooded soil is accompanied by a decrease of pH. Previous studies found

a negative correlation between soil pH and Eh (e.g., Frohne *et al.*, 2011; Rinklebe *et al.*, 2016b; Han *et al.*, 2019), which was mainly attributed to the consumption of protons during the reduction processes. Conversely, in our study, a positive correlation was obtained between the Eh_{6h} and pH_{6h} in the control and PB-treated soils (Table 2-5). Many factors including microbial activity, soil buffer capacity, and organic matter decomposition could affect the soil pH (Frohne *et al.*, 2015; Shaheen *et al.*, 2014). Therefore, we assume that some of these factors might have been changed in our experiment. For example, the decrease of Eh after flooding was accompanied by a sharply decrease of pH, which was due to the production of organic acids and the generation of carbon dioxide as the decomposition of natural organic matter (Reddy and Delaune, 2008; Shaheen *et al.*, 2014). The exogenous DOC from the addition of glucose and decomposition of straw may also contribute to the decrease of pH (Shaheen *et al.*, 2016). Additionally, the application of PB might change the dynamics of pH and Eh through altering the soil buffer capacity and organic compounds (Li *et al.*, 2018; El-Naggar *et al.*, 2019). Based on previous studies and our data, we proposed three possible mechanisms for the Eh and pH relationship as affected by biochar application: 1) PB might increase the amount of aromatic carbon and macromolecular substances due to its high aromaticity (Figure 2-2); 2) PB might enhance the reproduction and growth of microorganisms in soil by providing habitat and nutrients because of its highly porous structure and abundant mineral elements (Figure 2-2), thereby changing the pH buffer capacity of soil; (3) PB contained relatively high ash substances inorganic minerals (Figure 2-2, Table 2-1), thus it would consequently increase the electrical conductivity and pH of soil.

2.4.2 Alterations of Eh-dependent controlling factors

2.4.2.1 Impact on Fe and Mn

High concentrations of dissolved Fe and Mn were found under reducing conditions (Eh < 0 mV), and the concentrations decreased with increasing Eh (Figure 2-3). The concentrations of dissolved Fe and Mn were significantly ($P < 0.01$) negatively correlated with both Eh_{6h} and pH_{6h} (Table 2-5). The higher concentration of dissolved Fe and Mn under reducing conditions than under oxidizing conditions could be explained by the reduction of Fe³⁺ and Mn⁴⁺ to Fe²⁺ and Mn²⁺ through biotic (reducing bacteria) and/or abiotic pathways (Shaheen *et al.*, 2014; Rinklebe *et al.*, 2016b, 2020). Interestingly, the concentrations of dissolved Fe and Mn were lower at the 2nd sampling with Eh value of -400 mV than at the 3rd sampling with higher Eh value (around -300 mV). According to Frohne *et al.* (2015), the reduction of Fe-Mn (hydro)oxides was a microbial-catalyzed process, in which anaerobic microorganisms took time for reproduction. Hence, insufficient incubation time period of soil may lead to a poorly anaerobic environment. We postulate that the reaction time until the 2nd sampling (50 h) was insufficient to transfer all reducible Fe and Mn minerals to dissolved form.

Table 2-5 Pearson's correlations between As and controlling factors including Eh, Fe, Mn, dissolved organic carbon (DOC), specific UV absorbance (SUVA), Cl⁻ and SO₄²⁻ in the control and pig biochar-treated soils (n=32).

	Treatments	Eh _{6h}	pH _{6h}	As	Fe	Mn	Cl ⁻	SO ₄ ²⁻	DOC
pH _{6h}	Soil	ns							
	Soil+Pig biochar	0.642**							
As	Soil	-0.925**	ns						
	Soil+Pig biochar	-0.882**	-0.623**						
Fe	Soil	-0.858**	-0.463*	0.946**					
	Soil+Pig biochar	-0.910**	-0.694**	0.926**					
Mn	Soil	-0.626**	-0.707**	0.674**	0.823**				
	Soil+Pig biochar	-0.767**	-0.872**	0.770**	0.863**				
Cl ⁻	Soil	0.898**	ns	-0.845**	-0.788**	-0.527**			
	Soil+Pig biochar	0.792**	0.519**	-0.785**	-0.707**	-0.510**			
SO ₄ ²⁻	Soil	-0.583**	ns	0.588**	0.531**	ns	-0.578**		
	Soil+Pig biochar	ns	ns	0.540**	ns	ns	ns		
DOC	Soil	-0.856**	-0.475*	0.909**	0.967**	0.884**	-0.790**	0.533**	
	Soil+Pig biochar	-0.906**	-0.736**	0.901**	0.979**	0.913**	-0.683**	ns	
SUVA	Soil	0.629**	0.610**	-0.605**	-0.712**	-0.905**	0.528**	ns	-0.823**
	Soil+Pig biochar	0.816**	0.874**	-0.743**	-0.832**	-0.963**	0.565**	ns	-0.894**

** : correlation is significant at the 0.01 level.

* : correlation is significant at the 0.05 level.

ns: no significance.

With increasing Eh, the dissolved Fe and Mn could be immobilized through the formation of relatively stable (hydro)oxides (Shaheen *et al.*, 2016). Thus, a dramatic decrease of both elements was noticed at Eh = +200 and +100 mV for the control and PB treatment, respectively, indicating that the application of PB accelerated the oxidation of Fe²⁺ and Mn²⁺ in soils, even at moderately reducing conditions. This phenomenon was attributed to the dominant free cations (e.g., Fe³⁺ and Mn⁴⁺) in the soil solution could be bound by ligands via precipitation and complexation reactions (Kim *et al.*, 2018) with the increased ambient pH (up to 8.5) resulting from the application of PB (Figure 2-3).

2.4.2.2 Impact on SO₄²⁻ and Cl⁻

Microbial sulfate reduction is a crucial transformation that normally occurs under reducing conditions (Muyzer and Stams, 2008). Theoretically, reduction of sulfate starts at a reducing conditions with Eh values lower than -150 mV (Zhu *et al.*, 2018), thereby resulting in the precipitation of sulfate as metal sulfides. However, in our study, the concentration of SO₄²⁻ was higher under reducing conditions (Eh= -400 ~ -200 mV), especially in the control

(Figure 2-3). These results were in line with Rinklebe *et al.* (2016a), who indicated that the geochemical behavior of SO_4^{2-} was influenced by the pH of soil and the content of organic carbon. Therefore, the high concentration of SO_4^{2-} might be associated with the exogenous S-containing carbon source. The other reason could be the competition between different microbial metabolic pathways, since the microbial reduction of Fe oxides was more preferential than SO_4^{2-} reduction process (Zhu *et al.*, 2018). In this case, we assume that the electron shuttling to the SO_4^{2-} reduction might not be conducive as the reduction of Fe is relatively more active under the electron-limited conditions (Zhu *et al.*, 2018).

In the current study, higher concentrations of SO_4^{2-} under oxidizing conditions were observed in the PB treatment than in the control. In contrast, lower SO_4^{2-} concentrations were noticed in the PB treatment than in the control under reducing conditions (Figure 2-3). Zhao *et al.* (2017) conducted a SO_4^{2-} sorption experiment using rape straw biochar, loess soil and soil-biochar mixture, they found that biochar could efficiently adsorb SO_4^{2-} via electrostatic interactions and formation of stable precipitates (e.g., CaSO_4). We assume that the application of PB promoted the reduction of SO_4^{2-} to sulfide (S^{2-}) and subsequent precipitation as metal sulfide, thereby causing a sharp decrease of SO_4^{2-} under moderately reducing conditions ($E_h = -200 \sim 0$ mV) (Figure 2-3). Moreover, the previously generated S^{2-} would be oxidized to SO_4^{2-} again to be released. Consequently, we speculate that the application of PB altered the dynamics of sulfur reduction/oxidation reactions in soil. Significant ($P < 0.01$) positive correlations were found between the concentration of Cl^- and $E_{h\ 6h}$ in the control and PB-treated soils. However, no significant correlation was found between the concentration of Cl^- and pH_{6h} (Table 2-5). The application of PB slightly facilitated the release of Cl^- to the soil solution (Figure 2-3), which could be attributed to the relatively high content of Cl as proved by the EDS spectrum (Figure 2-2).

2.4.2.3 Impact on DOC and SUVA

In our study, a negative correlation ($P < 0.01$) was observed between DOC and $E_{h\ 6h}$ (Table 2-5), indicating the degradation of organic carbon with the increase of E_h . Under reducing conditions, the decomposition and hydrolysis of organic matter could cause enrichment of water-soluble intermediate metabolites, thereby increasing the concentration of DOC (Hanke *et al.*, 2013). The absence of Fe and Mn oxide sorption sites and decreased microbial activity could also cause an increase of in DOC concentration under reducing conditions (Karczewska *et al.*, 2018). Under oxidizing conditions, the elevated oxygen availability in water-soil system could result in a faster mineralization of DOC by enhancing the microbial activities (Hanke *et al.*, 2013), thus decreasing the concentration of DOC.

The application of PB resulted in a slight decrease in DOC irrespective of reducing or oxidizing conditions (Figure

2-3). It has been proved that biochar was a potential source of DOC (Kim *et al.*, 2018). However, the release amount was often negligible relative to the total carbon content in biochar (Eykelbosh *et al.*, 2015). In this study, even the total content of carbon was relatively low in the used PB (Table 2-1). Therefore, the release of DOC from PB could be negligible. Moreover, biochar could promote carbon sequestration via stabilizing DOC in soils (Eykelbosh *et al.*, 2015). It was confirmed that biochar with more C-H and C=O functional groups has stronger sorption capacity for small molecular organic compounds (Vithanage *et al.*, 2017). Consequently, we assume that the application of PB could increase the adsorption of organic ligands due to its porous structure and surface functional groups (Figure 2-2).

The SUVA values elevated with the increase of Eh, and positive correlations ($P < 0.01$) between Eh_{6h} and SUVA were noticed in both soils (Table 2-5). The smaller SUVA values imply the lower aromaticity levels of the organic carbon in soils (Li *et al.*, 2018). The results indicated that the proportion of aromatic DOC such as humic acids and organic carbon with high molecular weight was higher at oxidizing conditions than that at reducing conditions (Shaheen *et al.*, 2014). These results could be interpreted by the partial mineralization of DOC, as well as the selective preservation of the more aromatic and litter-derived molecules under oxidizing conditions (Karczewska *et al.*, 2018). The decrease of aromatic organic molecules under acidic conditions was mainly due to the adsorption of negatively charged organic molecules and formation of complexes (Shaheen *et al.*, 2014; El-Naggar *et al.*, 2018).

The SUVA values increased in the PB-treated soil when compared to the control, especially under oxidizing conditions (Figure 2-3). SUVA indicated various chemical compositions of DOC in soils under different redox conditions, the DOC under reducing conditions could be characterized as low molecular weight compounds, whereas the DOC under oxidizing conditions may be related to the higher molecular weight compounds (Shaheen *et al.*, 2014). Therefore, the application of PB might increase the higher molecular weight organic molecules such as humic-like substances and aromatic compounds under oxidizing conditions.

2.4.3 As mobilization

The higher concentrations of dissolved As were found under reducing conditions than oxidizing conditions (Figures 2-3 and 2-7). Therefore, the correlation between Eh_{6h} and the concentration of dissolved As in the control and the PB treatment was significantly ($P < 0.01$) negative (Table 2-5). The less mobile As(V) might be reduced to more mobile As(III) under reducing conditions as also reported by Rinklebe *et al.* (2016b). According to Yuan *et al.* (2017), we speculate that PB could either serve as catalyst shuttling electrons for the reduction of As(V), or be reduced as an electron donor to increase the solubility of As under reducing conditions.

Generally, the increase of pH caused by the change in Eh could be recognized as a possible mechanism leading to the increase of As solubility under reducing conditions (Karczewska *et al.*, 2018; Han *et al.*, 2019). In our study, however, the pH for both soils was relatively low (< 5.5) under reducing conditions (Figure 2-3), indicating that pH may play a subordinate role in affecting the concentration of dissolved As under these circumstances. Thus, the other factors, such as the reductive dissolution of Fe-Mn oxides, decomposition of DOC might play more important roles than pH in As mobilization under acidic reducing conditions (as discussed below).

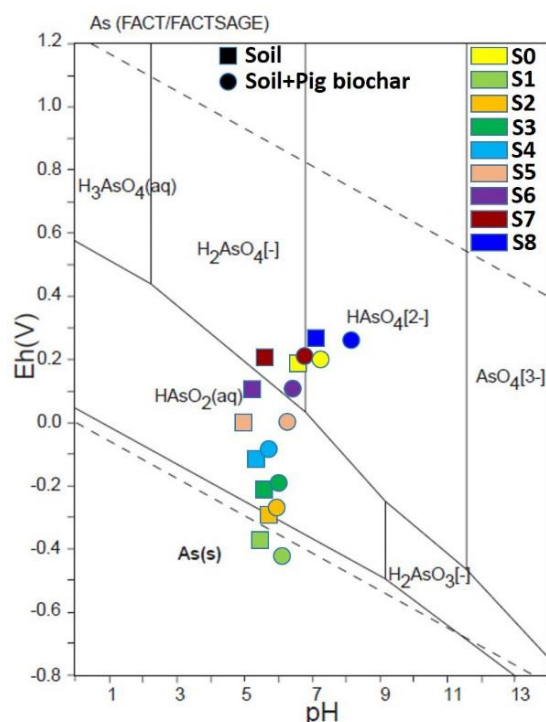


Figure 2-7 Distribution of sampling points on the As-Eh-pH diagram (Takeno, 2005). (Legends from S0 to S8 indicate the initial to the eighth samplings)

Under oxidizing conditions (+250 mV), the concentration of dissolved As in the PB treatment was higher than that in the control. This could be attributed to the higher pH caused by the addition of PB, leading to the release of As. Niazi *et al.* (2018) reported that the change in ambient pH could change the protonation of functional groups on biochar, thereby changing the chemistry of As. Van Vinh *et al.* (2014) indicated that the surface of biochar could be negatively charged under relatively alkaline conditions. Therefore, the increase in the concentration of dissolved As may be attributed to ‘anion exclusion’ resulting from the electrostatic repulsive force between negatively charged PB and the dominating negative As species, including $H_2AsO_4^-$, $HAsO_4^{2-}$ and AsO_4^{3-} (Beiyuan *et al.*, 2017; Frick *et al.*, 2019; Wen *et al.*, 2021). Additionally, we speculate that the application of this P-rich biochar (total P=8.1%; Table 2-1) may increase the soluble phosphate (PO_4^{3-}), which would compete with As

anions for the binding sites on soil (Pan *et al.*, 2021).

Significant ($P < 0.01$) positive correlations were found between As, and Fe and Mn concentrations in soil solutions (Table 2-5), implying that As was possibly released from Fe-Mn oxides, which have been assumed as the important binding substrates for As in oxidizing conditions (Rinklebe *et al.*, 2016b; Kim *et al.*, 2018). Nevertheless, in the paddy soil used in this study, negligible amount of Mn oxide-bound As was detected according to the fractionation analysis (Figure 2-1). Hence, the higher concentration of dissolved As in the PB-treated soil than the control under strongly reducing conditions ($E_h = -300$ mV) could be predominantly due to the reductive dissolution of Fe (hydro)oxides, rather than Mn (hydro)oxides (Shaheen *et al.*, 2014, 2016; Kim *et al.*, 2018). Based on the results from As K-edge XANES analysis (Figure 2-5, Table 2-4), the predominant phases of As in all collected solid samples were As(V)-sorbed Fe (hydro)oxides (e.g., ferrihydrite), and As-bound Fe organic compounds (e.g., Fe-humic-As(III)). Earlier studies proved that the rapid release of As from soil after flooding was owing to the dissolution of adsorbing phases such as Fe oxides and hydroxides (e.g., Aeppli *et al.*, 2019; Shi *et al.*, 2020). Under reducing conditions, consequently, the slightly higher concentration of dissolved As in the PB treatment than in the control could be attributed to the indirect effect of biochar by promoting the reduction of Fe. There might be two mechanisms: 1) the functional groups such as $-OH$, $-COOH$ and $C=O$ associated with the biochar (Figure 2-2) could act as electron-donors to facilitate the reduction reactions of Fe oxides (Kim *et al.*, 2018); 2) the application of biochar could promote the microbial reduction of As-bound Fe minerals (Yuan *et al.*, 2017). These mechanisms could be supported by the LCF results of the XANES spectra for soil samples (Figure 2-5; Table 2-4), where relatively low proportion of Fe-humic-As(III) was determined in the PB treatment irrespective of redox conditions as compared to the control. The LCF results also indicated that the As(III)-associated ferrihydrite might be the main source of the released As under reducing conditions, and this could explain the relatively high percentage of As(V)-sorbed ferrihydrite under oxidizing conditions, where the As(V) could be immobilized by ferrihydrite via oxidative precipitation.

Additionally, significant correlations ($P < 0.01$) between the concentrations of As, DOC and SUVA suggested that the mobilization of As was positively affected by the dissolved aliphatic carbon compounds, but negatively affected by the dissolved aromatic carbon compounds (Table 2-5). Guo *et al.* (2019) reported that the redox-active DOC could increase the release of As via desorption of As-sorbed organic matter and/or the microbially triggered reductive dissolution of As-bearing oxides under reducing conditions. However, in this study, the organic matter-induced pathway Guo *et al.* (2019) mentioned probably has not occurred, because of the low amount of organic-bound As in the pre-incubated soils (Figure 2-1). Moreover, the positive correlations ($P < 0.01$) between As, Fe,

and DOC could be explained by the formation of dissolved organo-Fe-As complexes and/or colloidal organo-Fe-As phase (Rinklebe *et al.*, 2016b), which could be linked to the transformation of As-sorbed ferrihydrite as discussed in the previous section. The factor analysis showed that As was associated in one cluster together with Fe, Mn, and DOC in both control and PB treatments (Figure 2-8), which was also a support for the affinities between As and Fe, Mn and DOC. Shaheen *et al.* (2016) reported that the complexation between aromatic DOC and As could also be an important mechanism in immobilization of As in soils. This could be employed to explain the negative correlation ($P < 0.01$) between SUVA and As in our study (Table 2-5). Li *et al.* (2018) indicated that biochar could modify soil DOC through releasing easily mineralizable carbon to soil, which may change the mobility, speciation and bioavailability of As, via altering soil redox conditions and simulating microbial activities. However, in our study, the effect of PB on As mobilization via increasing the concentration of DOC seemed to be subordinate, as a decrease of DOC concentration was found after PB application (Figure 2-3). This result could be supported by the As LCF results (Figure 2-5; Table 2-4), as under reducing conditions, higher relative percentage of the Fe-humic-As(III) was detected in the control soil as compared to that in the PB-treated soil. Furthermore, the co-existence of anions could also affect the mobilization of As from soil by competing with As(V) or As(III) for the available adsorption sites or altering the electrostatic charge on soil minerals (Sik *et al.*, 2017). For instance, SO_4^{2-} has been considered as an effective competitor of As oxyanions adsorption by Fe (hydro)oxides (Fu *et al.*, 2017). Under oxidizing conditions ($E_h = +250$ mV), the higher concentration of As after PB application might be due to the increase of SO_4^{2-} concentration. As shown in the factor analysis (Figure 2-8), the difference between the control and PB treatment was the grouping of SO_4^{2-} , implying that the application of PB might have changed the biogeochemical behavior of SO_4^{2-} .

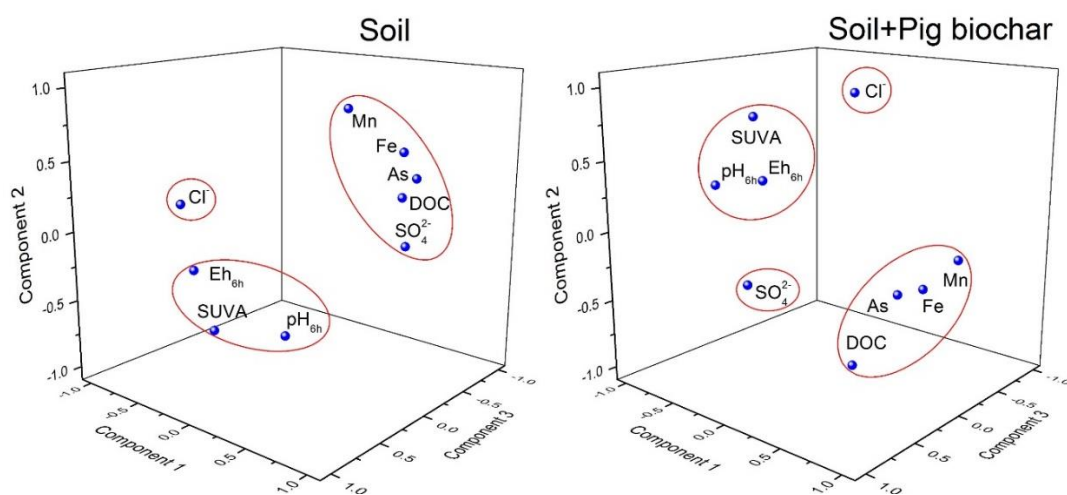


Figure 2-8 Factor analysis of the control and pig biochar-treated soils.

2.5 Conclusions

We conclude that the addition of pig carcass-derived biochar to paddy soils may cause a decrease in As mobilization and reduce the risk of As pollution in these soils under moderately reducing conditions (e.g., soils with Eh of +100 and +200 mV). However, this biochar material is not a good candidate for mitigating the bioavailability and toxicity of As in contaminated soils under highly reducing conditions (e.g., continuously flooded soils with Eh lower than -300 mV) and oxidizing conditions (e.g., upland or dry land soils with Eh higher than +300 mV). Future studies should elucidate the interactions between As and pig carcass-derived biochar-treated paddy soils by refining redox gradients. Also, As speciation in solution as well as microbial analysis should be conducted to further elucidate the role of As methylation genes in soils. In addition, future studies are also needed to verify the effect of different water management regimes on the mobilization and phytoavailability of As in pig biochar-treated paddy soils under field conditions.

2.6 Acknowledgements

This work was financially supported by the National Natural Science Foundation of China (Grant No. 21876027), and the Special Fund for the Science and Technology Innovation Team of Foshan, China (Grant No.1920001000083). Authors are also grateful to the National Synchrotron Radiation Research Center, Hsinchu 30076, Taiwan (NSRRC) and in particular Dr. Soo, Yun-Liang (TLS 07A1) and Dr. Lee, Jyh-Fu (TLS 17C1). We thank Claus Vandenhirtz and Kail Matuszak and the entire the team of the Laboratory of Soil- and Groundwater-Management, University of Wuppertal, Germany, for technical assistance.

2.7 References

- Aeppli, M., Vranic, S., Kaegi, R., Kretzschmar, R., Brown, A. R., Voegelin, A., Hofstetter, T. B., Sander, M., 2019. Decreases in iron oxide reducibility during microbial reductive dissolution and transformation of ferrihydrite. *Environ. Sci. Technol.* 53 (15), 8736-8746. <https://doi.org/10.1021/acs.est.9b01299>
- Antoniadis, V., Shaheen, S. M., Boersch, J., Frohne, T., Du Liang, G., Rinklebe, J., 2017. Bioavailability and risk assessment of potentially toxic elements in garden edible vegetables and soils around a highly contaminated former mining area in Germany. *J. Environ. Manage.* 186, 192-200. <https://doi.org/10.1016/j.jenvman.2016.04.036>
- Antoniadis, V., Shaheen, S. M., Levizou, E., Shahid, M., Niazi, N. K., Vithanage, M., Ok, Y. S., Bolan, N., Rinklebe, J., 2019. A critical prospective analysis of the potential toxicity of trace element regulation limits in soils worldwide: Are they protective concerning health risk assessment? - A review. *Environ. Int.* 127, 819-847. <https://doi.org/10.1016/j.envint.2019.03.039>
- Bandara, T., Franks, A., Xu, J., Bolan, N., Wang, H., Tang, C., 2020. Chemical and biological immobilization mechanisms of potentially toxic elements in biochar-amended soils. *Crit. Rev. Environ. Sci. Technol.* 50, 903-978. <https://doi.org/10.1080/10643389.2019.1642832>
- Beiyuan, J., Awad, Y. M., Beckers, F., Tsang, D. C. W., Ok, Y. S., & Rinklebe, J., 2017. Mobility and

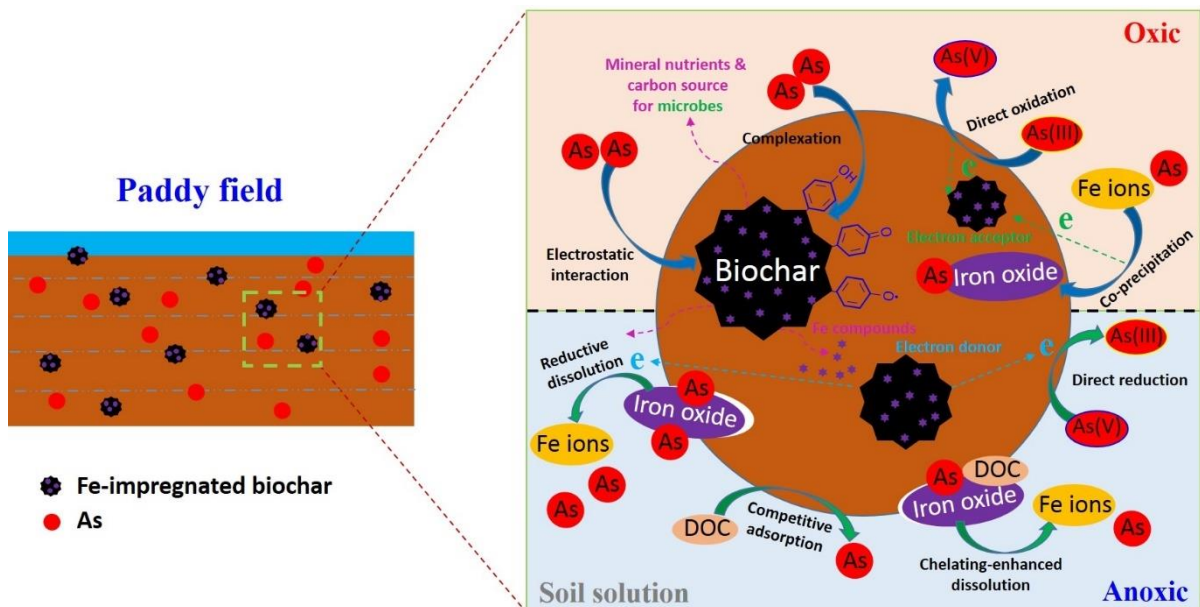
- phytoavailability of As and Pb in a contaminated soil using pine sawdust biochar under systematic change of redox conditions. *Chemosphere* 178, 110-118. <https://doi.org/10.1016/j.chemosphere.2017.03.022>
- Chen, H., Yang, X., Gielen, G., Mandal, S., Xu, S., Guo, J., Shaheen, S. M., Rinklebe, J., Che, L., Wang, H., 2019. Effect of biochars on the bioavailability of cadmium and di-(2-ethylhexyl) phthalate to *Brassica chinensis* L. in contaminated soils. *Sci. Total Environ.* 678, 43-52. <https://doi.org/10.1016/j.scitotenv.2019.04.417>
- Chen, H., Yang, X., Wang, H., Sarkar, B., Shaheen, S. M., Gielen, G., Bolan, N., Guo, J., Che, L., Sun, H., Rinklebe, J., 2020. Animal carcass- and wood-derived biochars improved nutrient bioavailability, enzyme activity, and plant growth in metal-phthalic acid ester co-contaminated soils: A trial for reclamation and improvement of degraded soils. *J. Environ. Manage.* 261, 110246. <https://doi.org/10.1016/j.jenvman.2020.110246>
- El-Naggar, A., Shaheen, S. M., Hseu, Z. Y., Wang, S. L., Ok, Y. S., Rinklebe, J., 2019. Release dynamics of As, Co, and Mo in a biochar treated soil under pre-definite redox conditions. *Sci. Total Environ.* 657, 686-695. <https://doi.org/10.1016/j.scitotenv.2018.12.026>
- El-Naggar, A., Shaheen, S. M., Ok, Y. S., Rinklebe, J., 2018. Biochar affects the dissolved and colloidal concentrations of Cd, Cu, Ni, and Zn and their phytoavailability and potential mobility in a mining soil under dynamic redox-conditions. *Sci. Total Environ.* 624, 1059-1071. <https://doi.org/10.1016/j.scitotenv.2017.12.190>
- Eykelbosh, A.J., Johnson, M. S., Couto, E. G., 2015. Biochar decreases dissolved organic carbon but not nitrate leaching in relation to vinasse application in a Brazilian sugarcane soil. *J. Environ. Manage.* 149, 9-16. <https://doi.org/10.1016/j.jenvman.2014.09.033>
- Feng, Y., Yang, X., Singh, B. P., Mandal, S., Guo, J., Che, L., Wang, H., 2020. Effects of contrasting biochars on the leaching of inorganic nitrogen from soil. *J. Soil. Sediment.* 20, 3017-3026. <https://doi.org/10.1007/s11368-019-02369-5>
- Frick, H., Tardif, S., Kandeler, E., Holm, P. E., Brandt, K. K., 2019. Assessment of biochar and zero-valent iron for in-situ remediation of chromated copper arsenate contaminated soil. *Sci. Total Environ.* 2019, 655, 414-422. <https://doi.org/10.1016/j.scitotenv.2018.11.193>
- Frohne, T., Diaz-Bone, R. A., Du Laing, G., Rinklebe, J., 2015. Impact of systematic change of redox potential on the leaching of Ba, Cr, Sr, and V from a riverine soil into water. *J. Soil. Sediment.* 15, 623-633. <https://doi.org/10.1007/s11368-014-1036-8>
- Frohne, T., Rinklebe, J., Diaz-Bone, R., Du Laing, G., 2011. Controlled variation of redox conditions in a floodplain soil: impact on metal mobilization and biomethylation of arsenic and antimony. *Geoderma* 160, 414-424. <https://doi.org/10.1016/j.geoderma.2010.10.012>
- Fu, D., He, Z., Su, S., Xu, B., Liu, Y., Zhao, Y., 2017. Fabrication of alpha-FeOOH decorated graphene oxide-carbon nanotubes aerogel and its application in adsorption of arsenic species. *J. Colloid. Interface Sci.* 505, 105-114. <https://doi.org/10.1016/j.jcis.2017.05.091>
- Guo, H., Li, X., Xiu, W., He, W., Cao, Y., Zhang, D., Wang, A., 2019. Controls of organic matter bioreactivity on arsenic mobility in shallow aquifers of the Hetao Basin, P.R. China. *J. Hydrol.* 571, 448-459. <https://doi.org/10.1016/j.jhydrol.2019.01.076>
- Han, Y. S., Park, J. H., Kim, S. J., Jeong, H. Y., Ahn, J. S., 2019. Redox transformation of soil minerals and arsenic in arsenic-contaminated soil under cycling redox conditions. *J. Hazard. Mater.* 378, 120745. <https://doi.org/10.1016/j.jhazmat.2019.120745>
- Hanke, A., Cerli, C., Muhr, J., Borken, W., Kalbitz, K., 2013. Redox control on carbon mineralization and dissolved organic matter along a chronosequence of paddy soils. *Eur. J. Soil Sci.* 64, 476-487. <https://doi.org/10.1111/ejss.12042>
- International Biochar Initiative, 2015. Standardized product definition and product testing guidelines for biochar

- that is used in soil. https://www.biochar-international.org/wp-content/uploads/2018/04/IBI_Biochar_Standards_V2.1_Final.pdf
- Karczewska, A., Lewińska, K., Siepak, M., Gałka, B., Dradrach, A., Szopka, K., 2018. Transformation of beech forest litter as a factor that triggers arsenic solubility in soils developed on historical mine dumps. *J. Soil. Sediment.* 18, 2749-2758. <https://doi.org/10.1007/s11368-018-2031-2>
- Khan, S., Chao, C., Waqas, M., Arp, H. P., Zhu, Y. G., 2013. Sewage sludge biochar influence upon rice (*Oryza sativa* L) yield, metal bioaccumulation and greenhouse gas emissions from acidic paddy soil. *Environ. Sci. Technol.* 47, 8624-8632. <https://doi.org/10.1021/es400554x>
- Kim, H. B., Kim, S. H., Jeon, E. K., Kim, D. H., Tsang, D. C. W., Alessi, D. S., Kwon, E. E., Baek, K., 2018. Effect of dissolved organic carbon from sludge, Rice straw and spent coffee ground biochar on the mobility of arsenic in soil. *Sci. Total Environ.* 636, 1241-1248. <https://doi.org/10.1016/j.scitotenv.2018.04.406>
- Li, G., Khan, S., Ibrahim, M., Sun, T. R., Tang, J. F., Cotner, J. B., Xu, Y. Y., 2018. Biochars induced modification of dissolved organic matter (DOM) in soil and its impact on mobility and bioaccumulation of arsenic and cadmium. *J. Hazard. Mater.* 348, 100. <https://doi.org/10.1016/j.jhazmat.2018.01.031>
- Lu, R., 2000. *Analytical Methods for Soil Agrochemistry*, Chinese Agricultural Science and Technology Publishing House, Beijing.
- Mikutta, C., Kretzschmar, R., 2011. Spectroscopic evidence for ternary complex formation between arsenate and ferric Iron complexes of humic substances. *Environ. Sci. Technol.* 45, 9550-9557. <https://doi.org/10.1021/es202300w>
- Ministry of Ecology and Environment of the People's Republic of China (MEEC), 2018. Soil environmental quality Risk control standard for soil contamination of agricultural land (GB 15618-2018).
- Muyzer, G., Stams, A. J., 2008. The ecology and biotechnology of sulphate-reducing bacteria. *Nat. Rev. Microbiol.* 6, 441-454. <https://doi.org/10.1038/nrmicro1892>
- Niazi, N. K., Bibi, I., Shahid, M., Ok, Y. S., Shaheen, S. M., Rinklebe, J., Wang, H., Murtaza, B., Islam, E., Nawaz, M. F., Luttge, A., 2018. Arsenic removal by Japanese oak wood biochar in aqueous solutions and well water: Investigating arsenic fate using integrated spectroscopic and microscopic techniques. *Sci. Total Environ.* 621, 1642-1651. <https://doi.org/10.1016/j.scitotenv.2017.10.063>
- Nie, C. R., Yang, X., Niazi, N. K., Xu, X., Wen, Y. H., Rinklebe, J., Ok, Y. S., Xu, S., Wang, H., 2018. Impact of sugarcane bagasse-derived biochar on heavy metal availability and microbial activity: A field study. *Chemosphere* 200, 274-282. <https://doi.org/10.1016/j.chemosphere.2018.02.134>
- Nie, T., Yang, X., Chen, H., Müller K., Shaheen, S. M., Rinklebe, J., Song, H., Xu, S., Wu, F., Wang, H., 2021. Effect of biochar aging and co-existence of diethyl phthalate on the mono-sorption of cadmium and zinc to biochar-treated soils. *J. Hazard. Mater.* 408, 124850. <https://doi.org/10.1016/j.jhazmat.2020.124850>
- Palansooriya, K. N., Shaheen, S. M., Chen, S. S., Tsang D. C. W., Hashimoto, Y., Hou, D., Bolan, N. S., Rinklebe, J., Ok, Y. S., 2020. Soil amendments for immobilization of potentially toxic elements in contaminated soils: A critical review. *Environ. Int.* 134, 105046. <https://doi.org/10.1016/j.envint.2019.105046>
- Pan, H., Yang, X., Chen, H., Sarkar, B., Bolan, N., Shaheen, S. M., Wu, F., Che, L., Ma, Y., Rinklebe, J., Wang, H., 2021. Pristine and iron-engineered animal- and plant-derived biochars enhanced bacterial abundance and immobilized arsenic and lead in a contaminated soil. *Sci. Total Environ.* 763, 144218. <https://doi.org/10.1016/j.scitotenv.2020.144218>
- Paul, R., Sarkar, C., Yan, Y., Trinh, Q. T., Rao, B. S., Pao, C. W., Lee, J. F., Liu, W., Mondal, J., 2020. Porous-Organic-Polymer-Triggered Advancement of Sustainable Magnetic Efficient Catalyst for Chemoselective Hydrogenation of Cinnamaldehyde. *ChemCatChem* 12, 3687-3704. <https://doi.org/10.1002/cctc.202000072>
- Prietzl, J., Thieme, J., Eusterhues, K., Eichert, D., 2007. Iron speciation in soils and soil aggregates by

- synchrotron-based X-ray microspectroscopy (XANES, μ -XANES). *Eur. J. Soil Sci.* 58, 1027-1041. <https://doi.org/10.1111/j.1365-2389.2006.00882.x>
- Ravel, B., Newville, M., 2005. ATHENA, ARTEMIS, HEPHAESTUS: data analysis for X-ray absorption spectroscopy using IFEFFIT. *J. Synchrotron Radiat.* 12, 537-541. <https://doi.org/10.1107/S0909049505012719>
- Reddy, R., Delaune, R.D., 2008. *Biogeochemistry of Wetlands: Science and Applications*, CRC Press: Boca Raton, FL.
- Rinklebe, J., Antoniadis, V., Shaheen, S. M., Rosche, O., Altermann, M., 2019. Health risk assessment of potentially toxic elements in soils along the Central Elbe River, Germany. *Environ. Int.* 126, 76-88. <https://doi.org/10.1016/j.envint.2019.02.011>
- Rinklebe, J., Shaheen, S. M., El-Naggar, A., Wang, H., Du Laing, G., Alessi, D. S., Ok, Y. S., 2020. Redox-induced mobilization of Ag, Sb, Sn, and Tl in the dissolved, colloidal and solid phase of a biochar-treated and untreated mining soil. *Environ. Int.* 140, 105754. <https://doi.org/10.1016/j.envint.2020.105754>
- Rinklebe, J., Shaheen, S. M., Frohne, T., 2016a. Amendment of biochar reduces the release of toxic elements under dynamic redox conditions in a contaminated floodplain soil. *Chemosphere* 142, 41-47. <https://doi.org/10.1016/j.chemosphere.2015.03.067>
- Rinklebe, J., Shaheen, S. M., Yu, K. W., 2016b. Release of As, Ba, Cd, Cu, Pb, and Sr under pre-definite redox conditions in different rice paddy soils originating from the USA and Asia. *Geoderma* 270, 21-32. <https://doi.org/10.1016/j.geoderma.2015.10.011>
- Shaheen, S. M., Antoniadis, V., Kwon, E., Song, H., Wang, S. L., Hseu, Z. Y., Rinklebe, J., 2020. Soil contamination by potentially toxic elements and the associated human health risk in geo- and anthropogenic contaminated soils: A case study from the temperate region (Germany) and the arid region (Egypt). *Environ. Pollut.* 262. <https://doi.org/10.1016/j.envpol.2020.114312>
- Shaheen, S. M., El-Naggar, A., Wang, J., Hassan, N. E. E., Niazi, N. K., Wang, H., Tsang, D. C. W., Ok, Y. S., Bolan, N., Rinklebe, J., 2019. Biochar as an (im)mobilizing agent for the potentially toxic elements in contaminated soils. In: Ok, Y.S., Tsang, D. (Eds.), *Biochar from Biomass and Waste*. Elsevier, New York, USA, pp. 256-274.
- Shaheen, S. M., Rinklebe, J., Frohne, T., White, J. R., DeLaune, R. D., 2014. Biogeochemical factors governing cobalt, nickel, selenium, and vanadium dynamics in periodically flooded Egyptian North Nile Delta rice soils. *Soil Sci. Soc. Am. J.* 78, 1065-1078. <https://doi.org/10.2136/sssaj2013.10.0441>
- Shaheen, S. M., Rinklebe, J., Frohne, T., White, J. R., DeLaune, R. D., 2016. Redox effects on release kinetics of arsenic, cadmium, cobalt, and vanadium in Wax Lake Deltaic freshwater marsh soils. *Chemosphere* 150, 740-748. <https://doi.org/10.1016/j.chemosphere.2015.12.043>
- Shi, Z., Hu, S., Lin, J., Liu, T., Li, X., Li, F., 2020. Quantifying microbially mediated kinetics of ferrihydrite transformation and arsenic reduction: role of the arsenate-reducing gene expression pattern. *Environ. Sci. Technol.* 54 (11), 6621-6631. <https://doi.org/10.1021/acs.est.9b07137>
- Sik, E., Kobya, M., Demirbas, E., Gengec, E., Oncel, M. S., 2017. Combined effects of co-existing anions on the removal of arsenic from groundwater by electrocoagulation process: Optimization through response surface methodology. *J. Environ. Chem. Eng.* 5, 3792-3802. <https://doi.org/10.1016/j.jece.2017.07.004>
- Takeño, N., 2005. *Atlas of Eh-pH diagrams*. National Institute of Advanced Industrial Science and Technology.
- Van Vinh, N., Zafar, M., Behera, S. K., Park, H. S., 2014. Arsenic(III) removal from aqueous solution by raw and zinc-loaded pine cone biochar: equilibrium, kinetics, and thermodynamics studies. *Int. J. Environ. Sci. Technol.* 12, 1283-1294. <https://doi.org/10.1007/s13762-014-0507-1>
- Vithanage, M., Herath, I., Joseph, S., Bundschuh, J., Bolan, N., Ok, Y. S., Kirkham, M. B., Rinklebe, J., 2017.

- Interaction of arsenic with biochar in soil and water: A critical review. *Carbon* 113, 219-230. <https://doi.org/10.1016/j.carbon.2016.11.032>
- Wang, N., Xue, X. M., Juhász, A. L., Chang, Z. Z., Li, H. B., 2017. Biochar increases arsenic release from an anaerobic paddy soil due to enhanced microbial reduction of iron and arsenic. *Environ. Pollut.* 220, 514-522. <https://doi.org/10.1016/j.envpol.2016.09.095>
- Wen, E., Yang, X., Chen, H., Shaheen, S. M., Sarkar, B., Xu, S., Song, H., Liang, Y., Rinklebe, J., Hou, D., Li, Y., Wu, F., Pohořelý, M., Wong, J. W. C., Wang, H., 2021. Iron-modified biochar and water management regime-induced changes in plant growth, enzyme activities, and phytoavailability of arsenic, cadmium and lead in a paddy soil. *J. Hazard. Mater.* 124344. <https://doi.org/10.1016/j.jhazmat.2020.124344>
- Wu, C., Cui, M., Xue, S., Li, W., Huang, L., Jiang, X., Qian, Z., 2018. Remediation of arsenic-contaminated paddy soil by iron-modified biochar. *Environ. Sci. Pollut. Res.* 25, 20792-20801. <https://doi.org/10.1007/s11356-018-2268-8>
- Yang, P.-T., Hashimoto, Y., Wu, W.-J., Huang, J.-H., Chiang, P.-N., Wang, S.-L., 2020. Effects of long-term paddy rice cultivation on soil arsenic speciation. *J. Environ. Manage.* 254, 109768. <https://doi.org/10.1016/j.jenvman.2019.109768>
- Yang, X., Liu, J., McGrouter, K., Huang, H., Lu, K., Guo, X., He, L., Lin, X., Che, L., Ye, Z., Wang, H., 2016. Effect of biochar on the extractability of heavy metals (Cd, Cu, Pb, and Zn) and enzyme activity in soil. *Environ. Sci. Pollut. Res.* 23, 974-984. <https://doi.org/10.1007/s11356-015-4233-0>
- Yang, X., Lu, K., McGrouter, K., Lei, C., Hu, G., Wang, Q., Liu, X., Shen, L., Huang, H., Ye, Z., Wang, H., 2017. Bioavailability of Cd and Zn in soils treated with biochars derived from tobacco stalk and dead pigs. *J. Soil. Sediment.* 17, 751-762. <https://doi.org/10.1007/s11368-015-1326-9>
- Yu, K.W., Rinklebe, J., 2011. Advancement in soil microcosm apparatus for biogeochemical research. *Ecol. Eng.* 37, 2071-2075. <https://doi.org/10.1016/j.ecoleng.2011.08.017>
- Yuan, Y., Bolan, N., PrevotEAU, A., Vithanage, M., Biswas, J. K., Ok, Y. S., Wang, H., 2017. Applications of biochar in redox-mediated reactions. *Bioresour. Technol.* 246, 271-281. <https://doi.org/10.1016/j.biortech.2017.06.154>
- Zeien, H., Brümmer, G. W., 1989. Chemische Extraktion zur Bestimmung von Schwermetallbindungsformen in Boden. *Mitt. Dtsch. Bodenk. Ges.* 59, 505-510.
- Zhao, B., Nan, X., Xu, H., Zhang, T., Ma, F., 2017. Sulfate sorption on rape (*Brassica campestris* L.) straw biochar, loess soil and a biochar-soil mixture. *J. Environ. Manage.* 201, 309-314. <https://doi.org/10.1016/j.jenvman.2017.06.064>
- Zhu, M., Zhang, L., Zheng, L., Zhuo, Y., Xu, J., He, Y., 2018. Typical Soil Redox Processes in Pentachlorophenol Polluted Soil Following Biochar Addition. *Front. Microbial.* 9, 579. <https://doi.org/10.3389/fmicb.2018.00579>
- Zhu, Y.-G., Xue, X.-M., Kappler, A., Rosen, B. P., Meharg, A. A., 2017. Linking Genes to Microbial Biogeochemical Cycling: Lessons from Arsenic. *Environ. Sci. Technol.* 51, 7326-7339. <https://doi.org/10.1021/acs.est.7b00689>

CHAPTER 3: Effects of Iron-Impregnated Green Waste Biochar on Arsenic Mobilization under Fluctuating Controlled Redox Conditions in Paddy Soil ²



² Adapted from Yang, X., Shaheen, S.M., Wang, J., Hou, D., Ok, Y.S., Wang, S.L., Wang, H., Rinklebe, J., 2022. Elucidating the redox-driven dynamic interactions between arsenic and iron-impregnated biochar in a paddy soil using geochemical and spectroscopic techniques. *Journal of Hazardous Materials* 422, 126808.

A supplementary data is provided in Appendix B.

Abstract

Iron (Fe)-modified biochar, a renewable amendment that synthesizes the functions of biochar and Fe materials, demonstrates a potential to remediate arsenic (As)-contaminated soils. However, the effectiveness of Fe-based biochar to immobilize As in paddy soils under varying redox conditions (Eh) has not been quantified. We tested the capability of raw (RBC) and Fe-impregnated (FeBC) biochars to immobilize As in a paddy soil under various Eh conditions (from -400 to +300 mV) using a biogeochemical microcosm system. In the control, As was mobilized ($686.2\text{--}1,535.8\ \mu\text{g L}^{-1}$) under reducing conditions and immobilized ($61.6\text{--}71.1\ \mu\text{g L}^{-1}$) under oxidizing conditions. The application of FeBC immobilized As at $Eh < 0$ mV by 32-81% compared to the control, due to the transformation of As-bound Fe (hydro)oxides (e.g., ferrihydrite) and the formation of complexes (e.g., ternary As-Fe-DOC). Application of RBC immobilized As at $Eh < -100$ mV by 61-41% compared to the control, due to its porous structure and oxygen-containing functional groups. Mobilized As at $Eh > +200$ mV was caused by the increase of pH after RBC application. Modification of biochar with Fe can be a suitable approach for alleviating the environmental risk of As under reducing conditions in paddy soils.

Keywords: Toxic metal(loid)s, Fe-based biochar, redox conditions, soil remediation, immobilization mechanisms

3.1 Introduction

Arsenic (As) is a highly hazardous element, which is originally sourced from natural geogenic sources, such as weathering processes, geochemical reactions and biological activities (Zhu et al., 2017; Shaheen et al., 2018). Moreover, anthropogenic activities, including mining and smelting industries, agricultural applications, sewage irrigations and fossil fuel combustions contribute to As contamination in soils (Wu *et al.*, 2018a). Soil contamination with As has adversely affected human health due to the environmental risk of As through bio-accumulation and bio-magnification in the food chain (Khan et al., 2021). Consequently, it is of great importance to develop cost-effective technologies or amendments (e.g., biochar) to remediate As-contaminated soils (Wu et al., 2018a; Amen et al., 2020).

Biochar has gained intensive interest as an effective and sustainable agent for remediation of contaminated soils (Yang et al., 2016; Vithanage et al., 2017; Lyu et al., 2020). Numerous studies confirmed that biochar has a potential to immobilize toxic elements (e.g., Cd, Cu, Ni, Pb, and Zn) in soils, as it can increase soil sorption capacity on these elements (e.g., Yang et al., 2017; Frick et al., 2019; Wen et al., 2021a). However, biochars produced from different feedstocks may immobilize or mobilize As in soils based on soil and biochar properties (Wu et al., 2018a; Shaheen et al., 2019). In general, As exists in soils as anionic forms, such as H_3AsO_3 , H_2AsO_4 , HAsO_3^{2-} , AsO_4^{3-} (Beiyuan et al., 2017; Pan et al., 2021), which may be weakly adsorbed by raw biochars (Vithanage et al., 2017; Frick et al., 2019). Therefore, the sole application of raw biochars might be less ideal for mitigating the mobilization and environmental toxicity of As in contaminated soils.

Recently, modified biochar has been employed to immobilize soil toxic elements including As (e.g., Premarathna et al., 2019; Wu et al., 2020; Yang et al., 2021). Biochar modified by iron (Fe) materials may render particular characteristics for As immobilization (Qiao et al., 2019; Fan et al., 2020; Wen et al., 2021b). Iron is an essential element that affects the fate of As in soils (Wu et al., 2018b; Han et al., 2019), where seasonal redox alteration may trigger the reversible reductive dissolution and oxidative precipitation of Fe (hydro)oxides, thereby affecting the mobilization and speciation of As (Aeppli et al., 2019; Amen et al., 2020; Shi et al., 2020). The Fe-modified biochar would synthesize the functions of biochar and Fe, and thus strengthen the effectiveness on immobilization of As in soils (Fan et al., 2021; Wen et al., 2021b). The presence of oxygen-containing functional groups, graphite-like structure and persistent free radicals on biochar (Lyu et al., 2020), coupled with the superior properties of Fe materials, such as catalysis (Jones et al., 2017), reduction (Wu et al., 2018b), and recrystallization (Xiao et al., 2017), would greatly alter the geochemical processes in soils, thereby affecting the transformation of As. The production and utilization of Fe-modified biochar for immobilization of As in soils have been investigated recently

(e.g., Wu et al., 2018a; El-Naggar et al., 2019; Frick et al., 2019). However, to the best of our knowledge, no attempt has been made to elucidate the potential ability of Fe-modified biochar for the immobilization of As in paddy soils with dynamic redox potentials (Eh conditions).

The transformation and speciation of As in soils are closely associated with the change in soil Eh and the redox-induced alterations of soil pH, Fe (hydro)oxides, sulfate/sulfide, and organic carbon (LeMonte et al., 2017; Shaheen et al., 2019). Biochar application may alter redox reactions and thus the behavior of As, since biochar could enhance electron transfer between oxidants and reductants in soils (Amen et al., 2020). Therefore, we hypothesized that the incorporation of the Fe-impregnated biochar would have some impacts on the biogeochemical reactions, including the change in Eh and pH, the redox cycling of Fe (hydro)oxides, the transformation of sulfur (S), and the composition of dissolved organic carbon (DOC), thus shifting the transformation and speciation of As in soils. However, a knowledge gap regarding the transformation and speciation of As triggered by the application of biochar, in particular Fe-modified biochar, in paddy soils under fluctuating redox conditions remains unaddressed. Moreover, synchrotron-based spectroscopic techniques are frequently used in different research areas to study the distribution and speciation of elements in diverse matrices (Feng et al., 2020). Synchrotron micro-X-ray absorption near-edge structure (XANES) spectroscopy analyses are being increasingly employed to study the distribution and speciation of As in contaminated soils (Mensah et al., 2020; Yang et al., 2020a,b). However, speciation and redistribution of As in biochar-treated paddy soils under systematic change in redox conditions using synchrotron-based techniques have not been investigated yet.

To fill the above knowledge gaps and test our hypothesis, in the current study, a raw biochar (RBC) derived from the branches of a green waste (*Platanus orientalis* L.), and the Fe-impregnated green waste biochar (FeBC) were applied to an As-contaminated paddy soil and then incubated under systematic changing Eh conditions using an automated biogeochemical microcosm (MC) system. The synchrotron-based XANES was exploited to analyze the species of As and Fe in soils. The aims of the current study were to 1) quantify the impact of RBC and FeBC application on the release and transformation of As under a series of controlled Eh conditions in a paddy soil, and 2) elucidate the potential mechanisms which may control the redox-mediated biogeochemical behavior of As in the RBC- and FeBC-amended paddy soils with the support of the synchrotron-based spectroscopic techniques (e.g., XANES).

3.2 Materials and methods

3.2.1 Collection and characterization of the studied soil

The studied paddy soil was collected from a rice paddy in the south of Shaoxing City, China (29°59' N, 120°46' E). This site was chosen because it is located in the Middle-Lower Yangtze plain, a main rice cultivation region in China; it is contaminated with As because of the runoff from adjacent mine tailings. The soil samples were mixed, air-dried, ground, and passed through a 3-mm sieve prior to use. The basic soil properties were analyzed using the standard methods (Lu, 2000) and are shown in Table 3-1.

Table 3-1 Selected physicochemical properties of the tested soil.

pH	CEC ^a (cmol kg ⁻¹)	EC ^b (dS m ⁻¹)	OC ^c (%)	Olsen P (mg kg ⁻¹)	Total As (mg kg ⁻¹)	Total Fe (g kg ⁻¹)	Sand (%)	Silt (%)	Clay (%)
5.8	13.4	0.05	1.3	1.8	141.3	32.1	33.5	45.9	20.6

^aCEC: cation exchange capacity. ^bEC: electrical conductivity. ^cOC: organic carbon.

The pH was measured on a 1:5 (w/v) water suspension of the soil sample after stirring manually for 1 minute. The organic carbon (OC) content was determined by the potassium dichromate external heating oxidation method. Total As was extracted by completely dissolved with HF-HClO₄-HNO₃ and analyzed using Inductively Coupled Plasma Optical Emission Spectroscopy (ICP-OES, Optima 2000, PerkinElmer Co., USA). It was an acidic soil (pH = 5.8) with an OC content of 1.3%. The total concentration of As in the soil was 141.3 mg kg⁻¹, which exceeded the risk screening value of As (30 mg kg⁻¹) in acidic paddy soils (5.5 < pH ≤ 6.5), based on the Soil Environmental Quality Risk Control Standard for Soil Contamination of Agricultural Land (MEE, 2018).

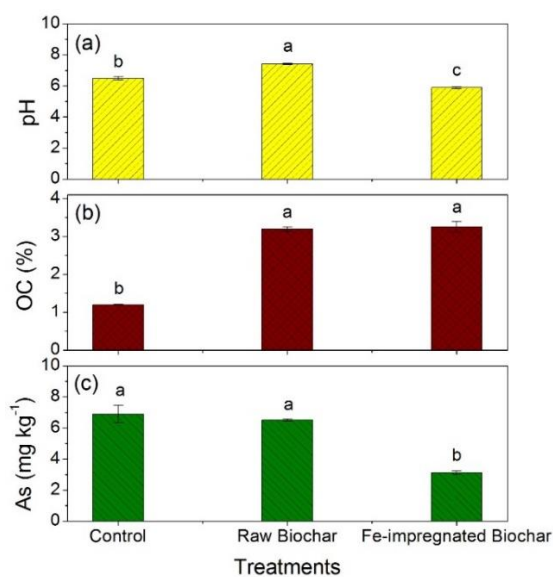


Figure 3-1 Effect of biochar application on soil pH (a), organic carbon (b, OC) and NH₄H₂PO₄-extractable As (c) after pre-incubation.

3.2.2 Biochar production and characterization

The branches of *Platanus orientalis* L. were pyrolyzed in a lab-scale furnace at approximately 650 °C for 2 h to produce the raw biochar (RBC). Subsequently, the obtained RBC was immersed in a $\text{FeCl}_3 \cdot 6\text{H}_2\text{O}$ solution at 20: 1 weight ratio (biochar: Fe) to produce the Fe-impregnated biochar (FeBC). In brief, the mixture of biochar and Fe solution was mixed thoroughly at 25 °C by stirring manually for 20 min and then ultrasound for 1 h. Thereafter, the mixture was oven-dried at 70 °C until constant weight. At last, the dried mixture was pyrolyzed at approximately 650 °C for 1 h to obtain FeBC (Wen et al., 2021a). The selected physicochemical properties of both biochars are shown in Table 3-2. The biochar morphological properties were examined under the scanning electron microscope (SEM) (Sirion-100, FEI, Poland) equipped with an energy-dispersive spectrometer at 20 kV (EDS, INCA X-sight, Oxford Instruments). The surface functional groups on biochars were characterized using a Fourier transform infrared spectroscopy (FTIR: Frontier, PerkinElmer, USA) at a resolution of 4 cm^{-1} .

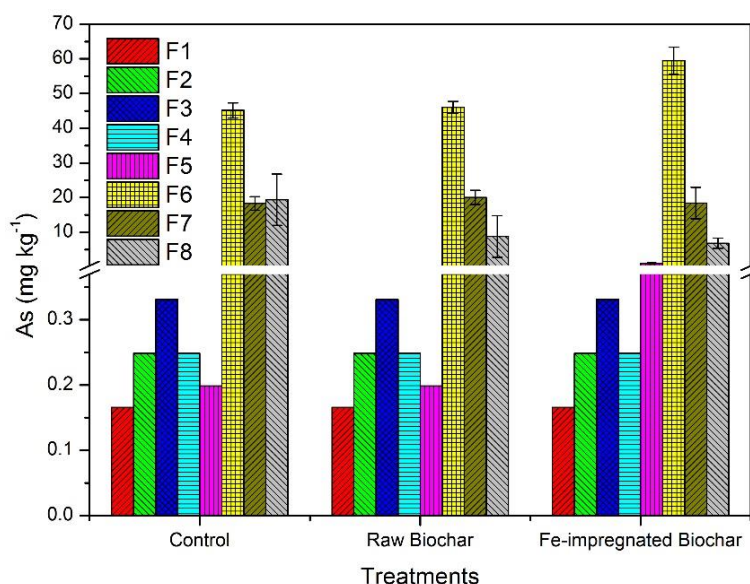


Figure 3-2 Effect of raw and Fe-impregnated biochar application on the geochemical fractions of As in soils after pre-incubation. F1: soluble + exchangeable; F2: carbonate; F3: manganese oxide; F4: organic matter; F5: sulfide; F6: amorphous iron oxide; F7: crystalline iron oxide; F8: residue. Control: non-treated soil; Raw Biochar: raw biochar-treated soil; Fe-impregnated Biochar: Fe-impregnated biochar-treated soil.

3.2.3 Pre-incubation of the non- and biochar-treated soils

The As-contaminated paddy soil was mixed with RBC or FeBC at the dose of 0% (non-treated control) and 3% (w/w). Thereafter, the control and biochar-treated soils were pre-incubated in four replicates under the laboratory conditions (25 °C) for 30 days to allow a proper stabilization of biochars after incorporation into the soil. During the pre-incubation, the soils were maintained under a flooding condition with deionized water (2 – 3 cm of water layer was maintained on the top of soil). Thereafter, the pre-incubated soil samples were retrieved, air-dried,

ground, and passed through a 2-mm sieve for the microcosm experiment. Meanwhile, the pre-incubated soil samples were characterized for pH, OC content (Lu, 2000), and the concentration of $\text{NH}_4\text{H}_2\text{PO}_4$ -extractable As (Wenzel et al., 2001); the results are provided in Figure 3-1. The geochemical fractions of As in the pre-incubated soils were analyzed using the method established by Zeien and Brümmer (1989), and modified by Beiyuan et al. (2017) and El-Naggar et al. (2019). The detailed sequential extraction method is given in Table 3-3 and the results are illustrated in Figure 3-2.

Table 3-2 Properties of the tested raw and Fe-impregnated biochars.

Properties	Raw biochar (RBC)	Fe-impregnated biochar (FeBC)
pH (H_2O)	9.3	4.4
Electrical conductivity (dS m^{-1})	0.4	4.5
Total C (%)	69.3	59.9
Total N (%)	1.1	0.9
Total H (%)	2.7	2.2
Total S (%)	0.4	0.2
Specific surface area ($\text{m}^2 \text{g}^{-1}$)	110.7	74.5
Surface alkalinity (cmol kg^{-1})	215.9	183.6
Total P (g kg^{-1})	1.9	3.0
Ash content (%)	9.7	15.3
Total Fe (%)	0.7	5.5
Total As (mg kg^{-1})	BDL ^a	BDL

^aBDL: Below the detection limit.

3.2.4 Microcosm experiment

A special automated biogeochemical microcosm (MC) setup (Figure 3-3) was employed to simulate the flooding conditions of paddy soils in the laboratory. The detailed description of this system is published in Yu and Rinklebe (2011). This MC system has been proven to be an efficient tool to study the redox-induced behaviors of trace elements including As in different soils (e.g., Frohne et al., 2011; Shaheen et al., 2014; El-Naggar et al., 2019; Rinklebe et al., 2020). A previous study proved that the results collected in the MC experiment are comparable to those in the field (Rupp et al., 2010). In the current study, each glass bottle was filled with 210 g of pre-incubated soils (section 3.2.3) and 1,680 mL of tap water (soil: water = 1: 8, w/v). Simultaneously, 10 g of rice straw and 5 g of glucose were applied to provide extra carbon sources for microorganisms, which were considered a vital factor for Eh alteration. Subsequently, the glass bottle was closed tightly and the slurry inside was stirred using a motor rotor throughout the experiment to maintain homogeneity. During the experiment, the Eh of slurry was regulated automatically by purging with synthetic air (oxygen) or nitrogen. Four replicates were run for each treatment. Two hours after origination, the initial sampling was conducted. The second to ninth samplings were

done minimum 48 h after reaching the targeted windows (Eh = -400, -300, -200, -100, 0, +100, +200, and +300 mV, respectively). At each sampling point, approximately 85 mL of slurry was taken from each glass bottle and then centrifuged at 5,000 rpm for 15 min. Afterwards, the samples were immediately transferred to an anaerobic glove box (Don Whitley Scientific, Shipley, UK) to pass through a 0.45- μm membrane filter (Whatman Inc., Maidstone, UK). Thereafter, sub-samples of the filtrate were prepared for the analyses of the concentrations of dissolved As and Fe, ferrous ion (Fe^{2+}), sulfate (SO_4^{2-}) and DOC. Meanwhile, soil samples (sediments after filtration) were collected and stored under $-80\text{ }^\circ\text{C}$ conditions for the synchrotron-based XANES analysis (section 3.2.5). Before XANES analysis, the collected soil samples were freeze-dried and ground in the anaerobic glove box. More information about the analytical methods, experimental conditions and sampling procedures is provided in the *Appendix B* (sections B1.1 and B1.2).

3.2.5 XANES analysis

The species of As and Fe in the freeze-dried soil samples collected from the microcosm experiment (Eh = -300, 0 and +250 mV) were analyzed using XANES on Beamlines 07 A and 17 C, respectively, in NSRRC, Taiwan, ROC. The fluorescence mode was used for all XANES spectra collection, and a Soller-slits Lytle detector was used in an energy range of 11,667 – 12,867 eV for As, and 6,912 – 7,912 eV for Fe, respectively. The XANES data were processed and analyzed using Athena (Ravel and Newville, 2005). Linear combination fitting (LCF) was performed to determine the species of As. More details about the data analysis are given in *Appendix B* (section B1.3).

3.2.6. Quality assurance and statistical analysis

Mean values of pH and Eh collected from 6 h prior to the sampling point ($\text{pH}_{6\text{h}}$ and $\text{Eh}_{6\text{h}}$) were calculated and used for statistical analyses (Rinklebe et al., 2020). A SPSS 18.0 (SPSS Inc., USA) program was used to conduct statistical analyses of the data. One-way analysis of variance (ANOVA) and Duncan's multiple range tests ($P < 0.05$) were used to assess the statistical significance of different treatments based on soil pH, OC content and the concentration of $\text{NH}_4\text{H}_2\text{PO}_4$ -extractable As. Correlations between the concentration of As and other controlling factors were analyzed using Pearson's correlation coefficient ($P < 0.05$). Figures were created using Origin 8.5. The quality assurance for determination of dissolved As was checked by analyzing certified references, standard solutions and reagent blanks. More details about quality assurance are provided in *Appendix B* (section B1.4).

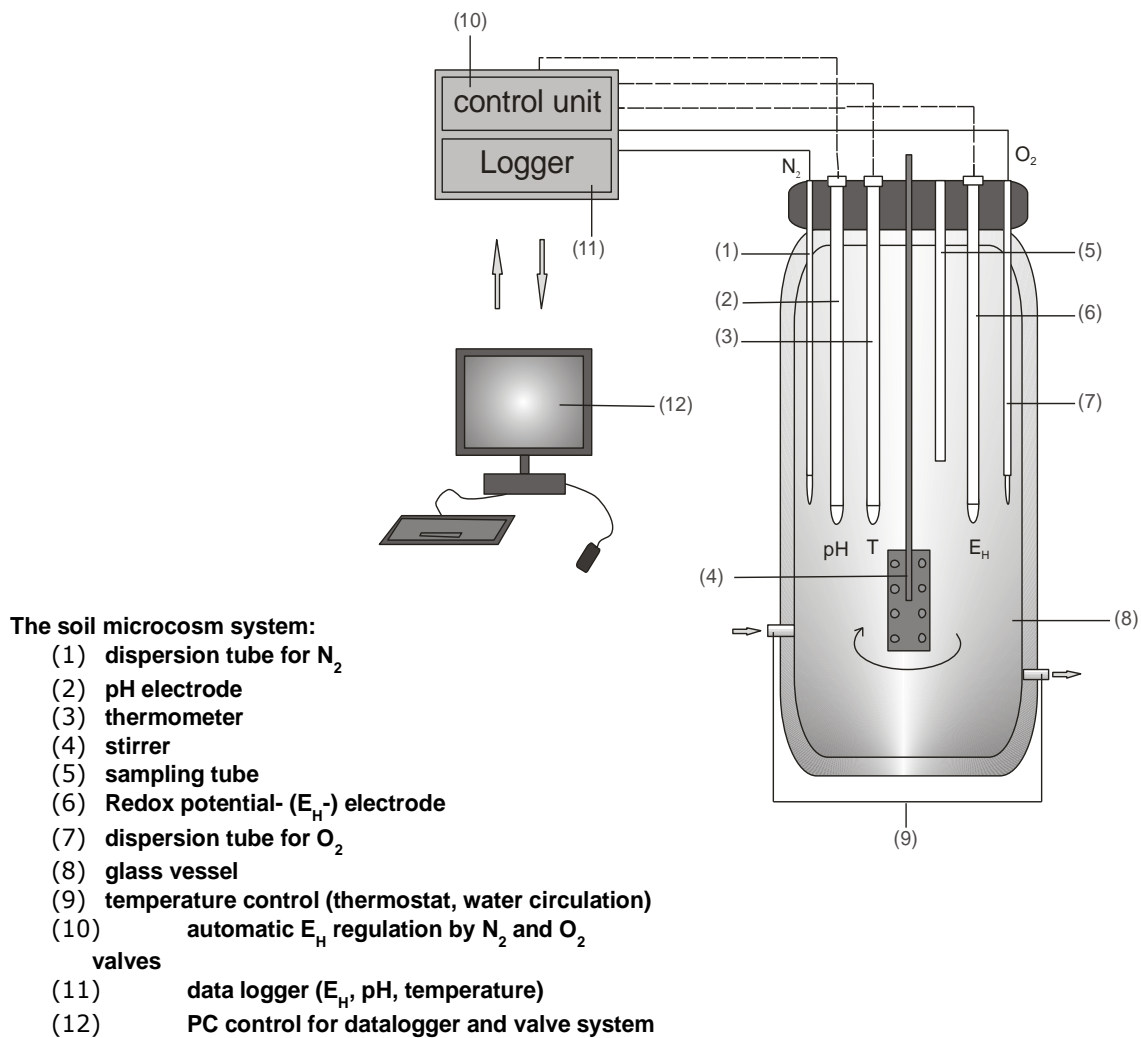


Figure 3-3 Biogeochemical microcosm setup.

3.3 Results and discussion

3.3.1 Characteristics of biochars: impact of modification

RBC was alkaline with a pH of 9.3, whereas FeBC was acidic with a pH of 4.4 (Table 3-2). The decline of biochar

pH after modification could be ascribed to the increase of H^+ caused by the hydrolysis of exogenous Fe compounds (Yin et al., 2017). The surface alkalinity of FeBC ($183.6 \text{ cmol kg}^{-1}$) was lower than that of RBC ($215.9 \text{ cmol kg}^{-1}$), which further confirmed the acidification of biochar after modification. In addition, the total content of Fe in FeBC (5.5%) was significantly higher than that in RBC (0.7%) (Table 3-2).

Table 3-3 Eight-step modified sequential extraction procedures.

Steps	Fractions	Extracting solution	Extraction conditions
1	Soluble + exchangeable	1 M NH_4OAc (pH 7.0)	24 h, room temperature
2	Bound to carbonate	1 M NH_4OAc (pH 6.0)	24 h, room temperature
3	Manganese oxide fraction	0.1 M $NH_2OH-HCl$ + 1 M NH_4OAc (pH 6.0)	0.5 h, room temperature
4	Organic matter fraction	0.025 M NH_4EDTA (pH 4.6)	1.5 h, room temperature
		3 mL 0.02 M HNO_3 + 5 mL 30% H_2O_2 (H_2O_2 pH = 2.0 with conc. HNO_3)	2 h, 85 °C in a water bath
5	Sulfide fraction	3 mL 30% H_2O_2 (H_2O_2 pH = 2.0)	3 h, 85 °C in a water bath
		5 mL 3.2 M NH_4OAc in 20% HNO_3 after cooling and diluted to 20 mL with DI water	
6	Amorphous Fe oxide fraction	0.2 M NH_4 -Oxalate (pH 3.25)	4 h, room temperature
7	Crystalline Fe oxide fraction	0.1 M ascorbic acid in 0.2 M NH_4 -oxalate buffer (pH 3.25)	0.5 h, 96 °C in a water bath
8	Residue	Aqua regia ($HCl:HNO_3 = 1:3 \text{ mL}$)	Microwave digestion

As shown in Figure 3-4, RBC exhibited a smooth surface with abundant small openings and irregularly arranged porous structures. However, FeBC had an inhomogeneous and rough surface, which was covered by numerous fine particles (Figure 3-4). We postulate that the porous structures on the raw biochar were partially destroyed or blocked after modification, therefore reducing the specific surface area of biochar (Table 3-2). The SEM-EDX $K\alpha$ map of Fe illustrated that the Fe compounds were evenly distributed on FeBC (Figure 3-4). However, the Fe map of RBC could not be obtained because of the low Fe abundance. The loading of Fe on FeBC after modification could be also proven by the presence of the peak at around 6.4 keV in the EDX spectra (Figure 3-4). The FTIR spectra showed that RBC contained more absorption peaks than FeBC (Figure 3-4), implying that the modification process decreased the number of functional groups on biochar. The modification-induced alterations on the surface characteristics of biochar could affect its ability for As (im)mobilization under different Eh conditions as will be discussed in the following sections.

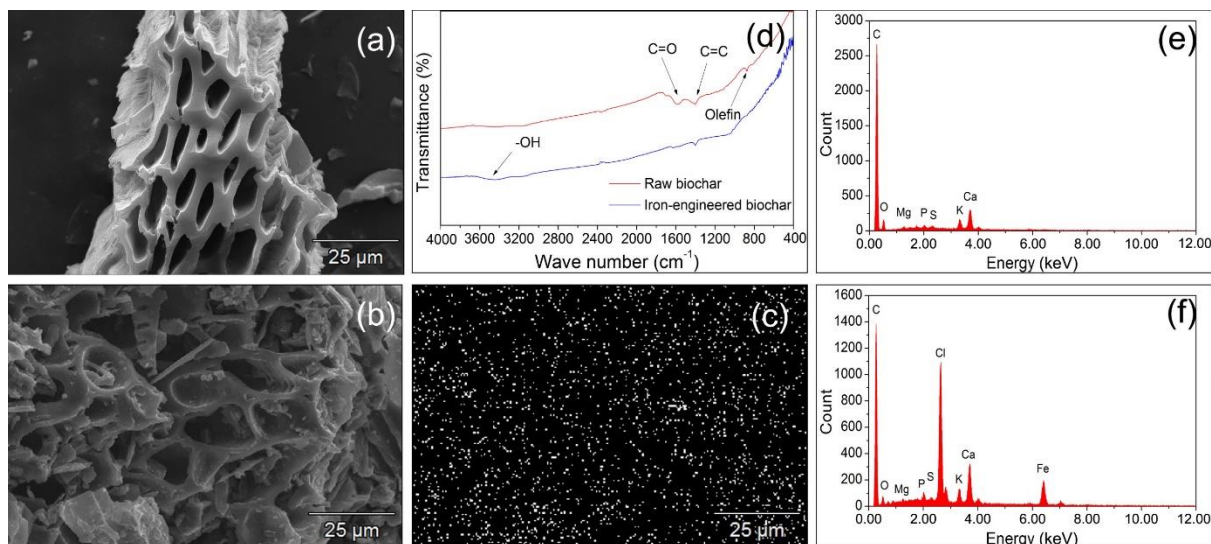


Figure 3-4 The scanning electron microscope (SEM) images of the raw (a) and Fe-impregnated biochar(b); SEM-EDX K α map of Fe in the Fe-impregnated biochar(c); Fourier transform infrared spectra of the raw and Fe-impregnated biochar (d); and the energy dispersive X-ray patterns of the raw biochar (e) and Fe-impregnated biochar (f).

3.3.2 Arsenic mobilization as affected by the biochar-induced alterations of Eh and pH

The temporal course of the average values of Eh and pH in the soil slurry and sampling timings are presented in Figure 3-5. Values of the four replicates of each treatment and the descriptive analyses of these values are presented in Table 3-4 and Figure 3-6. Application of different biochars caused a variation of Eh ranges, which followed an order of FeBC treatment (from -446 to +359 mV) > RBC treatment (from -484 to +281 mV) > control (from -465 to +293 mV). Such a biochar-induced change in soil Eh was reported in previous studies (e.g., Awad et al., 2018; Rinklebe et al., 2020).

Table 3-4 Variation of Eh, pH and concentrations of As, Fe, Fe²⁺, SO₄²⁻ and DOC in the control and biochar treatments.

Parameters	Control				RBC treatment				FeBC treatment			
	n	Minimum	Maximum	Mean	n	Minimum	Maximum	Mean	n	Minimum	Maximum	Mean
Eh _{all} (mV)	13,780	-465	+293	-13	13,780	-484	+281	-16.2	13,780	-446	+359	+44.9
Eh _{6h} (mV) ^a	36	-386	+248	-35	36	-436	+277	-35.5	36	-398	+352	+38.9
pH _{all}	13,775	4.3	7.6	5.6	13,780	4.8	8.8	6.1	13,780	4.6	7.8	5.9
pH _{6h} ^a	36	5.0	7.1	5.8	36	5.1	8.7	6.2	36	4.8	7.4	6.0
As (µg L ⁻¹)	32	BDL ^b	1,756.0	663.6	32	BDL	1,016.0	456.1	32	BDL	985.6	394.2
Fe (mg L ⁻¹)	32	0.05	240.1	110.1	32	0.05	193.7	88.0	32	0.03	250.4	95.7
Fe ²⁺ (mg L ⁻¹)	36	0	152.2	57.2	36	0	96.8	37.2	36	0	101.4	35.8
SO ₄ ²⁻ (mg L ⁻¹)	32	13.2	38.3	27.8	32	39.5	49.2	43.0	32	29.2	35.5	32.3
DOC (mg L ⁻¹)	28	46.6	826.4	511.0	28	112.0	751.2	481.1	28	20.6	663.5	395.9

^a Mean value of Eh and pH collected from 6 h prior to sampling.

^b Below the detection limit.

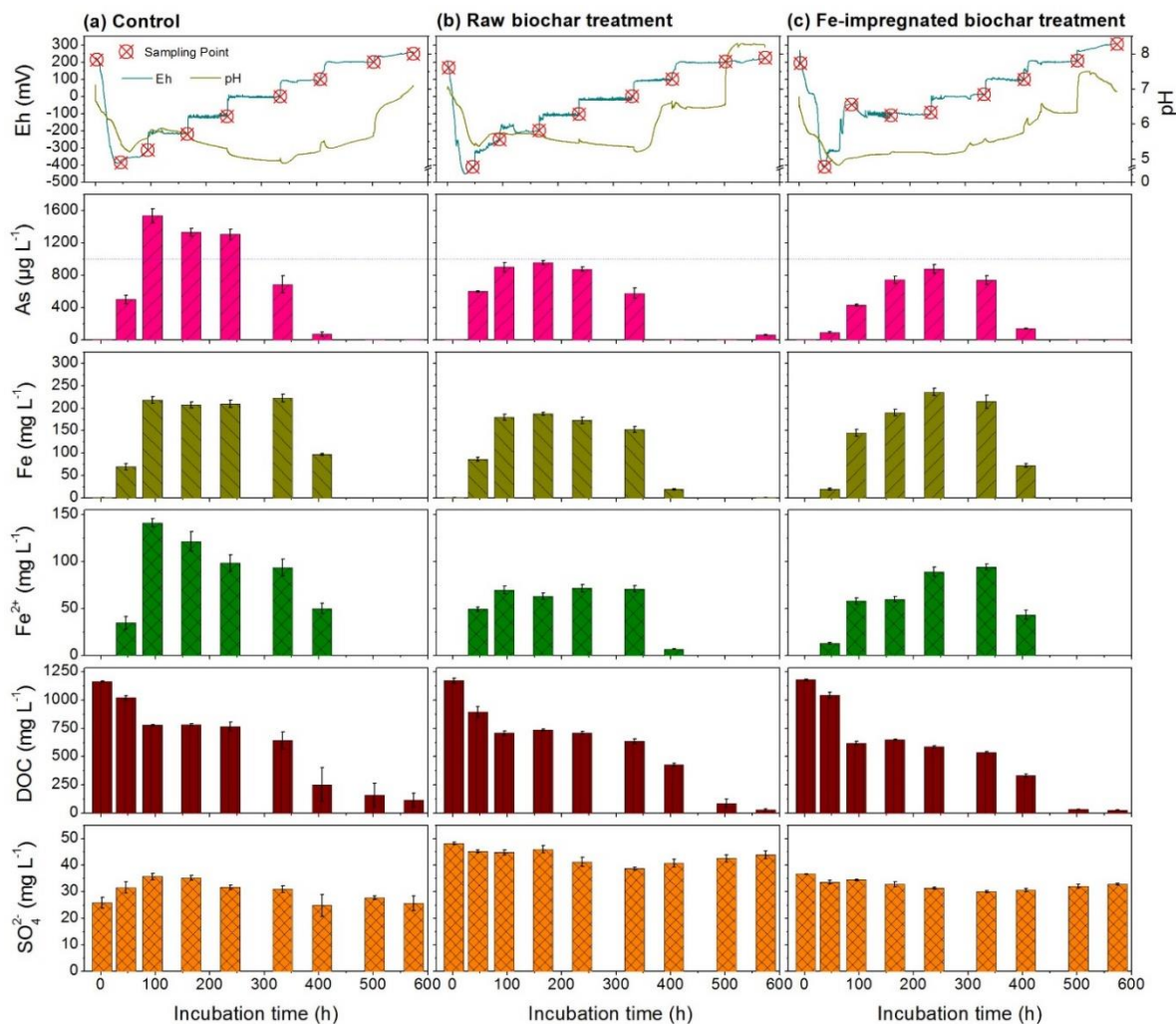


Figure 3-5 Effect of raw and Fe-impregnated biochars on the concentration of dissolved As and governing factors under dynamic and pre-defined redox conditions.

A decline of pH was found with decreasing Eh, and vice versa, in all treatments. The Eh_{6h} and pH_{6h} were positively correlated ($R= 0.51, P < 0.01$; Table 3-5). These results indicated that the change in redox processes affected soil pH. The declined pH under low Eh conditions may be due to the dissolution of microbe-generated CO₂ in the solution and the production of organic acids via the microbial decomposition of SOM (Shaheen et al., 2014). Application of RBC increased soil pH under varying Eh conditions (Figure 3-5), which might be attributed the high surface alkalinity of RBC (Table 3-2). However, FeBC-treated soil had a lower pH than the control, which may be attributed to the acidity of FeBC (Table 3-2), in particular under reducing conditions. Some studies showed that the decrease of soil pH caused by the application of Fe-modified biochar might be ascribed to the elevated H⁺ as a result of the hydrolysis of exogenous Fe (e.g., Yin et al., 2017; Zhang et al., 2020). These results revealed that RBC and FeBC have a potential to affect the mobilization of As via altering soil pH and the redox reactions in soil.

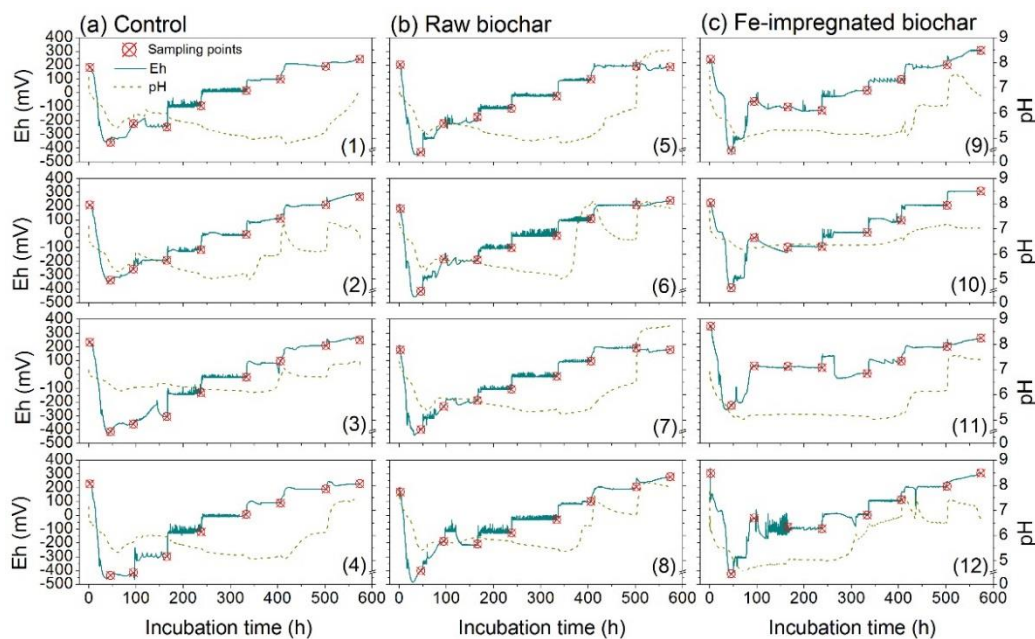


Figure 3-6 Dynamics of Eh and pH in each microcosm of control (1~4), raw biochar treatment (5~8) and Fe-impregnated biochar treatment (9~12). Control: non-treated soil; Raw Biochar: raw biochar-treated soil; Fe-impregnated Biochar: Fe-impregnated biochar-treated soil.

The average concentrations of dissolved As ranged from a value below the detection limit (BDL = $53 \mu\text{g L}^{-1}$) to $1,535.8 \mu\text{g L}^{-1}$ in the control, from BDL to $956.6 \mu\text{g L}^{-1}$ in the RBC treatment, and from BDL to $880.6 \mu\text{g L}^{-1}$ in the FeBC treatment. Higher concentrations of dissolved As were observed under reducing conditions than under oxidizing conditions in all treatments (Figure 3-5). For example, in the control, As was highly mobilized ($686.2 - 1,535.8 \mu\text{g L}^{-1}$) under reducing conditions and immobilized ($61.6 - 71.1 \mu\text{g L}^{-1}$) under oxidizing conditions. A higher concentration of dissolved As under reducing conditions indicated a relatively higher level of the environmental risk of As in contaminated paddy soils (Zhu et al., 2017; Pan et al., 2021). There was a significantly ($P < 0.01$) negative correlation between the concentration of dissolved As and $\text{Eh}_{6\text{h}}$ (Table 3-5), which further revealed the close affinity between Eh and the release of As. After flooding, the concentration of dissolved As increased rapidly with decreasing Eh (from approximately +200 to -300 mV), then maintained a slight fluctuation under reducing conditions ($\text{Eh} = -300 - 0 \text{ mV}$) (Figure 3-5). The relatively higher concentration of dissolved As under strongly reducing conditions than under oxidizing conditions might be due to the Eh- and pH-induced transformation of Fe (hydro)oxides (section 3.3.3) and/or mineralization of organic matter (section 3.3.4). However, the concentration of dissolved As rapidly decreased with the stepwise increase of Eh in all treatments (Figure 3-5), due to the oxidation of the relatively more mobile As(III) to less mobile As(V) along with Eh increasing (Amen et al., 2020).

Table 3-5 Correlation coefficients between As concentration and potential affecting factors. ^a

	As	Eh	pH	Fe	Fe ²⁺	DOC	SO ₄ ²⁻
As	1.000						
Eh	-0.68**	1.000					
pH	-0.51**	0.51**	1.000				
Fe	0.93**	-0.58**	-0.59**	1.000			
Fe ²⁺	0.94**	-0.63**	-0.57**	0.94**	1.000		
DOC	0.31**	-0.51**	-0.27**	0.26**	0.28**	1.000	
SO ₄ ²⁻	0.10	-0.24**	0.16	0.03	0.00	0.20*	1.000

^a n=32 for As, Eh, pH, Fe, Fe²⁺ and SO₄²⁻, n=28 for DOC.

**Correlation is significant at the 0.01 level.

*Correlation is significant at the 0.05 level.

Application of both RBC and FeBC decreased the concentration of dissolved As, in particular under reducing conditions, compared to the control (Figure 3-5). Biochars immobilized As compared to control with a higher effectiveness for FeBC (32.6 – 81.1%) than RBC (16.0 – 41.3%). In the third and fourth samplings, the concentrations of dissolved As decreased by 71.8 and 44.3% in the FeBC treatment, and 44.2 and 28.2% in the RBC treatment, respectively, compared to the control (Table 3-6). At these two sampling points, the Eh values of different treatments followed an order of FeBC treatment (-46 and -109 mV) > RBC treatment (-251 and -199 mV) > control (-313 and -219 mV). Thus, the decrease of dissolved As here, after the application of FeBC and RBC, could be tied to the biochar-induced change in Eh. As reported in a recently published study (Rinklebe et al., 2020), biochar may enhance the ability of soil in accepting and/or donating electrons through governing electron transfer reactions, thereby altering soil Eh, in turn changing the release feature of As in soils. Redox-active moieties (e.g., oxygen-containing groups and condensed aromatics) were detected in RBC (Figure 3-4). These moieties could be reversibly reduced and oxidized, thereby improving the redox buffer capacity of RBC, in turn changing soil Eh once amended (Klöpffel et al., 2014). Compared to the control, the increase of Eh as a result of the application of FeBC could be attributed to the presence of exogenous Fe. It is known that the redox transformation of Fe in soils is a result of electron transport (Gotoh and Patrick, 1974). The addition of Fe along with FeBC might further accelerate the electron transfer reactions in soil, thus causing an increase of Eh in the FeBC treatment, compared to the control and RBC treatment. Moreover, application of biochars might induce a more pronounced shift of Eh under strongly reducing conditions (e.g., the third and fourth samplings) than other sampling points with more oxidizing conditions. As indicated by Joseph et al. (2010), the aromatic carbon derived from biochar can serve as electron donors, which could be oxidized by alternative electron acceptors (e.g., Fe-Mn (hydro)oxides) in the absence of oxygen (under reducing conditions). Thus, both the high aromatic carbon-

containing RBC and the Fe-rich FeBC had a high potential to cause an increase of soil Eh, thereby decreasing the concentration of dissolved As under strongly reducing conditions.

Table 3-6 Average values (mean values of 4 replicates) of As dissolved concentrations and the induced changes (%) in the biochar-treated soils as compared to the control.

Targeted Eh (mV)	Control ($\mu\text{g L}^{-1}$)	RBC treatment ($\mu\text{g L}^{-1}$)	FeBC treatment ($\mu\text{g L}^{-1}$)	Changes in As (%) with RBC application	Change in As (%) with FeBC application
Initial sampling	LDL ^a	LDL	LDL	--	--
-400	502.5	599.8	95.1	19.3%	-81.1%
-300	1535.8	901.3	432.6	-41.3%	-71.8%
-200	1332.0	956.6	743.8	-28.2%	-44.2%
-100	1307.3	875.2	880.6	-33.0%	-32.6%
0	686.2	576.6	740.3	-16.0%	7.9%
+100	71.1	LDL	140.1	--	97.0%
+200	LDL	LDL	LDL	--	--
+300	LDL	61.6	LDL	--	--

^a Lower than the detection limit.

Soil pH plays a vital role in governing the mobilization of As (Karczewska et al., 2018). The concentration of dissolved As in the current study was negatively correlated ($P < 0.01$) with $\text{pH}_{6\text{h}}$ (Table 3-5), suggesting that the release of As could be linked to the biochar-induced change in pH. Under reducing conditions ($\text{Eh} < -100$ mV), the lower concentration of dissolved As in the FeBC treatment relative to that in the control and RBC treatment could be ascribed to the decline of pH caused by FeBC application (Figure 3-5). The decrease of pH might result in an increase of positive charges on soil colloids, thus promoting the adsorption of As via electrostatic attraction, particularly under reducing conditions (Zhong et al., 2019). Michalkova et al. (2016) and Van Vinh et al. (2014) concluded that a lower pH (< 7.0) could cause a stronger adsorption of As on the positively charged biochar, thereby promoting the immobilization of As by the biochar-treated soil. In contrast, the increased concentration of dissolved As under oxidizing conditions could be interpreted by the biochar-induced rise of pH. For example, in the last sampling ($\text{Eh} > +200$ mV), the concentrations of dissolved As were BDL in the control and the FeBC treatment, and the application of RBC increased the concentration to $61.6 \mu\text{g L}^{-1}$. It is obviously shown that the application of RBC significantly increased the pH (8.2), compared to the control (7.1) and the FeBC treatment (6.9). According to Van Vinh et al. (2014), biochar could be more negatively charged in a solution with higher pH. Moreover, in a solution with a pH between 3 and 8, As predominantly exists in anionic forms, such as H_2AsO_4^- , HAsO_4^{2-} and AsO_4^{3-} (Deng et al., 2008). Thus, application of RBC might promote the release of As through rising

pH, thereby enhancing the electrostatic repulsive force between the negatively charged RBC and As oxyanions.

3.3.3 Arsenic mobilization as affected by the biochar-induced changes in Fe (hydro)oxides

Similar to dissolved As, the concentrations of Fe^{2+} and dissolved Fe were higher under reducing conditions ($E_h = -400 - +100$ mV) than those under oxidizing conditions ($E_h > +200$ mV) in all treatments (Figure 3-5). Particularly, an abrupt decrease of dissolved Fe and Fe^{2+} was noticed after the seventh sampling ($E_h = +100$ mV). These findings might be tied to the redox chemistry of Fe (hydro)oxides, which could accept electrons abiotically from chemical electron donors, and/or biotically with the presence of Fe-reducing microorganisms under reducing conditions, thereby resulting in the reductive dissolution of Fe (hydro)oxides (Xiao et al., 2017; Aeppli et al., 2019). Under oxidizing conditions, the previously dissolved Fe ions might be immobilized through oxidation processes driven by Fe-oxidizing microorganisms (Shaheen et al., 2014). Application of both biochars decreased the concentration of Fe^{2+} but had no obvious impacts on total dissolved Fe, which might be linked to the elevated concentrations of SO_4^{2-} caused by the application of biochars (Figure 3-5). As reported by LeMonte et al. (2017), elevated SO_4^{2-} in a solution can competitively inhibit the reduction of Fe^{3+} by reductants, due to the preferential reduction of SO_4^{2-} at $\text{pH} > 5.0$.

Iron (hydro)oxides exhibit high reactivity and could control the release of As in soils through adsorption-desorption, precipitation-dissolution, and mineral transformation-structural incorporation (Aeppli et al., 2019; Amen et al., 2020; Shi et al., 2020). The reductive dissolution of Fe (hydro)oxides in wetland soils occurs at $E_h < +100$ mV (LeMonte et al., 2014), which agrees with the critical point where the release of As begins (Reddy and Delaune, 2008). In this study, positive correlations were found between the concentrations of dissolved As and Fe, and Fe^{2+} (Table 3-5). Additionally, the sequential extraction results revealed that As was predominantly occluded with the amorphous and crystalline iron oxides in the control and biochar-treated soils (Figure 3-2). Accordingly, we assume that the application of both biochars, in particular FeBC, might alter the geochemical fractions and species of Fe, thereby affecting the transformation and speciation of As in soils.

To verify the above assumption, Fe and As species in the soil samples were analyzed using K-edge XANES spectroscopy (Figures 3-7 and 3-8). Generally, it is difficult to use Fe K-edge XANES to exactly quantify specific Fe phases in soils, where the Fe compounds are complicated because of weathering and pedogenesis (Prietz et al., 2007). However, the contribution of different mineral classes and oxidation states of Fe in soils can be fairly estimated by Fe K-edge XANES. In the current study, FeO and $\alpha\text{-Fe}_2\text{O}_3$ were selected as the Fe(II) and Fe(III) reference materials, respectively, to estimate the oxidation states of Fe in the soil samples, after the principal component analysis (PCA) for all reference materials.

The first derivative XANES spectra of Fe showed that the predominant oxidation state of Fe in all soils was Fe(III) (Figure 3-7), indicating that Fe mainly existed as Fe(III)-bearing minerals (e.g., ferrihydrite, goethite, hematite, lepidocrocite). Moreover, application of biochars and change in Eh had no obvious impact on the oxidation states of Fe in soils. The standard spectra of hematite, goethite, ferrihydrite and lepidocrocite were very similar, thus the LCF results were not suitable for distinguishing among these Fe(III) (hydro)oxides in soils (Prietz et al., 2007). Meanwhile, the presence of Fe(II) in our samples cannot be completely ruled out because of the restriction from the sensitivity of XAS (Graser et al., 2015).

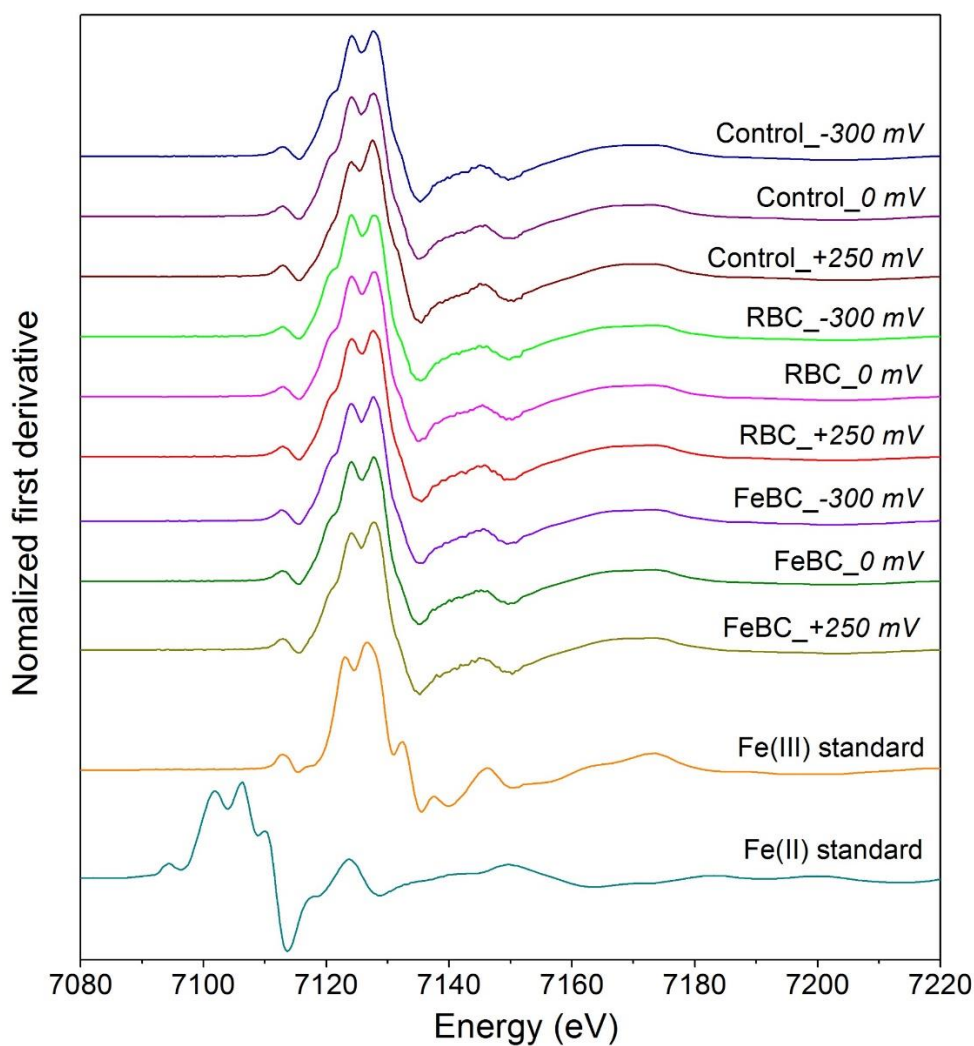


Figure 3-7 First derivative Fe K-edge XANES spectra of soils collected under pre-defined redox conditions against reference materials.

Based on the LCF of As XANES spectra (Figure 3-8) and sequential extraction results (Figure 3-2), As was predominantly bound to amorphous Fe oxides (e.g., ferrihydrite) in the tested soils. Consequently, we assume that ferrihydrite, a thermodynamically metastable iron oxide (Perez et al., 2019), could be considered as a predominant Fe phase in our samples. Ferrihydrite can readily undergo redox transformation to form more crystalline Fe

(hydro)oxides (e.g., goethite, lepidocrocite, hematite and magnetite) with the catalysis of Fe(II) under reducing conditions (Rawson et al., 2016; Aepli et al., 2019; Perez et al., 2019). In general, the Fe(II)-catalyzed mineralogical transformation of Fe (hydro)oxides is closely associated with the biogeochemical behaviors of nutrient elements (e.g., C, N, P, and S) and contaminants (e.g., As) in soils (Jones et al., 2017; Xiao et al., 2017; Wu et al., 2018b; Shi et al., 2020). Therefore, we postulate that the application of biochars may change the abundance of adsorbed Fe(II), thereby driving the transformation and/or recrystallization of Fe (hydro)oxides, and concomitantly altering the transformation and speciation of As.

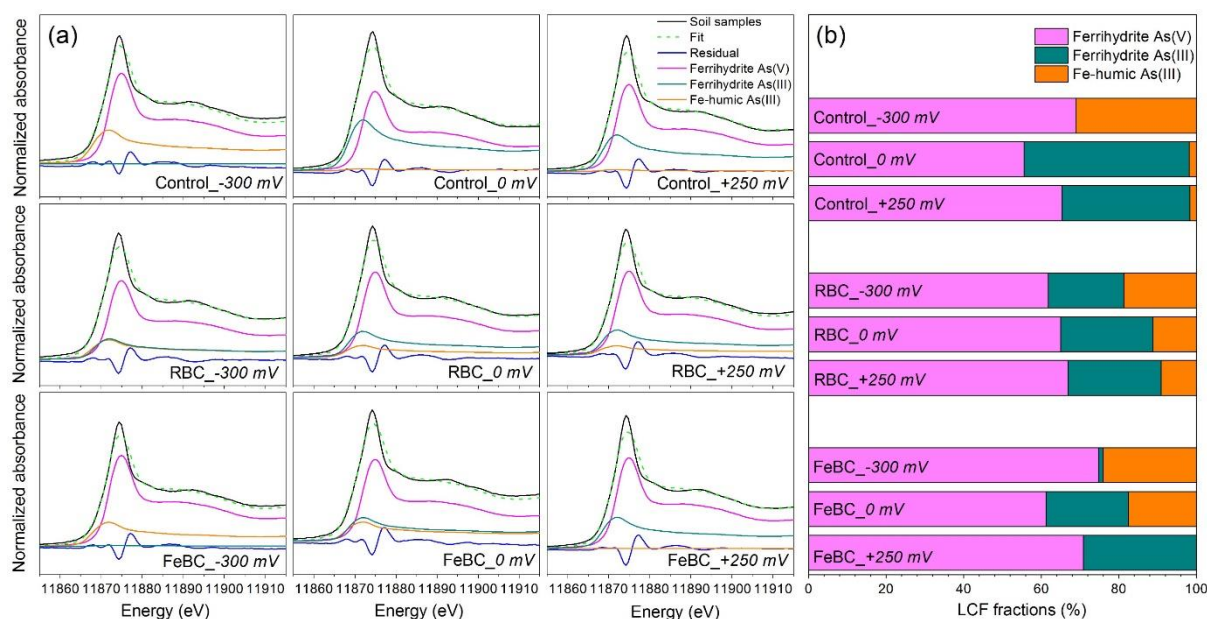


Figure 3-8 Linear combination fitting results of As K-edge XANES spectra of soils collected under pre-defined redox conditions (a), and the relatively proportions of different representative As species in soils (b).

The first derivative XANES spectra of As showed that the edges of the soil XANES spectra are closer to As(V) than As(III), indicative of the dominance of As(V) in our soil samples (Figure 3-9). The distinct spectral features of different reference materials were applied to analyze the speciation of As in soils using LCF. The results showed that the best fits for all samples were obtained with three reference materials, comprising As(V)- and As(III)-bearing ferrihydrite and As(III)-bearing ferric iron complexes of humic substances (Fe-humic As(III)) (Figure 3-8; Table 3-7). Although the inclusion of any other reference materials could not improve the LCF results, the association of As with other Fe minerals cannot be completely ruled out because of the detection limit of XAS, as well as the similar XANES spectra feature at near-edge ranges. The error of the LCF for As XANES spectra was $\pm 10\%$ and the detection limit of XAS for As species was approximately 5% (Yang et al., 2020b). Meanwhile, the detected As-bearing ferrihydrite and humic substances could not be interpreted as the actual presence of such

phases in the soils, but those with a similar configuration on soil minerals. These results revealed that As was predominantly associated with Fe (hydro)oxides, which agreed with the fractionation results, where As in soils existed primarily as Fe oxides-bound forms in soils (Figure 3-2). Previous studies have also proven that Fe minerals, such as ferrihydrite, goethite, hematite and magnetite, had strong affinity with both As(III) and As(V) in soils via adsorption, precipitation, and complexation (e.g., Aeppli et al., 2019; Yang et al., 2020a,b). Mikutta and Kretzschmar (2011) and Liu et al. (2011) indicated the formation of a ternary complex between As oxyanions and Fe-humic substances in soils, and the former study has proven the existence of these complexes using XAS. Thus, As bound to Fe (hydro)oxides (e.g., As(III)- and As(V)-bearing ferrihydrite) and organic compounds (e.g., Fe-humic As(III)) could be considered as the representative As species in our soil samples.

Table 3-7 Linear combination fitting (LCF) results of As K-edge XANES spectra of soil samples collected from different redox conditions and bulk soil.

Soil samples	Sampling condition	As components (%)			R-factor
		Ferrihydrite As(V)	Ferrihydrite As(III)	Fe-humic As(III)	
Bulk soil	--	76.7	11.5	11.8	0.017
Control	-300 mV	68.9	0.0	31.1	0.010
	0 mV	55.5	42.7	1.8	0.010
	+250 mV	65.3	33.0	1.7	0.013
RBC treatment	-300 mV	61.8	19.5	18.7	0.012
	0 mV	65.0	23.8	11.2	0.011
	+250 mV	66.9	24.0	9.1	0.014
FeBC treatment	-300 mV	74.8	1.2	24.0	0.013
	0 mV	61.2	21.3	17.5	0.013
	+250 mV	70.9	29.1	0.0	0.015

The LCF results from the XANES spectra demonstrated that As predominantly existed as As(V)-bearing ferrihydrite (from 55.5 to 74.8%), and higher proportion of As(III) (sum of the ferrihydrite As(III) and Fe-humic As(III)) was found in all soil samples compared to the bulk soil (Figure 3-8; Table 3-7). The initial As(V)-bearing ferrihydrite could be partially reduced to As(III) under anoxic conditions with the presence of aqueous Fe(II) (Perez et al., 2019). This could explain the higher proportion of As(III) under moderately reducing conditions ($E_h = 0$ mV), compared to that under oxidizing conditions ($E_h = +250$ mV). Under strongly reducing conditions ($E_h = -300$ mV), we assume that the previously formed As(III)-bearing ferrihydrite dissolved as the reaction progressed, indicating that the released As under reducing conditions was primarily from the reductive dissolution and Fe(II)-catalyzed transformation of As(III)-bearing ferrihydrite.

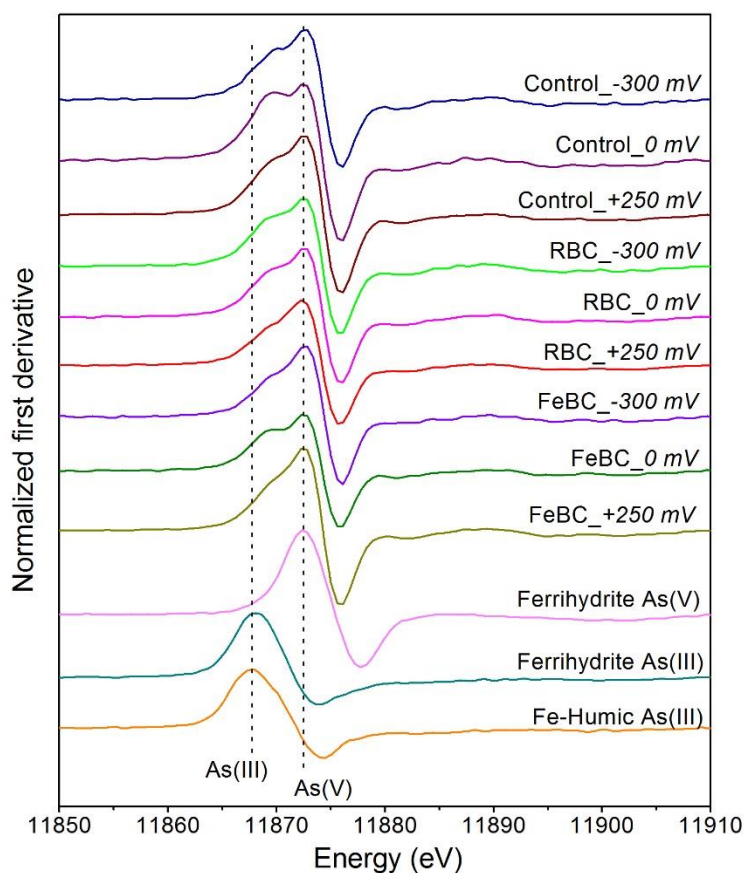


Figure 3-9 First derivative As K-edge XANES spectra of reference materials and soil samples collected from different redox conditions. Control: non-treated soil; RBC: raw biochar-treated soil; FeBC: Fe-impregnated biochar-treated soil.

In the present study, the concentration of Fe^{2+} in both biochar treatments was lower than that in the control, especially under reducing conditions (Figure 3-5). In contrast, previous studies suggested that biochar serving as “electron shuttles” can facilitate microbial reduction of ferrihydrite, thereby yielding the dissolution of Fe^{2+} and increasing its concentration in soil (Chen et al., 2016; Wu et al., 2018b). In our study, the functional groups, such as $-\text{OH}$, $\text{C}=\text{C}$ and $\text{C}=\text{O}$ were determined in both biochars (Figure 3-4). These functional groups could act as electron donors to facilitate the reduction of As-bearing Fe minerals in the soil, thereby promoting the reductive dissolution of both Fe^{2+} and As (Kim et al., 2018). On the other hand, application of biochar might appear to stimulate the microbial oxidation of organic compounds under anaerobic conditions. In turn, the microbial community could exchange electrons through organic compounds in soils as a quinone-like group, which normally acts as electron donors to promote the microbial reduction of Fe (hydro)oxides and the release of As (Van der Zee and Cervantes, 2009; Chen et al., 2016). With regard to the decrease of the concentrations of Fe^{2+} and dissolved As caused by the application of both RBC and FeBC under reducing conditions (Figure 3-5), we speculate that over incubation time, the reductively dissolved As and Fe might further form secondary minerals via precipitation

(Wu et al., 2018b) and/or complexation under reducing conditions (Liu et al., 2011). The the presence of biochar as an electron shuttles may mediate and/or accelerate these redox-induced reactions in soils, thereby promoting the formation of the secondary minerals (Van der Zee and Cervantes, 2009; Chen et al., 2016; Zhu et al., 2017). The LCF results showed that As could bind to organic matter via metastable inner-sphere complexation (e.g., Fe-humic As(III)) under reducing conditions (section 3.3.4). These findings could further prove that the application of biochar, in particular FeBC, could promote the immobilization of As under reducing conditions through formation of stable minerals, thus alleviating the environmental risk of As in paddy soils.

3.3.4 Arsenic mobilization as affected by the biochar-induced changes in DOC

The concentrations of DOC under reducing conditions were higher than those under oxidizing conditions in all treatments (Figure 3-5). The elevated DOC under reducing conditions might be due to the absence of oxide sorption sites, as well as the dramatically decrease of the oxygen-favored microorganism activities caused by the lack of oxygen (Karczewska et al., 2018). Under oxidizing conditions, the increase of oxygen availability might accelerate the aerobically microbial mineralization of DOC, thereby decreasing the concentration of DOC (Hanke et al., 2013). Under reducing conditions, application of both RBC and FeBC reduced the concentration of DOC, compared to the control (Figure 3-5). As aforementioned, both RBC and FeBC could serve as a quinone-like group to stimulate the microbial oxidation and decomposition of DOC under anaerobic conditions (Chen et al., 2016; Beiyuan et al., 2017), thereby resulting in a lower concentration of DOC under reducing conditions, compared to the control. In addition, the RBC-induced decrease of DOC could be also attributed to its abundant oxygen-containing functional groups and high porous structures (Figure 3-4). As reported by Vithanage et al. (2017), biochar with more functional groups and higher porous structures has stronger sorption capacity on small molecular organic compounds. For the FeBC treatment, the decrease of DOC might be linked to the formation of insoluble ternary As-Fe-DOC complexes under reducing conditions (see more details in the next paragraph). Under oxidizing conditions, application of both biochars, in particular FeBC, decreased the concentration of DOC. Due to the highly porous structures and abundant content of C, N and other mineral elements in the biochars (Figure 3-4), application of these biochars can be beneficial for enhancing microbial activities through providing a habitat and supplying carbon source and mineral elements (Nie et al., 2018), thus resulting in a higher microbial decomposition rate of DOC. In particular, the relatively higher number of mineral elements on FeBC (Figure 3-4) could promote the growth and reproduction of microorganisms and accelerate the decomposition of DOC. Therefore, a lower concentration of DOC was noticed in the FeBC treatment, compared to the control and RBC treatment, in particular under oxidizing conditions.

The release of As in our study could be also associated with the biochar-induced change in DOC composition in soils. Pearson's correlation analysis showed a positive correlation ($P < 0.01$) between the concentrations of dissolved As and DOC (Table 3-5). In the RBC treatment, the change in DOC concentration under reducing conditions might be attributed to the high aromatics and abundant functional groups on RBC (Figure 3-4). These high molecular weight aromatic carbon and functional groups could bind As through surface complexation and ligand exchange (Liu et al., 2011; Vithanage et al., 2017). Under oxidizing conditions ($E_h > +200$ mV), the concentrations of DOC and dissolved As decreased in the RBC treatment, compared to the control (Figure 3-5). This could be mainly interpreted by the presence of highly porous structures and functional groups (Figure 3-4), which may increase the surface adsorption of As and DOC on the RBC-treated soil. With regard to the FeBC treatment, the exogenous Fe added along with FeBC may act as a bridge between As and DOC, and ultimately form a ternary As-Fe-DOC complex (Sharma et al., 2010; Liu et al., 2011), thereby decreasing the concentration of dissolved As, particularly under reducing conditions. As aforementioned (section 3.3.3), As(III)-bearing ferric iron complexes of humic substances was possibly formed through Fe-involved As and DOC complexation, which was supported by the As K-edge XANES results (Figures 3-8 and 3-9; Table 3-7). The LCF results demonstrated that a higher proportion of the Fe-humic As(III) was determined in the FeBC treatment than that in the RBC treatment, in particular under reducing conditions (Figure 3-8). Therefore, we assume that the exogenous Fe on FeBC might be released and reduced to form Fe^{2+} under reducing conditions, thereby being involved in the Fe-catalyzed interactions between As and DOC, in turn mitigating the mobilization and environmental toxicity of As in the paddy soil.

3.3.5 Arsenic mobilization as affected by the biochar-induced changes in SO_4^{2-}

The tendency of SO_4^{2-} concentrations in different treatments varied over incubation time (Figure 3-5). In brief, the concentration of SO_4^{2-} in the control increased until the third sampling (targeted $E_h = -300$ mV), then decreased with the increase of E_h . In the RBC treatment, the concentration of SO_4^{2-} gradually decreased until the sixth sampling (targeted $E_h = 0$ mV) and then gradually increased with increasing E_h . However, in the FeBC treatment, the concentration of SO_4^{2-} declined throughout the experiment. Compared to the control, application of RBC notably increased the concentration of SO_4^{2-} throughout the experiment, which was primarily due to the variation of DOC after biochar application (Rinklebe et al., 2020). We assume that abundant sulfur-containing groups might be attached to the biochar-generated organic compounds, and the decomposition of those sulfur-containing organic compounds might contribute to the increase of SO_4^{2-} over incubation. However, application of FeBC caused a slighter increase of the concentration of SO_4^{2-} than RBC, when both were compared to the control (Figure 3-5).

The total S content in RBC (0.4%) was twice as high as that in FeBC (0.2%) (Table 3-2), which agreed with our above assumption that the biochar-generated S caused an increase of SO_4^{2-} in the solution over incubation.

Sulfide (S^{2-}) might be formed under reducing conditions due to the reduction of SO_4^{2-} (El-Naggar et al., 2019). However, in the present study, the concentration of S^{2-} was not detectable in all samples. We assume that S^{2-} was likely formed under reducing conditions, whereas the formed S^{2-} might have rapidly reacted with As anions and/or Fe^{2+} to generate unstable precipitates and/or complexes (e.g., $\text{HAS}_3\text{S}_6^{2-}$) (LeMonte et al., 2017). The elevated SO_4^{2-} caused by the application of RBC may inhibit the reduction of As(V) and Fe(III), which plausibly may mitigate the release of As from soil (LeMonte et al., 2017), thus decreasing its environmental risk. Nevertheless, no significant correlation was found between the concentrations of dissolved As and SO_4^{2-} (Table 3-5). This could be explained by the low concentration of sulfide-bound As in the control and biochar-treated soils (Figure 3-2). Consequently, we speculate that the Eh- and biochar-induced change in SO_4^{2-} had inappreciable effect on the release of As in the current study, as compared to other governing factors such as pH, Fe and DOC.

We summarize that application of RBC and FeBC decreased the concentration of dissolved As, in particular under reducing conditions (up to 41.3 and 81.1%, respectively). The RBC mobilized As under oxidizing conditions ($\text{Eh} > +200$ mV), caused by the associated increase of pH, which increased the potential risk of As to the environment and human health. The modification of RBC with Fe materials increased its effectiveness for As immobilization under reducing conditions, which could be mainly attributed to its abundant oxygen-containing functional groups and high aromaticity. The immobilization of As after FeBC application could be predominantly ascribed to the Fe-catalyzed transformation of As-bearing Fe (hydro)oxides (e.g., ferrihydrite) and the formation of insoluble complexes (e.g., ternary As-Fe-DOC complex).

3.4 Conclusions

Our findings demonstrate that the concentrations of dissolved As were higher under reducing conditions and lower under oxidizing conditions, which indicate the high potential environmental and human health risk of As in contaminated flooded paddy soils and emphasize the need for remediation. We also found that the green waste biochar modified by Fe materials (e.g., FeCl_3) is able to reduce the mobilization thus, the environmental toxicity of As in the contaminated paddy soil, in particular under reducing conditions. In addition, it is feasible to produce and use green waste biochar in long-term and large-scale trials in the future, since green wastes such as tree branches, leaves, residual flowers, and roots are abundant and low-cost. Application of the Fe-impregnated biochar could decrease the concentrations of dissolved As in the soil solutions, in particular under reducing conditions,

thus alleviating the environmental risks of As to be accumulated in the food chain and/or transported into groundwater. However, most of the decreased values in the current study were still higher than the permissible threshold values for drinking water of $10 \mu\text{g L}^{-1}$ set by the World Health Organization (WHO). Therefore, more efforts, such as increasing application dose and testing different types of biochars and Fe materials, etc. are needed to achieve an ideal remediation effectiveness of As-contaminated paddy soils using Fe-modified biochars.

In the future, integrating various advanced chemical analyses (e.g., speciation of As in soil solutions), microbiological methods (e.g., As transformation genes) and spectroscopic techniques (e.g., XANES) will offer deeper insights into the biogeochemical behavior of As in biochar-treated paddy soils under varying Eh conditions. Future studies are also needed to extend the current results to realistic environment in the field (natural paddy soils). With regard to the application of Fe-modified biochars, urgent tasks are to optimize the modification of biochar with Fe materials, investigate the application rate of various biochars, and monitor the long-term effect of Fe-modified biochar on As immobilization in paddy soils. In addition, the feasibility of using alternative low-cost and eco-friendly Fe materials (e.g., natural iron ores and minerals) for the modification of biochars is also worth to be assessed in the future large-scale studies.

3.5 Acknowledgements

This work was supported by the National Key Research and Development Program of China (2020YFC1807704), the National Natural Science Foundation of China (Grant No. 21876027), and the Fundamental Research Program of Department of Science and Technology of Guizhou, China (ZK[2021]-key-045), and the Special Fund for the Science and Technology Innovation Team of Foshan, China (Grant No. 1920001000083). Authors are also grateful to the team in NSRRC, Hsinchu 30076, Taiwan, ROC, and in particular Dr. Soo, Yun-Liang (TLS 07A1) and Dr. Lee, Jyh-Fu (TLS 17C1). We thank the team of the Laboratory of Soil- and Groundwater-Management, University of Wuppertal, Germany, in particular Ilya Mironov, Claus Vandenhirtz and Kail Matuszak for technical assistance.

3.6 References

- Aeppli, M., Vranic, S., Kaegi, R., Kretzschmar, R., Brown, A.R., Voegelin, A., Hofstetter, T.B., Sander, M., 2019. Decreases in iron oxide reducibility during microbial reductive dissolution and transformation of ferrihydrite. *Environ. Sci. Technol.* 53, 8736-8746. <https://doi.org/10.1021/acs.est.9b01299>
- Amen, R., Bashir, H., Bibi, I., Shaheen, S.M., Niazi, N.K., Shahid, M., Hussain, M.M., Antoniadis, V., Shakoor, M.B., Al-Solaimani, S.G., Wang, H., Bundschuh, J., Rinklebe, J., 2020. A critical review on arsenic removal from water using biochar-based sorbents: The significance of modification and redox reactions. *Chem. Eng. J.* 396, 125195. <https://doi.org/10.1016/j.cej.2020.125195>
- Awad, Y.M., Ok, Y.S., Abridgata, J., Beiyuan, J.Z., Beckers, F., Tsang, D.C.W., Rinklebe, J., 2018. Pine sawdust biomass and biochars at different pyrolysis temperatures change soil redox processes. *Sci. Total Environ.* 625, 147-154. <https://doi.org/10.1016/j.scitotenv.2017.12.194>
- Beiyuan, J., Awad, Y.M., Beckers, F., Tsang, D.C.W., Ok, Y.S., Rinklebe, J., 2017. Mobility and phytoavailability of As and Pb in a contaminated soil using pine sawdust biochar under systematic change of redox conditions. *Chemosphere* 178, 110-118. <https://doi.org/10.1016/j.chemosphere.2017.03.022>
- Chen, Z., Wang, Y., Xia, D., Jiang, X., Fu, D., Shen, L., Wang, H., Li, Q.B., 2016. Enhanced bioreduction of iron and arsenic in sediment by biochar amendment influencing microbial community composition and dissolved organic matter content and composition. *J. Hazard. Mater.* 311, 20-29. <https://doi.org/10.1016/j.jhazmat.2016.02.069>
- Deng, S., Yu, G., Xie, S., Yu, Q., Huang, J., Kuwali, Y., Iseki, M., 2008. Enhanced adsorption of arsenate on the aminated fibers: sorption behavior and uptake mechanism. *Langmuir* 24, 10961-10967. <https://doi.org/10.1021/la8023138>
- El-Naggar, A., Shaheen, S.M., Hseu, Z.Y., Wang, S.L., Ok, Y.S., Rinklebe, J., 2019. Release dynamics of As, Co, and Mo in a biochar treated soil under pre-definite redox conditions. *Sci. Total Environ.* 657, 686-695. <https://doi.org/10.1016/j.scitotenv.2018.12.026>
- Fan, J., Chen, X., Xu, Z., Xu, X., Zhao, L., Qiu, H., Cao, X., 2020. One-pot synthesis of nZVI-embedded biochar for remediation of two mining arsenic-contaminated soils: Arsenic immobilization associated with iron transformation. *J. Hazard. Mater.* 398, 122901. <https://doi.org/10.1016/j.jhazmat.2020.122901>
- Feng, Y., Liu, P., Wang, Y., Finfrook, Y.Z., Xie, X., Su, C., Liu, N., Yang, Y., Xu, Y., 2020. Distribution and speciation of iron in Fe-modified biochars and its application in removal of As(V), As(III), Cr(VI), and Hg(II): An X-ray absorption study. *J. Hazard. Mater.*, 384, 121342. <https://doi.org/10.1016/j.jhazmat.2019.121342>
- Frick, H., Tardif, S., Kandeler, E., Holm, P.E., Brandt, K.K., 2019. Assessment of biochar and zero-valent iron for in-situ remediation of chromated copper arsenate contaminated soil. *Sci. Total Environ.* 2019, 655, 414-422. <https://doi.org/10.1016/j.scitotenv.2018.11.193>
- Frohne, T., Rinklebe, J., Diaz-Bone, R.A., Du Laing, G., 2011. Controlled variation of redox conditions in a floodplain soil: Impact on metal mobilization and biomethylation of arsenic and antimony. *Geoderma* 160, 414-424. <https://doi.org/10.1016/j.geoderma.2010.10.012>
- Gotoh S., Patrick, W.H.J., 1974. Transformation of iron in a waterlogged soil as influenced by redox potential and pH. *Soil Sci. Soc. Am. J.* 38. <https://doi.org/10.2136/sssaj1974.03615995003800010024x>
- Graser, C.-H., Banik, N.I., Bender, K.A., Lagos, M., Marquardt, C.M., Marsac, R., Montoya, V., Geckeis, H., 2015. Sensitive redox speciation of iron, neptunium, and plutonium by capillary electrophoresis hyphenated to inductively coupled plasma sector field mass spectrometry. *Anal. Chem.* 87, 9786-9794. <https://doi.org/10.1021/acs.analchem.5b02051>
- Han, Y.S., Park, J.H., Kim, S.J., Jeong, H.Y., Ahn, J.S., 2019. Redox transformation of soil minerals and arsenic in arsenic-contaminated soil under cycling redox conditions. *J. Hazard. Mater.* 378, 120745.

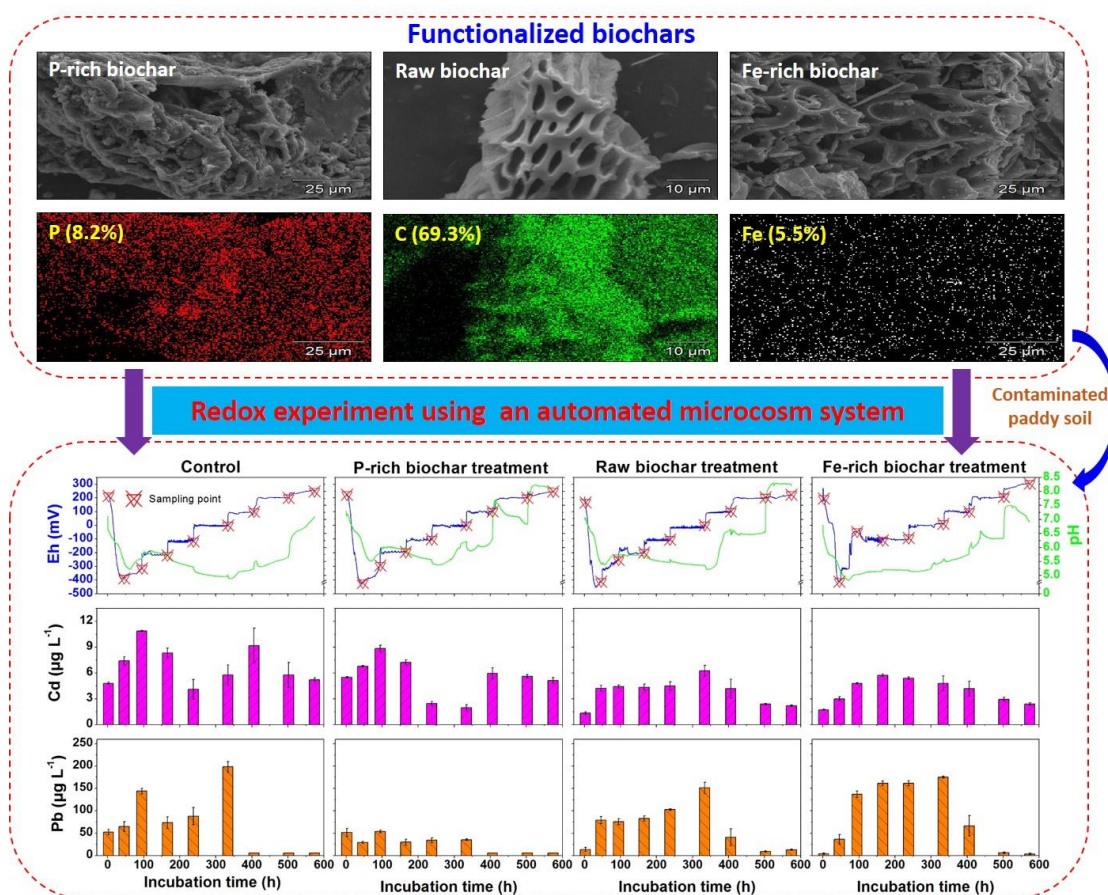
- <https://doi.org/10.1016/j.jhazmat.2019.120745>
- Hanke, A., Cerli, C., Muhr, J., Borken, W., Kalbitz, K., 2013. Redox control on carbon mineralization and dissolved organic matter along a chronosequence of paddy soils. *Eur. J. Soil Sci.* 64, 476-487. <https://doi.org/10.1111/ejss.12042>
- Jones, A.M., Collins, R.N., Waite, T.D., 2017. Redox characterization of the Fe(II)-catalyzed transformation of ferrihydrite to goethite. *Geochim. Cosmochim. Ac.* 218, 257-272. <https://doi.org/10.1016/j.gca.2017.09.024>
- Joseph, S.D., Camps-Arbestain, M., Lin, Y., Munore, P., Chia, C.H., Hook, J., Van Zwieten, L., Kimber, S., Cowie, A., Singh, B.P., Lehmann, J., Foidl, N., Smernik, R.J., Amonette, J.E., 2010. An investigation into the reactions of biochar in soil. *Aust. J. Soil Res.* 48, 501-515. <https://doi.org/10.1071/SR10009>
- Karczewska, A., Lewińska, K., Siepak, M., Gałka, B., Dradrach, A., Szopka, K., 2018. Transformation of beech forest litter as a factor that triggers arsenic solubility in soils developed on historical mine dumps. *J. Soil. Sediment.* 18, 2749-2758. <https://doi.org/10.1007/s11368-018-2031-2>
- Khan, I., Awan, S.A., Rizwan, M., Ali, S., Zhang, X., Huang, L., 2021. Arsenic behavior in soil-plant system and its detoxification mechanisms in plants: A review. *Environ. pollut.* 286, 117389. <https://doi.org/10.1016/j.envpol.2021.117389>
- Kim, H.B., Kim, S.H., Jeon, E.K., Kim, D.H., Tsang, D.C.W., Alessi, D.S., Kwon, E.E., Baek, K., 2018. Effect of dissolved organic carbon from sludge, Rice straw and spent coffee ground biochar on the mobility of arsenic in soil. *Sci. Total Environ.* 636, 1241-1248. <https://doi.org/10.1016/j.scitotenv.2018.04.406>
- Klöpffel, L., Keiluweit, M., Kleber, M., Sander, M., 2014. Redox properties of plant biomass-derived black carbon (Biochar). *Environ. Sci. Technol.* 48, 5601-5611. <https://doi.org/10.1021/es500906d>
- LeMonte, J.J., Stuckey, J.W., Sanchez, J.Z., Tappero, R., Rinklebe, J., Sparks, D.L., 2017. Sea level rise induced arsenic release from historically contaminated coastal soils. *Environ. Sci. Technol.* 51, 5913-5922. <https://doi.org/10.1021/acs.est.6b06152>
- Liu, G., Fernandez, A., Cai, Y., 2011. Complexation of arsenite with humic acid in the presence of ferric iron. *Environ. Sci. Technol.* 45, 3210-3216. <https://doi.org/10.1021/es102931p>
- Lu, R., 2000. *Analytical Methods for Soil Agrochemistry*, Chinese Agricultural Science and Technology Publishing House, Beijing.
- Lyu, H., Tang, J., Cui, M., Gao, B., Shen, B., 2020. Biochar/iron (BC/Fe) composites for soil and groundwater remediation: Synthesis, applications, and mechanisms. *Chemosphere* 246, 125609. <https://doi.org/10.1016/j.chemosphere.2019.125609>
- MEE, C., 2018. Soil Environmental Quality Risk Control Standard for Soil Contamination of Agricultural Land.
- Mensah, A.K., Marschner, B., Shaheen, S.M., Wang, J., Wang, S.-L., Rinklebe, J., 2020. Arsenic contamination in abandoned and active gold mine spoils in Ghana: Geochemical fractionation, speciation, and assessment of the potential human health risk. *Environ. Pollut.*, 114116. <https://doi.org/10.1016/j.envpol.2020.114116>
- Michalkova, Z., Komarek, M., Veselska, V., Cihalova, S., 2016. Selected Fe and Mn (nano)oxides as perspective amendments for the stabilization of As in contaminated soils. *Environ. Sci. Pollut. Res.* 23, 10841-10854. <https://doi.org/10.1007/s11356-016-6200-9>
- Mikutta, C., Kretzschmar, R., 2011. Spectroscopic evidence for ternary complex formation between arsenate and ferric Iron complexes of humic substances. *Environ. Sci. Technol.* 45, 9550-9557. <https://doi.org/10.1021/es202300w>
- Nie, C., Yang, X., Niazi, N.K., Xu, X., Wen, Y., Rinklebe, J., Ok, Y.S., Xu, S., Wang, H., 2018. Impact of sugarcane bagasse-derived biochar on heavy metal availability and microbial activity: A field study. *Chemosphere* 200, 274-282. <https://doi.org/10.1016/j.chemosphere.2018.02.134>
- Pan, H., Yang, X., Chen, H., Sarkar, B., Bolan, N., Shaheen, S. M., Wu, F., Che, L., Ma, Y., Rinklebe, J., Wang,

- H., 2021. Pristine and iron-engineered animal- and plant-derived biochars enhanced bacterial abundance and immobilized arsenic and lead in a contaminated soil. *Sci. Total Environ.* 763, 144218. <https://doi.org/10.1016/j.scitotenv.2020.144218>
- Perez, J.P.H., Tobler, D.J., Thomas, A.N., Freeman, H.M., Dideriksen, K., Radnik, J., Benning, L.G., 2019. Adsorption and reduction of arsenate during the Fe²⁺-induced transformation of ferrihydrite. *ACS Earth Space Chem.* 3, 884-894. <https://doi.org/10.1021/acsearthspacechem.9b00031>
- Premarathna, K.S.D., Rajapaksha, A.U., Sarkar, B., Kwon, E.E., Bhatnagar, A., Ok, Y.S., Vithanage, M., 2019. Biochar-based engineered composites for sorptive decontamination of water: A review. *Chem. Eng. J.* 372, 536-550. <https://doi.org/10.1016/j.cej.2019.04.097>
- Prietzl, J., Thieme, J., Eusterhues, K., Eichert, D., 2007. Iron speciation in soils and soil aggregates by synchrotron-based X-ray microspectroscopy (XANES, μ -XANES). *Eur. J. Soil Sci.* 58, 1027-1041. <https://doi.org/10.1111/j.1365-2389.2006.00882.x>
- Qiao, J., Yu, H., Wang, X., Li, F., Wang, Q., Yuan, Y., Liu, C., 2019. The applicability of biochar and zero-valent iron for the mitigation of arsenic and cadmium contamination in an alkaline paddy soil. *Biochar* 1, 203-212. <https://doi.org/10.1007/s42773-019-00015-4>
- Ravel, B., Newville, M., 2005. ATHENA, ARTEMIS, HEPHAESTUS: data analysis for X-ray absorption spectroscopy using IFEFFIT. *J. Synchrotron Radiat.* 12, 537-541. <https://doi.org/10.1107/S0909049505012719>
- Rawson, J., Prommer, H., Siade, A., Carr, J., Berg, M., Davis, J.A., Fendorf, S., 2016. Numerical modeling of arsenic mobility during reductive iron-mineral transformations. *Environ. Sci. Technol.* 50, 2459-2467. <https://doi.org/10.1021/acs.est.5b05956>
- Reddy, R., Delaune, R.D., 2008. *Biogeochemistry of Wetlands: Science and Applications*, CRC Press: Boca Raton, FL.
- Rinklebe, J., Shaheen, S.M., Yu, K.W., 2016b. Release of As, Ba, Cd, Cu, Pb, and Sr under pre-definite redox conditions in different rice paddy soils originating from the USA and Asia. *Geoderma* 270, 21-32. <https://doi.org/10.1016/j.geoderma.2015.10.011>
- Rupp, H., Rinklebe, J., Bolze, S., Meissner, R., 2010. A scale-dependent approach to study pollution control processes in wetland soils using three different techniques. *Ecological Engineering* 36, 1439-1447. <https://doi.org/10.1016/j.ecoleng.2010.06.024>
- Shaheen, S.M., Antoniadis, V., Kwon, E., Song, H., Wang, S.L., Hseu, Z.Y., Rinklebe, J., 2020. Soil contamination by potentially toxic elements and the associated human health risk in geo- and anthropogenic contaminated soils: A case study from the temperate region (Germany) and the arid region (Egypt). *Environ. Pollut.* 262. <https://doi.org/10.1016/j.envpol.2020.114312>
- Shaheen, S. M., El-Naggar, A., Wang, J., Hassan, N. E. E., Niazi, N. K., Wang, H., Tsang, D. C. W., Ok, Y. S., Bolan, N., Rinklebe, J., 2019. Biochar as an (im)mobilizing agent for the potentially toxic elements in contaminated soils. In: Ok, Y.S., Tsang, D. (Eds.), *Biochar from Biomass and Waste*. Elsevier, New York, USA, pp. 256-274.
- Shaheen, S.M., Rinklebe, J., Frohne, T., White, J.R., DeLaune, R.D., 2014. Biogeochemical Factors Governing Cobalt, Nickel, Selenium, and Vanadium Dynamics in Periodically Flooded Egyptian North Nile Delta Rice Soils. *Soil Sci. Soc. Am. J.* 78, 1065-1078. <https://doi.org/10.2136/sssaj2013.10.0441>
- Sharma, P., Ofner, J., Kappler, A., 2010. Formation of binary and ternary colloids and dissolved complexes of organic matter, Fe and As. *Environ. Sci. Technol.* 44, 4479-4485. <https://doi.org/10.1021/es100066s>
- Shi, Z., Hu, S., Lin, J., Liu, T., Li, X., Li, F., 2020. Quantifying microbially mediated kinetics of ferrihydrite transformation and arsenic reduction: role of the arsenate-reducing gene expression pattern. *Environ. Sci.*

- Technol. 54 (11), 6621-6631. <https://doi.org/10.1021/acs.est.9b07137>
- Van der Zee, F.P., Cervantes, F.J., 2009. Impact and application of electron shuttles on the redox (bio)transformation of contaminants: A review. *Biotechnol. Adv.* 27, 256-277. <https://doi.org/10.1016/j.biotechadv.2009.01.004>
- Van Vinh, N., Zafar, M., Behera, S.K., Park, H.S., 2014. Arsenic(III) removal from aqueous solution by raw and zinc-loaded pine cone biochar: equilibrium, kinetics, and thermodynamics studies. *Int. J. Environ. Sci. Technol.* 12, 1283-1294. <https://doi.org/10.1007/s13762-014-0507-1>
- Vithanage, M., Herath, I., Joseph, S., Bundschuh, J., Bolan, N., Ok, Y.S., Kirkham, M.B., Rinklebe, J., 2017. Interaction of arsenic with biochar in soil and water: A critical review. *Carbon* 113, 219-230. <https://doi.org/10.1016/j.carbon.2016.11.032>
- Wen, E., Yang, X., Chen, H., Shaheen, S.M., Sarkar, B., Xu, S., Song, H., Liang, Y., Rinklebe, J., Hou, D., Li, Y., Wu, F., Pohořelý, M., Wong, J.W.C., Wang, H., 2021a. Iron-modified biochar and water management regime-induced changes in plant growth, enzyme activities, and phytoavailability of arsenic, cadmium and lead in a paddy soil. *J. Hazard. Mater.* 407, 124344. <https://doi.org/10.1016/j.jhazmat.2020.124344>
- Wenzel, W.W., Kirchbaumer, N., Prohaska, T., Stingeder, G., Lombi, E., Adriano, D.C., 2001. Arsenic fractionation in soils using an improved sequential extraction procedure. *Anal. Chim. Acta* 436, 309-323. [https://doi.org/10.1016/S0003-2670\(01\)00924-2](https://doi.org/10.1016/S0003-2670(01)00924-2)
- Wen, Z., Xi, J., Lu, J., Zhang, Y., Cheng, G., Zhang, Y., Chen, R., 2021b. Porous biochar-supported MnFe₂O₄ magnetic nanocomposite as an excellent adsorbent for simultaneous and effective removal of organic/inorganic arsenic from water. *J. Hazard. Mater.* 411, 124909. <https://doi.org/10.1016/j.jhazmat.2020.124909>
- Wu, C., Cui, M., Xue, S., Li, W., Huang, L., Jiang, X., Qian, Z., 2018a. Remediation of arsenic-contaminated paddy soil by iron-modified biochar. *Environ. Sci. Pollut. Res.* 25, 20792-20801. <https://doi.org/10.1007/s11356-018-2268-8>
- Wu, S., Fang, G., Wang, D., Jaisi, D.P., Cui, P., Wang, R., Wang, Y., Wang, L., Sherman, D.M., Zhou, D., 2018b. Fate of As(III) and As(V) during microbial reduction of arsenic-bearing ferrihydrite facilitated by activated carbon. *ACS Earth Space Chem.* 2, 878-887. <https://doi.org/10.1021/acsearthspacechem.8b00058>
- Xiao, W., Jones, A.M., Li, X., Collins, R.N., Waite, T.D., 2017. Effect of shewanella oneidensis on the kinetics of Fe(II)-catalyzed transformation of ferrihydrite to crystalline iron oxides. *Environ. Sci. Technol.* 52, 114-123. <https://doi.org/10.1021/acs.est.7b05098>
- Yang, P.-T., Hashimoto, Y., Wu, W.-J., Huang, J.-H., Chiang, P.-N., Wang, S.-L., 2020a. Effects of long-term paddy rice cultivation on soil arsenic speciation. *J. Environ. Manage.* 254, 109768. <https://doi.org/10.1016/j.jenvman.2019.109768>
- Yang, P.-T., Wu, W.-J., Hashimoto, Y., Huang, J.-H., Huang, S.-T., Hseu, Z.-Y., Wang, S.-L., 2020b. Evolution of As speciation with depth in a soil profile with a geothermal As origin. *Chemosphere* 241, 124956. <https://doi.org/10.1016/j.chemosphere.2019.124956>
- Yang, X., Liu, J., McGrouther, K., Huang, H., Lu, K., Guo, X., He, L., Lin, X., Che, L., Ye, Z., Wang, H., 2016. Effect of biochar on the extractability of heavy metals (Cd, Cu, Pb, and Zn) and enzyme activity in soil. *Environ. Sci. Pollut. Res.* 23, 974-984. <https://doi.org/10.1007/s11356-015-4233-0>
- Yang, X., Lu, K., McGrouther, K., Lei, C., Hu, G., Wang, Q., Liu, X., Shen, L., Huang, H., Ye, Z., Wang, H., 2017. Bioavailability of Cd and Zn in soils treated with biochars derived from tobacco stalk and dead pigs. *J. Soil. Sediment.* 17, 751-762. <https://doi.org/10.1007/s11368-015-1326-9>
- Yu, K., Rinklebe, J., 2011. Advancement in soil microcosm apparatus for biogeochemical research. *Ecol. Eng.* 37, 2071-2075. <https://doi.org/10.1016/j.ecoleng.2011.08.017>

- Yang, X., Pan, H., Shaheen, S.M., Wang, H., Rinklebe, J., 2021a. Immobilization of cadmium and lead using phosphorus-rich animal-derived and iron-modified plant-derived biochars under dynamic redox conditions in a paddy soil. *Environ. Int.* 156, 106628. <https://doi.org/10.1016/j.envint.2021.106628>
- Yin, D., Wang, X., Peng, B., Tan, C., Ma, L.Q., 2017. Effect of biochar and Fe-biochar on Cd and As mobility and transfer in soil-rice system. *Chemosphere* 186, 928-937. <https://doi.org/10.1016/j.chemosphere.2017.07.126>
- Yu, K.W., Rinklebe, J., 2011. Advancement in soil microcosm apparatus for biogeochemical research. *Ecol. Eng.* 37, 2071-2075. <https://doi.org/10.1016/j.ecoleng.2011.08.017>
- Zeien, H., Brümmer, G.W., 1989. Chemische Extraktion zur Bestimmung von Schwermetallbindungsformen in Boden. *Mitt. Dtsch. Bodenkd. Ges.* 59, 505-510.
- Zhang, J.Y., Zhou, H., Gu, J.F., Huang, F., Yang, W.J., Wang, S.L., Yuan, T.Y., Liao, B.H., 2020. Effects of nano-Fe₃O₄-modified biochar on iron plaque formation and Cd accumulation in rice (*Oryza sativa* L.). *Environ. Pollut.* 260, 113970. <https://doi.org/10.1016/j.envpol.2020.113970>
- Zhong, D., Jiang, Y., Zhao, Z., Wang, L., Chen, J., Ren, S., Liu, Z., Zhang, Y., Tsang, D.C.W., Crittenden, J.C., 2019. pH dependence of arsenic oxidation by rice-husk-derived biochar: roles of redox-active moieties. *Environ. Sci. Technol.* 53, 9034-9044. <https://doi.org/10.1021/acs.est.9b00756>
- Zhu, Y.-G., Xue, X.-M., Kappler, A., Rosen, B.P., Meharg, A.A., 2017. Linking Genes to Microbial Biogeochemical Cycling: Lessons from Arsenic. *Environ. Sci. Technol.* 51, 7326-7339. <https://doi.org/10.1021/acs.est.7b00689>

CHAPTER 4: Effects of Phosphorus- and Iron-Rich Biochars on Cadmium and Lead Mobilization under Fluctuating Controlled Redox Conditions in Paddy Soil ³



³ Adapted from Yang, X., Pan, H., Shaheen, S.M., Wang, H., Rinklebe, J., 2021. Immobilization of cadmium and lead using phosphorus-rich animal-derived and iron-modified plant-derived biochars under dynamic redox conditions in a paddy soil. *Environment International* 156, 106628.

A supplementary data is provided in Appendix C.

Abstract

Functionalized biochar has gained extensive interests as a sustainable amendment for an effective remediation of paddy soils contaminated with heavy metals (HMs). We examined the efficiency of pig carcass-derived biochar (P-rich biochar, total P = 8.3%) and pristine (raw biochar, total Fe = 0.76%) and Fe-modified (Fe-rich biochar, total Fe = 5.5%) green waste-derived biochars for the immobilization of cadmium (Cd) and lead (Pb) in a paddy soil under pre-defined redox conditions (Eh, from -400 to +300 mV). Average concentrations ($\mu\text{g L}^{-1}$) of dissolved Cd increased under reducing conditions up to 10.9 in the control soil, and decreased under oxidizing conditions to below the detection limit (LDL= 2.7) in the raw and Fe-rich biochar treated soils. Application of the raw biochar decreased the concentrations of dissolved Cd by 43-59% under $E_h \leq -100$ mV, compared to the non-treated control, which was more effective than the Fe-rich biochar (31-59%) and the P-rich biochar (8-19%). The immobilization of Cd under low Eh might be due to its precipitation with sulfide (S^{2-}), whereas its immobilization under high Eh might be due to the associated increase of pH. Concentrations ($\mu\text{g L}^{-1}$) of Pb ranged from 29.4 to 198.2 under reducing conditions, and decreased to LDL (12.5) under oxidizing conditions. The P-rich biochar was more effective on immobilizing Pb than the raw and Fe-rich biochars, particularly under $E_h \leq 0$ mV (55-82%), which might be due to the retention of Pb by phosphates. The raw and Fe-rich biochars immobilized Pb under low Eh (≤ -300 mV), but both biochars, particularly the Fe-rich biochar mobilized Pb under Eh higher than -200 mV, especially at +100 mV, due to the decrease of pH at this point (pH = 6.0 to 6.5). These results improved our understanding of using P-rich and Fe-rich functionalized biochars for the immobilization of Cd and Pb in a paddy soil under stepwise redox changes. The amendment of P-rich pig carcass-derived biochar to paddy soils could be a promising approach for mitigating the risk of Pb for human health and the environment. The raw and Fe-rich green waste-derived biochars can be used for immobilizing Cd and mitigating its risk in paddy soils under both reducing and oxidizing conditions.

Keywords: Heavy metal; Paddy soil; Redox change; Feedstock; Modified biochar; Gentle remediation

4.1 Introduction

Contamination of agricultural soils with heavy metals (HMs), such as cadmium (Cd) and lead (Pb), is a global concern due to its severe risks to the food security and human health (Isinkaye, 2018; Antoniadis et al., 2019; El Rasafi et al., 2021). Cadmium and Pb are released into the soil often by anthropogenic activities such as excessive agricultural inputs, wastewater irrigation, coal burning, mining and smelting, waste dumping (Palansooriya et al., 2020; Wang et al., 2021). Between 2005 and 2013, an intensive Chinese national survey of soils was conducted covering more than 70% of land area in China (Zhao et al., 2015). The results demonstrated that 19.4% of the collected agricultural soil samples (equivalent to approximately 26 million ha) are contaminated according to the China National Environmental Quality Standard for Soils (Zhao et al., 2015), whereas Cd and Pb rank at the first (7.0%) and fifth (1.5%) positions, respectively (Ministry of Environmental Protection P.R.C. and Ministry of Land and Resources P.R.C., 2014). Rice is one of the most important cereal foods for half of the population worldwide; it can accumulate HMs and can be an important source of HMs in the human body (Kashif Irshad et al., 2020; Li et al., 2020). In China, a considerable area of paddy soils is co-contaminated with Cd and Pb, rather than single-metal contamination (Hamid et al., 2020). A sustainable management of those soils with a view to mitigating the mobilization and availability of Cd and Pb simultaneous in paddy soils is therefore an urgent issue for maintaining human health.

Considerable studies showed that soil contaminated with Cd and Pb could be remediated by biochar, due to its favorable properties, such as liming effect, large surface area, high cation exchange capacity, porous structure, negatively charged surface and presence of oxygen-containing functional groups (e.g., Yang et al., 2016; Beiyuan et al., 2020). However, the remediation efficiency of pristine biochar for HMs is limited and could be enhanced by physical and chemical modifications (e.g., Chen et al., 2019a; Lyu et al., 2020; Wang et al., 2020). The modification of biochar aiming to achieve superior performance in HM immobilization is a hot spot of recent research, including introduction of organic or inorganic materials such as iron (Fe) compounds (Bian et al., 2018; Kashif Irshad et al., 2020) and phosphate (P) materials (Chen et al., 2019a; Zhang et al., 2020). In addition, the fluctuation of Eh in paddy soils, generally caused by dynamic and variable hydrological regimes, critically affects the transformation and speciation of Fe and P, thereby influencing the geochemical transformation of HMs (Yuan et al., 2017; Rapin et al., 2019; Cui et al., 2020). Moreover, the mobilization of Cd and Pb could be also influenced by the redox-induced changes such as pH, dissolved organic carbon (DOC), sulfur (S), manganese (Mn), in temporarily flooded paddy soils (e.g., Rinklebe et al., 2016a; El-Naggar et al., 2018; Beiyuan et al., 2020).

Phosphorus-rich materials can stabilize Cd and Pb in soils through formation of insoluble metal-phosphate

precipitates (Xenidis et al., 2010; Cui et al., 2020; Azeem et al., 2021; Wang et al., 2021). For instance, Zhang et al. (2020) indicated that husk and cornstalk biochars modified by potassium phosphate had high immobilization efficiency for Cd. Netherway et al. (2019) found a higher amount of stable Pb-phosphate and pyromorphite in the P-rich biochar-treated soil as compared to the non-treated control. In our previous studies, a biochar produced through pyrolyzing pig carcasses at a final temperature of 650°C was effective on remediating contaminated soils (Chen et al., 2019b), promoting plant growth (Yang et al., 2017a), improving soil nutrient status (Chen et al., 2020), and mitigating the leaching loss of nitrogen from soils (Feng et al., 2020). However, no attempt has been made to investigate the impact of pig biochar as a P-rich material for a simultaneous immobilization of Cd and Pb in co-contaminated paddy soils, especially under dynamic redox (Eh) conditions.

Iron-containing materials, such as Fe (hydro)oxides, Fe sulfides, nano zero-valent Fe and goethite have been used for the modification of biochar to improve its effectiveness on immobilization of HMs (e.g., Bian et al., 2018; Rajendran et al., 2019). For example, Kashif Irshad et al. (2020) reported that the incorporation of the goethite-modified biochar was more effective on decreasing Cd mobilization than the raw biochar. Yu et al. (2020) reported that application of *Pennisetum sinense Roxb* and coffee grounds biochars coupled with the iron fertilizer significantly decreased the exchangeable and reducible Cd and Pb in a contaminated soil. Wen et al. (2021) indicated that the modification of green waste biochar using FeCl₃ enhanced its ability for reducing the uptake of As by rice plants. However, to our knowledge, no study has focused on the impact of Fe-based biochar amendment on (im)mobilization of Cd and Pb, as well as the underlying geochemical mechanisms in paddy soils under a wide range of pre-defined Eh conditions.

We hypothesized that the incorporation of animal-derived P-rich biochar and raw and Fe-rich plant-derived biochar have a certain impact on the Eh and the redox-induced soil biochemical processes and controlling factors (e.g., pH, Fe-Mn oxides, DOC, sulfur). In turn, the redox-induced transformation and speciation of P and Fe may enhance the immobilization of Cd and Pb in the paddy soil via formation of stable metal-P and metal-Fe precipitates and complexes. To test our hypothesis, we aimed to 1) quantify the impact of two functionalized biochars i.e., the pig carcass-derived (P-rich) biochar and the iron-modified green waste-derived (Fe-rich) biochar, as well as the pristine green waste-derived (raw) biochar (as a comparison) on the release dynamics of Cd and Pb in a paddy soil under a wide range of controlled redox conditions, and 2) to elucidate the interactions between biochars and Cd and Pb as affected by the redox-dependent changes in controlling factors (e.g., pH, Fe-Mn oxides, DOC, sulfur).

4.2 Materials and methods

4.2.1 Soil collection and characterization

Soil was taken from a paddy field in a small village in the east of Shaoxing City, Zhejiang Province, China (29°59' N, 120°46' E). This site is located in the Middle-Lower Yangtze plain, which is one of the main rice cultivation regions in China. Soil samples were passed through a 3-mm sieve after air-drying. The total concentrations of Cd (0.5 mg kg⁻¹) and Pb (736 mg kg⁻¹) exceeded the risk screening value of Cd (0.4 mg kg⁻¹) and the risk intervention value of Pb (500 mg kg⁻¹), respectively, according to the Soil Environmental Quality Risk Control Standard for Soil Contamination of Agricultural Land (GB15618-2018) (Ministry of Ecology and Environment of China, 2018). The soil had a content of 1.3% of organic carbon. The electrical conductivity and cation exchange capacity were 0.05 dS m⁻¹ and 13.4 cmol kg⁻¹, respectively. The total concentrations of Fe and Mn were 30.5 and 0.9 g kg⁻¹, respectively.

Table 4-1 Properties of used P-rich, raw and Fe-rich biochars.

Properties	P-rich biochar	Raw biochar	Fe-rich biochar
pH (H ₂ O)	10.6	9.3	4.4
Electrical conductivity (mS cm ⁻¹)	2.0	0.4	4.5
Total C (%)	30.8	69.3	59.9
Total N (%)	2.1	1.1	0.9
Total H (%)	1.3	2.7	2.2
Total S (%)	0.2	0.4	0.2
Surface area (m ² g ⁻¹)	18.4	110.7	74.5
Ash content (%)	50.9	9.7	15.3
Total P (g kg ⁻¹)	82.8	1.9	3.0
Total Fe (g kg ⁻¹)	20.6	7.6	54.6
Total Cd (mg kg ⁻¹)	ldl	ldl	ldl
Total Pb (mg kg ⁻¹)	1.6	7.0	11.4

ldl: lower than detection limits.

4.2.2 Biochar preparation and methods of characterization

The pig carcass-derived biochar, produced via pyrolyzing dead pig bodies at a final temperature of 650°C for approximately 2 h using a batch pyrolysis facility according to the description of the local producer (Zhejiang Eco Environmental Technology Co., Ltd.), was defined as “P-rich biochar” due to its high total P concentration (> 80 g kg⁻¹) (Table 4-1). The biochar defined here as “raw biochar” was produced from pyrolyzing the branches of oriental plane (*Platanus orientalis* L.) in a lab-scaled pyrolysis facility at a peak temperature of 650°C for approximately 2 h. The “Fe-rich biochar” was produced by immersing the raw biochar into a FeCl₃ solution with a weight ratio of 1: 20 for Fe and biochar (Dong et al., 2016; Wen et al., 2021). Briefly, the mixture was stirred

and then thoroughly mixed under ultrasound for approximately 1 h. Subsequently, the substance was oven-dried at around 70°C until only the solid materials were left. At last, the solid substances were pyrolyzed once more at 650°C for 1 h using the same facility to obtain the Fe-rich biochar (Fe concentration = 54.6 mg kg⁻¹) (Table 4-1). The biochar samples were crushed and sieved through a 2-mm sieve. Selected properties of biochars (Table 4-1) were analyzed according to IBI Biochar Standards (2015). Furthermore, various advanced spectroscopic techniques including scanning electron microscopy (SEM) coupled with an energy dispersive X-ray spectroscopy (EDX) (Hitachi S-4800 with ISIS 310, Japan) and Fourier transform infrared spectrometer (FTIR) (Nicolet iS10, USA) were used to characterize the biochars.

4.2.3 Biochar characteristics

The SEM images (Figure 4-1) exhibited that the P-rich biochar had an irregular structure, where a porous structure was not obvious. The raw biochar had a porous structure where the pores were distributed in honeycomb shape with distinct edges. The Fe-rich biochar presented a destroyed porous structure with rough and irregular morphology, as the cell walls were fragmentary and the pores were partly blocked by some small debris. The contrasting difference between the animal-derived P-rich biochar and the plant-derived raw biochar could be attributed to the nature of feedstocks. However, the difference between the Fe-rich biochar and the raw biochar might be caused by the mechanical damage during the Fe-loading process. The morphological characteristics of biochars agreed with their surface areas, as the raw biochar had larger surface area than the other two biochars (Table 4-1).

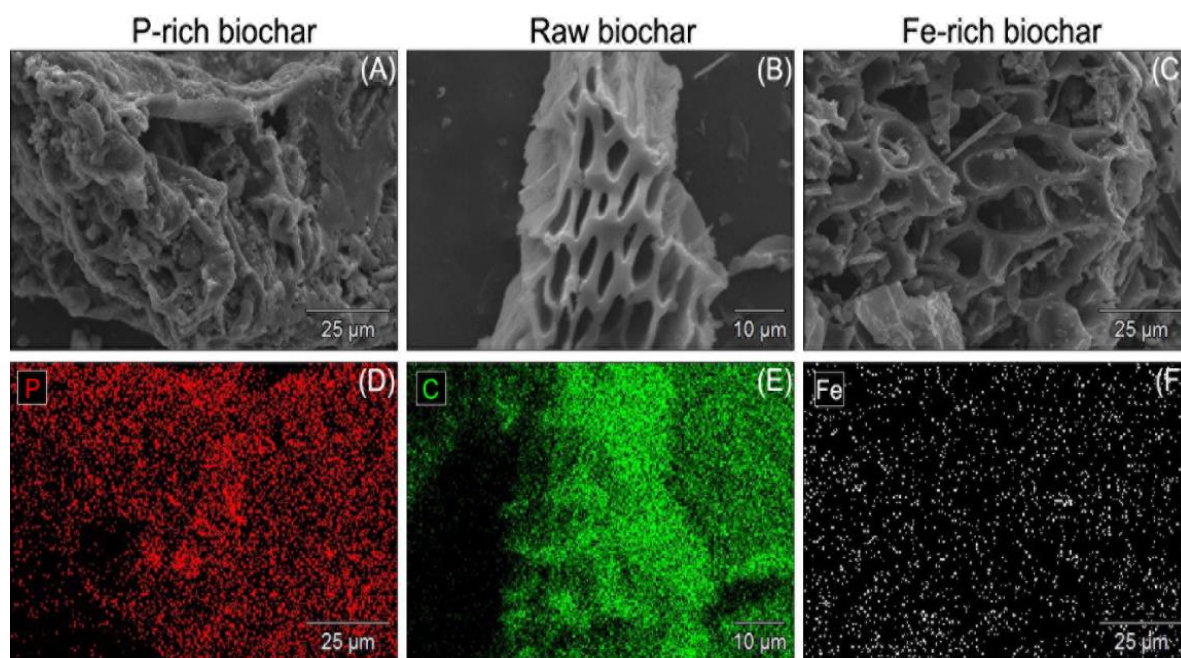


Figure 4-1 Scanning electron microscope images (SEM, A-C) and SEM-EDX K α maps (D-F) of biochars.

The SEM-EDX $K\alpha$ maps showed that P, C and Fe were evenly distributed on the surface of the P-rich biochar, raw biochar and Fe-rich biochar, respectively (Figure 4-1). Moreover, high abundance of P, C and Fe were illustrated in the EDX patterns, respectively (Figure 4-2). Higher abundance of the mineral elements in the Fe-rich biochar might be due to the concentrating during the modification process (e.g., re-pyrolysis). This assumption agreed with the lower C and N content but higher ash content of the Fe-rich biochar compared to those of the raw biochar (Table 4-1), as the mineral elements might be concentrated after the loss of volatile materials from the further decomposition of organic matters caused by re-pyrolysis (Yang et al., 2017b). The FTIR spectrum of the P-rich biochar (Figure 4-2) indicated the presence of functional groups such as hydroxyl groups ($-\text{OH}$, 3400 cm^{-1}), aromatic $\text{C}=\text{C}$, $\text{C}=\text{O}$ and/or $-\text{COO}^-$ anti-symmetric stretching ($1400\sim 1600\text{ cm}^{-1}$) and $\text{C}-\text{OH}/\text{C}-\text{C}$ stretching or carbonate (1100 cm^{-1}) (Yang et al., 2017a; Chen et al., 2019b). However, less and weaker adsorption peaks were found on the FTIR spectra of the other two biochars, indicating less functional groups on these two biochars than that on the P-rich biochar. The presence of different oxygen containing functional groups will affect their ability to immobilize dissolved Cd and Pb species as discussed in section 4.3.3.

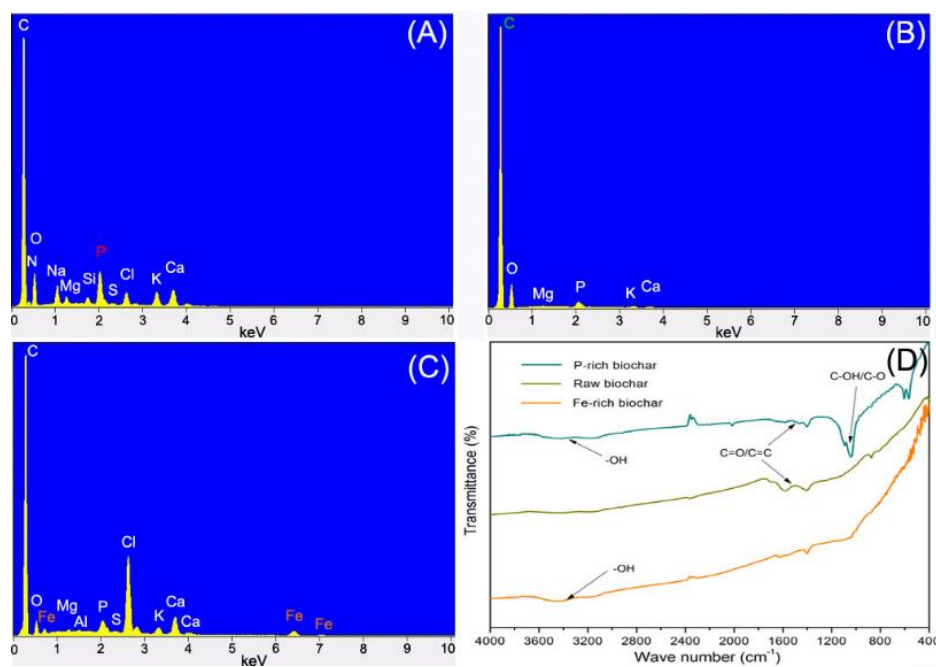


Figure 4-2 Energy dispersive X-ray patterns (A: P-rich biochar; B: raw biochar; C: Fe-rich biochar) and Fourier transform infrared spectra (D) of biochars.

4.2.4 Pre-incubation of soil

A 30-day pre-incubation experiment was carried out to allow a proper stabilization of biochars after application into the soil. The pre-incubation was performed using 800 g of air-dried contaminated soil enclosed in a series of plastic beakers. The biochars were added into the beakers at 3% of the dry soil weight and mixed thoroughly with

soil. The non-treated soil served as control. Four independent replications were used for each treatment. All treatments including the control were incubated under continuous flooded conditions at 25°C. All beakers were watered with deionized water by maintaining 2~3 cm water layer on the top of the soil. After pre-incubation, the soil sample was collected from each beaker, air-dried, and ground to pass through a 2-mm sieve prior to the redox experiment. The sub-samples were used for the analyses of organic carbon, available P and Fe, as well as the geochemical fractions of Cd and Pb in soils. The analytical methods and results are provided in *Appendix C* (sections C1.1 and C2.1).

4.2.5 Redox experiment set up

A redox experiment was conducted using an automated biogeochemical microcosm (MC) system to simulate the flooding of the paddy soil in the laboratory conditions. Technical details about this system were described earlier (Frohne et al., 2011; Yu and Rinklebe, 2011). This equipment has been successfully used in earlier studies for assessing the release behaviors of HMs in soils and sediments (e.g., Shaheen and Rinklebe, 2017; Rinklebe et al., 2020; Shaheen et al., 2020). In total, sixteen MCs were employed for the redox experiment using the control and the three biochar-amended soils in four independent replicates each. For each MC, 210 g of pre-incubated soil and 1.68 L of tap water were added into a glass vessel with an air-tight lid to maintain a ratio of 1:8 for soil and water. Additionally, 5 g of glucose and 10 g of rice straw were added to provide sufficient amount of organic carbon, which served as nutrients for microorganisms. The system is equipped with a stirrer, a platinum (Pt) Eh electrode with a silver-silver chloride (Ag/AgCl) reference electrode (EMC 33), a pH electrode (EGA 153), and a temperature electrode (Pt 100) (all: Meinsberger Elektroden, Ziegra-Knobeldorf, Germany). The MC system enables us to adjust the Eh to pre-defined conditions, which allows the simulation of various anoxic/oxic cycles that may occur in the soils when the water level changes. The system allows automatic control of Eh by adding nitrogen to lower Eh or synthetic air/oxygen to increase Eh. At first, the soil samples were incubated and left to react naturally. Two h after flooding we performed the initial sampling at ca. +200 mV. Thereafter, the redox potential was forced to reducing conditions (targeted -400 mV) by purging with nitrogen; thereafter from reducing to oxidizing conditions (targeted +300 mV) by purging with synthetic air (20% oxygen+80% nitrogen) or pure oxygen. The slurry was stirred continuously throughout the experiment. A data logger was used to record the Eh and pH values from each MC every 10 minutes. The Eh values were not calculated as a reference to the standard hydrogen electrode aiming to present the actual redox potential in relation to the solution.

The initial sampling was carried out 2 h after the start of the experiment. The 1st to 8th samplings were taken 48~72 h after reaching the stepwise targeted Eh window (-400, -300, -200, -100, 0, +100, +200 and +300 mV,

respectively). The slurry samples were taken from each MC at each defined Eh window, centrifuged at 5,000 rpm for 15 minutes, thereafter, the supernatant was passed through a 0.45- μm membrane filter (Whatman Inc., Maidstone, UK) in an anaerobic glove box (Whitley A35 Anaerobic Work Station, Don Whitley Scientific, Shipley, UK). The obtained filtrate was divided into several parts to analyze the concentrations of dissolved Cd, Pb, Fe, Mn, phosphate (PO_4^{3-}), sulfate (SO_4^{2-}), and ferrous iron (Fe^{2+}). The concentration of dissolved Cd, Pb, Fe and Mn in the filtrate was measured by an inductively coupled plasma optical spectroscopy (ICP-OES, Horiba Jobin Yvon, Uterhaching, Germany). The concentration of Fe^{2+} was measured using a colorimeter (CADAS 200, Dr. Lange, Germany) at 510 (Harvey et al., 1955), respectively. The concentration of PO_4^{3-} and SO_4^{2-} was measured using an ion chromatograph (Metrohm, Filderstadt, Germany). The concentration of DOC was analyzed by a total carbon analyzer (Analytik Jena, Germany).

4.2.6 Quality control and statistical analysis

Triplicate measurements and blanks were used in all analyses. The detected values with relative standard deviations larger than 10% were excluded. Analytical grade reagents were purchased from Sigma Aldrich and used in the analyses. Certified reference standard solutions (Merck) were used to guarantee high-quality results. The certified reference soil materials (BRM12, TMC, and TML) were used for the quality control of the extraction efficiency of the total content of Cd and Pb and the extraction recovery was 88-91% and 87-89%, respectively. The limits of quantification of Cd and Pb were 2.7 and 12.5 $\mu\text{g L}^{-1}$, respectively. For those values with relative standard deviation larger than 10% or lower than the limit of quantification, 1/8 of the limit of quantification was used for statistics.

The average values of Eh and pH collected at 6 h before sampling ($\text{Eh}_{6\text{h}}$ and $\text{pH}_{6\text{h}}$) were used for statistics according to Rinklebe et al. (2016a). The SPSS 18.0 software (SPSS Institute, USA) was employed to carry out statistical analyses. One-way analysis of variance (ANOVA) and Duncan's multiple range tests were used to assess the statistical significance between the treatments ($P < 0.05$). The correlations between Cd and Pb concentrations and the controlling factors (e.g., $\text{Eh}_{6\text{h}}$, $\text{pH}_{6\text{h}}$, Fe, Mn, Fe^{2+} , DOC and SO_4^{2-}) were analyzed based on the Pearson's correlation coefficients ($P < 0.05$). The factor analysis (principal component analysis) was conducted to determine the affinities among the Cd and Pb concentrations and the measured controlling factors. The canonical discrimination analysis was carried out to analyze the differences/similarities of the measured parameters in different treatments.

4.3 Results and discussion

4.3.1 Eh and pH

The Eh-pH diagrams of the average data are presented in Figure 4-3 and the data of the four replicates are presented in Figure 4-4. After flooding, the Eh of all treatments decreased rapidly in the first 50 h of the redox experiment, which shall be attributed to the oxygen consumption by microorganisms in the early stage of flooding. The achieved minimum redox values of the control, P-rich biochar, raw biochar and Fe-rich biochar treatments were -465, -457, -484 and -446 mV, and the maximum values were +293, +278, +281 and +359 mV, respectively (Table 4-2).

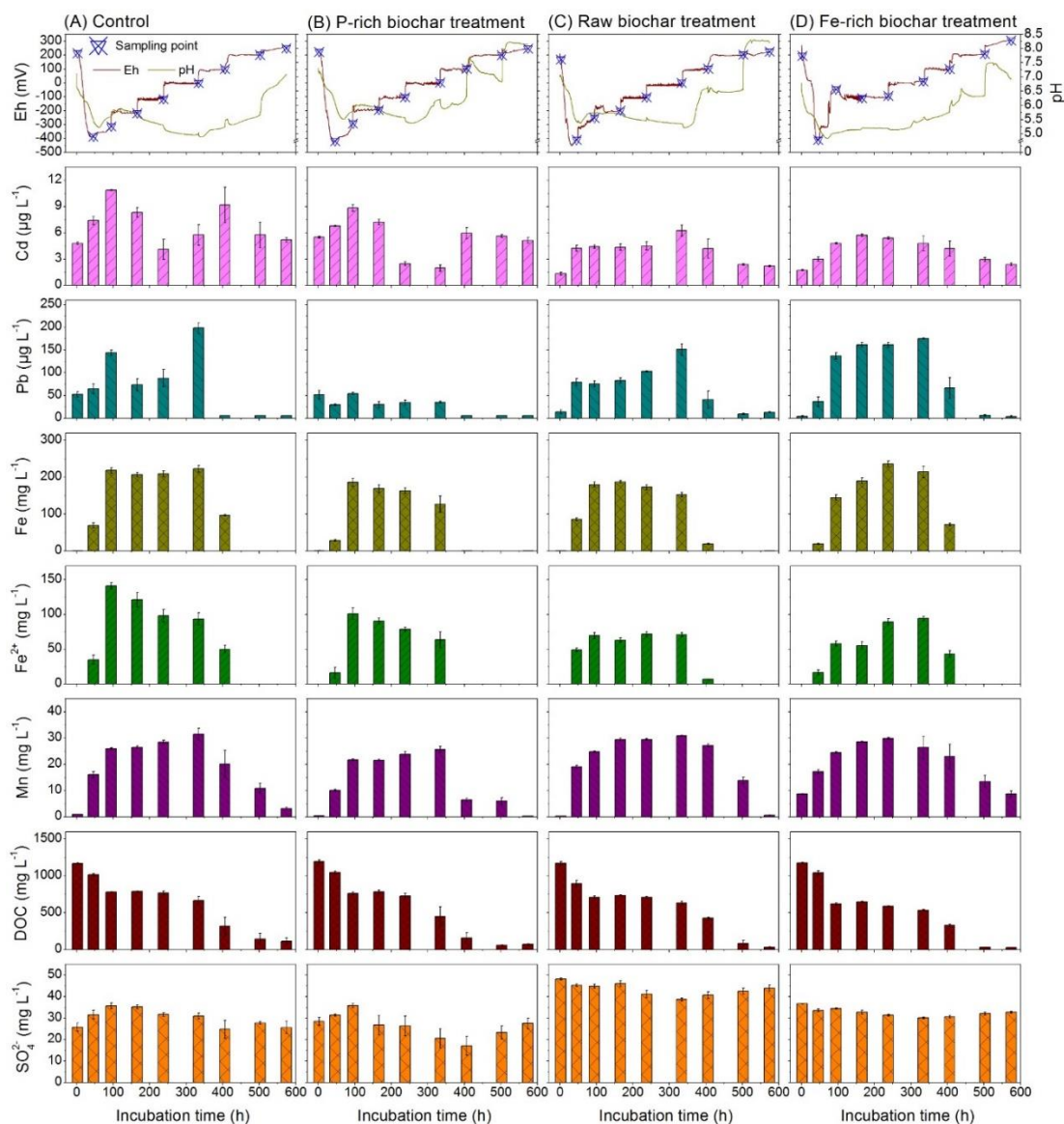


Figure 4-3 Effect of pre-defined Eh conditions on the concentration of dissolved Cd and Pb, as well as concentration of dissolved Fe, Mn and Fe^{2+} , DOC, SO_4^{2-} in control and biochar-treated soils.

Table 4-2 Variation of concentration of Eh, dissolved Cd and Pb and measured governing factors in the slurry of soil treated with different biochars (four replicates).

Parameter	Control				P-rich biochar treatment				Raw biochar treatment				Fe-rich biochar treatment			
	n	Minimum	Maximum	Mean	n	Minimum	Maximum	Mean	n	Minimum	Maximum	Mean	n	Minimum	Maximum	Mean
E _{H all} (mV)	13,778	-465	+293	-13.2	13,764	-457	+278	-15.2	13,774	-484	+281	-15.3	13,779	-446	+359	+44.8
E _{H 6h} (mV)	36	-386	+248	-34.8	36	-420	+247	-30.9	36	-436	+277	-35.5	36	-398	+352	+38.9
pH _{all}	13,775	4.3	7.6	5.6	13,777	5.1	8.9	6.4	13,779	4.8	8.8	6.1	13,780	4.6	7.8	5.9
pH _{6h}	36	5.0	7.1	5.8	36	5.5	8.1	6.5	36	5.1	8.7	6.2	36	4.8	7.4	6.0
Cd ($\mu\text{g L}^{-1}$)	36	2.5	13.2	7.0	36	1.5	9.6	5.6	36	1.0	7.6	3.8	36	1.6	6.3	4.0
Pb ($\mu\text{g L}^{-1}$)	36	5.3	221.5	67.2	36	5.3	76.9	28.3	36	6.1	171.9	68.1	36	5.3	179.1	105.2
Fe (mg L^{-1})	36	0.05	240.1	116.6	36	0.03	211.3	77.2	36	0.05	193.7	93.1	36	0.03	250.4	103.3
Mn (mg L^{-1})	36	0.9	35.2	18.8	36	0.4	28.1	13.5	36	0.35	28.09	12.90	36	6.8	31.2	20.1
Fe ²⁺ (mg L^{-1})	36	0	152.2	57.2	36	0	123.5	37.1	36	0	96.8	37.2	36	0	101.4	35.8
DOC (mg L^{-1})	36	46.5	1185.0	640.1	36	52.04	1257.2	584.8	36	15.4	1208.0	610.8	36	20.5	1198.2	564.1
SO ₄ ²⁻ (mg L^{-1})	36	13.2	42.1	28.5	36	8.0	38.5	26.4	36	37.0	49.6	43.6	36	29.2	37.0	32.8

The decrease of Eh at the beginning of the redox experiment was associated with a decrease in pH, which might be due to the formation of organic acids and CO₂ caused by the microbial decomposition of organic matters under anoxic conditions (Shaheen et al., 2014; Rinklebe et al., 2020). Increasing Eh values caused an increase of pH from 4.3, 5.1, 4.8, and 4.6 to 7.6, 8.9, 8.8, and 7.8 in the control, P-rich, raw, and Fe-rich biochar treatments, respectively (Figure 4-3, Table 4-2). Thus, a significant positive correlation ($P < 0.01$) between pH_{6h} and Eh_{6h} was observed (Figure 4-5). The increase of pH due to the addition of raw and P-rich biochars was stronger than the Fe-rich biochar as compared to the control, particularly under oxidizing conditions (Eh > +100 mV). The raw and P-rich biochars increased pH, whereas the Fe-rich biochar slightly decreased the pH, particularly under strongly reducing conditions (Figure 4-3). The modification of the raw biochar with FeCl₃ decreased its pH from 9.3 to 4.4 and thus the Fe-rich biochar application decreased pH as compared to the raw biochar treatment and control. These results agreed with the pH of soils after 30 days of pre-incubation, where the addition of P-rich and raw biochars increased, whereas Fe-rich biochar decreased the pH of soil (Figure 4-6). The change in soil pH could be ascribed to the alkalinity of P-rich and raw biochars as compared to those of the Fe-rich biochar (Table 4-1).

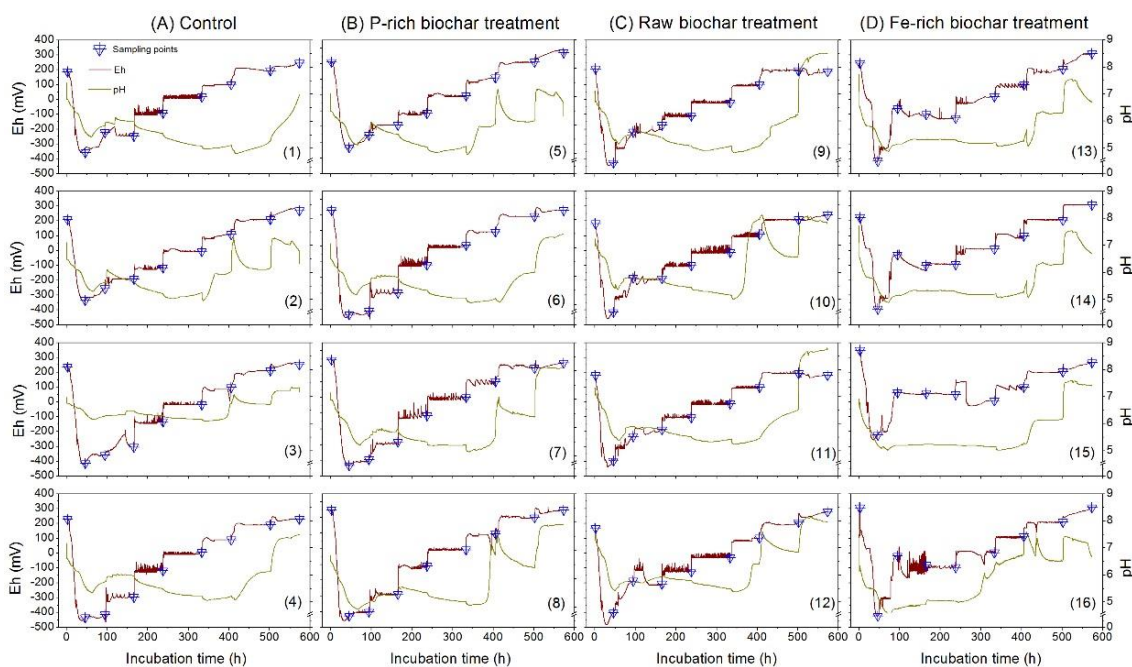


Figure 4-4 Dynamics of redox potential and pH in the microcosms with biochar-treated soils (each MC).

4.3.2 Redox-induced changes in pH, Fe, Mn, DOC, and S affect the mobilization of Cd and Pb

The concentrations of dissolved Cd and Pb varied with the change in Eh conditions in all treatments (Figure 4-3). The data of the four replicates (Table 4-2) showed that the concentrations of dissolved Cd ($\mu\text{g L}^{-1}$) varied from a value lower than detection limit (LDL=2.7) to 13.2 in the control, from LDL to 9.6 in the P-rich biochar, from

LDL to 7.6 in the raw biochar treatment, and from LDL to 6.3 in the Fe-rich biochar treatment. The concentrations of dissolved Pb ($\mu\text{g L}^{-1}$) ranged from LDL to 221.5 in the control, from 5.3 to 76.9 in the P-rich biochar treatment, from 6.1 to 171.9 in the raw biochar treatment, and from 5.3 to 179.1 in the Fe-rich biochar treatment, respectively (Table 4-2). The geochemical behaviors of Cd and Pb in soils seem to be influenced by the Eh and redox-induced alterations of pH, Fe, Mn, DOC, and sulfur (Rinklebe et al., 2016a; El-Naggar et al., 2018). The correlation analysis (Figure 4-5) and the factor analysis (use all treatments together) have been conducted (Figure 4-7) to test the impact of these governing factors on the mobilization of Cd and Pb.

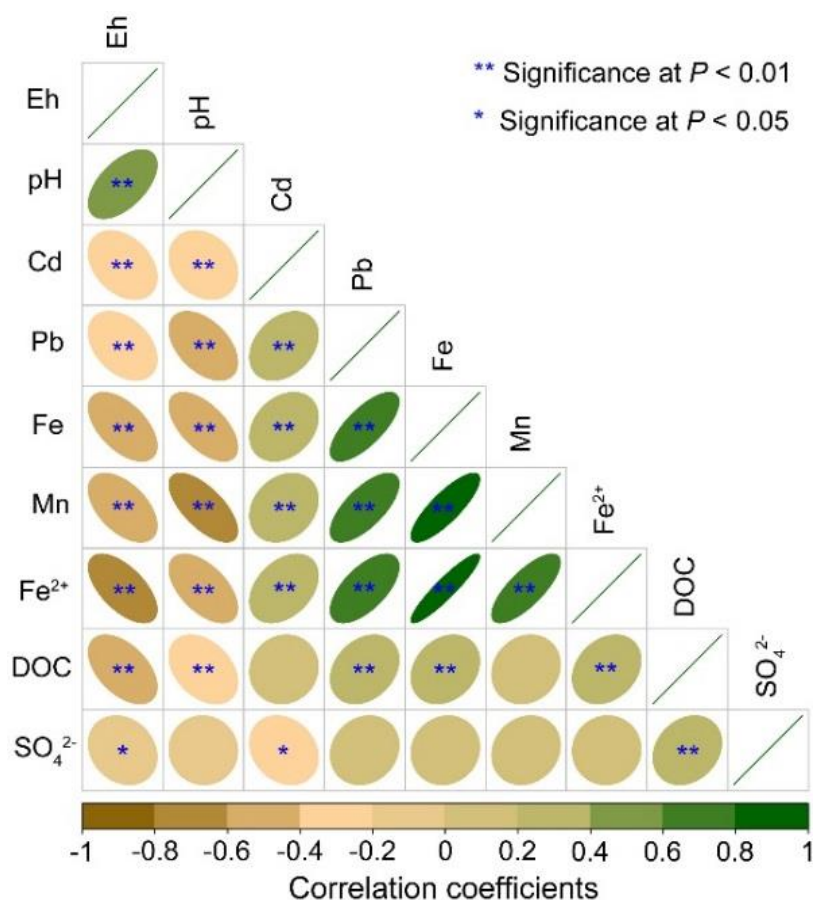


Figure 4-5 Correlation coefficients between the concentration of dissolved Cd, Pb and other measured geochemical factors (n=144).

According to the data, we proposed several possible mechanisms to interpret the variability of the observed dynamics of Cd and Pb as influenced by the Eh changes. The detected dissolved Cd and Pb in the initial sampling primarily depended on the concentration of water-soluble metals in the pre-incubated soils. Especially for Cd, the exchangeable fraction ranged between 18.3% and 23.7% (Figure 4-8), which was possibly a contributory factor for the presence of soluble metals in the initial samples. The rapid decrease of pH after flooding might result in an increase of the Cd and Pb mobilization, as a lower pH may trigger the formation of the soluble species of metals

and accelerate the desorption of metals from soil colloids due to the decreased cationic exchange sites (Rinklebe et al., 2016a; Beiyuan et al., 2020; Kashif Irshad et al., 2020). The low Cd and Pb mobilization under oxidizing conditions (> 100 mV) might be due to the elevated pH (Figure 4-3), which may cause an increase of the cationic exchange capacity of soil colloids and thus increase metal sorption (Shaheen et al., 2013; Seshadri et al., 2016; Rinklebe et al., 2020). Therefore, we postulate that the redox-induced change in pH is a predominant factor affecting the release dynamics of both metals. This assumption could be supported by the negative ($P < 0.01$) correlations between the concentrations of dissolved Cd and Pb and $\text{pH}_{6\text{h}}$ (Figure 4-5).

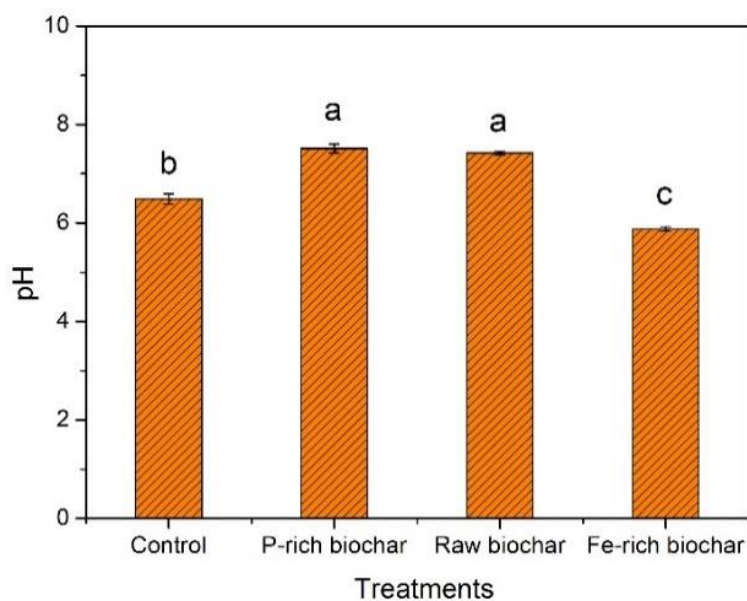


Figure 4-6 Effect of biochar application on the pH of the pre-incubated soils.

The factor analysis showed that Cd was associated in one cluster with SO_4^{2-} (Figure 4-7), indicating that the chemical behavior of sulfur was an important factor in altering the mobilization of Cd in our study. We assume that SO_4^{2-} could be reduced to sulfide (S^{2-}) under reducing conditions, according to the Eh-pH diagram described by Takeno (2005), the formation of S^{2-} occurred around -100 mV under acidic conditions. Thus, the formed S^{2-} may react with Cd to form insoluble precipitates, thereby decreasing the mobilization of Cd (Shaheen et al., 2016; Meng et al., 2019). In our experiment, insoluble CdS might be formed under reducing conditions (Eh = -200 ~ -100 mV), where a slight decrease of dissolved Cd was noticed (Figure 4-3). Later, the formed stable S^{2-} can be again oxidized to soluble SO_4^{2-} when the conditions changed from reducing to oxidizing (Rinklebe et al., 2016b; Shaheen et al. 2016). Hence, the high concentration of dissolved Cd under high Eh conditions ($> +100$ mV) might be ascribed to the oxidation of CdS and the release of Cd to soil solution. However, a negative correlation ($P < 0.05$) was found between the concentration of Cd and SO_4^{2-} in our study (Figure 4-5). This could be attributed to

the different orders of magnitude for Cd (LDL $\sim 13.2 \mu\text{g L}^{-1}$) and SO_4^{2-} ($8.0 \sim 49.6 \text{ mg L}^{-1}$) in our samples (Table 4-2). Therefore, we speculate that a small portion of SO_4^{2-} might be reduced to form S^{2-} under reducing conditions, which could immobilize the dissolved Cd through precipitation. As reported by Shaheen et al. (2016), even a small amount of reductively formed S^{2-} might be sufficient to precipitate considerable portion of dissolved Cd.

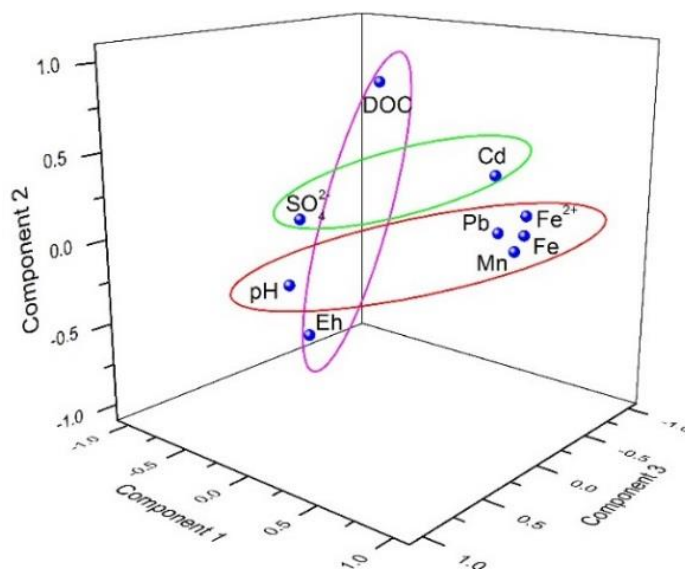


Figure 4-7 Factor analysis of the concentration of dissolved Cd, Pb and other measured geochemical factors (all treatments).

The concentration of dissolved Pb clustered together with $\text{pH}_{6\text{h}}$ and the concentrations of dissolved Fe, Mn and Fe^{2+} (Figure 4-7), implying that the pH could affect the geochemical behavior of Pb in our study. The reduction/oxidation cycling of Fe and Mn might be primarily coupled to the mobilization of Pb. In addition, the concentration of dissolved Pb showed negative ($P < 0.01$) correlations with $\text{pH}_{6\text{h}}$ and the concentrations of dissolved Fe, Mn and Fe^{2+} (Figure 4-5). The Fe-Mn (hydro)oxides have been considered as an important carrier for HMs under oxidizing conditions (e.g., Yu et al., 2016; El-Naggar et al., 2018; Rinklebe et al., 2020). Thus, the mobilization of HMs might be increased with decreasing Eh because of the reductive dissolution of Fe-Mn (hydro)oxides, and vice versa (Rinklebe et al. (2016b)). In our study, the concentrations of Fe^{2+} and dissolved Fe and Mn were higher under reducing conditions than oxidizing conditions (Figure 4-3). Consequently, the rapid decline of the concentration of dissolved Pb when conditions change from moderately reducing to oxidizing conditions may be due to the formation of co-precipitates with Mn-Fe (hydro)oxides. Moreover, the formed Fe-Mn (hydro)oxides likely had a relatively high cation exchange capacity and surface area which favored the adsorption of Pb (Beiyuan et al., 2020).

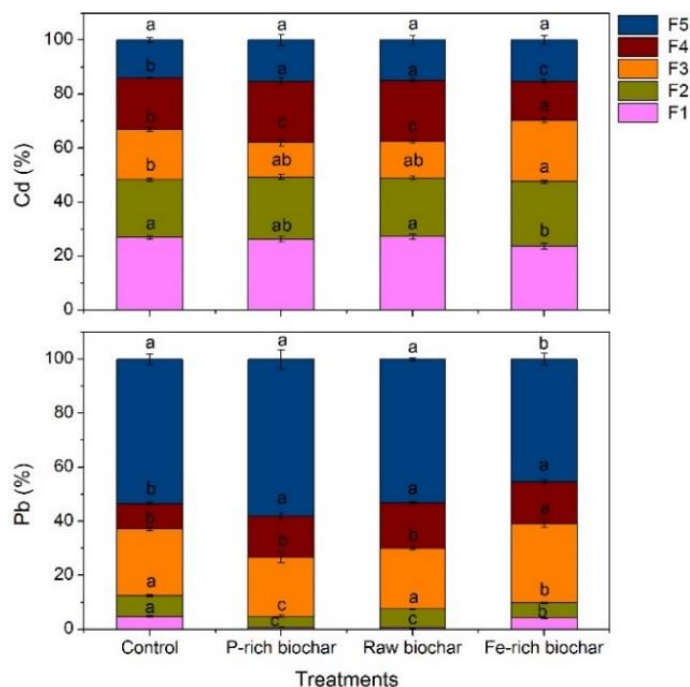


Figure 4-8 Effect of biochar application on the geochemical fractions of Cd and Pb in the pre-incubated soils.

4.3.3 Effect of biochar application on the redox-induced mobilization of Cd and Pb

The addition of biochars affected the redox-induced mobilization of Cd and Pb under varying redox conditions (Figure 4-3). The impact of biochars on the concentrations of dissolved Cd and Pb varied primarily depending on the Eh conditions. The raw biochar was more effective on reducing the concentrations of dissolved Cd under $Eh \leq -100$ mV (after 238 h incubation time) (43-59%), followed by the Fe-rich biochar (31-59%), as compared to the control. The application of the P-rich biochar reduced the concentration of dissolved Cd by 8-19% under reducing and < 3% under oxidizing conditions as compared to the control (Table 4-3). Under moderately reducing conditions ($Eh = 0 \sim -100$ mV; 238-334 h incubation time), the P-rich biochar was more effective on reducing Cd mobilization than the raw and Fe-rich biochars. The P-rich biochar was more effective on immobilizing Pb than the raw and Fe-rich biochars, particularly under $Eh \leq 0$ mV (55-82%), which might be due to the retention of Pb with phosphate compounds (Table 4-3). The raw and Fe-rich biochars immobilized Pb under low Eh (≤ -300 mV), but both biochars, particularly the Fe-rich biochar mobilized Pb under Eh higher than -200 mV, especially at +100 mV. These results indicate that the raw and Fe-rich biochars exhibited more advantages than the P-rich biochar in decreasing the dissolved Cd under strongly reducing and oxidizing conditions, whereas under moderately reducing conditions ($Eh = -100 \sim 0$ mV), the P-rich biochar was more effective than the other two biochars (Figures 4-3 and 4-9). Under both strongly and moderately reducing conditions ($Eh = -400 \sim 0$ mV), the application of the P-rich biochar significantly ($P < 0.05$) reduced the concentration of dissolved Pb. In contrast, the application of the

Fe-rich biochar significantly increased the concentration of dissolved Pb under moderately reducing conditions (Eh = -100 ~ 0 mV).

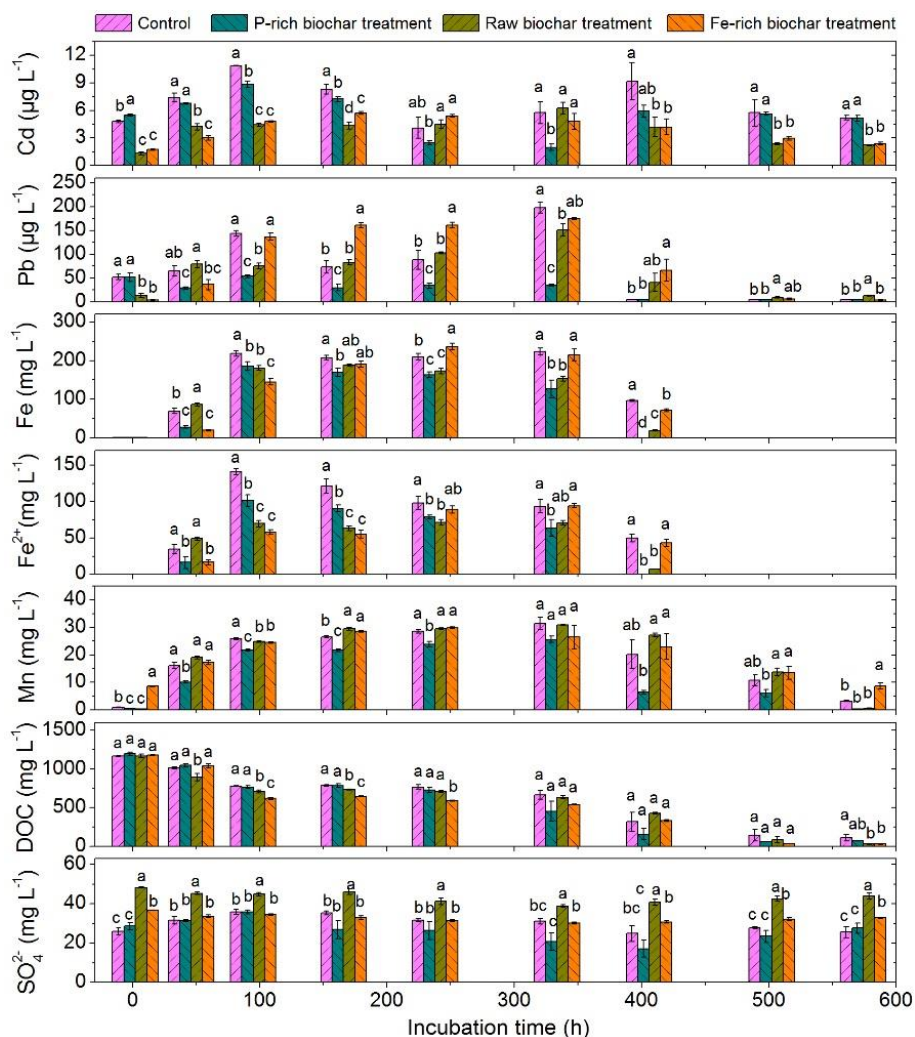


Figure 4-9 Effect of biochar application on the concentrations of Cd, Pb, Fe, Mn, Fe²⁺, DOC and SO₄²⁻ in soil solutions collected from the redox experiment. (Different letters indicate significant differences between treatments in each sampling.)

Factor analysis (Figure 4-10) was conducted within each treatment to evaluate the influence of biochars on the redox-dependent geochemical processes, thus the mobilization of Cd and Pb in the treated soil. The total explained variances of the first two components for the control, P-rich biochar, raw biochar and Fe-rich biochar treatments were 67.9% (Component 1: 54.0; Component 2: 13.9), 70.6% (Component 1: 50.7; Component 2: 19.9), 81.1% (Component 1: 61.9; Component 2: 19.2) and 78.6% (Component 1: 58.8; Component 2: 19.8), respectively. The patterns showed that Cd and Pb were clustered with pH_{6h}, Fe, Mn and Fe²⁺ in one group in the control, raw biochar- and Fe-rich biochar-treated soils, indicating that the concentrations of dissolved Cd and Pb were closely associated with pH and the cycling of Fe-Mn (hydro)oxides in these three treatments. However, in the P-rich biochar

treatment, the concentrations of dissolved Cd and Pb were associated in one cluster with Eh_{6h} , DOC and SO_4^{2-} , implying a slight difference in the geochemical behaviors of Cd and Pb in the P-rich biochar treatment as compared to the control and the other two biochar treatments.

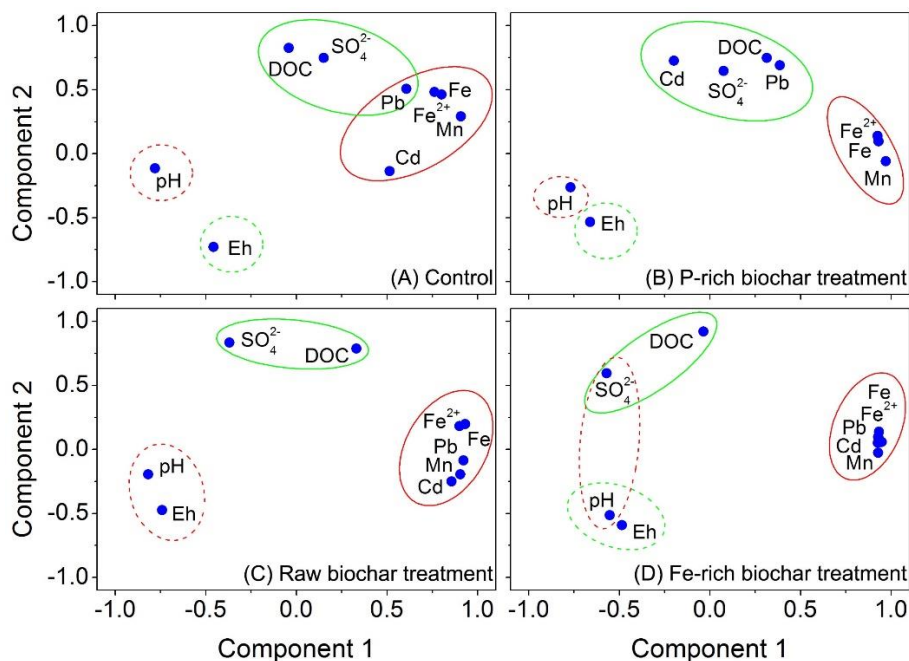


Figure 4-10 Factor analysis of the dissolved Cd, Pb and other measured geochemical factors in control soil(A) and soils treated with P-rich biochar (B), raw biochar (C) and Fe-rich biochar (D) (The solid and dotted ellipses with the same color represent the same cluster).

The decrease of dissolved Cd and Pb caused by the addition of the raw biochar might be attributed to the relatively high pH of this biochar (pH= 9.3, Table 4-1), which increased the pH of the soil, especially under moderately reducing conditions (Figure 4-3). Soil pH affects surface charge characteristics, thus influencing adsorption and precipitation of metal ions. The solubility of metals that can occur as free hydrated cations generally decreases with increasing pH. Therefore, the biochar-induced increase in soil pH is expected to increase the sorption of Cd and Pb from soil solution, and thus decrease their solubility and mobilization (Chen et al., 2019b; Azeem et al., 2021; Bolan et al., 2021). Furthermore, the application of the raw biochar significantly ($P < 0.05$) decreased the concentrations of dissolved Fe, Mn and Fe^{2+} ($Eh \leq 100$ mV, Figures 4-3 and 4-9). Iron-Mn compounds are important binding agents for HMs, especially under oxidizing conditions (Rinklebe et al., 2020; Rajendran et al., 2019; Beiyuan et al., 2020). Thus, decreasing concentrations of dissolved Cd and Pb after raw biochar application might be linked to the stabilization of the dissolved Fe and Mn through co-precipitation and corporation. Firstly, the raw biochar application may promote the formation of Fe-Mn oxides through elevating soil pH (Su et al., 2016; Wen et al., 2021). Secondly, the application of biochar could increase the formation of stable complexes between

Fe ions and organic matters (Fe-OC complexes), thereby promoting the stabilization of Fe (Giannetta et al., 2020). Consequently, we assume that the dissolved Cd and Pb could be stabilized via co-precipitation, complexation with Fe-Mn oxides and incorporation with Fe organic compounds. Moreover, the increased soil organic carbon caused by the raw biochar application (Figure 4-11) and the presence of oxygen-containing functional groups on the raw biochar (Figure 4-2) might also contribute to the adsorption and immobilization of Cd and Pb, as these functional groups and organic carbon can provide binding sites for HMs (Rinklebe et al., 2016a; 2020; Li et al., 2018). In addition, the highly porous structure (Figure 4-1) and large specific surface area (Table 4-1) of the raw biochar may promote the electrostatic adsorption on Cd and Pb, especially under oxidizing and alkaline conditions. Van Vinh et al. (2015) indicated that the surface of biochar can be negatively charged under alkaline conditions. Consequently, the Cd and Pb might be adsorbed due to the attractive force between cationic metals (Cd²⁺ and Pb²⁺) and negatively charged raw biochar (Figure 4-2) under oxidizing conditions.

Table 4-3 Impact of biochars on the changes (%) in the mobilization Cd and Pb in the treated soil as compared to the control

Elements	Eh (mV)	P-rich biochar treatment	Raw biochar treatment	Fe-rich biochar treatment
Cd	+200	14.58	-72.40	-64.06
	-400	-8.56	-42.91	-59.46
	-300	-18.62	-59.31	-55.86
	-200	-13.11	-47.75	-31.23
	-100	-39.84	9.76	31.71
	0	-65.65	8.70	-16.52
	+100	-35.15	-54.22	-54.22
	+200	-2.46	-58.82	-48.84
	+300	-1.44	-57.69	-54.33
Pb	+200	-0.48	-73.76	-92.65
	-400	-54.75	22.27	-44.07
	-300	-62.48	-47.64	-4.82
	-200	-59.31	12.28	119.21
	-100	-61.18	16.43	83.04
	0	-82.06	-23.73	-11.55
	+100	0.00	679.52	1168.57
	+200	0.00	79.05	19.52
	+300	0.00	150.00	-31.43

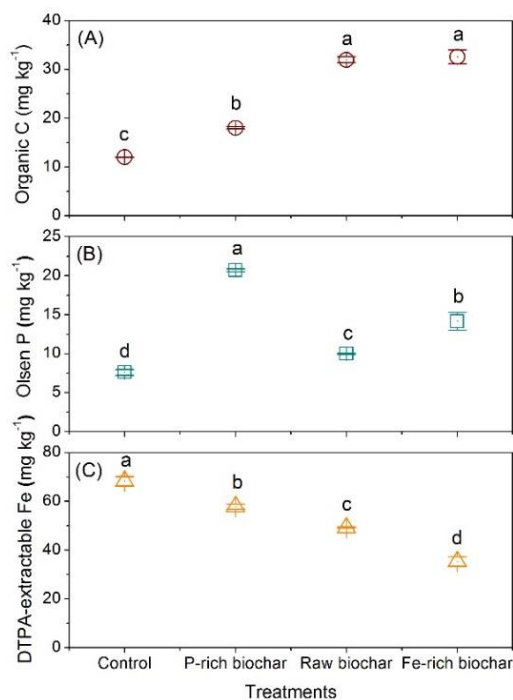


Figure 4-11 Effect of biochar application on the organic carbon content, concentrations of Olsen P and potential available Fe in the pre-incubated soils.

In the case of the Fe-rich biochar treatment, the pH decreased to 6.0 and thus the mobilization of Pb increased under Eh higher than -200 mV, especially at +100 mV. Therefore, the modification of the raw biochar with Fe decreased its immobilization efficiency for Pb because of the acidity effect. The factor analysis demonstrated that the concentration of dissolved Cd was rather associated with the transformation of Fe and Mn than other factors (Figure 4-10). A significant decrease in the concentrations of dissolved Fe and Fe²⁺ was found under reducing conditions (Eh ≤ -100 mV). However, the application of the Fe-modified biochar created no significant difference in the concentration of dissolved Mn as compared to the control (Figure 4-3). In general, the solubility of Fe is negatively correlated with the pH (Zhang et al., 2018). In our study, a slight decrease of pH (less than 0.5 unit) was noticed after the Fe-rich biochar application as compared to the control, especially under reducing conditions (Eh ≤ -100 mV) (Figure 4-3). This minor alteration of pH is unlikely to have driven the entire negative impact of the Fe-rich biochar on the solubility and reduction of Fe in the soil solution (Su et al., 2016). Therefore, we speculate that the formation of Fe-organic matter complexes may play a major role on the decrease of dissolved Fe and Fe²⁺ (Gannett et al., 2020), whereas the influence of this slight pH alteration cannot be completely ruled out. This assumption could be supported by the concomitant decrease of DOC in the Fe-rich biochar treatment as compared to the control (Eh ≤ -100 mV) (Figures 4-3 and 4-9). The lower concentration of Fe in the dissolved phase of the Fe-rich biochar treatment than in the control may indicate conversely a higher amount of insoluble

Fe compounds (e.g., Fe oxides, Fe-organic matter complexes) bound in the Fe-rich biochar-treated soil solid phase than that in the control. Moreover, the potentially higher abundance of Fe compounds in the Fe-rich biochar-treated soil may be also attributed to the exogenous Fe in the Fe-rich biochar (Table 4-1 and EDX spectrum, Figure 4-2). We observed that the application of the Fe-rich biochar could reduce the concentration of Cd in soil solution under reducing conditions. This might be via sorption and/or incorporation by Fe (hydro)oxides and Fe-organic matter complexes. Seshadri et al. (2016) also reported that Fe (hydro)oxides could provide adsorption sites for Cd even under acidic and reducing conditions. Under oxidizing conditions, Fe oxides could promote the immobilization of Cd via re-sorption and co-precipitation (Li et al., 2019; Lyu et al., 2020). In addition, the application of the Fe-rich biochar significantly ($P < 0.05$) increased the concentration of dissolved Pb under moderately reducing conditions ($E_h = -100 \sim +100\text{mV}$). It is likely that under moderately reducing conditions, the released Fe^{2+} would compete with Pb^{2+} for the adsorption sites on soil colloids, which may lead to an increased concentration of dissolved Pb (Fulda et al., 2013). Additionally, the low concentration of dissolved Pb in the Fe-rich biochar treatment under oxidizing conditions might be due to the formation of organic Pb complexes, or sorption of inorganic Pb by the previously formed Fe- Mn (hydro)oxides (Oustriere et al., 2017).

The considerably high efficiency of the P-rich biochar in reducing the concentration of dissolved Pb and Cd, particularly Pb, may be attributed to its high alkalinity ($\text{pH} = 10.4$) and high P and ash content (Table 4-1). The elevated pH might cause a decline in the concentrations of dissolved Cd and Pb due to enhanced electrostatic sorption and precipitation, where the immobilization of Cd and Pb was closely tied to pH (section 4.3.3). A significant ($P < 0.05$) higher pH was observed in the pre-incubated P-rich biochar treatment as compared to the control (Figure 4-6). Higher pH values in the P-rich biochar treatment were also noticed over the entire experiment (Figure 4-3). Additionally, the interactions between Pb and the P-rich biochar under different redox conditions were expected due to the superior ability of phosphate in immobilizing Pb (Zhang et al., 2020; Wang et al., 2021). The P level in the soil was elevated once the P-rich biochar was added due to the high concentration of P in the P-rich biochar (Table 4-1). The concentration of Olsen P significantly ($P < 0.05$) increased after the application of the P-rich biochar (Figure 4-11). However, PO_4^{3-} was not detected in our samples. The most stable Pb form, Pb-phosphates, could rapidly form in the presence of adequate phosphate and Pb^{2+} (Xenidis et al. (2010). Penido et al. (2019) reported that the concentration of P in solution significantly decreased after Cd adsorption by a phosphorus/magnesium-engineered biochar, which was mainly ascribed to the formation of amorphous $\text{Cd}_3(\text{PO}_4)_2$, an insoluble precipitate. Consequently, we assume that similar reactions between phosphate and both metals may have occurred in our experiment, especially in the P-rich biochar treatment, which conversely could explain the

low concentration of PO_4^{3-} in the solutions.

The canonical discriminant analysis was able to discriminate the raw and Fe-rich biochar treatments from the control and the P-rich biochar treatment (Figure 4-12). More than 89% of the variability of different biochar-treated and non-treated soils can be explained by function 1, and function 2 explained only 6.8% of the variability. Based on the standardized canonical discrimination coefficient, only SO_4^{2-} could explain the discrimination of the treatments according to function 1, and only Eh_{6h} could explain the discrimination based on function 2. Consequently, the observed dissimilarity among the treatments in Figure 4-12 was mainly due to the difference of the concentrations of SO_4^{2-} in different treatments. This is in line with our interpretations, as significant higher concentration of SO_4^{2-} was found in the raw biochar treatment during the entire experiment (Figures 4-3 and 4-9). Overall, application of the raw biochar could immobilize Cd and Pb, the former particularly, based on its liming effect and high content of organic carbon and sulfur. The Fe-rich biochar was more effective on immobilizing Cd than Pb, which was primarily due to the redox interactions between the applied Fe and Cd, including re-sorption and co-precipitation. The P-rich biochar had higher efficiency in immobilizing Pb than Cd, which might be due to its alkalinity and high ash content. Moreover, the rich phosphate might contribute to immobilization Pb through precipitation. The application of both raw and Fe-rich biochars enable to immobilize Cd in paddy soils, particularly under strongly reducing conditions. However, the application of the Fe-rich acidic biochar may decrease the pH and thus mobilize Pb and increase its eco-toxicity under moderately reducing conditions.

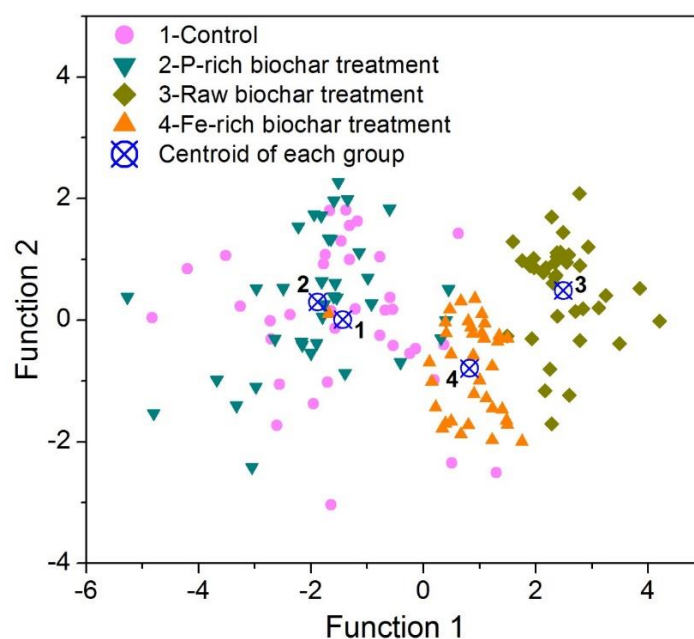


Figure 4-12 Canonical discriminant analysis of dissolved Cd, Pb and other measured geochemical factors.

4.4 Conclusions

This study reveals the biogeochemical interactions between Cd, Pb and P-rich pig carcass-derived biochar as well as raw and Fe-modified green waste-derived biochars under varying redox conditions in a paddy soil. The various characteristics of different biochars affected their ability for Cd and Pb immobilization. For instance, the efficacy of the raw green waste-derived biochar for immobilizing Pb and Cd could be linked to its high content of organic carbon and sulfur, as well as its high alkalinity. The Fe-rich biochar can immobilize Cd rather than Pb through the interactions between the exogenous Fe and Cd. The P-rich biochar had higher efficiency of immobilization of Pb than Cd, which was due to its high phosphate and ash content. Our findings provide implications on the sustainable management of Cd and Pb in contaminated paddy soils using functionalized biochars for mitigating the risks for human health and the environment. We conclude that the amendment of P-rich pig carcass biochar could be a promising approach for mitigating the environmental and human health risk of Pb in paddy soils, whereas the raw and Fe-rich green waste-derived biochars can be used for immobilizing Cd under both reducing and oxidizing conditions and mitigate its potential risk in paddy soils. Future field studies are needed to verify the feasibility of these biochars for remediation of Cd and Pb co-contaminated paddy soils under field conditions. Also, the mobilization of Cd and Pb and their interactions with different biochars under various redox cycling conditions need to be further clarified in the future.

4.5 Acknowledgements

We thank the National Natural Science Foundation of China (Grant No. 21876027) for funding.

4.6 References

- Antoniadis, V., Shaheen, S.M., Levizou, E., Shahid, M., Niazi, N.K., Vithanage, M., Ok, Y.S., Bolan, N., Rinklebe, J., 2019. A critical prospective analysis of the potential toxicity of trace element regulation limits in soils worldwide: Are they protective concerning health risk assessment? - A review. *Environ. Int.* 127, 819-847. <https://doi.org/10.1016/j.envint.2019.03.039>
- Azeem, M., Ali, A., Soundari, P.G., Yiman, L., Zhang, Z., 2021. Bone-derived biochar improved soil quality and reduced Cd and Zn phytoavailability in a multi-metal contaminated mining soil. *Environ. Pollut.* 277, 116800. <https://doi.org/10.1016/j.envpol.2021.116800>
- Beiyuan, J., Awad, Y.M., Beckers, F., Wang, J., Tsang, D.C.W., Ok, Y.S., Wang, S.L., Wang, H., Rinklebe, J., 2020. (Im)mobilization and speciation of lead under dynamic redox conditions in a contaminated soil amended with pine sawdust biochar. *Environ. Int.* 135, 105376. <https://doi.org/10.1016/j.envint.2019.105376>
- Bian, P., Zhang, J., Zhang, C., Huang, H., Rong, Q., Wu, H., Li, X., Xu, M., Liu, Y., Ren, S., 2018. Effects of silkworm excrement biochar combined with different iron-based materials on the speciation of cadmium and lead in soil. *Appl. Sci.* 8, 1999. <https://doi.org/10.3390/app8101999>
- Bolan, N., Hoang, S.A., Beiyuan, J., Gupta, S., Hou, D., Karakoti, A., Joseph, S., Jung, S., Kim, K.-H., Kirkham, M.B., Kua, H.W., Kumar, M., Kwon, E.E., Ok, Y.S., Perera, V., Rinklebe, J., Shaheen, S.M., Sarkar, B., Sarmah, A.K., Singh, B.P., Singh, G., Tsang, D.C.W., Vikrant, K., Vithanage, M., Vinu, A., Wang, H., Wijesekara, H., Yan, Y., Younis, S.A., Van Zwieten, L., 2021. Multifunctional applications of biochar beyond carbon storage. *Int. Mater. Rev.* 67, 150-200. <https://doi.org/10.1080/09506608.2021.1922047>
- Chen, H., Li, W., Wang, J., Xu, H., Liu, Y., Zhang, Z., Li, Y., Zhang, Y., 2019a. Adsorption of cadmium and lead ions by phosphoric acid-modified biochar generated from chicken feather: Selective adsorption and influence of dissolved organic matter. *Bioresour. Technol.* 292, 121948. <https://doi.org/10.1016/j.biortech.2019.121948>
- Chen, H., Yang, X., Gielen, G., Mandal, S., Xu, S., Guo, J., Shaheen, S.M., Rinklebe, J., Che, L., Wang, H., 2019b. Effect of biochars on the bioavailability of cadmium and di-(2-ethylhexyl) phthalate to *Brassica chinensis* L. in contaminated soils. *Sci. Total Environ.* 678, 43-52. <https://doi.org/10.1016/j.scitotenv.2019.04.417>
- Chen, H., Yang, X., Wang, H., Sarkar, B., Shaheen, S.M., Gielen, G., Bolan, N., Guo, J., Che, L., Sun, H., Rinklebe, J., 2020. Animal carcass- and wood-derived biochars improved nutrient bioavailability, enzyme activity, and plant growth in metal-phthalic acid ester co-contaminated soils: A trial for reclamation and improvement of degraded soils. *J. Environ. Manage.* 261, 110246. <https://doi.org/10.1016/j.jenvman.2020.110246>
- Cui, H., Zhang, X., Wu, Q., Zhang, S., Xu, L., Zhou, J., Zheng, X., Zhou, J., 2020. Hematite enhances the immobilization of copper, cadmium and phosphorus in soil amended with hydroxyapatite under flooded conditions. *Sci. Total Environ.* 708, 134590. <https://doi.org/10.1016/j.scitotenv.2019.134590>
- Dong, S., Xu, W., Wu, F., Yan, C., Li, D., Jia, H., 2016. Fe-modified biochar improving transformation of arsenic form in soil and inhibiting its absorption of plant. *Transactions of the Chinese Society of Agricultural Engineering* 32, 204-212. (in Chinese)
- El-Naggar, A., Shaheen, S.M., Ok, Y.S., Rinklebe, J., 2018. Biochar affects the dissolved and colloidal concentrations of Cd, Cu, Ni, and Zn and their phytoavailability and potential mobility in a mining soil under dynamic redox-conditions. *Sci. Total Environ.* 624, 1059-1071. <https://doi.org/10.1016/j.scitotenv.2017.12.190>
- El Rasafi, T., Oukarroum, A., Haddioui, A., Song, H., Kwon, E. E., Bolan, N., Tack, F. M. G., Sebastian, A., Prasad, M. N. V., Rinklebe, J., 2021. Cadmium stress in plants: A critical review of the effects, mechanisms, and tolerance strategies. *Crit. Rev. Environ. Sci. Technol.* <https://doi.org/10.1080/10643389.2020.1835435>
- Feng, Y., Yang, X., Singh, B.P., Mandal, S., Guo, J., Che, L., Wang, H., 2020. Effects of contrasting biochars on

- the leaching of inorganic nitrogen from soil. *J. Soil. Sediment.* 20, 3017-3026. <https://doi.org/10.1007/s11368-019-02369-5>
- Frohne, T., Rinklebe, J., Diaz-Bone, R., Du Laing, G., 2011. Controlled variation of redox conditions in a floodplain soil: impact on metal mobilization and biomethylation of arsenic and antimony. *Geoderma* 160. 414-424. <https://doi.org/10.1016/j.geoderma.2010.10.012>
- Fulda, B., Voegelin, A., Ehlert, K., Kretzschmar, R., 2013. Redox transformation, solid phase speciation and solution dynamics of copper during soil reduction and reoxidation as affected by sulfate availability. *Geochim. Cosmochim. Ac.* 123, 385-402. <https://doi.org/10.1016/j.gca.2013.07.017>
- Giannetta, B., Plaza, C., Siebecker, M.G., Aquilanti, G., Vischetti, C., Plaisier, J.R., Juanco, M., Sparks, D.L., Zaccane, C., 2020. Iron speciation in organic matter fractions isolated from soils amended with biochar and organic fertilizers. *Environ. Sci. Technol.* 54, 5093-5101. <https://doi.org/10.1021/acs.est.0c00042>
- Hamid, Y., Tang, L., Hussain, B., Usman, M., Gurajala, H.K., Rashid, M.S., He, Z., Yang, X., 2020. Efficiency of lime, biochar, Fe containing biochar and composite amendments for Cd and Pb immobilization in a co-contaminated alluvial soil. *Environ. Pollut.* 257, 113609. <https://doi.org/10.1016/j.envpol.2019.113609>
- Harvey, A.E., Smart, J.A., Amis, E.S., 1955. Simultaneous spectrophotometric determination of iron (II) and total iron with 1, 10-phenanthroline. *Anal. Chem.* 27, 26-29. <https://doi.org/10.1021/ac60097a009>
- International Biochar Initiative, 2015. Standardized product definition and product testing guidelines for biochar that is used in soil. https://www.biochar-international.org/wp-content/uploads/2018/04/IBI_Biochar_Standards_V2.1_Final.pdf
- Isinkaye, O. M. 2018. Distribution and multivariate pollution risks assessment of heavy metals and natural radionuclides around abandoned iron-ore mines in north central Nigeria. *Earth Systems and Environment*, 2, 331-343.
- Kashif Irshad, M., Chen, C., Noman, A., Ibrahim, M., Adeel, M., Shang, J., 2020. Goethite-modified biochar restricts the mobility and transfer of cadmium in soil-rice system. *Chemosphere* 242, 125152. <https://doi.org/10.1016/j.chemosphere.2019.125152>
- Li, G., Khan, S., Ibrahim, M., Sun, T.R., Tang, J.F., Cotner, J.B., Xu, Y.Y., 2018. Biochars induced modification of dissolved organic matter (DOM) in soil and its impact on mobility and bioaccumulation of arsenic and cadmium. *J. Hazard. Mater.* 348, 100-108. <https://doi.org/10.1016/j.jhazmat.2018.01.031>
- Li, J., Wang, S.-L., Zhang, J., Zheng, L., Chen, D., Shaheen, S.M., Rinklebe, J., Ok, Y.S., Wang, H., Wu, W., 2020. Coconut-fiber biochar reduced the bioavailability of lead but increased its translocation rate in rice plants: Elucidation of immobilization mechanisms and significance of iron plaque barrier on roots using spectroscopic techniques. *J. Hazard. Mater.* 389, 122117. <https://doi.org/10.1016/j.jhazmat.2020.122117>
- Li, X., Yang, Z., Zhang, C., Wei, J., Zhang, H., Li, Z., Ma, C., Wang, M., Chen, J., Hu, J., 2019. Effects of different crystalline iron oxides on immobilization and bioavailability of Cd in contaminated sediment. *Chem. Eng. J.* 373, 307-317. <https://doi.org/10.1016/j.cej.2019.05.015>
- Lyu, H., Tang, J., Cui, M., Gao, B., Shen, B., 2020. Biochar/iron (BC/Fe) composites for soil and groundwater remediation: Synthesis, applications, and mechanisms. *Chemosphere* 246, 125609. <https://doi.org/10.1016/j.chemosphere.2019.125609>
- Meng, D., Li, J., Liu, T., Liu, Y., Yan, M., Hu, J., Li, X., Liu, X., Liang, Y., Liu, H., Yin, H., 2019. Effects of redox potential on soil cadmium solubility: Insight into microbial community. *J. Environ. Sci.* 75, 224-232. <https://doi.org/10.1016/j.jes.2018.03.032>
- Netherway, P., Reichman, S.M., Laidlaw, M., Scheckel, K., Pingitore, N., Gasco, G., Mendez, A., Surapaneni, A., Paz-Ferreiro, J., 2019. Phosphorus-rich biochars can transform lead in an urban contaminated soil. *J. Environ. Qual.* 48, 1091-1099. <https://doi.org/10.2134/jeq2018.09.0324>
- Oustriere, N., Marchand, L., Rosette, G., Friesl-Hanl, W., Mench, M., 2017. Wood-derived-biochar combined

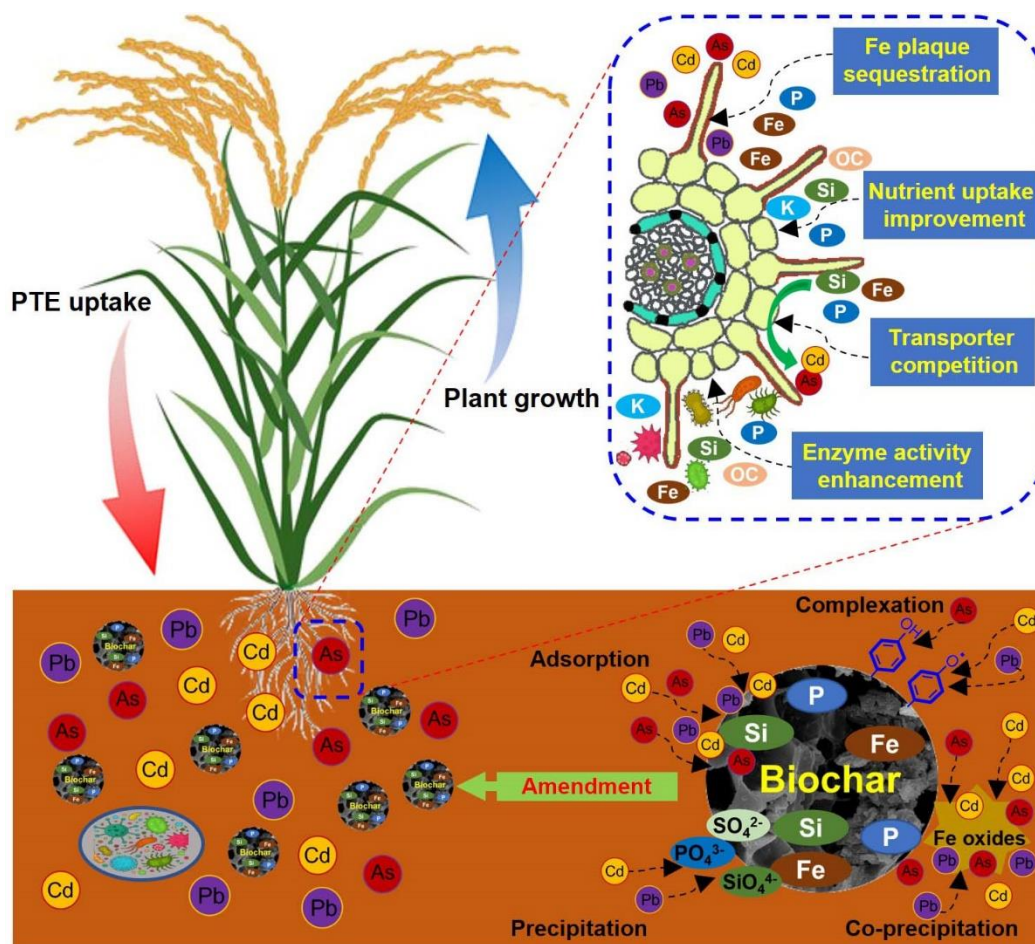
- with compost or iron grit for in situ stabilization of Cd, Pb, and Zn in a contaminated soil. *Environ. Sci. Pollut. Res.* 24, 7468-7481. <https://doi.org/10.1007/s11356-017-8361-6>
- Palansooriya, K.N., Shaheen, S.M., Chen, S.S., Tsang D.C.W., Hashimoto, Y., Hou, D., Bolan, N.S., Rinklebe, J., Ok, Y.S., 2020. Soil amendments for immobilization of potentially toxic elements in contaminated soils: A critical review. *Environ. Int.* 134, 105046. <https://doi.org/10.1016/j.envint.2019.105046>
- Penido, E.S., Melo, L.C.A., Guilherme, L.R.G., Bianchi, M.L., 2019. Cadmium binding mechanisms and adsorption capacity by novel phosphorus/magnesium-engineered biochars. *Sci. Total Environ.* 671, 1134-1143. <https://doi.org/10.1016/j.scitotenv.2019.03.437>
- Rajendran, M., Shi, L., Wu, C., Li, W., An, W., Liu, Z., Xue, S., 2019. Effect of sulfur and sulfur-iron modified biochar on cadmium availability and transfer in the soil-rice system. *Chemosphere* 222, 314-322. <https://doi.org/10.1016/j.chemosphere.2019.01.149>
- Rapin, A., Grybos, M., Rabiet, M., Mourier, B., Deluchat, V., 2019. Phosphorus mobility in dam reservoir affected by redox oscillations: An experimental study. *J. Environ. Sci.* 77, 250-263. <https://doi.org/10.1016/j.jes.2018.07.016>
- Rinklebe, J., Shaheen, S.M., El-Naggar, A., Wang, H., Du Laing, G., Alessi, D.S., Sik Ok, Y., 2020. Redox-induced mobilization of Ag, Sb, Sn, and Tl in the dissolved, colloidal and solid phase of a biochar-treated and untreated mining soil. *Environ. Int.* 140, 105754. <https://doi.org/10.1016/j.envint.2020.105754>
- Rinklebe, J., Shaheen, S.M., Frohne, T., 2016a. Amendment of biochar reduces the release of toxic elements under dynamic redox conditions in a contaminated floodplain soil. *Chemosphere* 142, 41-47. <https://doi.org/10.1016/j.chemosphere.2015.03.067>
- Rinklebe, J., Shaheen, S.M., Yu, K.W., 2016b. Release of As, Ba, Cd, Cu, Pb, and Sr under pre-definite redox conditions in different rice paddy soils originating from the USA and Asia. *Geoderma* 270, 21-32. <https://doi.org/10.1016/j.geoderma.2015.10.011>
- Seshadri, B., Bolan, N.S., Wijesekara, H., Kunhikrishnan, A., Thangarajan, R., Qi, F., Matheyarasu, R., Rocco, C., Mbene, K., Naidu, R., 2016. Phosphorus-cadmium interactions in paddy soils. *Geoderma* 270, 43-59. <https://doi.org/10.1016/j.geoderma.2015.11.029>
- Shaheen, S.M., Rinklebe, J., 2017. Sugar beet factory lime affects the mobilization of Cd, Co, Cr, Cu, Mo, Ni, Pb, and Zn under dynamic redox conditions in a contaminated floodplain soil. *J. Environ. Manage.* 186, 253-260. <https://doi.org/10.1016/j.jenvman.2016.07.060>
- Shaheen, S.M., El-Naggar, A., Antoniadis, V., Moghanm, F.S., Zhang, Z., Tsang, D.C.W., Ok, Y.S., Rinklebe, J., 2020: Release of toxic elements in fishpond sediments under dynamic redox conditions: Assessing the potential environmental risk for a safe management of fisheries systems and degraded waterlogged sediments. *J. Environ. Manage.* 255, 109778. <https://doi.org/10.1016/j.jenvman.2019.109778>
- Shaheen, S.M., Rinklebe, J., Frohne, T., White, J.R., DeLaune, R.D., 2016. Redox effects on release kinetics of arsenic, cadmium, cobalt, and vanadium in Wax Lake Deltaic freshwater marsh soils. *Chemosphere* 150, 740-748. <https://doi.org/10.1016/j.chemosphere.2015.12.043>
- Shaheen, S.M., Rinklebe, J., Frohne, T., White, J.R., DeLaune, R.D., 2014. Biogeochemical factors governing cobalt, nickel, selenium, and vanadium dynamics in periodically flooded Egyptian North Nile Delta rice soils. *Soil Sci. Soc. Am. J.* 78, 1065-1078. <https://doi.org/10.2136/sssaj2013.10.0441>
- Shaheen, S.M., Tsadilas, C.D., Rinklebe, J., 2013. A review of the distribution coefficients of trace elements in soils: Influence of sorption system, element characteristics, and soil colloidal properties. *Adv. Colloid Interface Sci.* 201-202, 43-56. <https://doi.org/10.1016/j.cis.2013.10.005>
- Su, H., Fang, Z., Tsang, P.E., Fang, J., Zhao, D., 2016. Stabilisation of nanoscale zero-valent iron with biochar for enhanced transport and in-situ remediation of hexavalent chromium in soil. *Environ. Pollut.* 214, 94-100.

- <https://doi.org/10.1016/j.envpol.2016.03.072>
- Takeo, N., 2005. Atlas of Eh-pH diagrams. National Institute of Advanced Industrial Science and Technology.
- Van Vinh, N., Zafar, M., Behera, S.K., Park, H.S., 2015. Arsenic(III) removal from aqueous solution by raw and zinc-loaded pine cone biochar: equilibrium, kinetics, and thermodynamics studies. *Int. J. Environ. Sci. Technol.* 12, 1283-1294. <https://doi.org/10.1007/s13762-014-0507-1>
- Wang, Q., Shaheen, S.M., Jiang, Y., Li, R., Slaný, M., Kwon, Bolan, N., Rinklebe, J., Zhang, Z. 2021. Fe/Mn- and P-modified drinking water treatment residuals decreased Cu and Pb phytoavailability and uptake in a mining soil. *Journal of Hazardous Materials* 403, 123628. <https://doi.org/10.1016/j.jhazmat.2020.123628>
- Wang, L., Ok, Y.S., Tsang, D.C.W., Alessi, D.S., Rinklebe, J., Wang, H., Mašek, O., Hou, R., O'Connor, D., Hou, D., Nicholson, F., 2020. New trends in biochar pyrolysis and modification strategies: feedstock, pyrolysis conditions, sustainability concerns and implications for soil amendment. *Soil Use Manag.* 36, 358-386. <https://doi.org/10.1111/sum.12592>
- Wen, E., Yang, X., Chen, H., Shaheen, S.M., Sarkar, B., Xu, S., Song, H., Liang, Y., Rinklebe, J., Hou, D., Li, Y., Wu, F., Pohořelý, M., Wong, J.W.C., Wang, H., 2021. Iron-modified biochar and water management regime-induced changes in plant growth, enzyme activities, and phytoavailability of arsenic, cadmium and lead in a paddy soil. *J. Hazard. Mater.* (in press) <https://doi.org/10.1016/j.jhazmat.2020.124344>
- Xenidis, A., Stouraiti, C., Papassiopi, N., 2010. Stabilization of Pb and As in soils by applying combined treatment with phosphates and ferrous iron. *J. Hazard. Mater.* 177, 929-937. <https://doi.org/10.1016/j.jhazmat.2010.01.006>
- Yang, X., Liu, J., McGrouther, K., Huang, H., Lu, K., Guo, X., He, L., Lin, X., Che, L., Ye, Z., Wang, H., 2016. Effect of biochar on the extractability of heavy metals (Cd, Cu, Pb, and Zn) and enzyme activity in soil. *Environ. Sci. Pollut. Res.* 23, 974-984. <https://doi.org/10.1007/s11356-015-4233-0>
- Yang, X., Lu, K., McGrouther, K., Lei, C., Hu, G., Wang, Q., Liu, X., Shen, L., Huang, H., Ye, Z., Wang, H., 2017a. Bioavailability of Cd and Zn in soils treated with biochars derived from tobacco stalk and dead pigs. *J. Soil. Sediment.* 17, 751-762. <https://doi.org/10.1007/s11368-015-1326-9>
- Yang, X., Wang, H., Strong, P., Xu, S., Liu, S., Lu, K., Sheng, K., Guo, J., Che, L., He, L., Ok, Y.S., Yuan, G., Shen, J., Chen, X., 2017b. Thermal Properties of Biochars Derived from Waste Biomass Generated by Agricultural and Forestry Sectors. *Energies* 10(4): 469. <https://doi.org/10.3390/en10040469>
- Yuan, Y., Bolan, N., PrevotEAU, A., Vithanage, M., Biswas, J.K., Ok, Y.S., Wang, H.L., 2017. Applications of biochar in redox-mediated reactions. *Bioresour. Technol.* 246, 271-281. <https://doi.org/10.1016/j.biortech.2017.06.154>
- Yu, B., Li, D., Wang, Y., He, H., Li, H., Chen, G., 2020. The compound effects of biochar and iron on watercress in a Cd/Pb-contaminated soil. *Environ. Sci. Pollut. Res.* 27, 6312-6325. <https://doi.org/10.1007/s11356-019-07353-7>
- Yu, K., Rinklebe, J., 2011. Advancement in soil microcosm apparatus for biogeochemical research. *Ecol. Eng.* 37, 2071-2075. <https://doi.org/10.1016/j.ecoleng.2011.08.017>
- Yu, H.Y., Li, F.B., Liu, C.S., Huang, W., Liu, T.X., Yu, W.M., 2016. Iron redox cycling coupled to transformation and immobilization of heavy metals: implications for paddy rice safety in the red soil of south China. *Adv. Agron.* 137, 279-317. <https://doi.org/10.1016/bs.agron.2015.12.006>
- Zhang, H., Shao, J., Zhang, S., Zhang, X., Chen, H., 2020. Effect of phosphorus-modified biochars on immobilization of Cu (II), Cd (II), and As (V) in paddy soil. *J. Hazard. Mater.* 390, 121349. <https://doi.org/10.1016/j.jhazmat.2019.121349>
- Zhang, Q., Zhang, L., Liu, T., Liu, B., Huang, D., Zhu, Q., Xu, C., 2018. The influence of liming on cadmium accumulation in rice grains via iron-reducing bacteria. *Sci. Total Environ.* 645, 109-118.

<https://doi.org/10.1016/j.scitotenv.2018.06.316>

Zhao, F.J., Ma, Y., Zhu, Y.G., Tang, Z., McGrath, S.P., 2015. Soil contamination in China: current status and mitigation strategies. *Environ. Sci. Technol.* 49, 750-759. <https://doi.org/10.1021/es5047099>

CHAPTER 5: Influences of Iron-Modified Phosphorus- and Silicon-Rich Biochars on Arsenic, Cadmium, and Lead Accumulation in Rice and Microbial Activities in Paddy Soil ⁴



⁴ Adapted from **Yang, X.**, Wen, E., Ge, C., El-Naggar, A., Wang, S., Kwon, E.E., Song, H., Shaheen, S.M., Wang, H., Rinklebe, J. Iron-modified phosphorus- and silicon-based biochars exhibited various influences on arsenic, cadmium and lead accumulation in rice and enzyme activities in a paddy soil. Ready for being submitted to *Journal of Cleaner Production*.

A supplementary data is provided in Appendix D.

Abstract

Application of functionalized biochar in rice cultivation has been proposed as an effective means to reduce environmental hazards of potentially toxic elements (PTEs) in paddy soils. Employing functionalized biochar could also enhance the yield and quality of rice. Nevertheless, the role of functionalized biochar in the remediation of soils contaminated with multi-PTEs has not been fully implemented. As such, this work was undertaken to seek the positive effects of a rice husk-derived silicon (Si)-rich biochar (Si-BC) and a pig carcass-derived phosphorus (P)-rich biochar (P-BC), as well as their Fe-modified biochars (Fe-Si-BC and Fe-P-BC) on the enzyme activity and PTE availability in an As-Cd-Pb-contaminated soil, and the impacts of those functionalized biochars on rice growth and uptake for PTEs. Our results showed that Si-BC decreased the concentrations of As in rice grain and straw by 59.4 and 61.4%, respectively, compared to the control, without compromising plant growth and grain yield, while Fe-Si-BC significantly ($P<0.05$) enhanced plant growth, increasing grain yield (by 38.6%). However, Si-BC had no significant impacts on plant-Cd and plant-Pb, whereas Fe-Si-BC significantly ($P<0.05$) elevated Cd and Pb accumulation in rice plants, posing a higher environmental risk. Application of P-BC enhanced the activities of soil enzymes (dehydrogenase, catalase, and urease), and reduced grain-Pb and straw-Pb by 49.3 and 43.2%, respectively, without affecting plant-As and -Cd, plant growth and rice yield. However, Fe-P-BC reduced plant-As in rice grain and straw by 12.2 and 51.2%, respectively, but increased plant-Cd and plant-Pb, compared to the control. Thus, Fe-modified Si-rich (rice husk) and P-rich (pig carcass) biochars could be used to remediate paddy soils contaminated with As, and in turn enhance the yield and quality of rice. Application of pristine P-rich biochar could be also a promising strategy to remediate the Pb-contaminated paddy soils and limit Pb accumulation in rice.

Keywords: Heavy metal; Paddy field; Rice growth; Fe-functionalized biochar; Soil remediation; Waste management

5.1 Introduction

Contamination of agricultural soils with potentially toxic elements (PTEs) has become a severe global agricultural, environmental and public health problem (Bandara *et al.*, 2019; Zhao and Wang, 2019). Arsenic (As), cadmium (Cd), and lead (Pb) are three PTEs that have been ranked respectively first, seventh, and second as hazardous substances by the Agency for Toxic Substance and Disease Registry (ATSDR, 2019). Rice plants exhibit a high ability to accumulate PTEs (Liu *et al.*, 2020), which is a common dietary source for PTE exposure, posing a severe risk to the environment and human health (Shaheen *et al.*, 2022). Simultaneous immobilization of As, Cd, and Pb could be technically challenging due to their distinct biogeochemical behaviors in soils (El-Naggar *et al.*, 2021). In this context, it is essential to seek for effective soil remediation technologies for simultaneously alleviating the bioavailability of PTEs in paddy soils and controlling their uptake by rice plants to maintain food security and human health (Palansooriya *et al.*, 2020; Ok *et al.*, 2020).

Biochar is a promising amendment that could mitigate the bioavailability and toxicity of cationic PTEs (e.g., Cd and Pb) in paddy soils (Palansooriya *et al.*, 2020; Yang *et al.*, 2021a), owing to its alkalinity, large specific surface area, abundant porous structure, negatively-charged surface groups, and high cationic exchange capacity (Yang *et al.*, 2017; Pan *et al.*, 2021; Wen *et al.*, 2021). The liming effect of biochar could generally mobilize As due to the electrostatic repulsion between negative As anions (e.g., H_2AsO_4^- , HAsO_4^{2-} , and AsO_4^{3-}) and the negatively charged biochar (Frick *et al.*, 2019; El-Naggar *et al.*, 2020). Thus, it is critical to design and apply highly effective functionalized biochars for remediation of paddy soils contaminated with multi-PTEs (Wen *et al.*, 2021). The biochar modification process could be tailored by either selecting precursors (e.g., silicon (Si)-rich and phosphorus (P)-rich biomass) or loading other organic or inorganic materials (e.g., iron (Fe)-rich compounds) on biochar (Xiao *et al.*, 2018; Wang *et al.*, 2019; Yang *et al.*, 2021a).

Silicon (Si) is a vital mineral element for soil-plant interactions, which is not considered to be essential, yet confers high benefits to plant growth because of its ability to alleviate abiotic/biotic stresses (e.g., PTEs) in the soil-plant system (Wang *et al.*, 2019). Moreover, application of Si fertilizers and/or Si-rich soil amendments is a cost-effective agronomic practice for preventing the adverse effects of PTEs while, promoting plant growth, and ameliorating the accumulation of PTEs in rice plants (Zhao *et al.*, 2017; Sohail *et al.*, 2020; Xiao *et al.*, 2021). Biochars derived from silicophilic plants, such as rice, wheat, barley, and maize, are considered as Si-rich biochars (Xiao *et al.*, 2018; Wang *et al.*, 2020), which have been used for remediation of soils contaminated with PTEs and soil quality improvement (Zama *et al.*, 2018; Seyfferth *et al.*, 2019).

Phosphorus (P) is not only an essential nutrient for plant and microbe growth (Xiao *et al.*, 2018), but also an

effective material for the immobilization of PTEs (especially Cd and Pb) in soils, due to the formation of stable phosphate precipitates and complexes (Xiao *et al.*, 2018; Yang *et al.*, 2021a). Several studies have recently paid attention to using P-rich biochar for the remediation of soils contaminated with PTEs. For instance, Azeem *et al.* (2021) indicated that the sheep bone-derived biochar immobilized Cd in a contaminated mining soil by the formation of insoluble $\text{Cd}_3(\text{PO}_4)_2$ and Ca-Cd phosphates. The pig carcasses biochar was proven to be a promising soil amendment for alleviating release of Pb in a paddy soil (Yang *et al.*, 2021a). Furthermore, phosphate could inhibit As uptake in rice plants, because As(V) uses the same phosphate-uptake transporters (OsPT1, OsPT4, and OsPT8) (Seyfferth and Fendorf, 2012; Zhao and Wang, 2019).

Iron (Fe)-based biochar has been frequently used for remediation of soils contaminated with PTEs (in particular As) (Li *et al.*, 2020; Pan *et al.*, 2021; Wen *et al.*, 2021). Kumarathilaka *et al.* (2021) indicated that an addition of the iron-modified Si-rich biochar reduced the concentrations of As in different rice tissues by 37-79%. Peng *et al.* (2019) found that loading of Fe materials (nanoscale zerovalent iron and ferrous sulfide) on fruit shell biochar expedited the Pb immobilization rate in soil by 9.9 and 2.4%, respectively, compared to the raw biochar treatment. Also, a recent study observed that application of 2 and 3% of goethite-modified biochar minimized the Cd uptake in rice grains by 85 and 59%, respectively (Kashif Irshad *et al.*, 2022).

Biological properties of soil have been proven to be vastly responsible for the biogeochemical behaviors of PTEs (Tang *et al.*, 2020). Soil enzymes play critical roles in organic carbon turnover, nutrient cycling, and catalyzing biochemical reactions in soils, serving as a vital indicator for evaluating the toxicity and stress of PTEs in soils (Yang *et al.*, 2016a; Nie *et al.*, 2018; Wen *et al.*, 2021). It has been proven that the application of biochar (Yang *et al.*, 2016b; Chen *et al.*, 2020) or mineral elements such as Fe, P and Si (Gomez-Sagasti *et al.*, 2019; Jinger *et al.*, 2022) can directly and indirectly affect soil enzymes activity. However, their combined effects on enzyme activities are still scarcely studied. We hypothesized that the Fe-modified Si- or P-rich functionalized biochars would synergize the merits of different materials (Si-, P- and Fe-rich compounds and biochars), thereby improving soil microbial properties and fertility, in turn promoting rice plant growth, reducing PTE bioavailability, and eventually ameliorating the accumulation of PTEs in rice. Based on these hypotheses, we tested the feasibility of different functionalized biochars, including a rice husk-derived Si-rich biochar, a pig carcass-derived P-rich biochar, as well as their Fe-modified biochars, for the simultaneous immobilization of As, Cd, and Pb in paddy soils. Furthermore, the changes in rice growth parameters, grain yield, nutrient bioavailability, and soil enzyme activities were also scrutinized to seek the potential mechanisms for simultaneous remediation of those PTEs.

5.2 Materials and methods

5.2.1 Soil collection and characterization

The multi-PET contaminated soil was collected from a paddy field at 0 - 20 cm soil depth. The sampling site was a few kilometers away from an abandoned Pb-Zn mine in the southeast of Shaoxing City, Zhejiang Province, China. This soil was intentionally chosen since it was well-weathered and has a long history for rice cultivation (personal communication), and the sampling site was geologically located in the Middle-Lower Yangtze River region, a well-known region for rice production in China. Soil samples were air-dried and mechanically sieved to < 3 mm particle size. Subsamples of the air-dried soil were taken for soil characterization and the remained was used for the pot experiment. The soil was contaminated with 141 mg kg⁻¹ of As, 0.5 mg kg⁻¹ of Cd, and 736 mg kg⁻¹ of Pb. The properties of this soil have been reported in our previous works (Pan *et al.*, 2021; Wen *et al.*, 2021), and more details could be found in *Appendix D* (section D1).

5.2.2 Preparation of functionalized biochars

Si-rich biochar (Si-BC) was produced through pyrolysis of rice husk at 650 °C for 2 h using a lab-scale furnace in an oxygen-free environment. A local producer (Zhejiang Eco Environmental Technology Co., Ltd.) provided the P-rich biochar (P-BC), which was derived from pig carcasses using a batch pyrolysis facility at a final temperature of 650 °C for 2 h. Si-BC and P-BC were milled and passed through a 2-mm sieve. Afterwards, a portion of Si-BC or P-BC was immersed into a ferric chloride solution at 1: 20 of Fe-to-biochar ratio. The mixture was stirred for 20 min and then sonicated for 1 h for homogeneity. Thereafter, the mixture was oven-dried under 70 °C for 2 d, and then pyrolyzed under 650 °C for 1 h to obtain the Fe-modified Si-rich biochar (Fe-Si-BC) and P-rich biochar (Fe-P-BC). In *Appendix D*, the selected basic properties of functionalized biochars (Figure 5-1; Table 5-1) and the relevant analytical methods (section D2) are given.

5.2.3 Experimental design

Rice plants (*Oryza sativa* L.) were cultivated in PTE-contaminated soils with/without biochar application under intermittent water management practice. The pot experiment was conducted in a greenhouse at Zhejiang A & F University in Hangzhou City, Zhejiang Province, China. Different biochars were mixed with contaminated soil at 3 wt.% and the non-treated soil served as control. Biochar treatments (Si-BC, Fe-Si-BC, P-BC, and Fe-P-BC) and the control were conducted in four replicates. Each 10-L plastic pot (22 cm high, 24 cm in diameter) received 8.0 kg of non- or biochar-treated soils. Twenty pots were placed in a randomized blocked design. Prior to rice transplanting, all pots were flooded to 2-3 cm above the soil surface for a 7-day equilibration.

Table 5-1 Physicochemical properties of functionalized biochars.

Properties	Si-rich biochar	Fe-Si-rich biochar	P-rich biochar	Fe-P-rich biochar
pH	9.0	3.1	10.6	3.6
Specific surface area (m ² g ⁻¹)	237.3	69.3	18.4	43.6
Ash content (%)	28.0	46.3	60.0	76.3
Total C (%)	43.7	38.8	30.8	40.4
Total N (%)	0.8	1.7	2.1	1.8
Total H (%)	2.4	1.4	1.3	1.5
Total S (%)	0.20	0.10	0.19	0.16
C/N	67.3	22.8	14.7	22.9
C/H	22.4	27.1	24.6	27.5
Total As (mg kg ⁻¹)	LDL	LDL	LDL	LDL
Total Cd (mg kg ⁻¹)	LDL	LDL	LDL	LDL
Total Pb (mg kg ⁻¹)	LDL	LDL	1.6	4.6

Rice seeds (cultivar Xiushui-519) provided by a local rice farmer were germinated in the greenhouse using a non-contaminated soil. Five healthy seedlings at the 3-4 leaf stage were transplanted to each pot. As per the local rice production practice, 0.68 g (equivalent to 450 kg ha⁻¹) of a commercial compound fertilizer (N: P: K=15:12:18) was added in each pot as base fertilizer. Ten days after transplantation, 0.68 g (equivalent to 450 kg ha⁻¹) of commercial compound fertilizer and 0.34 g (equivalent to 225 kg ha⁻¹) of urea were incorporated as topdressing. Pots were intermittently flooded during the entire growing phase and drained 10 d before harvest. In brief, water was always added until flooding (with a 2-3 cm water level on the soil surface) when fine cracks could be noticed on the surface.

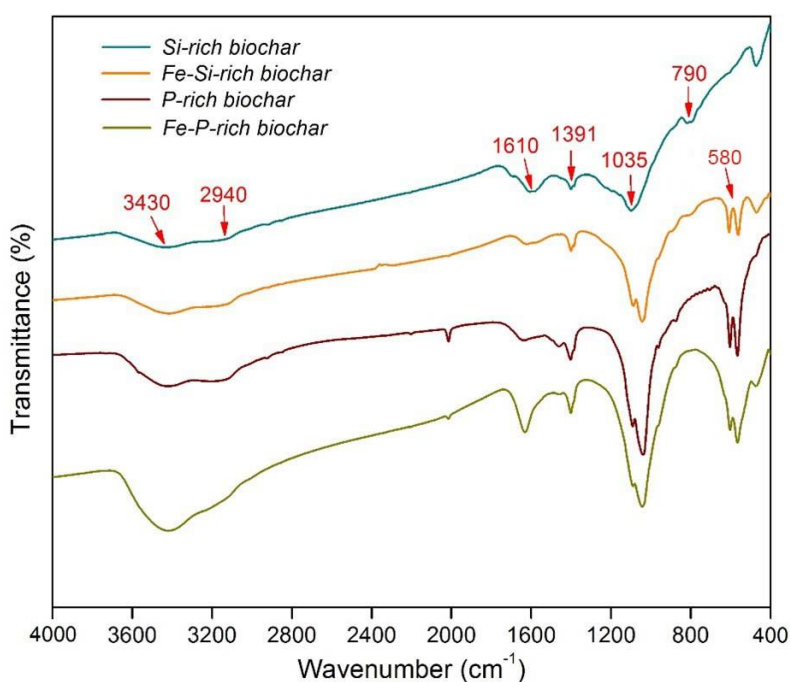


Figure 5-1 Fourier transform infrared (FTIR) spectra of different functionalized biochars.

5.2.4 Plant harvesting, soil collection and chemical analyses

At grain maturity (132 d post-transplantation), rice plants were cut 3 cm above the soil surface. Grain and straw samples were separated, oven-dried (65 °C), and ground to powder prior to analyses. Simultaneously, plant height, straw biomass, number of panicles, and grain yield per pot were measured after harvest. The ground plant samples were microwave-digested using HNO₃-H₂O₂ mixture for total As, Cd, Pb, Fe, and plant nutrient (P and K) analyses. Total Si in plant samples was extracted separately using a lithium metaborate digestion method according to Yang *et al.* (2020). Briefly, about 50 mg of ground plant samples were fused with 0.3 g of lithium metaborate in a muffle furnace at 950 °C for 30 min. Thereafter, the fused mixture was dissolved in 30 mL of 4% nitric solution, and then the concentration of Si in the solution was determined using the molybdenum blue colorimetric method as described in Lu (2000).

Soil samples were retrieved from each pot and placed in the greenhouse for air-drying. After sieved (< 2 mm), soil pH, organic carbon content, and concentrations of available nutrients (N, P, and K) were determined according to the standard methods presented in Lu, (2000). Soil As extracted with 0.05 M NH₄H₂PO₄ at a soil/solution ratio of 1: 25 (w/v) was considered as plant available. Potentially available Cd, Pb, and Fe were extracted using a solution consisting of 0.005 M DTPA (diethylenetriaminepentaacetic acid), 0.1 M triethanolamine, and 0.01 M CaCl₂ (Lindsay and Norvell, 1978). Available Si was extracted with 1 M NaAc-HAc buffer (pH = 4) according to Yang *et al.* (2020), and measured using the molybdenum blue colorimetric method (Lu, 2000). The freeze-dried (after freezing under -70 °C) soil subsamples were used for the analyses of enzyme activities, including 2 oxidoreductases (dehydrogenase and catalase), 1 carbon-cycling enzyme (β -glucosidase), 1 nitrogen-cycling enzyme (urease), and 1 phosphorus-cycling enzyme (acid phosphatase). The analytical methods of the enzyme activities are given in Table 5-2.

Table 5-2 Analytical methods of various enzyme activities.

Enzyme type	Substrate	Metabolite	Reaction time	Unit	References
Dehydrogenase	2,3,5-triphenyltetrazolium chloride	Triphenyl formazan	24 h	$\mu\text{g TPF g}^{-1} \text{ soil h}^{-1}$	(Casida <i>et al.</i> , 1964)
Catalase	H ₂ O ₂	H ₂ O	20 min	$\text{mL } 0.1 \text{ M KMnO}_4 \text{ g}^{-1} \text{ soil } 20 \text{ min}^{-1}$	(Johnson and Temple, 1964)
β -glucosidase	<i>p</i> -nitrophenyl- β -D-glucopyranoside	<i>p</i> -nitrophenol	1 h	$\mu\text{g PNP g}^{-1} \text{ soil h}^{-1}$	(Eivazi and Tabatabai, 1988)
Urease	Urea	NH ₃ -N	24 h	$\text{mg NH}_3\text{-N g}^{-1} \text{ soil } 24 \text{ h}^{-1}$	(Kandeler and Gerber, 1988)
Acid phosphatase	<i>p</i> -nitrophenol phosphate	<i>p</i> -nitrophenol	1 h	$\mu\text{g PNP g}^{-1} \text{ soil h}^{-1}$	(Tabatabai and Bremner, 1969)

5.2.5 Data processing and quality control

All data including characteristics, potentially available nutrients and enzyme activities of soil, and PTEs in soil and plants were tested for normality and homogeneity of distribution, and presented as means \pm standard errors ($n=4$). Statistical analyses were performed using SPSS 23.0 program (SPSS Inc. USA). A comparison between different treatments with varying parameters was conducted using one-way analysis of variance (ANOVA), followed by Tukey's multiple comparison test ($P<0.05$). Correlations between different parameters were analyzed based on Pearson's correlation coefficients ($P<0.05$). The intricate associations among enzyme activities, PTEs, and environmental variables were assayed by redundancy analysis (RDA). Principal component analysis (PCA) was carried out to depict the statistical correlations among rice growth parameters and soil pH, organic carbon, available nutrients, and PTEs. Details about quality assurance and quality control during analysis are given in *Appendix D* (section D3).

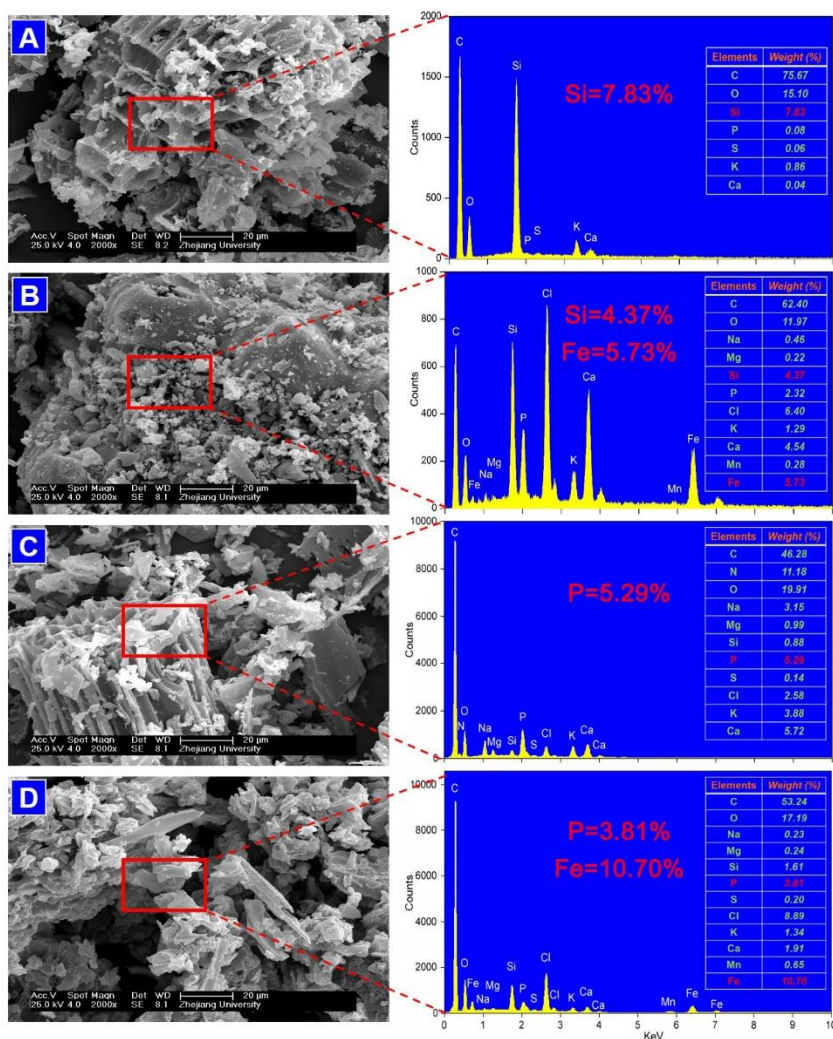


Figure 5-2 The scanning electron microscope (SEM) images and the energy dispersive X-ray (EDX) patterns of functionalized biochars (A: Si-BC; B: Fe-Si-BC; C: P-BC; D: Fe-P-BC).

5.3 Results

5.3.1 Characteristics of the functionalized biochars

The scanning electron microscope (SEM) images showed that there were obvious cellular and tubular porous structures in the pristine biochars (Si-BC and P-BC), whereas those porous structures were likely clogged after modification (Figure 5-2). The specific surface area of Fe-Si-BC ($69.3 \text{ m}^2 \text{ g}^{-1}$) was smaller than that of Si-BC ($237.3 \text{ m}^2 \text{ g}^{-1}$) (Table 5-1). The presence of Si (7.83 wt.%) and P (5.29 wt.%) in Si-BC and P-BC, respectively, was confirmed by the energy dispersive X-ray (EDX) spectroscopy spectra (Figure 5-2). The content of Fe in the modified biochars was noticeably higher than that of the pristine ones, indicating a successful loading of Fe after modification. Moreover, P-BCs were richer in ash and nitrogen (N) but poorer in carbon (C) and nitrogen (H) than Si-BCs, and an increase of biochar ash content was observed after modification (Table 5-1). Fourier transform infrared (FTIR) spectra of all biochars exhibited characteristic peaks at 3430, 2940, 1610, 1391, 1035, and 790 cm^{-1} , and the intensity of those peaks was strengthened after modification; moreover, the peaks of both P-BCs were stronger than those of Si-BCs (Figure 5-1). The functional groups were assigned as follows: 3430 cm^{-1} to O-H vibrations of hydroxyl groups, and N-H vibrations; 2940 cm^{-1} to C-H stretching of aliphatic CH_3 and CH_2 ; 1610 cm^{-1} to aromatic C=C vibration, and C=O stretching of quinones and ketonic acids; 1391 cm^{-1} to O-H deformation, phenolic C-O stretching groups, and C=N stretching of amide III band; 1035 cm^{-1} to C-O stretching of polysaccharides and polysaccharides-like compounds and Si-O-Si groups; 790 cm^{-1} to C-H bending CH out of plane deformation (Wu *et al.*, 2012; Fan *et al.*, 2018). The spectrum of Fe-Si-BC contained a characteristic peak at around 580 cm^{-1} , indicating the presence of ferrite bond (Fe-O) (Zhu *et al.*, 2020), which was not detected in Si-BC; meanwhile, a larger peak at 580 cm^{-1} was observed in the spectrum of Fe-P-BC relative to that of P-BC (Figure 5-1). These results further proved a successful loading of Fe on both biochars after modification. The concentrations of As, Cd, and Pb were minimal or undetected, avoiding the incorporation of exogenous PTE pollution.

5.3.2 Plant growth and grain yield

Application of functionalized biochars exhibited varying effects on rice plant growth and grain yield (Figure 5-3). The panicle number (per plant) and aboveground biomass (per plant) increased by 72.5% and 32.9% in the Si-BC treatment, and by 87.5% and 53.6% in the Fe-Si-BC treatment, respectively, compared to the control. Meanwhile, application of Fe-P-BC increased the panicle number and aboveground biomass by 47.5% and 35.7%, respectively, compared to the control. Fe-Si-BC was the only amendment that significantly ($P < 0.05$) increased the grain yield, by 38.6% as compared to the control. For the plant height, there were no significant ($P > 0.05$) differences among

different treatments, although a slight increased tendency was noticed in the Si-BC, Fe-Si-BC, and Fe-P-BC treatments, compared to the control.

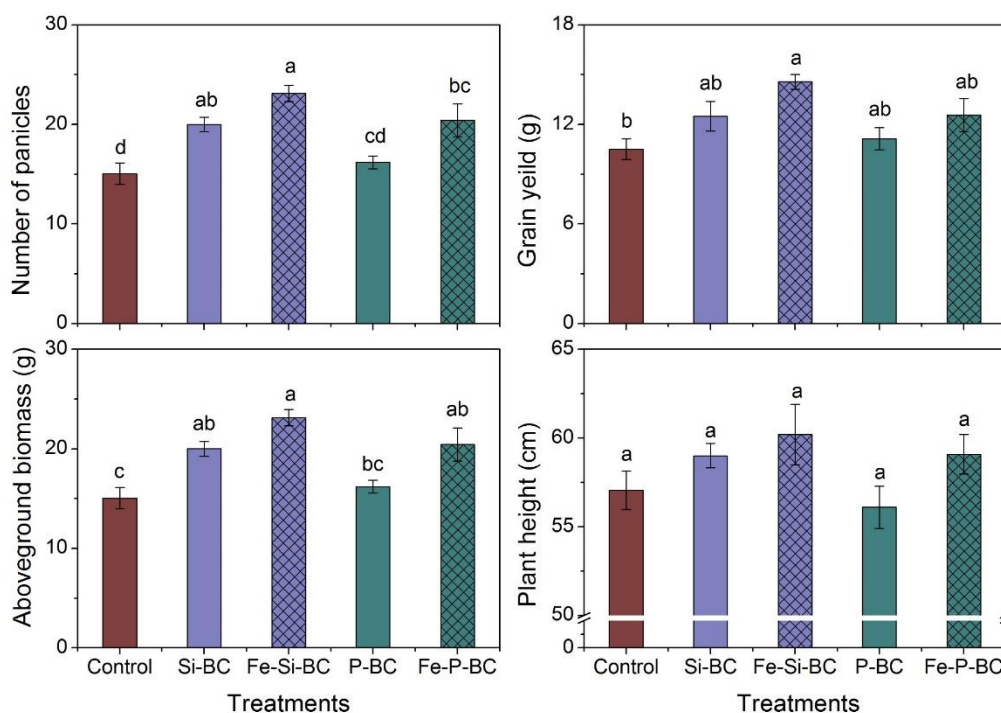


Figure 5-3 Effect of functionalized biochars on plant growth and grain yield.

5.3.3 Potential availability and plant accumulation of PTEs

The concentration of NaH_2PO_4 -extractable (available) As in the P-BC treatment increased by 13.9%, whereas Si-BC application did not significantly affect the concentration of available As in the soil, compared to the control (Figure 5-4). Application of both Fe-modified biochars led to a significant ($P < 0.05$) increase in available As, by 46.9% and 20.5% for Fe-Si-BC and Fe-P-BC, respectively, compared to the control. A similar trend of plant-As was noticed in the Fe-Si-BC, P-BC, and Fe-P-BC treatments. It is worth mentioning that, grain-As significantly ($P < 0.05$) decreased by 59.4% in the Si-BC treatment, compared to the control, whereas the concentration (0.73 mg kg^{-1}) was still higher than the permissible limit of As in brown rice regulated by the National Food Standard of China (GB 2762-2017, 0.20 mg kg^{-1}). Plants grown in all functionalized biochar-treated soils had significantly ($P < 0.05$) lower straw-As than those grown in the control soil. In general, both Si-rich biochars were slightly more effective on decreasing the accumulation of As in rice plants than the P-rich biochars.

Application of Si-BC did not affect the DTPA-extractable (available) Cd in soil, whereas Fe-Si-BC significantly ($P < 0.05$) decreased the concentration of available Cd, by 14.2%, compared to the control (Figure 5-4). The concentrations of available Cd also decreased significantly ($P < 0.05$) after the application of both P-BC (by 35.0%)

and Fe-P-BC (by 21.1%) as compared to the control. However, compared to the control, application of Fe-Si-BC and Fe-P-BC increased the concentrations of grain-Cd, by 1.3-fold and 1.3-fold, respectively. Similar to grain-Cd, application of Si-BC and P-BC did not affect straw-Cd, whereas the Fe-modified biochars promoted the accumulation of Cd in rice straw. Although the uptake of Cd in rice grain significantly ($P<0.05$) increased after the application of Fe-BCs, the concentrations (0.064 and 0.064 mg kg⁻¹, respectively) were still much lower than the permissible limit of Cd in brown rice (GB 2762-2017, 0.20 mg kg⁻¹).

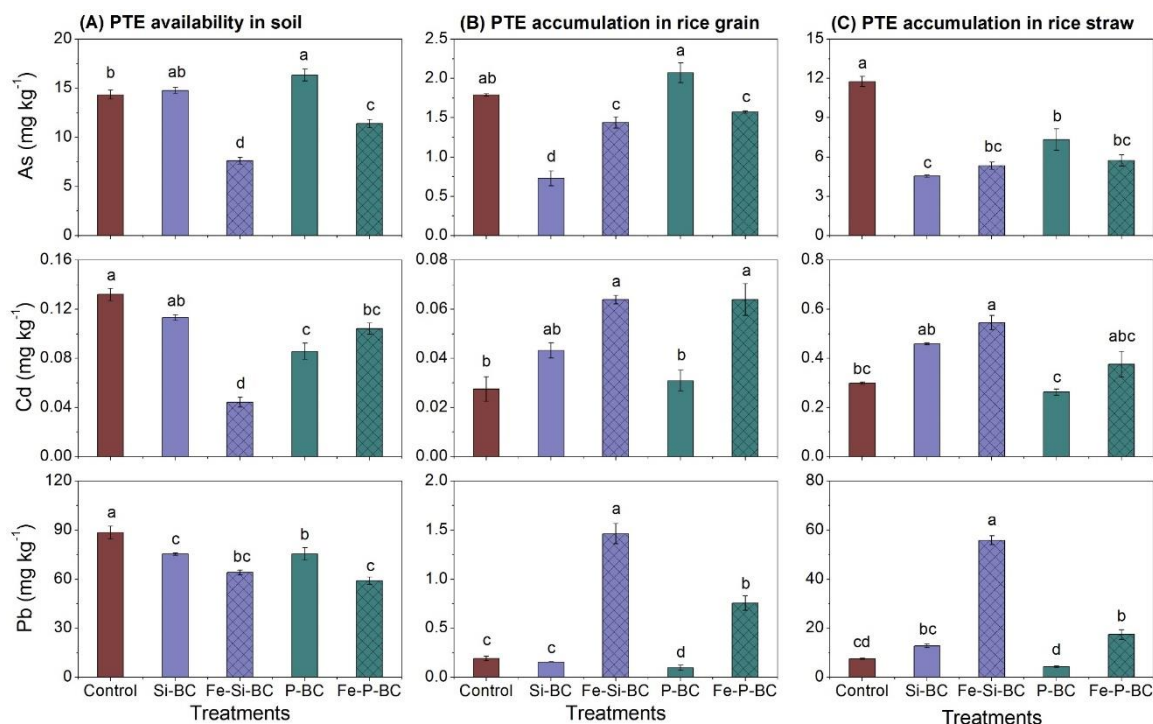


Figure 5-4 Effect of functionalized biochars on the availability of As, Cd, Pb, and their accumulation in rice grain and straw.

Application of all functionalized biochars decreased the DTPA-extractable (available) Pb in the soil (Figure 5-4). Compared to the control, the concentration of available Pb declined by 14.9% in the Si-BC treatment, by 27.5% in the Fe-Si-BC treatment, by 14.7% in the P-BC treatment, and by 33.3% in the Fe-P-BC treatment. Application of Si-BC did not significantly ($P>0.05$) affect either grain-Pb or straw-Pb, whereas the addition of Fe-Si-BC increased grain-Pb and straw-Pb by 6.6-fold and 6.3-fold, respectively, compared to the control. The P-BC amendment significantly ($P<0.05$) decreased grain-Pb and straw-Pb by 49.3% and 43.2%, respectively, whereas application of Fe-P-BC caused increased concentrations of grain-Pb (by 2.9-fold) and straw-Pb (by 1.3-fold) when both compared to the control. Overall, application of P-BC alleviated accumulation of Pb in rice grain to a value (0.10 mg kg⁻¹) lower than the permissible limit of Pb in brown rice (GB 2762-2017, 0.20 mg kg⁻¹), whereas

application of Fe-Si-BC and Fe-P-BC elevated the grain-Pb to 1.46 and 0.76 mg kg⁻¹, respectively.

5.3.4 Soil enzyme activities

Application of Si-BC significantly ($P < 0.05$) enhanced dehydrogenase and catalase activities, inhibited acid phosphatase activity, and did not affect β -glucosidase and urease activities in soil (Table 5-3). After Fe-Si-BC application, the activities of dehydrogenase and catalase were significantly ($P < 0.05$) inhibited by 49.6% and 40.0%, respectively, whereas the activity of acid phosphatase was promoted by 14.1%, compared to the control (Table 5-3). Application of P-BC improved the activities of all tested enzymes, except for acid phosphatase for which the activity was significantly ($P < 0.05$) inhibited. The change in enzyme activities in the Fe-P-BC treatment was nearly opposite to that in the P-BC treatment, showing a significant ($P < 0.05$) improvement of the activities of dehydrogenase (by 59.8%) and urease (by 22.7%), but a depression of the activities of catalase (by 29.5%) and acid phosphatase (by 21.0%), compared to the control (Table 5-3).

Table 5-3 Enzyme activities in non- and functionalized biochar-treated soils (mean \pm standard error, n = 4).

Treatments	Dehydrogenase ($\mu\text{g TPF g}^{-1} \text{ soil h}^{-1}$)	Catalase (mL 0.1 M KMnO ₄ $\text{g}^{-1} \text{ soil } 20 \text{ min}^{-1}$)	β -glucosidase ($\mu\text{g PNP g}^{-1} \text{ soil h}^{-1}$)	Urease (mg NH ₃ -N g ⁻¹ $\text{ soil } 24 \text{ h}^{-1}$)	Acid phosphatase ($\mu\text{g PNP g}^{-1} \text{ soil h}^{-1}$)
Control	1.66 \pm 0.02c	33.88 \pm 0.13b	15.20 \pm 0.66ab	0.16 \pm 0.01cd	0.27 \pm 0.00b
Si-BC	2.95 \pm 0.05b	36.63 \pm 0.13a	19.03 \pm 2.92a	0.18 \pm 0.00bc	0.22 \pm 0.00c
Fe-Si-BC	0.84 \pm 0.04d	20.33 \pm 0.14d	9.03 \pm 0.70b	0.14 \pm 0.01d	0.31 \pm 0.01a
P-BC	4.05 \pm 0.06a	36.00 \pm 0.00a	19.33 \pm 1.46a	0.23 \pm 0.01a	0.19 \pm 0.01c
Fe-P-BC	2.66 \pm 0.08b	23.88 \pm 0.24c	13.50 \pm 0.61ab	0.20 \pm 0.00ab	0.21 \pm 0.00c

5.4 Discussion

5.4.1 Effect of functionalized biochars on the potential availability of PTEs in soils and their accumulation in rice plants

5.4.1.1 Arsenic

Soil available As was positively correlated ($P < 0.01$) with pH (Figures 5-5 and 5-6). Soil pH plays an important role in affecting the mobilization of As in soils (Zama *et al.*, 2018; Pan *et al.*, 2021; Yang *et al.*, 2022a). Upon P-BC application, soil particles could be more negatively charged due to the elevated ambient pH relative to the control (Pan *et al.*, 2021). Meanwhile, As is present as anions, such as AsO₄³⁻, HAsO₄²⁻, and H₂AsO₄⁻ at the pH range from 3 to 8 (Yang *et al.*, 2022a). Thus, the elevated pH caused by P-BC application (Figure 5-6) may cause an enhanced release of As due to the electrostatic repulsive force; vice versa, the decline of pH caused by Fe-Si-BC application (Figure 5-7) might depress As availability because of the electrostatic attraction between the protonated soil particles and anionic As (Wen *et al.*, 2021). It is unlikely that the decrease of available As in the

Fe-Si-BC treatment could be linked to pH because there was no significant ($P>0.05$) change in pH as compared to the control (Figure 5-7). However, the decrease of available As in the Fe-modified biochar treatments might be associated with the redox chemistry of Fe. Seyfferth *et al.* (2019) reported that soil As has been immobilized due to the incorporation and co-precipitation with Fe oxides under non-flooded soil conditions. In addition, the enhanced competition among dissolved organic carbon (DOC), phosphate, and As after P-BC application could be employed to explain the elevated As availability in soil (Zama *et al.*, 2018), due to the P-BC-induced rising of available P and organic carbon content (Figure 5-6).

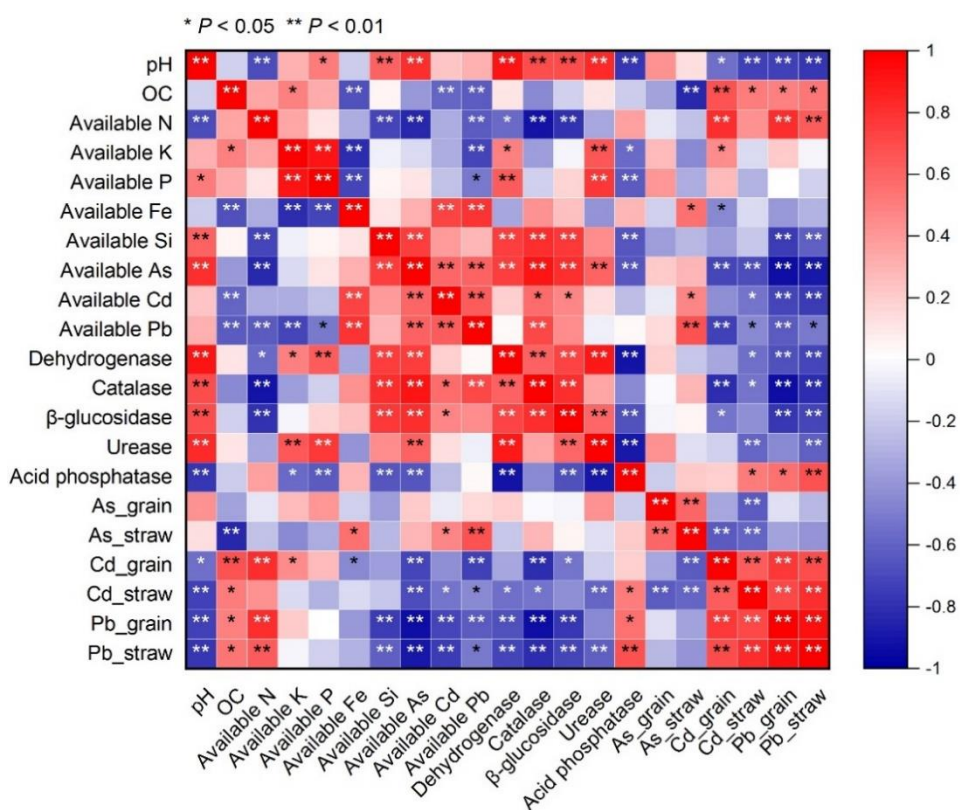


Figure 5-5 Pearson's correlation coefficients among different parameters.

The concentrations of available As in soil were not correlated with the concentrations of As in rice grain and straw (Figure 5-5), which indicated that functionalized biochars affected As accumulation in rice plants in different ways. For instance, the significant ($P<0.05$) decrease of As concentrations in rice grain and straw in the Si-BC treatment could be primarily attributed to the high availability of Si (Figure 5-6). Arsenite, mainly under anaerobic (flooding) conditions, is absorbed by rice roots primarily through Si transporters (Lsi1 and Lsi2), thus the presence of available Si may limit As uptake by rice plants through competing for the transporters (Seyfferth *et al.*, 2019). This mechanism could be further proven by the significantly ($P<0.05$) increased concentrations of straw-Si and grain-Si as compared to the control (Table 5-4). On the other hand, Si could also inhibit As uptake through down-

regulating the expression of those two transporters (Zhao and Wang, 2019). Both P-BCs can ameliorate As uptake, particularly in rice straw, because of the increased P availability (Figure 5-6). Phosphate, which exhibits similar chemical behavior as arsenate (mostly under drainage conditions), could inhibit As uptake by rice plants, since arsenate shares the same uptake transporters (OsPT1, OsPT4, and OsPT8) with phosphate (Seyfferth and Fendorf, 2012; Zhao and Wang, 2019). This could be evidenced by the significant ($P < 0.05$) increase in straw-P and rice-P in the P-BC treatment, compared to the control (Table 5-4). The significant ($P < 0.05$) decrease in both straw-As and grain-As levels in the Fe-biochar treatments could be interpreted by the formation of iron plaque, which may attract soluble As from soil solution and/or act as a barrier to As uptake in rice roots (Seyfferth *et al.*, 2010). In our study, the content of iron plaque extracted from rice roots in the Fe-biochar treatments was significantly ($P < 0.05$) higher than that in the control (Table 5-4).

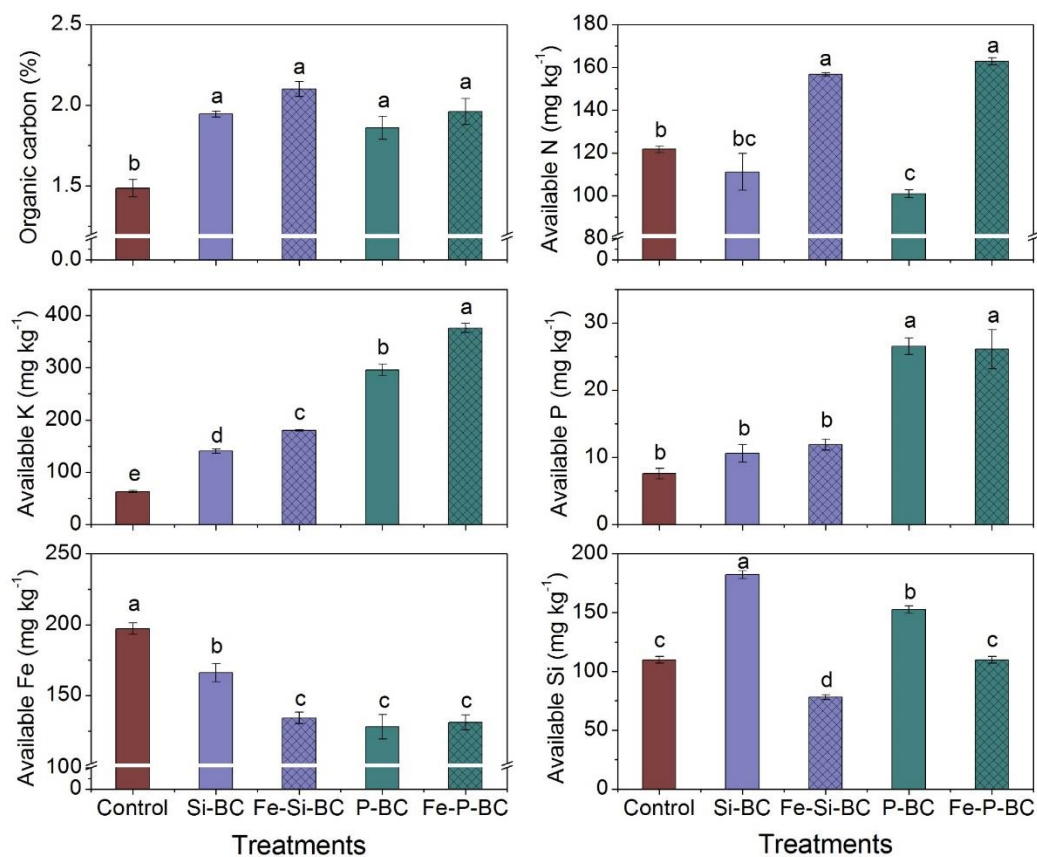


Figure 5-6 Effect of functionalized biochars on organic carbon content and concentrations of available nutrients in the soil.

Table 5-4 Effect of functionalized biochars on uptake of K, P and N in rice grain and straw, and iron plaque content on rice root.

Treatments	Grain-K (g kg ⁻¹)	Straw-K (g kg ⁻¹)	Grain-P (g kg ⁻¹)	Straw-P (g kg ⁻¹)	Grain-Si (g kg ⁻¹)	Straw-Si (g kg ⁻¹)	Grain-Fe (mg kg ⁻¹)	Straw-Fe (mg kg ⁻¹)	Iron plaque (g kg ⁻¹)
Control	1.57 ± 0.06ab	6.77 ± 0.38b	1.70 ± 0.03bc	0.96 ± 0.02c	6.01 ± 0.65d	29.42 ± 1.84c	60.53 ± 7.79b	803.5 ± 41.9a	6.11 ± 0.44c
Si-BC	1.25 ± 0.00c	8.71 ± 0.12a	1.46 ± 0.17c	0.51 ± 0.04d	19.31 ± 0.48a	63.19 ± 0.43a	113.43 ± 3.78a	712.3 ± 143.5a	8.15 ± 1.26bc
Fe-Si-BC	1.48 ± 0.03b	8.69 ± 0.10a	1.62 ± 0.05bc	0.62 ± 0.04d	11.52 ± 0.30b	52.33 ± 0.78b	119.50 ± 4.76a	889.3 ± 124.5a	11.90 ± 0.67a
P-BC	1.65 ± 0.04a	6.66 ± 0.39b	2.10 ± 0.03a	2.22 ± 0.03a	9.24 ± 0.38c	28.19 ± 1.37c	68.10 ± 3.68b	583.3 ± 46.8a	7.99 ± 0.28bc
Fe-P-BC	1.58 ± 0.03ab	8.62 ± 0.21a	1.84 ± 0.03ab	1.12 ± 0.04b	7.29 ± 0.21cd	28.30 ± 0.38c	110.97 ± 11.99a	1034.7 ± 42.9a	8.85 ± 0.28b

5.4.1.2 Cadmium

All functionalized biochar treatments, except for the case of Si-BC, reduced the concentrations of available Cd in the soil, compared to the control (Figure 5-4). The decreased soil Cd availability in the P-BC treatment could be mainly explained by the presence of large porous structure and abundant functional groups on the surface of P-BC (Figures 5-1 and 5-2) and the P-BC-induced elevated soil pH (Figure 5-7), which may promote the immobilization of Cd via electrostatic interactions and formation of complexes and precipitates (Wang *et al.*, 2019; Wen *et al.*, 2021). In addition, the increased availability of P (soluble phosphate) in soil (Figure 5-6) might form insoluble compounds with Cd, such as $Cd_3(PO_4)_2$ and Ca-Cd phosphates (Azeem *et al.*, 2021; Yang *et al.*, 2021a). This mechanism could also be employed for the interpretation of the alleviated Cd availability in the Fe-P-BC treatment. It was assumed that the decrease of available Cd in both Fe-modified biochar treatments could be rather linked to the exogenous Fe added along with biochars than the change in pH, since available Cd was positively correlated ($P < 0.01$) with available Fe, but non-correlated ($P > 0.01$) with pH (Figure 5-5). Iron (hydro)oxides are the predominant forms of iron in soils; their redox transformation and speciation might change the characteristics of clay minerals, thereby influencing the mobility and bioavailability of Cd (Yu *et al.*, 2020; Yang *et al.*, 2021a). Thus, it was speculated that the application of Fe-modified biochars could immobilize Cd through complexation, co-precipitation, and incorporation with Fe (hydro)oxides and Fe organic compounds, in particular during drainage period (under aerobic conditions).

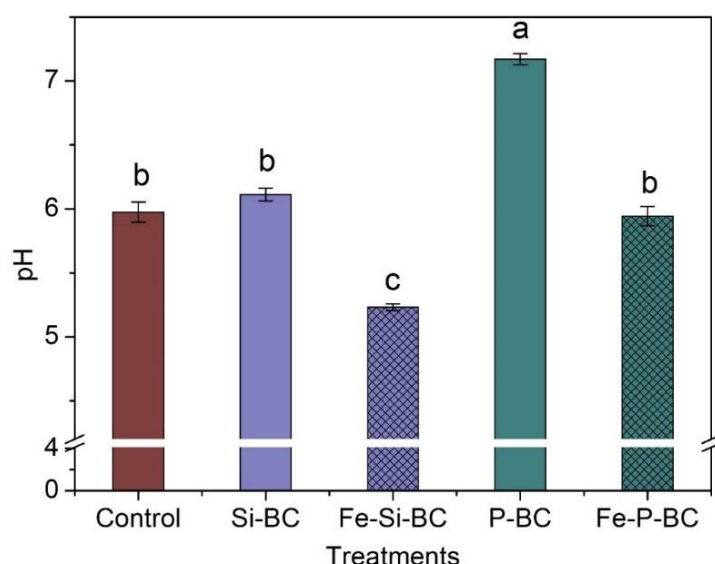


Figure 5-7 Effect of functionalized biochars on soil pH.

Application of Fe-modified biochars significantly ($P < 0.05$) increased the accumulation of Cd in plant tissues (particularly in rice grain), while no significant differences were found between the control and the pristine biochar

treatments. These results disagreed with the potential availability of Cd in soil treated with different treatments (Figure 5-4). Our previous study confirmed that biochar-induced change in soil pH was a main factor that controlled the uptake of Cd by rice plants (Wen *et al.*, 2021). Although a significantly ($P < 0.01$) negative correlation between soil pH and plant-Cd was found (Figure 5-5), it is unlikely to associate the concentration of plant-Cd with soil pH in the pristine biochar treatments, since no decline tendency of pH was found in either treatment (Figure 5-7). However, it might be that the acidic Fe-modified biochars, in particular Fe-Si-BC caused an increased plant-Cd due to the decrease of soil pH. In general, soil acidification is considered to be one of the key contributors to high Cd concentrations in rice grain in southern China (Zhao and Wang, 2019). Furthermore, considering the intermittent water management applied in this study, the effects of the fluctuated redox conditions (Eh) during rice grown cannot be ruled out. Cadmium is generally presented as free ions and/or soluble complexes in soil solutions (Zhao and Wang, 2019). Under drainage conditions, application of organic matter along with the Fe-modified biochars might promote the transformation of Cd from the soluble form to stable Fe-complexes (e.g., Fe-OC complex) (Yang *et al.*, 2021a) and Fe-precipitates (e.g., $\text{CdCO}_3\text{-FeCO}_3\text{-CaCO}_3$ mineral) (Bian *et al.*, 2018), thereby decreasing the mobility and bioavailability of Cd. After flooding, it is likely that the bound Cd could be released because of the reductive dissolution and decomposition of those stable Fe minerals, thereby promoting Cd accumulation in rice plants (Yang *et al.* 2021b). On the other hand, Huang *et al.* (2021) reported that the mobility of Cd could be increased upon soil drainage due to the formation of hydroxyl free radicals, which can promote the oxidative dissolution of CdS.

5.4.1.3 Lead

Similar to Cd, the potential availability of Pb decreased in soils treated with different functionalized biochars, compared to that in the control (Figure 5-4). Also, the Fe-modified biochars were more effective than the pristine ones (especially PBC). For the Si-BC treatment, the immobilization of Pb in the soil depended mainly on the relatively high surface area of Si-BC (Table 5-1), which likely offered a chance to promote the physical/electrostatic adsorption of Pb (Wan *et al.*, 2020). The presence of SiO_3^{2-} and Si-rich particles could also enhance the formation of Si-Pb precipitates (e.g., $5\text{PbO}\cdot\text{P}_2\text{O}_5\cdot\text{SiO}_2$) (Xiao *et al.*, 2018). With regard to the P-BC treatment, the adsorption of Pb depended primarily on the presence of high phosphorus and functional groups on P-BC, as well as its high alkalinity (Figures 5-1 and 5-2). It has been proven that Pb and phosphate can react rapidly to form insoluble Pb-phosphate compounds (e.g., $\text{Pb}_5(\text{PO}_4)_3$) (Wen *et al.*, 2021; Yang *et al.*, 2021a), thereby decreasing Pb mobility and availability in soils. The elevated soil pH, caused by P-BC application in this study (Figure 5-7), is a well-known mechanism that leads to immobilization of Pb in soil, which may promote the

formation of insoluble Pb minerals (Yu *et al.*, 2020). In addition, the functional groups on P-BC could immobilize Pb through the formation of stable complexes (Pan *et al.*, 2021). Similarly, this mechanism could also be engaged in explaining the decreased Pb availability in both Fe-modified biochar treatments, since the Fe loading process increased the variety and number of functional groups on biochars (Figure 5-1), consequently promoting the immobilization of Pb. Moreover, the redox cycling of Fe compounds might be coupled with the mobility and availability of Pb (Yang *et al.*, 2021a). Wan *et al.* (2020) found that Pb could be attached to the Fe oxides in soils, as proven by the micro-X-ray fluorescence mapping; they also proved that Pb could be adsorbed on biochar and Fe oxides after the application of iron-modified magnetic biochar. In addition, the modification process might have concentrated the content of cationic mineral elements (Ca^{2+} , K^+ , Mg^{2+}) (Figure 5-2), which could also contribute to the immobilization of Pb in soils (Igalavithana *et al.*, 2019).

Although application of Si-BC decreased the concentration of available Pb in soil, no significant difference was found in either straw-Pb or grain-Pb content between the Si-BC treatment and control; however, application of P-BC significantly ($P < 0.05$) decreased the accumulation of Pb in both rice tissues (Figure 5-4). These infer that the incorporation of SiO_3^{2-} and Si-rich compounds along with Si-BC played only a limited role in affecting accumulation of Pb in rice plants, although Zhao *et al.* (2017) indicated that the application of silicate reduced the concentration of Pb in brown rice. However, the decrease in Pb bioavailability in soil induced by P-BC application could be considered as one of the main causes for the reduction of Pb in rice plants (Wen *et al.*, 2021). Therefore, P-BC was more effective on obstructing Pb uptake by rice straw and grain than Si-BC in the current study. On the other hand, the raised soil pH after P-BC application (Figure 5-7) could be the other major factor that caused an alleviation of Pb accumulation in rice plants (Wan *et al.*, 2020). Conversely, the decreased soil pH caused by application of the acidic Fe-modified biochars might be responsible for the elevated Pb concentration in rice plants grown in both Fe-modified biochar-treated soils, particularly in the Fe-Si-BC treatment (Figure 5-4). Additionally, the redox-induced cycling of Fe (hydro)oxides and organic compounds resulted from the intermittent water management could also be employed to explain the significant ($P < 0.05$) increase of straw-Pb and grain-Pb levels after Fe-modified biochar application (similar to Cd as discussed in section 4.1.2).

5.4.2 Effect of functionalized biochars on soil enzyme activities

Soil enzymes are sensitive to changes in PTE toxicity, nutrient availability, and soil physicochemical property (Chen *et al.*, 2020). In the current study, therefore, it was deduced that the changes in soil enzyme activities could be linked to the variations of the environmental parameters (e.g., soil pH, organic carbon content, and available nutrients and PTEs) caused by the application of functionalized biochars. Redundancy analysis (RDA) was

conducted to assess the multivariate relationships between soil enzyme activities and those environmental parameters (Figure 5-8). The results showed that soil pH is the most crucial factor determining the soil enzyme activities (64.6%, $P=0.002$). Thus, promotion of all enzyme activities, except for acid phosphatase after pristine biochar application, in particular P-BC, could be predominantly attributed to the elevated soil pH (Figure 5-7). Conversely, application of acidic Fe-modified biochars had either inhibition or no effect on enzyme activities except for dehydrogenase and urease in the Fe-P-BC treatment and acid phosphatase in the Fe-Si-BC treatment. Positive correlations ($P<0.01$) were found between soil pH and dehydrogenase, catalase, β -glucosidase, and urease activities (Figure 5-5), which further confirmed that soil pH played an important role in regulating enzyme activities. The optimum pH for acid phosphatase ranged from 4.0 to 5.0 (Chen *et al.*, 2020). Thus, the Fe-Si-BC-induced decrease in pH (5.2) and P-BC-induced increase in pH (7.2) could cause promotion and inhibition, respectively of soil acid phosphatase activity.

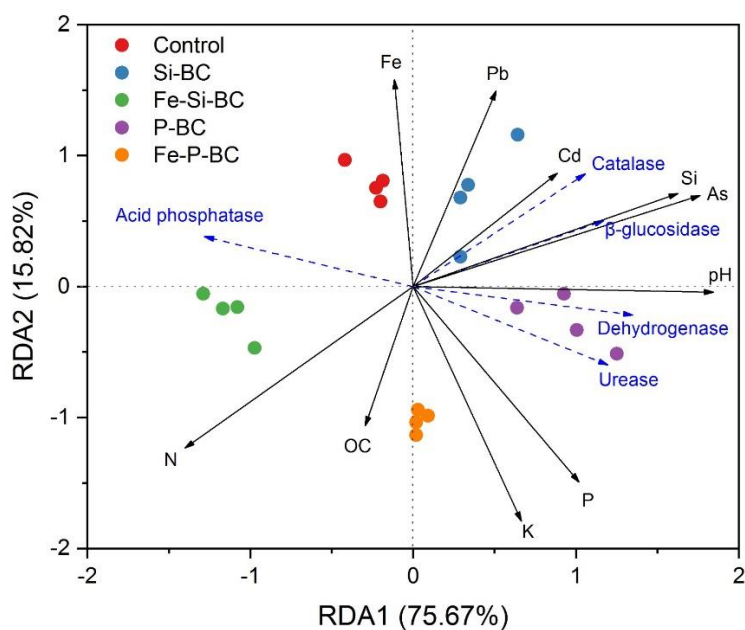


Figure 5-8 Redundancy analysis (RDA) between enzyme activities and environmental factors (soil pH, organic carbon, and available nutrients and PTEs).

RDA results also suggested that the second and third most critical environmental factors that contributed to the variant activities of soil enzymes were available K and Si, which respectively accounted for 14.2% ($P=0.002$) and 8.6% ($P=0.006$) of the total variance (Figure 5-8). Although available P indicated non-significant influence on enzyme activities, its impact cannot be ruled out, as positive correlations ($P<0.01$) between available P and dehydrogenase and urease activities were found in the correlation matrix (Figure 5-5). Soil nutrients, such as available P, K, and Si generated from biochar, might alleviate the nutrient limitation, thus promoting microbial

metabolism, and enhancing microbial activities and enzyme excretion (Zama *et al.*, 2018; Tang *et al.*, 2020). Previous studies also reported that soil nutrients are responsible for plant growth and a vital symptom of soil microbial productivity (Yang *et al.*, 2016a; Nie *et al.*, 2018; Tang *et al.*, 2020). Therefore, it can be presumed that the enhanced soil enzyme activities (dehydrogenase, catalase, and urease) after P-BC application might be ascribed to the increase of soil available K and P (Figure 5-6). On the other hand, Si-BC could promote the activities of enzymes (e.g., dehydrogenase and catalase) through increasing Si bioavailability (Figure 5-6). The direct interactions between microbes and biochar particles could contribute to the increased enzyme activities after the application of pristine biochars. For instance, the porous structure on pristine biochars (Figure 5-2) might serve as a reliable habitat, protecting microbes from predators (Nie *et al.*, 2018), thereby promoting their growth and reproduction.

In the current study, RDA results showed that the available As significantly (3.3%, $P=0.006$) contributed to the variability in enzyme activities (Figure 5-8), and all enzymes except for acid phosphatase were positively correlated ($P<0.01$) with the soil available As (Figure 5-5). A similar result was reported by Tang *et al.* (2020), where they found that the increased As availability could promote soil enzyme activities, and interpreted this phenomenon by the PTE-enhanced coordination between enzyme active sites and substrate in soils. However, soil available Cd and Pb made no significant contributions to the variability in enzyme activities (Figure 5-8), which was inconsistent with the previous studies (e.g., Nie *et al.*, 2018; Chen *et al.*, 2020). Yang *et al.* (2016a) indicated that soil enzyme activities exhibited various (positive, negative, or none) correlations with PTE availability, which depended on different factors, including soil types, contamination levels, analytical methods, *etc.*

5.4.3 Effect of functionalized biochars on plant growth

As aforementioned in the above sections, application of functionalized biochars have, to some extent, adjusted soil pH, improved soil fertility status, ameliorated PTE availability, and promoted enzymatic activities in soils, providing better soil conditions and cleaner environment for rice production. As shown in the PCA, vectors of plant height, aboveground biomass, grain yield, and number of panicles are all pointing to the similar direction as those of organic carbon and available P and K (Figure 5-9), indicating a positive effect of these parameters on rice plant growth. Previous studies also pointed out that biochar could promote plant growth by improving soil fertility and enhancing nutrient use efficiency (Zeeshan *et al.*, 2020; Zhang *et al.*, 2020; Wen *et al.*, 2021). Therefore, we speculate that the promoted plant growth and increased rice yield might be attributed to the increase of nutrient availability after the addition of functionalized biochars, in particular both P-BCs (Figure 5-7).

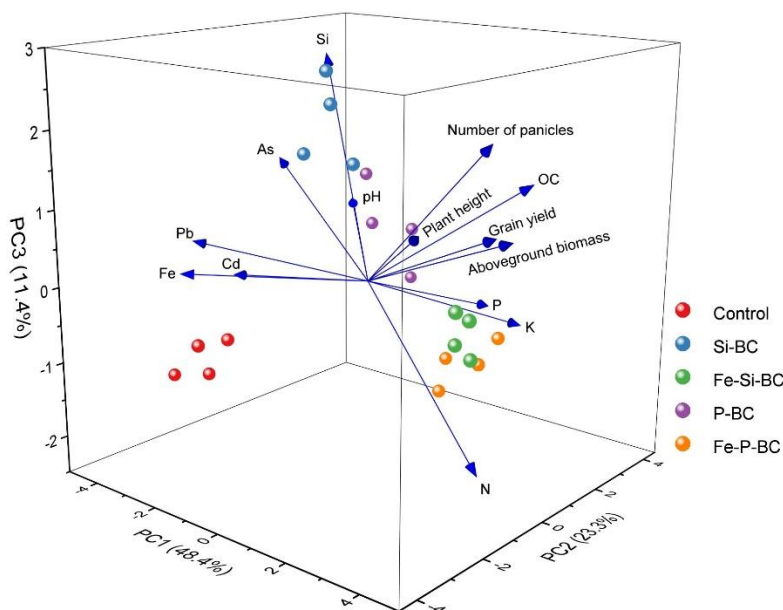


Figure 5-9 Principal analysis (PCA) among rice plant growth parameters and soil pH, organic carbon, and available nutrients and PTEs.

Negative correlations were found between available PTEs and rice plant growth parameters (Figure 5-9), suggesting that the availability and toxicity of PTEs could affect the growth of rice plants (Wen *et al.*, 2021). Moreover, Zeeshan *et al.* (2020) reported that the quality along with the yield of crop is seriously affected if the accumulative contents of PTEs in plant tissues are over the certain threshold values. Biochar application can improve plant growth and protect plants from abiotic stress resulting from heavy metal pollution by enhancing the uptake of mineral elements in plants (Sui *et al.*, 2021). In this study, although the application of functionalized biochars did not ideally reduce the concentrations of PTEs to values lower than the limits (Figure 5-6), it promoted uptake of mineral elements in rice tissues. Namely, both Si-BCs increased the concentrations of straw-K, grain-Si, straw-Si, grain-Fe and straw-Fe, while application of both P-BCs increased the concentrations of grain-P, straw-P, grain Si, and grain-Fe, compared to the control (Table 5-4).

Consequently, it was inferred that the promoted plant growth and improved rice yield after the application of functionalized biochars could be attributed to the increase of accumulation of mineral elements in rice plants. In particular, the increased plant-Si caused by Si-BCs could help rice plants to avoid abiotic/biotic stresses and enhanced susceptibility to diseases and pests (Seyfferth *et al.*, 2013; Wang *et al.*, 2019). The optimum pH condition for rice growth was between 5.0 and 6.5 (Yu *et al.*, 2021). Therefore, the slightly lower growth indices for plants grown in P-BC-treated soil than those in other functionalized biochar-treated one could be explained by the P-BC-induced increase of pH (up to 7.2).

5.5 Conclusions

Different functionalized biochars exerted various effects on soil fertility, enzyme activity and PTEs (i.e., As, Cd, and Pb) phytoavailability, thus influencing the yield and quality of rice differently. In particular, the pristine Si-rich biochar reduced As accumulation in rice grain and straw, and improved soil fertility and microbial activities without negative impacts on rice yield, whereas the Fe-modified Si-rich biochar alleviated As uptake, and meanwhile promoted plant growth, thus increasing rice yield. Nevertheless, Fe-modified Si-rich biochar is unlikely to be used for the remediation of multi-PTE contaminated paddy soils since it dramatically promoted the uptake of Cd and Pb by rice plants and elevated their environmental risks. P-rich biochar reduced the accumulation of Pb in rice grain and straw, without affecting plant-As and -Cd and compromising rice yield. However, application of Fe-modified P-rich biochar significantly ($P < 0.05$) decreased As in rice grain and straw, improved soil fertility, and promoted plant growth, whereas increased the plant-Cd and -Pb levels. Therefore, it was concluded that the Fe-modified Si-rich (rice husk) and P-rich (pig carcass) biochar could be suitable amendments for improving soil quality and increasing the yield and quality of rice when As is the only concern in soils. If Pb is a concern, application of pristine P-rich biochar could be a strategic measure to limit Pb accumulation in rice. However, application of Fe-modified biochars might induce an increasing accumulation of Cd and Pb in rice, thus posing a high risk of these elements to food security and human health. Overall, none of the tested functionalized biochars could reach an appropriate effectiveness on a simultaneous mitigation of multi-PTEs in the paddy soil. Future studies are warranted to select suitable feedstocks for producing functionalized biochars, optimize practical techniques for biochar modification, and investigate the suitable application manners and dosages of functionalized biochars to achieve cleaner rice production.

5.6 Acknowledgments

This work was supported by the National Natural Science Foundation of China (21876027), the Key Scientific and Technological Project of Foshan City, China (2120001008392), and the Special Fund for the Science and Technology Innovation Team of Foshan City, China (1920001000083).

5.7 References

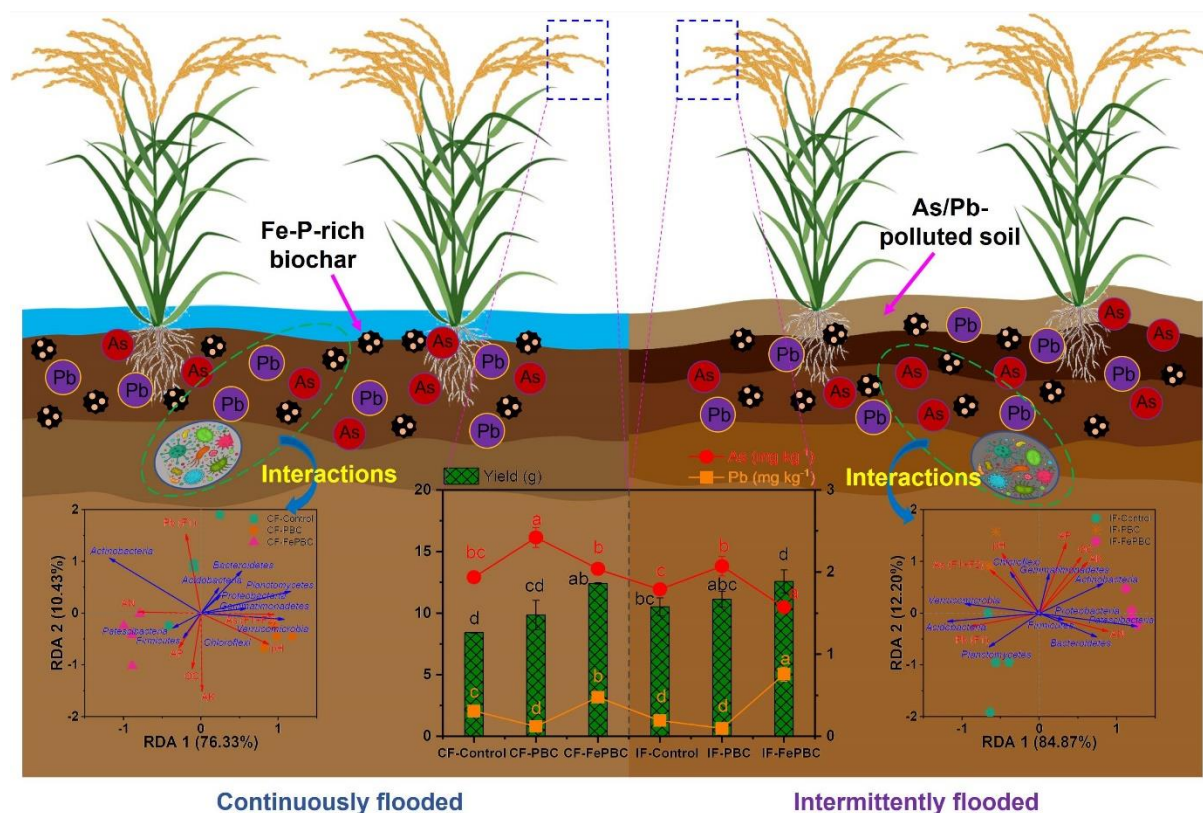
- ATSDR's substance priority list., Available from: <https://www.atsdr.cdc.gov/spl/index.html#2019spl>.
- Azeem, M., Ali, A., Soundari, P.G., Yiman, L., Zhang, Z., 2021. Bone-derived biochar improved soil quality and reduced Cd and Zn phytoavailability in a multi-metal contaminated mining soil. *Environ. Pollut.* 277, 116800. <https://doi.org/10.1016/j.envpol.2021.116800>
- Bandara, T., Franks, A., Xu, J., Bolan, N., Wang, H., Tang, C., 2019. Chemical and biological immobilization mechanisms of potentially toxic elements in biochar-amended soils. *Crit. Rev. Environ. Sci.* 50, 903-978. <https://doi.org/10.1080/10643389.2019.1642832>
- Bian, P., Zhang, J., Zhang, C., Huang, H., Rong, Q., Wu, H., Li, X., Xu, M., Liu, Y., Ren, S., 2018. Effects of Silk-worm Excrement Biochar Combined with Different Iron-Based Materials on the Speciation of Cadmium and Lead in Soil. *Appl. Sci.* 8, 1999. <https://doi.org/10.3390/app8101999>
- Chen, H., Yang, X., Wang, H., Sarkar, B., Shaheen, S.M., Gielen, G., Bolan, N., Guo, J., Che, L., Sun, H., Rinklebe, J., 2020. Animal carcass- and wood-derived biochars improved nutrient bioavailability, enzyme activity, and plant growth in metal-phthalic acid ester co-contaminated soils: A trial for reclamation and improvement of degraded soils. *J. Environ. Manage.* 261, 110246. <https://doi.org/10.1016/j.jenvman.2020.110246>
- El-Naggar, A., Lee, M.H., Hur, J., Lee, Y.H., Igalavithana, A.D., Shaheen, S.M., Ryu, C., Rinklebe, J., Tsang, D.C.W., Ok, Y.S., 2020. Biochar-induced metal immobilization and soil biogeochemical process: An integrated mechanistic approach. *Sci. Total Environ.* 698, 134112. <https://doi.org/10.1016/j.scitotenv.2019.134112>
- El-Naggar, A., Chang, S.X., Cai, Y., Lee, Y.H., Wang, J., Wang, S.L., Ryu, C., Rinklebe, J., Sik Ok, Y., 2021. Mechanistic insights into the (im)mobilization of arsenic, cadmium, lead, and zinc in a multi-contaminated soil treated with different biochars. *Environ. Int.* 156, 106638. <https://doi.org/10.1016/j.envint.2021.106638>
- Fan, W., Wu, J., Li, J., Hu, J., 2018. Comparative effects of different maize straw returning modes on soil humus composition and humic acid structural characteristics in Northeast China. *Chem. Ecol.* 34, 355-370. <https://doi.org/10.1080/02757540.2018.1437147>
- Frick, H., Tardif, S., Kandeler, E., Holm, P.E., Brandt, K.K., 2019. Assessment of biochar and zero-valent iron for in-situ remediation of chromated copper arsenate contaminated soil. *Sci. Total Environ.* 655, 414-422. <https://doi.org/10.1016/j.scitotenv.2018.11.193>
- Gomez-Sagasti, M.T., Epelde, L., Anza, M., Urrea, J., Alkorta, I., Garbisu, C., 2019. The impact of nanoscale zero-valent iron particles on soil microbial communities is soil dependent. *J. Hazard. Mater.* 364, 591-599. <https://doi.org/10.1016/j.jhazmat.2018.10.034>
- Huang, H., Ji, X., Cheng, L., Zhao, F., Wang, P., 2021. Free radicals produced from the oxidation of ferrous sulfides promote the remobilization of cadmium in paddy soils during drainage. *Environ. Sci. Technol.* 55, 9845-9853. <https://doi.org/10.1021/acs.est.1c00576>
- Igalavithana, A.D., Kwon, E.E., Vithanage, M., Rinklebe, J., Moon, D.H., Meers, E., Tsang, D.C.W., Ok, Y.S., 2019. Soil lead immobilization by biochars in short-term laboratory incubation studies. *Environ. Int.* 127, 190-198. <https://doi.org/10.1016/j.envint.2019.03.031>
- Jinger, D., Dhar, S., Dass, A., Sharma, V.K., Shukla, L., Paramesh, V., Parihar, M., Joshi, N., Joshi, E., Gupta, G., Singh, S., 2022. Residual Silicon and Phosphorus Improved the Growth, Yield, Nutrient Uptake and Soil Enzyme Activities of Wheat. *Silicon*. <https://doi.org/10.1007/s12633-022-01676-w>
- Kashif Irshad, M., Noman, A., Wang, Y., Yin, Y., Chen, C., Shang, J., 2022. Goethite modified biochar simultaneously mitigates the arsenic and cadmium accumulation in paddy rice (*Oryza sativa*) L. *Environ. Res.* 206, 112238. <https://doi.org/10.1016/j.envres.2021.112238>
- Kumarathilaka, P., Bundschuh, J., Seneweera, S., Marchuk, A., Ok, Y.S., 2021. Iron modification to silicon-rich

- biochar and alternative water management to decrease arsenic accumulation in rice (*Oryza sativa* L.). Environ. Pollut. 286, 117661. <https://doi.org/10.1016/j.envpol.2021.117661>
- Li, Z., Wang, L., Wu, J., Xu, Y., Wang, F., Tang, X., Xu, J., Ok, Y.S., Meng, J., Liu, X., 2020. Zeolite-supported nanoscale zero-valent iron for immobilization of cadmium, lead, and arsenic in farmland soils: Encapsulation mechanisms and indigenous microbial responses. Environ. Pollut. 260, 114098. <https://doi.org/10.1016/j.envpol.2020.114098>
- Liu, L., Han, J., Xu, X., Xu, Z., Abeysinghe, K.S., Atapattu, A.J., De Silva, P., Lu, Q., Qiu, G., 2020. Dietary exposure assessment of cadmium, arsenic, and lead in market rice from Sri Lanka. Environ. Sci. Pollut. Res. 27, 42704-42712. <https://doi.org/10.1007/s11356-020-10209-0>
- Lu, R., 2000. Analytical Methods for Soil Agrochemistry. Chinese Agricultural Science and Technology Publishing House, Beijing.
- Nie, C., Yang, X., Niazi, N.K., Xu, X., Wen, Y., Rinklebe, J., Ok, Y.S., Xu, S., Wang, H., 2018. Impact of sugarcane bagasse-derived biochar on heavy metal availability and microbial activity: A field study. Chemosphere 200, 274-282. <https://doi.org/10.1016/j.chemosphere.2018.02.134>
- Ok, Y.S., Rinklebe, J., Hou, D., Tsang, D.C., Tack, F.M.G., 2020. Soil and Groundwater Remediation Technologies: A Practical Guide (pp. 1-350). CRC Press.
- Palansooriya, K.N., Shaheen, S.M., Chen, S.S., Tsang, D.C.W., Hashimoto, Y., Hou, D., Bolan, N.S., Rinklebe, J., Ok, Y.S., 2020. Soil amendments for immobilization of potentially toxic elements in contaminated soils: A critical review. Environ. Int. 134, 105046. <https://doi.org/10.1016/j.envint.2019.105046>
- Pan, H., Yang, X., Chen, H., Sarkar, B., Bolan, N., Shaheen, S.M., Wu, F., Che, L., Ma, Y., Rinklebe, J., Wang, H., 2021. Pristine and iron-engineered animal- and plant-derived biochars enhanced bacterial abundance and immobilized arsenic and lead in a contaminated soil. Sci. Total Environ. 763, 144218. <https://doi.org/10.1016/j.scitotenv.2020.144218>
- Peng, D., Wu, B., Tan, H., Hou, S., Liu, M., Tang, H., Yu, J., Xu, H., 2019. Effect of multiple iron-based nanoparticles on availability of lead and iron, and micro-ecology in lead contaminated soil. Chemosphere 228, 44-53. <https://doi.org/10.1016/j.chemosphere.2019.04.106>
- Seyfferth, A.L., Amaral, D., Limmer, M.A., Guilherme, L.R.G., 2019. Combined impacts of Si-rich rice residues and flooding extent on grain As and Cd in rice. Environ. Int. 128, 301-309. <https://doi.org/10.1016/j.envint.2019.04.060>
- Seyfferth, A.L., Fendorf, S., 2012. Silicate mineral impacts on the uptake and storage of arsenic and plant nutrients in rice (*Oryza sativa* L.). Environ. Sci. Technol. 46, 13176-13183. <https://doi.org/10.1021/es3025337>
- Seyfferth, A.L., Kocar, B.D., Lee, J.A., Fendorf, S., 2013. Seasonal dynamics of dissolved silicon in a rice cropping system after straw incorporation. Geochim. Cosmochim. Acta 123, 120-133. <https://doi.org/10.1016/j.gca.2013.09.015>
- Seyfferth, A.L., Webb, S.M., Andrews, J.C., Fendorf, S., 2010. Arsenic localization, speciation, and co-occurrence with iron on rice (*Oryza sativa* L.) roots having variable Fe coatings. Environ. Sci. Technol. 44, 8108-8113. <https://doi.org/10.1021/es101139z>
- Shaheen, S.M., Vasileios Antoniadis, V., Muhammad Shahid, Yang, Y., Abdelrahman, H., Zhang, T., Hassan, N.E.E., Bibi, I., Niazi, N.K., Younis, S.A., Almazroui, M., Tsang, Y.F., Sarmah, A.K., Kim, K., Rinklebe, J., 2022. Sustainable applications of rice feedstock in agro-environmental and construction sectors: A global perspective. Renew. Sustain. Energy Rev. 153, 111791. <https://doi.org/10.1016/j.rser.2021.111791>
- Sohail, M.I., Zia Ur Rehman, M., Rizwan, M., Yousaf, B., Ali, S., Anwar Ul Haq, M., Anayat, A., Waris, A.A., 2020. Efficiency of various silicon rich amendments on growth and cadmium accumulation in field grown cereals and health risk assessment. Chemosphere 244, 125481.

- <https://doi.org/10.1016/j.chemosphere.2019.125481>
- Sui, F., Kang, Y., Wu, H., Li, H., Wang, J., Joseph, S., Munroe, P., Li, L., Pan, G., 2021. Effects of iron-modified biochar with S-rich and Si-rich feedstocks on Cd immobilization in the soil-rice system. *Ecotoxicol. Environ. Saf.* 225, 112764. <https://doi.org/10.1016/j.ecoenv.2021.112764>
- Tang, J., Zhang, L., Zhang, J., Ren, L., Zhou, Y., Zheng, Y., Luo, L., Yang, Y., Huang, H., Chen, A., 2020. Physicochemical features, metal availability and enzyme activity in heavy metal-polluted soil remediated by biochar and compost. *Sci. Total Environ.* 701, 134751. <https://doi.org/10.1016/j.scitotenv.2019.134751>
- Wan, X., Li, C., Parikh, S.J., 2020. Simultaneous removal of arsenic, cadmium, and lead from soil by iron-modified magnetic biochar. *Environ. Pollut.* 261, 114157. <https://doi.org/10.1016/j.envpol.2020.114157>
- Wang, Y., Xiao, X., Xu, Y., Chen, B., 2019. Environmental Effects of Silicon within Biochar (Sichar) and Carbon-Silicon Coupling Mechanisms: A Critical Review. *Environ. Sci. Technol.* 53, 13570-13582. <https://doi.org/10.1021/acs.est.9b03607>
- Wang, Y., Zhang, K., Lu, L., Xiao, X., Chen, B., 2020. Novel insights into effects of silicon-rich biochar (Sichar) amendment on cadmium uptake, translocation and accumulation in rice plants. *Environ. Pollut.* 265, 114772. <https://doi.org/10.1016/j.envpol.2020.114772>
- Wen, E., Yang, X., Chen, H., Shaheen, S.M., Sarkar, B., Xu, S., Song, H., Liang, Y., Rinklebe, J., Hou, D., Li, Y., Wu, F., Pohořelý, M., Wong, J.W.C., Wang, H., 2021. Iron-modified biochar and water management regime-induced changes in plant growth, enzyme activities, and phytoavailability of arsenic, cadmium and lead in a paddy soil. *J. Hazard. Mater.* 407, 124344. <https://doi.org/10.1016/j.jhazmat.2020.124344>
- Wu, W., Yang, M., Feng, Q., McGrouther, K., Wang, H., Lu, H., Chen, Y., 2012. Chemical characterization of rice straw-derived biochar for soil amendment. *Biomass Bioenergy* 47, 268-276. <https://doi.org/10.1016/j.biombioe.2012.09.034>
- Xiao, X., Chen, B., Chen, Z., Zhu, L., Schnoor, J.L., 2018. Insight into multiple and multilevel structures of biochars and their potential environmental applications: A critical review. *Environ. Sci. Technol.* 52, 5027-5047. <https://doi.org/10.1021/acs.est.7b06487>
- Xiao, Z., Peng, M., Mei, Y., Tan, L., Liang, Y., 2021. Effect of organosilicone and mineral silicon fertilizers on chemical forms of cadmium and lead in soil and their accumulation in rice. *Environ. Pollut.* 283, 117107. <https://doi.org/10.1016/j.envpol.2021.117107>
- Yang, J., Yang, F., Yang, Y., Xing, G., Deng, C., Shen, Y., Luo, L., Li, B., Yuan, H., 2016a. A proposal of “core enzyme” bioindicator in long-term Pb-Zn ore pollution areas based on topsoil property analysis. *Environ. Pollut.* 213, 760-769. <https://doi.org/10.1016/j.envpol.2016.03.030>
- Yang, X., Hinzmann, M., Pan, H., Wang, J., Bolan, N., Tsang, D.C.W., Ok, Y.S., Wang, S.-L., Shaheen, S.M., Wang, H., Rinklebe, J., 2022a. Pig carcass-derived biochar caused contradictory effects on arsenic mobilization in a contaminated paddy soil under fluctuating controlled redox conditions. *J. Hazard. Mater.* 421, 126647. <https://doi.org/10.1016/j.jhazmat.2021.126647>
- Yang, X., Li, J., Liang, T., Yan, X., Zhong, L., Shao, J., El-Naggar, A., Guan, C.Y., Liu, J., Zhou, Y., 2021b. A combined management scheme to simultaneously mitigate As and Cd concentrations in rice cultivated in contaminated paddy soil. *J. Hazard. Mater.* 416, 125837. <https://doi.org/10.1016/j.jhazmat.2021.125837>
- Yang, X., Liu, J., McGrouther, K., Huang, H., Lu, K., Guo, X., He, L., Lin, X., Che, L., Ye, Z., Wang, H., 2016b. Effect of biochar on the extractability of heavy metals (Cd, Cu, Pb, and Zn) and enzyme activity in soil. *Environ. Sci. Pollut. Res.* 23, 974-984. <https://doi.org/10.1007/s11356-015-4233-0>
- Yang, X., Lu, K., McGrouther, K., Lei, C., Hu, G., Wang, Q., Liu, X., Shen, L., Huang, H., Ye, Z., 2017. Bioavailability of Cd and Zn in soils treated with biochars derived from tobacco stalk and dead pigs. *J. Soils Sediments* 17, 751-762. <https://doi.org/10.1007/s11368-015-1326-9>

- Yang, X., Pan, H., Shaheen, S.M., Wang, H., Rinklebe, J., 2021a. Immobilization of cadmium and lead using phosphorus-rich animal-derived and iron-modified plant-derived biochars under dynamic redox conditions in a paddy soil. *Environ. Int.* 156, 106628. <https://doi.org/10.1016/j.envint.2021.106628>
- Yang, X., Shaheen, S.M., Wang, J., Hou, D., Ok, Y.S., Wang, S.L., Wang, H., Rinklebe, J., 2022b. Elucidating the redox-driven dynamic interactions between arsenic and iron-impregnated biochar in a paddy soil using geochemical and spectroscopic techniques. *J. Hazard. Mater.* 422, 126808. <https://doi.org/10.1016/j.jhazmat.2021.126808>
- Yang, X., Song, Z., Qin, Z., Wu, L., Yin, L., Van Zwieten, L., Song, A., Ran, X., Yu, C., Wang, H., 2020. Phytolith-rich straw application and groundwater table management over 36 years affect the soil-plant silicon cycle of a paddy field. *Plant Soil* 454, 343-358. <https://doi.org/10.1007/s11104-020-04656-4>
- Yu, B., Li, D., Wang, Y., He, H., Li, H., Chen, G., 2020. The compound effects of biochar and iron on watercress in a Cd/Pb-contaminated soil. *Environ. Sci. Pollut. Res.* 27, 6312-6325. <https://doi.org/10.1007/s11356-019-07353-7>
- Yu, M., Su, W.-q., Parikh, S.J., Li, Y., Tang, C., Xu, J., 2021. Intact and washed biochar caused different patterns of nitrogen transformation and distribution in a flooded paddy soil. *J. Clean. Prod.* 293, 126259. <https://doi.org/10.1016/j.jclepro.2021.126259>
- Zama, E.F., Reid, B.J., Sun, G.-X., Yuan, H.-Y., Li, X.-M., Zhu, Y.-G., 2018. Silicon (Si) biochar for the mitigation of arsenic (As) bioaccumulation in spinach (*Spinacia oleracea*) and improvement in the plant growth. *J. Clean. Prod.* 189, 386-395. <https://doi.org/10.1016/j.jclepro.2018.04.056>
- Zeeshan, M., Ahmad, W., Hussain, F., Ahamd, W., Numan, M., Shah, M., Ahmad, I., 2020. Phytostabilization of the heavy metals in the soil with biochar applications, the impact on chlorophyll, carotene, soil fertility and tomato crop yield. *J. Clean. Prod.* 255, 120318. <https://doi.org/10.1016/j.jclepro.2020.120318>
- Zhang, Q., Song, Y., Wu, Z., Yan, X., Gunina, A., Kuzyakov, Y., Xiong, Z., 2020. Effects of six-year biochar amendment on soil aggregation, crop growth, and nitrogen and phosphorus use efficiencies in a rice-wheat rotation. *J. Clean. Prod.* 242, 118435. <https://doi.org/10.1016/j.jclepro.2019.118435>
- Zhao, F.-J., Wang, P., 2019. Arsenic and cadmium accumulation in rice and mitigation strategies. *Plant Soil* 446, 1-21. <https://doi.org/10.1007/s11104-019-04374-6>
- Zhao, M., Liu, Y., Li, H., Cai, Y., Wang, M.K., Chen, Y., Xie, T., Wang, G., 2017. Effects and mechanisms of meta-sodium silicate amendments on lead uptake and accumulation by rice. *Environ. Sci. Pollut. Res.* 24, 21700-21709. <https://doi.org/10.1007/s11356-017-9746-2>
- Zhu, S., Zhao, J., Zhao, N., Yang, X., Chen, C., Shang, J., 2020. Goethite modified biochar as a multifunctional amendment for cationic Cd(II), anionic As(III), roxarsone, and phosphorus in soil and water. *J. Clean. Prod.* 247. <https://doi.org/10.1016/j.jclepro.2019.119579>

CHAPTER 6: Influences of the Iron-Modified Phosphorus-Rich Biochar on Rice Yield, Arsenic and Lead Redistribution, and Bacterial Community Structure in Paddy Soil ⁵



⁵ Adapted from Yang, X., Dai, Z., Ge, C., Bolan, N., Tsang, D.C.W., Song, H., Hou, D., Shaheen, S.M., Wang, H., Rinklebe, J. Multiple-functionalized biochar enhances rice yield via regulating arsenic and lead redistribution and bacterial community structure in soils under different hydrological conditions. Ready for being submitted to *Environment International*.

A supplementary data is provided in Appendix E.

Abstract

Rice grown in soils contaminated with arsenic (As) and lead (Pb) will accumulate these elements in rice grain, thereby resulting in lower rice yield due to the toxic stress. Herein, we examined the roles of functionalized biochars (raw and iron (Fe)-modified phosphorus (P)-rich, PBC and FePBC, respectively) coupled with different water regimes (continuously and intermittently flooded, CF and IF) in affecting the rice yield and the accumulation of As and Pb in rice grain. Results showed that FePBC increased the rice yield under both CF (47.4%) and IF (19.6%) conditions compared to the controls, mainly because FePBC application improved the soil nutrient availability and shifted the abundance of genera *Bacillus*, *Arthrobacter* and *Gemmatimonas*. Both biochars treatments changed the accumulation of As and Pb in the rice grain through regulating their redistribution and bacterial community structure (especially at the genus level) in the soil. Grain As concentration was higher under CF (1.94-2.42 mg kg⁻¹) than under IF conditions (1.56-2.31 mg kg⁻¹), while the concentration of grain Pb was higher under IF (0.10-0.76 mg kg⁻¹) than CF (0.12-0.48 mg kg⁻¹) conditions. The application of PBC reduced grain Pb by 60.1% under CF conditions, whereas FePBC reduced grain As by 12.2% under IF conditions, and increased grain Pb by 2.9 and 6.6 times under CF and IF conditions, respectively, compared to the controls. Therefore, the application of the Fe-modified P-rich biochar is effective on raising the rice yield and reducing the accumulation of As in rice grain (particularly under IF conditions). However, it may undesirably elevate the environmental risks of Pb to rice production.

Keywords: engineered biochar; potentially toxic elements; food security/safety; soil remediation; rice paddy management; sustainable waste management.

6.1 Introduction

Soil contamination with potentially toxic elements including heavy metals and metalloids is an increasingly severe ecological and environmental concern in China and other regions (Zhao and Wang, 2019). Industrial and agricultural activities, such as mining and smelting, fossil fuels combustion, sewage irrigation and sewage sludge application, agrochemical over-use often cause widespread contamination of heavy metals and metalloids in soils (Palansooriya *et al.*, 2020). Arsenic (As) and lead (Pb) are prevalent metalloid and heavy metal, respectively, in arable soils in the industrial zones and mining areas (Wu *et al.*, 2021). For example, according to the Report on the National Soil Contamination Survey in China, 2.7% and 1.5% of the investigated sites covering over 65% of China's land area exceeded the regulatory limit of As and Pb, respectively, ranked third and sixth among the eight monitored inorganic contaminants (MEE and MNR, 2014). Exposure of As and Pb in paddy soils poses a serious threat to human health via rice consumption and other food crops (Wu *et al.*, 2021; Yang *et al.*, 2021). Arsenic is well-known to be associated with neurological problems, skin lesions, cardiovascular diseases, infertility and diabetes (Yang *et al.*, 2022a), and Pb may cause serious diseases such as neurasthenia, anorexia, and anemia (Qu *et al.*, 2022). Given that As and Pb in soils are difficult to extract/recover and cannot be degraded, altering their bioaccessible fractions to reduce their mobility and bioavailability has become a research hotspot (Lan *et al.*, 2021). Agronomic management strategies (e.g., water management or irrigation pattern) and the judicious application of soil amendments (e.g., biochar) have been increasingly adopted to reduce the accumulation of As and Pb in rice, while maintaining or even enhancing the rice yield.

Water/irrigation management in rice cultivation significantly affects the redox reactions in paddy soil, eventually controlling the transformation and redistribution of As and Pb in rice paddy (Das *et al.*, 2016; Wang *et al.*, 2019; Yang *et al.*, 2021). Under aerobic conditions, As is present as As(V), which is less mobile than As(III), and can be strongly absorbed by Fe-Mn (hydro)oxides in soils (Yang *et al.*, 2022b). In contrast, prolonged submergence of paddy soil may promote the reduction of As(V) to As(III) and the reductive dissolution of As-bearing Fe-Mn (hydro)oxides, thus elevating As mobility and bioavailability (Das *et al.*, 2016). However, water management has an opposite effect on the accumulation of As and Pb in rice crops (Wu *et al.*, 2021). Xia *et al.* (2018) found that Pb could be immobilized under anaerobic conditions through the formation of insoluble sulfide. Thus, it is challenging to simultaneously immobilize As and Pb in paddy soils through regulating water management regimes. Even though it has been well-proven that biochar application could (1) ameliorate soil physicochemical and microbial conditions (Shaheen *et al.*, 2018), and (2) enhance the immobilization of cationic metals (e.g., Pb) in soils (Palansooriya *et al.*, 2020), it is less effective on immobilizing anionic metalloids such as As, and can even

increase its mobility in some cases, owing to the elevated soil pH (Pan *et al.*, 2021). Thus, biochar has limited capability in remediating soils co-contaminated with As and Pb, unless it is modified or functionalized to impart specific moieties reactive to both cationic and anionic contaminants (Yang *et al.*, 2021). For instance, iron-based materials, such as Fe oxides, nano zero-valent Fe, and Fe sulfides have been used for biochar modification due to their promising prospects in immobilization of heavy metals and metalloids (Wan *et al.*, 2020; Wen *et al.*, 2021; Qu *et al.*, 2022). Phosphorus-rich materials have been widely used for immobilizing Pb in soils since soluble phosphate (PO_4^{3-}) could transform labile Pb into stable compounds such as $\text{Pb}_5(\text{PO}_4)_3\text{OH}$ and $\text{Pb}_5(\text{PO}_4)_3\text{Cl}$ (Bolan *et al.*, 2003; Chen *et al.*, 2022; Qu *et al.*, 2022). In addition, PO_4^{3-} shared the same transporters (OsPT1, OsPT4, and OsPT8) with As(V) to rice roots due to their chemical similarity, thus the elevated concentration of PO_4^{3-} may inhibit the uptake of As by rice plants (Bolan *et al.*, 2015; Zhao and Wang, 2019).

Our previous study demonstrated that Fe- and P-rich functionalized biochars can effectively immobilize As, Cd, and Pb under dynamic redox conditions in a paddy soil (an incubation experiment) (Yang *et al.*, 2021; Yang *et al.*, 2022b). We found that the Fe-rich biochar could immobilize As, particularly under reducing conditions, while it had little effect on Pb. In contrast, the application of the P-rich biochar alleviated the mobility of Pb, whereas increasing As release under both strongly reducing and oxidizing conditions. Based on these findings, we hypothesized that a multiple-functionalized biochar, Fe-modified P-rich biochar, would capitalize on the merits of various materials, i.e., Fe, P, and biochar, thus improving the effectiveness on multi-PTE immobilization. To this end, several types of functionalized biochars, including the Fe-modified P-rich biochars were prepared and applied to rice cultivation to investigate their performance in immobilizing As and Pb in soils under different water management regimes. Moreover, soil microorganisms are considered the most sensitive soil biota to the subtle changes in soil properties and stress of As and Pb in contaminated soils (Wan *et al.*, 2022). Since both water management and biochar application are likely to have profound effects on soil microbial activity in arable soils, the change and evolution of soil microcosms were scrutinized by microbial assay (Smith *et al.*, 2010; Bastida *et al.*, 2017; Zhang *et al.*, 2019). Therefore, the coupling synergetic effects of water management regimes and functionalized biochar application on the redistribution of As and Pb and soil microbial community structure need to be rigorously verified. Here, a Fe-loaded pig carcass-derived P-rich biochar was exploited (1) to investigate the potential impacts of this Fe-P-rich biochar on the geochemical redistribution and bioavailability of As and Pb in a contaminated paddy soils under different water management regimes, and (2) to assess the influences of Fe-P-rich biochar on the ecotoxicity of As and Pb, as well as the responses of soil bacterial communities.

6.2 Materials and methods

6.2.1 Soil and biochar preparation

Soil was collected in a farmland near an abandoned lead mine in Shaoxing City, Zhejiang Province, China (29°59'N, 120°46'E). This site was selected because it has a long history of being used as a paddy field. Due to occasional runoff from the adjacent mine tailings, the paddy soils are enriched in As and Pb. Total concentrations of As and Pb in this soil were 141 and 736 mg kg⁻¹, which exceeded regulatory limit of 30 and 500 mg kg⁻¹, respectively, with pH range from 5.5 to 6.5 (MEE, 2018). More details about the soil properties could be found in our previous studies (Pan *et al.*, 2021; Yang *et al.*, 2021). Top layer (0-20 cm) soils were collected from several sampling points and mixed as one composite, and then shipped to the laboratory for air-drying, milling, and sieving prior to use. The virgin biochar produced from pig carcass was obtained from Zhejiang Eco Environmental Technology Co., Ltd (Zhejiang, China), and it was proven to be rich in P in our previous studies (Yang *et al.*, 2017; Yang *et al.*, 2022a). According to the manufacturer, pig carcasses were placed in a batch pyrolysis reactor and kept for 2 h at a final temperature of approximately 650°C to obtain the raw P-rich biochar (PBC). For preparation of the Fe-modified P-rich biochar (FePBC), predetermined amount of PBC was put in a FeCl₃·6H₂O solution at 1: 20 of Fe-to-biochar ratio, and then followed by mixing, drying, and re-pyrolysis (Wen *et al.*, 2021). The selected characteristics of those two biochars are shown in the Table 6-1 and Figures 6-1 and 6-2. It is noteworthy that the concentrations of As and Pb in both biochars are low and negligible.

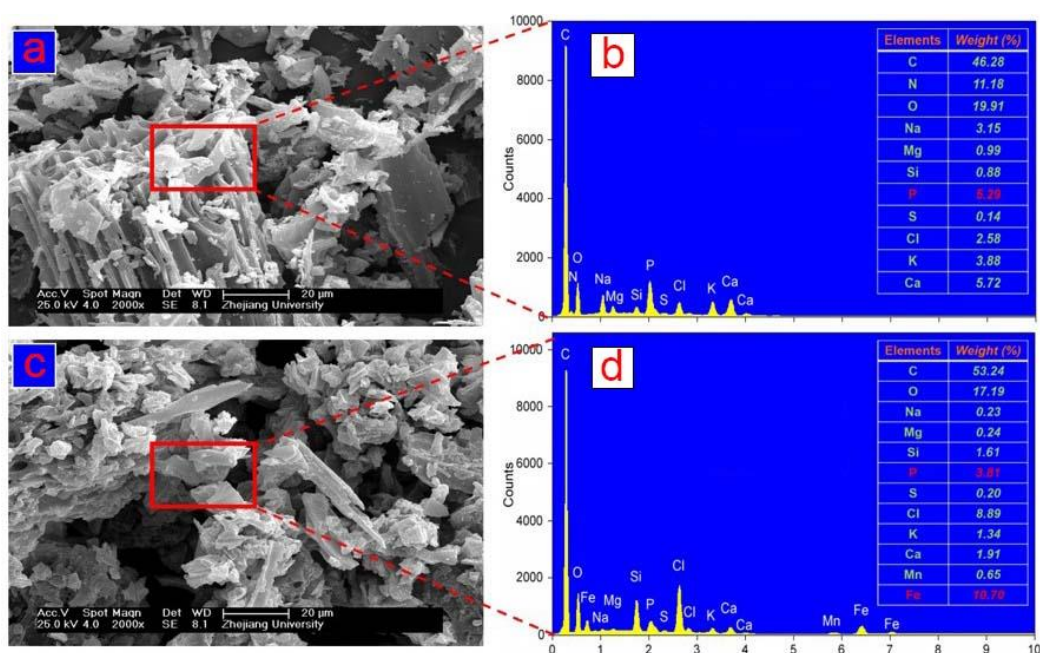


Figure 6-1 The scanning electron microscope (SEM) images and the energy dispersive X-ray patterns (EDS) of biochars (a: PCB-SEM; b: PBC-EDS; c: FePCB-SEM; d: FePBC-EDS).

Table 6-1 Physicochemical properties of the studied biochars.

Properties	PBC	FePBC
pH	10.6	3.6
Specific surface area (m ² g ⁻¹)	18.4	43.6
Ash content (%)	60.0	76.3
Total C (%)	30.8	40.4
Total N (%)	2.1	1.8
Total H (%)	1.3	1.5
Total S (%)	0.19	0.16
molar N/C	0.06	0.04
molar H/C	0.5	0.4
Total As (mg kg ⁻¹)	LDL	LDL
Total Pb (mg kg ⁻¹)	1.6	4.6

6.2.2 Rice cultivation experiment

Both biochars were thoroughly mixed with the contaminated soil at a rate of 3 wt.% biochar relative to soil dry weight. Non-treated soil served as control. The cultivation experiment was designed to simulate two different water management regimes (continuously flooded (CF) and intermittently flooded (IF)), and a total of six treatments were set as follows: CF-Control, CF-PBC, CF-FePBC, IF-Control, IF-PBC, IF-FePBC. Each plastic pot (22 cm high, 24 cm in diameter) was filled with 8.0 kg of the non- and biochar-treated soils. Four replications for each treatment were arranged as a randomized block design. Twenty-four pots were placed in a greenhouse at Zhejiang A & F University in China. Based on the local rice cultivation practice, 0.68 g (equivalent to 450 kg ha⁻¹) of compound fertilizer (N: P: K=15: 12: 18) was incorporated into each pot as base fertilizer, and another 0.68 g (equivalent to 450 kg ha⁻¹) of compound fertilizer and 0.34 g (equivalent to 225 kg ha⁻¹) of urea were added as topdressing 10 days after transplantation. The agronomic design of irrigation patterns, i.e., CF and IF, has been described elsewhere (Wen *et al.*, 2021). Seven days after the first irrigation, five uniform-sized rice seedlings (cultivar Xiushui-519) at 3-4 leaf stage were selected and transplanted into each pot. The irrigation patterns for both CF and IF groups were maintained until harvest. After harvest (i.e., 132 days after transplantation), rice grain yield in each pot was recorded and then was ground to powder for total As and Pb analysis. Soil samples were collected for further analyses. The analytical methods for soil pH, organic carbon content, and nutrient availability were given in *Appendix E* (section E1).

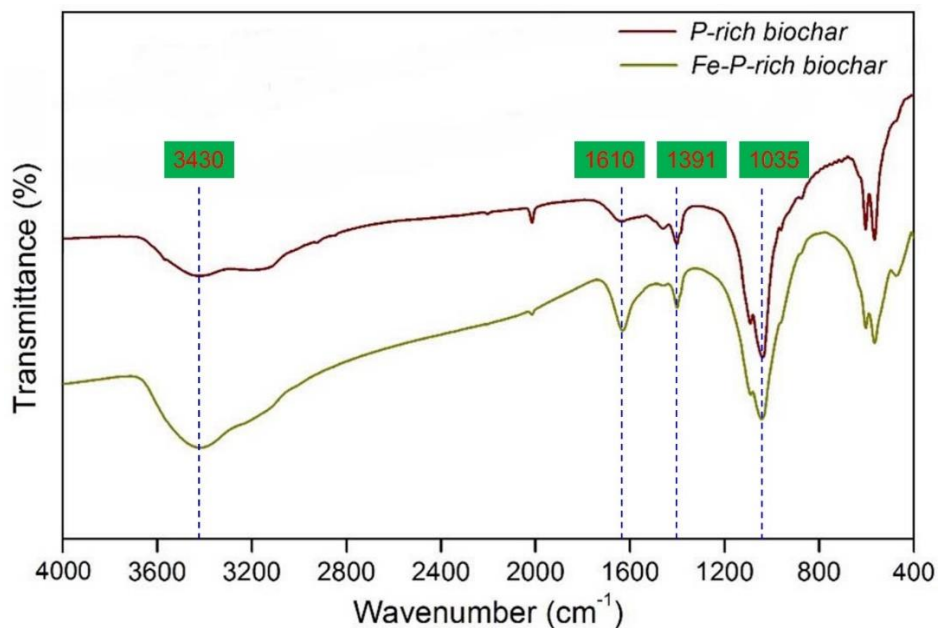


Figure 6-2 Fourier transform infrared (FTIR) spectra of both biochars.

6.2.3 Fractionation of As and Pb

A five-step sequential extraction method was used for the fractionation of As (Wenzel *et al.*, 2001). Those five steps represented non-specifically adsorbed fraction (F1), specifically adsorbed fraction (F2), amorphous Fe/Mn oxides bound fraction (F3), crystalline Fe-Mn oxides bound fraction (F4), and residual fraction (F5). A four-step sequential extraction procedure established by the European Union Bureau of Reference (EUBCR) was employed for the fractionation of Pb (Zembyova *et al.*, 2006). Based on the procedure, four Pb fractions were acid extractable fraction (F1), fraction bound to Fe/Mn oxides (F2), fraction bound to organic matter (F3), and residual fraction (F4). More details about the sequential extraction procedures are presented in *Appendix E* (section E4).

6.2.4 DNA extraction and high-throughput sequencing

DNA in different soil samples was extracted using an E.Z.N.A.®Soil DNA Kit (D4015, Omega, Inc., USA) based on the manufacturer's recommendations. After quantity verification using the NanoDrop spectrophotometer (Nano), the isolated DNA was eluted and diluted to approximately $1 \text{ ng } \mu\text{L}^{-1}$ (minimum $25 \text{ } \mu\text{L}$ for reaction), and then stored at -80°C prior to the further processing. For bacterial diversity analysis, V3-V4 variable regions of 16S rRNA gene were amplified using universal primers of 341F (5'-CCTACGGGNGGCWGCAG-3') and 805R (5'-GACTACHVGGGTATCTAATCC-3'). The PCR conditions were set as follows: an initial denaturation at 98°C for 30 s; 32 cycles of denaturation at 98°C for 10 s, annealing at 54°C for 30 s, and then extension at 72°C for 45 s; finally, an extension at 72°C for 10 min. The PCR crude products were confirmed using 2% agarose gel electrophoresis, and then purified by Agencourt AMPure XP beads (Beckman Coulter Genomics, Danvers, MA,

USA) and quantified by Qubit (Invitrogen, USA). Equal amounts of purified amplicon were pooled for subsequent sequencing.

6.2.5 Data processing and statistical analysis

The sequencing analysis was conducted using the Illumina NovaSeq platform provided by LC-Bio Technology Co., Ltd. (Hangzhou, China) following the manufacturer's instructions. Paired-end reads were assigned to samples according to their unique barcode and truncated by cutting off the barcode and primer sequence, and then merged using the FLASH program. Chimeric sequences were filtered using Vsearch software (v2.3.4). Operational Units (OTUs) were clustered using UPARSE (version 7.1) at 97% sequence identity. Before statistical analysis, the dataset was analyzed for the homogeneity of variance and normality. Statistical analyses, including a univariate analysis of variance (ANOVA) with Duncan's multiple tests ($P < 0.05$), Pearson's correlation analysis, principal component analysis (PCA), and redundancy analysis (RDA) were performed using SPSS software (IBM SPSS Statistics 23.0). Figures were created using software OriginPro 2022.

6.3 Results and discussion

6.3.1 Soil pH, organic carbon content and nutrient availability

6.3.1.1 pH

The application of PBC increased soil pH by approximately 1.0 unit under CF conditions, while it increased by 1.2 units under IF conditions (Table 6-2). However, the addition of FePBC decreased ($P < 0.05$) the pH of soils under CF and IF conditions from 6.25 and 5.98 to 6.19 and 5.94, respectively. The elevated pH caused by PBC application in both water regimes might be explained by its relatively high alkalinity (pH=10.6) and ash content (60.0%) (Table 6-1), associated with the presence of mineral elements, such as Na, K, Ca, and Mg (Figure 6-1). As reported earlier, the liming effect of the animal-derived biochar and its high content of alkali elements could account for the increase of soil pH (Chen *et al.*, 2022). However, the application of FePBC caused a slight decrease of soil pH, which might be attributed to the acidity of FePBC (Table 6-1). Zhang *et al.* (2020a) reported that the decreased soil pH caused by the addition of Fe materials can be ascribed to the hydrolysis and precipitation of Fe(III)-hydroxides. In addition, with the presence of oxygen in paddy soils under IF conditions, ferrous ions might be rapidly oxidized to the trivalent state, this oxidization process releases protons and lowers the pH (Rong *et al.*, 2019). Water management showed no significant ($P > 0.05$) difference in the soil pH regardless of the control or biochar treatments (Table 6-2), presumably owing to the relatively high soil buffer capacity (Yang *et al.*, 2022b). In general, the liming effect of biochar may result in an elevated soil pH, which can effectively reduce the mobility

and phytoavailability of cationic Pb, but increase those of anionic As (Zama *et al.*, 2018; Zhang *et al.*, 2020a). Conversely, the decline of soil pH after the addition of Fe-modified biochars might lead to opposite effects on mobility of Pb and As. In addition, soil pH plays a vital role in regulating plant growth, through controlling the mobility and transformation of As and Pb and adjusting nutrient availability in soils (Yang *et al.*, 2017; Tang *et al.*, 2020).

Table 6-2 Soil pH, organic carbon content and available nutrient in soils as affected by biochar application and water management regime. (mean \pm standard error, n = 4).

Treatments	pH	Organic carbon (%)	Available N (mg kg ⁻¹)	Available P (mg kg ⁻¹)	Available K (mg kg ⁻¹)
CF-Control	6.25 \pm 0.06 b	1.51 \pm 0.01 b	153.5 \pm 2.2 b	15.1 \pm 1.18 b	76.5 \pm 1.6 d
CF-PBC	7.20 \pm 0.08 a	1.87 \pm 0.09 a	134.0 \pm 1.3 c	16.0 \pm 0.95 b	373.3 \pm 9.1 b
CF-FePBC	6.19 \pm 0.03 c	1.99 \pm 0.18 a	185.7 \pm 11.3 a	21.5 \pm 2.47 a	399.5 \pm 4.1 a
IF-Control	5.98 \pm 0.08 b	1.49 \pm 0.06 b	120.4 \pm 0.7 c	7.6 \pm 0.80 c	64.7 \pm 1.3 d
IF-PBC	7.17 \pm 0.04 a	1.86 \pm 0.08 a	102.7 \pm 0.7 d	25.3 \pm 0.24 a	295.5 \pm 11.2 c
IF-FePBC	5.94 \pm 0.07 c	1.96 \pm 0.09 a	164.3 \pm 0.8 b	23.5 \pm 1.26 a	376 .0 \pm 8.9 b

6.3.1.2 Organic carbon

The application of PBC and FePBC significantly ($P < 0.05$) increased soil organic carbon content, by 24.4% and 32.2% under CF conditions, and by 25.1% and 31.9% under IF conditions, respectively, compared to the controls (Table 6-2). These results are in accordance with previous studies reporting the beneficial aspects of biochar application (Chen *et al.*, 2020a; Han *et al.*, 2020; Pan *et al.*, 2021). As reported by Han *et al.* (2020), approximately 80-97% of the organic carbon derived from biochar exists in stable forms, which are not mineralized to CO₂ even for a long time (over hundreds of years). In addition, biochar can indirectly influence the biogeochemical processes, including soil pH, particle aggregation, moisture retention, and microbiological activities, thus regulating the turnover of organic carbon in soils (Han *et al.*, 2020). Sun *et al.* (2020) found that a mixed biomass-derived biochar indirectly changed the soil organic carbon content through altering soil aggregation. In our previous studies, the changes in redox conditions and the Fe chemistry in soils play vital roles in the mineralization and composition of organic carbon (Yang *et al.*, 2021; Yang *et al.*, 2022b). In the current study, however, no significant difference in organic carbon content was found between different water management regimes; furthermore, the loading of Fe did not change biochar's functions on adjusting the content of soil organic carbon (Table 6-2). Consequently, we assume that the direct input of organic carbon along with biochar played a predominant role in enriching soil organic carbon.

6.3.1.3. Nitrogen availability

After PBC application, soil available nitrogen (N) significantly ($P < 0.05$) decreased under both CF and IF conditions, whereas the application of FePBC increased the concentrations of available N under CF and IF conditions by 22.3% and 25.2%, respectively, compared to the controls (Table 6-2). In agro-ecosystems, soil N availability generally limits the growth and productivity of rice (Yu *et al.*, 2021). The availability of N significantly ($P < 0.05$) increased in the FePBC treatments, whereas it declined in the PBC treatments (Table 6-2), although the N content in PBC (2.1%) was slightly higher than that in FePBC (1.8%) (Table 6-1). Our previous study has proven that most of N in biomass feedstock was converted into unavailable forms during pyrolysis and that the change in soil N availability did not arise from direct input of biochar (Feng *et al.*, 2019). Nevertheless, biochar may affect the mineralization-immobilization turnover of N through regulating the soil pH, organic carbon content, aeration level, and microbial activity (He *et al.*, 2019). Pearson's correlation analysis showed a significantly ($P < 0.01$) negative correlation between soil available N and soil pH under both CF and IF conditions (Figure 6-3), suggesting that biochar-induced change in soil pH played a key role in regulating the soil N cycling. According to He *et al.* (2019), the application of acidic Fe-modified biochars could lower the denitrification in soil, thus improving the bioavailability of N. In addition, the decrease of N bioavailability in the PBC treatment could be attributed to the presence of porous structure and functional groups in PBC (Figures 6-1 and 6-2), which might enhance the adsorption of NH_4^+ (Yu *et al.*, 2021), thereby decreasing soil N availability. However, no significant correlations were observed between available N and organic carbon content (Figure 6-3), revealing that organic carbon had insignificant effects on the N availability in the soil. It was also found that the concentrations of available N in soils under CF conditions were higher than those under IF conditions (Table 6-2). It has been proven that alternate wetting and drying irrigation practice increased the loss of N from the soil, probably due to the increase of N_2O emission as a consequence of enhanced denitrification in wetting-drying cycles (Reddy and Patrick, 1975; Liu *et al.*, 2012).

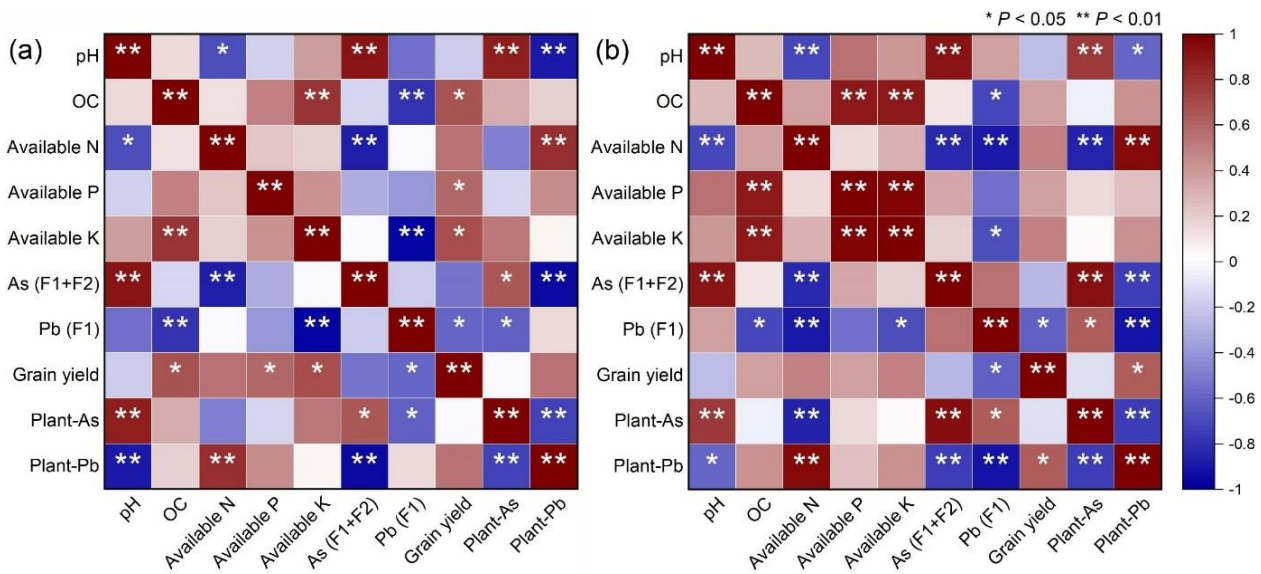


Figure 6-3 Pearson's correlation matrix of various parameters as affected by water management regimes (a: CF treatments; b: IF treatments).

6.3.1.4 Phosphorus availability

The concentration of available P increased by 234.1% in the IF-PBC treatment as compared to IF-Control, but no significant difference was found between the CF-PBC treatment and CF-Control. For the FePBC treatments, the concentrations of P increased by 42.6% and 209.8% under CF and IF conditions, respectively, compared to the controls (Table 6-2). Both biochars, i.e., PBC (5.29% of P) and FePBC (3.81% of P) are rich in P, due to the enrichment of P during pyrolysis of the P-rich pig carcasses (Xiao *et al.*, 2018; Yang *et al.*, 2022a). The significant increase of available P after biochar application could be ascribed to the direct release of PO_4^{3-} from biochars (Yu *et al.*, 2021). Moreover, biochar may affect the formation of P complexes and/or the adsorption-desorption equilibrium of P via modifying the soil pH (Zhang *et al.*, 2020b). The increase in P availability after PBC application might also be attributed to the hydrolysis of Al and Fe phosphates with the elevated pH (Zhang *et al.*, 2021). Thus, the increased P availability after the application of both PBCs might be plausibly due to the change in soil pH. In the current study, however, pH might have played a secondary role in affecting P availability, since no significant correlation was obtained between available P and soil pH (Figure 6-3). As affected by the water management regimes, the available P in CF-Control (15.1 mg kg^{-1}) are higher than that in IF-Control (7.6 mg kg^{-1}) (Table 6-2). It has been well-documented that flooding the soil usually increases the solubility and availability of P (Zhang *et al.*, 2021; Shaheen *et al.*, 2022), due to the reduction of ferric phosphates to the more soluble ferrous forms, as well as the dissolution of Ca phosphates because of the production of CO_2 under anaerobic conditions (Shaheen *et al.*, 2022). However, the application of PBC changed the scenario, where a significantly

($P < 0.05$) higher concentration of soil available P was observed under IF conditions (25.3 mg kg^{-1}) than that under CF conditions (16.0 mg kg^{-1}) (Table 6-2). It is likely that the application of the PBC has tipped the balance of P in the soil, where the mineralization of organic forms of P might have contributed predominantly to the additional pool of available P in the soil (Patrick *et al.*, 1985), and the supply of oxygen under IF conditions enhanced the breakdown of P-containing organic compounds (Zhang *et al.*, 2021).

6.3.1.5 Potassium availability

The concentrations of available potassium (K) in the PBC-treatments under CF and IF conditions were 3.9 and 3.6 times, respectively, higher than that in the controls. In the FePBC treatments, even higher concentrations of available K were noticed, which were 4.2 and 4.8 times higher than that in the controls (Table 6-2). Similar to P, the elevated available K in the soil could be attributed to the direct input of K along with biochar application, due to the presence of K in both biochars (Figure 6-1). Purakayastha *et al.* (2019) reviewed that the water-soluble K in biochar is usually high (up to 65-70% of the total content). Moreover, the concentrations of K in soils under CF conditions were higher than those under IF conditions (Table 6-2). This is because soil flooding can enhance the release of K through the reductive dissolution of Fe and Mn (hydro)oxides (Patrick *et al.*, 1985).

6.3.2 Redistribution of As and Pb

6.3.2.1 Arsenic

In CF-Control, the distribution of As was 0.2% in non-specifically adsorbed fraction (F1), 5.6% in specifically adsorbed fraction (F2), 24.3% in amorphous Fe-Mn oxides bound fraction (F3), 12.7% in crystalline Fe-Mn oxides bound fraction (F4), and 57.3% in residual fraction (F5). In IF-Control, F5 contributed more than half of the As (55.2%), followed by F3 (25.2%), F4 (14.1%), F2 (5.4%), and F1 (0.1%) (Figure 6-4, Table 6-3). The sum of F1 and F2 is considered bioavailable, whereas F3 and F4 less bioavailable As, and F5 non-available (Wenzel *et al.*, 2001; Kashif Irshad *et al.*, 2022). The application of PBC significantly ($P < 0.05$) increased the proportion of bioavailable As fractions to 7.5% (10.7 mg kg^{-1}) and 7.6% (10.8 mg kg^{-1}) under CF and IF conditions, respectively, whereas FePBC significantly ($P < 0.05$) decreased the bioavailable fractions of As to 4.3% (6.1 mg kg^{-1}) and 4.7% (6.6 mg kg^{-1}) under CF and IF conditions, respectively (Figure 6-4, Table 6-3). No significant difference in the redistribution of As was noticed between the CF and IF treatments, suggesting that biochar application might have played a more pivotal role than water management regime in governing the mobility and bioavailability of As in this study.

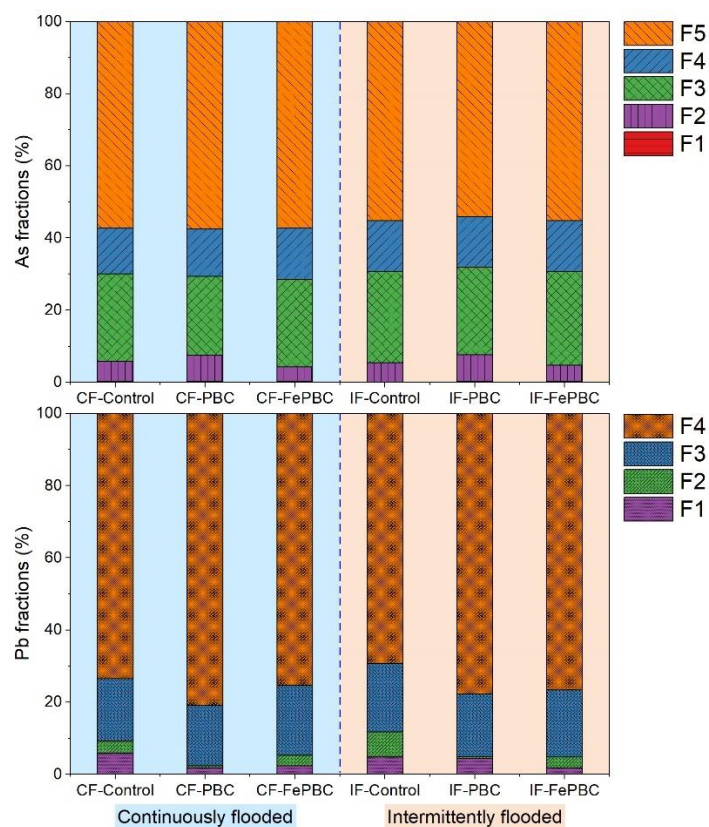


Figure 6-4 As (a) and Pb (b) fractions in soils as affected by biochar application and water management regime. The above results indicated that FePBC application triggered the transformation of As from bioavailable forms to immobile forms that are bound with amorphous and crystalline hydrous oxides (Kashif Irshad *et al.*, 2022; Pan *et al.*, 2021). It might provide a reason to explain the significantly ($P < 0.01$) positive correlations between As (F1+F2) and soil pH under both CF and IF conditions (Figure 6-3), indicating that soil pH plays a vital role in controlling the bioavailability of As (Okkenhaug *et al.*, 2012; Wen *et al.*, 2021). In the current study, the application of FePBC caused a decline of pH (Table 6-2) and in turn accelerated the protonation on soil colloids, thereby immobilizing As which existed as anions (e.g., AsO_4^{3-} , HAsO_4^{2-} , and H_2AsO_4^-) (Zhong *et al.*, 2019; Yang *et al.*, 2022b). In addition, various oxygen-containing functional groups (e.g., $-\text{OH}$, $\text{C}=\text{O}$, and $-\text{COOH}$) were detected on the surface of FePBC, those moieties could also be protonated under relatively acidic conditions; consequently, the mobility and bioavailability of As could be reduced through electrostatic attraction between protonated functional groups and anionic As (Shaheen *et al.*, 2018). Furthermore, the oxidation of As(III) under low pH to form less mobile As(V) may contribute to the decrease of As bioavailability. Zhong *et al.* (2019) reported that As(III) could be oxidized by hydroxyl free radicals ($\bullet\text{OH}$) and H_2O_2 derived from activation of O_2 by redox-active moieties, such as semiquinone-type persistent free radicals. Nevertheless, an expected mechanism, the co-precipitation of As with the formation of Fe oxides in the presence of O_2 might not occur, since the application of FePBC caused

non-significant changes in either F4 or F5 under IF conditions (intermittently oxidizing) (Figure 6-4, Table 6-3).

Table 6-3 Distribution of different fractions of As and Pb in soils as affected by biochar application and water regime.

Elements	Treatments	F1 (%)	F2 (%)	F3 (%)	F4 (%)	F5 (%)	F1+F2 (%)	F3+f4 (%)
As	CF-Control	0.2±0.04b	5.6±0.3b	24.3±1.8ab	12.7±0.5b	57.3±1.4a	5.7±0.3b	37.0±1.5bc
	CF-PBC	0.2±0.03b	7.3±0.3a	21.8±1.3b	13.0±1.2ab	57.6±1.4a	7.5±0.3a	34.9±1.6c
	CF-FePBC	0.4±0.06a	3.9±0.2c	24.2±1.1ab	14.2±0.3a	57.3±1.4a	4.3±0.2c	38.4±1.3ab
	IF-Control	0.1±0.01c	5.4±0.3b	25.2±1.8a	14.1±1.0a	55.2±2.6ab	5.5±0.3b	39.3±2.4ab
	IF-PBC	0.2±0.06b	7.4±0.7a	24.3±1.5ab	14.0±0.8ab	54.1±1.4b	7.6±0.7a	38.2±1.1ab
	IF-FePBC	0.2±0.04b	4.5±0.3c	26.0±1.7a	14.1±1.0a	55.2±1.0ab	4.7±0.4c	40.1±1.0a
Pb	CF-Control	5.9±0.1a	3.3±0.3b	17.3±0.6b	73.5±0.7d	--	--	--
	CF-PBC	1.8±0.3e	0.5±0.1c	16.7±1.3b	81.0±1.1a	--	--	--
	CF-FePBC	2.4±0.1d	2.9±0.1b	19.4±0.2a	75.3±0.2c	--	--	--
	IF-Control	4.8±0.1b	6.9±0.8a	18.9±0.4a	69.4±1.2e	--	--	--
	IF-PBC	4.3±0.1c	0.6±0.2c	17.3±0.3b	77.8±0.6b	--	--	--
	IF-FePBC	1.8±0.0e	3.1±1.2b	18.6±0.3a	76.6±1.0bc	--	--	--

Conversely, the elevated pH caused by PBC application (Table 6-2) may cause an enhanced release of As due to the electrostatic repulsive force between negatively charged biochar/soil particles and anionic As (especially As(V)), thus increasing the bioavailability of As (Yang *et al.*, 2022a). Moreover, as is well-known, phosphate is a chemical analog of As(V) (Lee *et al.*, 2016); under aerobic conditions, both anions compete strongly for the same charged adsorption sites on soil (Bolan *et al.*, 2013; Anawar *et al.*, 2018). Hence, the increased available P (Table 6-2), particularly under IF conditions could provide evidence to explain the increase of As bioavailability after PBC application (Figure 6-4). In addition, the competition between dissolved organic carbon (DOC) and As after PBC application could contribute to the elevated As availability (Zama *et al.*, 2018), due to the PBC-induced increase of organic carbon content (Table 6-2). Hartley *et al.* (2009) reported that large concentrations of DOC could promote the release of As due to the competition between DOC and As for sorption sites on iron oxides and soil particles, thus leading to the increase in As mobility and bioavailability.

6.3.2.2 Lead

Acid soluble fraction of Pb (F1) was considered to be bioavailable, whereas reducible (F2), oxidizable (F3), and residual (F4) fractions were recognized as immobilized Pb that cannot be readily used by plants (Ure *et al.*, 1993). A large portion of Pb was present in residual fraction in all treatments and accounted for 70-80% of the total Pb content (Figure 6-4), indicating that most Pb in the soil was of geogenic origin (Shetaya *et al.*, 2019). This result agreed with Li *et al.* (2015), where they found that Pb was present predominantly as residual fraction in soils

collected from mining regions. The application of PBC and FePBC reduced the proportion of F1 from 5.9% (43.4 mg kg⁻¹) to 1.8% (13.1 mg kg⁻¹) and 2.4% (17.5 mg kg⁻¹) under CF conditions, and from 4.8% (35.6 mg kg⁻¹) to 4.3% (31.5 mg kg⁻¹) and 1.8% (13.0 mg kg⁻¹) under IF conditions (Figure 6-4, Table 6-3), respectively. In addition, the proportion of F2 was significantly ($P < 0.05$) reduced with the addition of PBC under both water management regimes. The application of FePBC significantly ($P < 0.05$) decreased the proportion of F2 under IF conditions, whereas increased that of F3 under CF conditions. Meanwhile, the application of PBC and FePBC also caused a significant ($P < 0.05$) increase in the residual fraction of Pb under both CF and IF conditions (Figure 6-4, Table 6-3). With regard to the bioavailable fraction (F1), a more noticeable decrease was found under CF conditions than under IF conditions, indicating that flooding promoted Pb immobilization by PBC-treated soil. Conversely, compared to the controls, the application of FePBC resulted in a slightly larger decline of Pb bioavailability under IF conditions (by 59.3%) than under CF conditions (by 62.5%).

It was obvious that PBC application could promote the transfer of Pb from mobile fractions to comparatively stable fractions, thus decreasing its bioavailability (Figure 6-4). In previous studies, P has been effective to immobilize Pb in soils through formation of stable precipitates, such as Pb₅(PO₄)₃OH (Qu *et al.*, 2022). The exogenous P amended along with PBC may be responsible for the decreased mobility and availability of Pb in the soil. The immobilization of Pb using P-containing compounds has been well-documented (Bolan *et al.*, 2003; Pei *et al.*, 2021; Wu *et al.*, 2021; Chen *et al.*, 2022). For instance, Pei *et al.* (2021) reported that the P-enriched biochar derived from dairy manure exhibited good affinity to Pb sorption via the formation of insoluble Pb phosphates, i.e., β-Pb₉(PO₄)₆ or Pb₁₀(PO₄)₆F₂. The PBC-triggered increase of soil pH (Table 6-2) could also contribute to reduced Pb mobility. Chen *et al.* (2022) found that rise of pH caused by biochar application could induce stronger electrostatic attraction between negatively-charged biochar particles and positive Pb ions. Pearson's correlation matrix showed that the available Pb was positively ($P < 0.01$) correlated with pH, but not correlated with available P (Figure 6-5), indicating that pH played a more important role than available P in immobilizing Pb after PBC application. In addition, PBC contained abundant O-containing functional groups (Figure 6-2), which could provide effective adsorption sites to chelate Pb, thereby reducing Pb mobility and availability (Pan *et al.*, 2021). In a recent study, Chen *et al.* (2022) also attributed the decrease of Pb mobility to the formation of Pb-containing stable complexes (e.g., Pb-O-C and C-O-Pb-O-C), due to the presence of O-containing functional groups, such as carboxyl and hydroxyl. However, the formation of Pb-containing complexes might have not occurred to a large extent in this study, as no increase of organic-bound Pb (F3) was found under either water management regime (Figure 6-4; Table 6-3). A significantly ($P < 0.01$) lower concentration of bioavailable Pb was found under CF

conditions than that under IF conditions, which could be linked to the redox transformation of sulfur (S) after the application of the S-containing PBC, thereby contributing to Pb immobilization (Table 6-1). Previous studies proved that Pb could be immobilized by S via the formation of insoluble Pb-sulfides under anaerobic conditions caused by long-term flooding (Wu *et al.*, 2021).

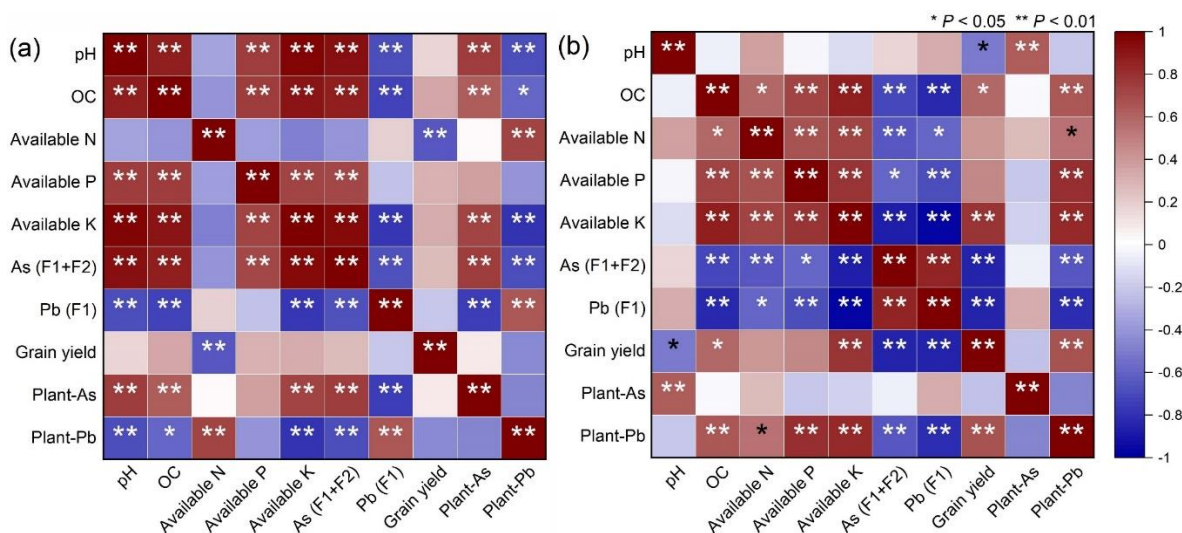


Figure 6-5 Pearson's correlation matrix of various parameters as affected by biochar application (a: control + PBC treatments; b: control + FePBC treatments).

Some of the above-mentioned mechanisms could also explain the decreased Pb availability after the application of FePBC. For instance, relatively high P content was also detected in FePBC (Figure 6-1), which also caused a significant increase in soil available P (Table 6-2). Hence, the retention of Pb with phosphate generated from FePBC might be responsible for the declined Pb mobility (Yang *et al.*, 2021). In addition, the intensity of characteristic peaks on the FTIR spectrum of FePBC was greater than those on the PBC spectrum, indicating that the loading of Fe increased the abundance of oxygen-containing functional groups on the biochar. Therefore, the immobilization of Pb after the application of FePBC could be also explained by the complexation of Pb by organic moieties and functional groups (Zhong *et al.*, 2019; Pan *et al.*, 2021). As a result, the proportion of organic-bound Pb significantly ($P < 0.05$) increased, especially under CF conditions, compared to the control (Figure 6-4, Table 6-3). On the other hand, the redox cycling of Fe compounds might contribute to the immobilization of Pb (Yang *et al.*, 2021). With the support of an X-ray fluorescence (XRF) technique, Wan *et al.* (2020) proved that Pb could be attached to Fe oxides in soils, and the application of the iron-modified magnetic biochar promoted the immobilization of Pb in soils. With regard to the higher bioavailability of Pb under CF conditions than under IF conditions (Figure 6-4, Table 6-3), it is likely that the applied Fe was reduced to Fe^{2+} under anaerobic conditions caused by continuous flooding (Wen *et al.*, 2021). The dissolved Fe^{2+} could therefore compete with Pb^{2+} for

adsorption sites on the soil particles (Fulda *et al.*, 2013), thereby leading to a higher Pb bioavailability under CF conditions than that under IF conditions. Also, the adsorbed and/or precipitated Pb could be released during the reductive dissolution of Fe (hydro)oxides under CF conditions (Yang *et al.*, 2021).

6.3.3 Bacterial community structure

In the CF-treated soils, the bacterial community was dominated by phylum *Firmicutes* (30.6-37.9%), followed by *Actinobacteria* (14.5-25.5%), *Proteobacteria* (12.3-17.5%), *Acidobacteria* (4.7-7.1%), *Chloroflexi* (4.5-5.4%), and *Bacteroidetes* (3.4-5.2%), which in total accounted for over 80% of the bacterial community at the phylum level (Figure 6-6; Table 6-4). For IF conditions, however, the dominant bacterial communities were *Proteobacteria* (26.6-31.6%), *Actinobacteria* (17.0-25.8%), *Acidobacteria* (4.1-14.8%), *Chloroflexi* (7.1-9.4%), *Bacteroidetes* (5.8-8.8%), and *Planctomycetes* (3.7-7.4%). These findings demonstrated that the change in water management regimes remarkably shifted the composition of soil bacterial communities, especially for *Firmicutes* and *Proteobacteria*. Previous studies reported that both *Firmicutes* and *Proteobacteria* were frequently observed in soils in mining areas (Tang *et al.*, 2021), and both have been depicted as dominant members of the rhizosphere bacteria (Philippot *et al.*, 2013). In addition, *Firmicutes* and *Proteobacteria* could be involved in the transformation of As in the paddy agroecosystem (Kumarathilaka *et al.*, 2021). The relative abundance of *Firmicutes* in the CF-treated soils was significantly ($P < 0.05$) higher than that in the IF-treated soils. Zhang *et al.* (2019) reached a conclusion that *Firmicutes* were sensitive to drought stress in soil, under which the relative abundance of *Firmicutes* was reduced. In contrast, a significant ($P < 0.05$) lower relative abundance of *Proteobacteria* was found in soils under IF conditions as compared to those under CF conditions. Das *et al.* (2016) also found that the relative abundance of *Proteobacteria* in rhizosphere soil was higher in the alternate wetting and drying irrigation practice than that in the flooded practice. This could be linked to the inherent nature of the *Proteobacteria*, which were described as fast-growing r-strategists that thrive under unstable and/or fluctuating conditions where nutrients are adequate (Philippot *et al.*, 2013).

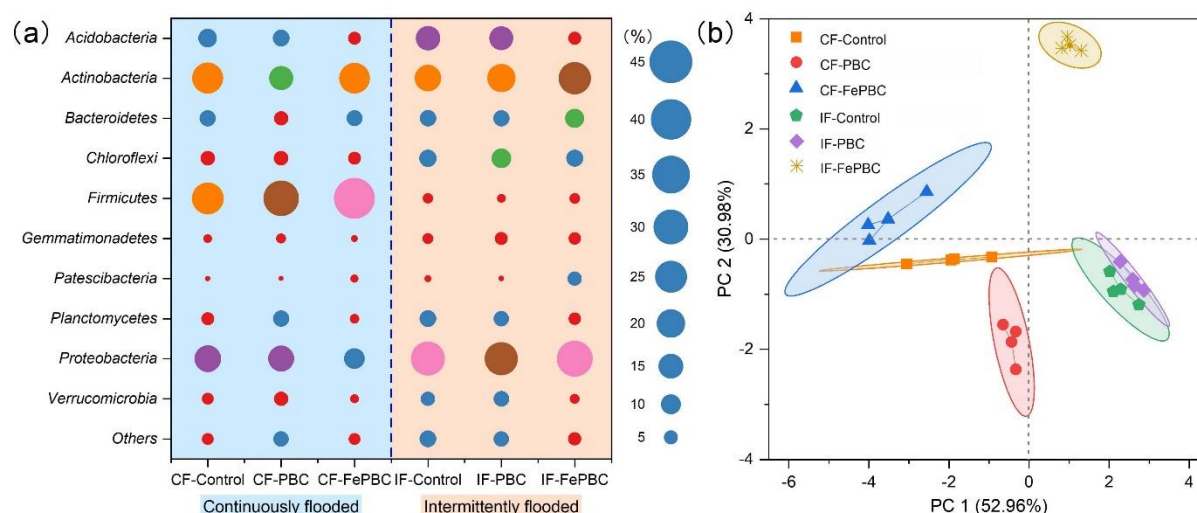


Figure 6-6 Relative abundance of top 10 bacterial phyla in soils as affected by biochar application and water management regime (a) and their principal component analysis (PCA) (b).

Our results demonstrated that most of the detected bacteria at the phylum level were unaffected by the application of PBC (Figure 6-6; Table 6-4). Although PBC application caused a significant ($P < 0.05$) increase in the abundance of *Gemmatimonadetes* under both CF and IF conditions and *Verrucomicrobia* only under CF conditions, these bacteria were non-dominant because of their low relative abundances ($< 6\%$) in all treatments. Interestingly, the abundance of *Actinobacteria*, a dominant phylum, significantly ($P < 0.05$) decreased in response to PBC application under CF conditions, by 38.6% as compared to the control; however, a significant ($P < 0.05$) increase of this clan was noticed in the IF-FePBC treatment as compared to the control (Figure 6-6; Table 6-4). These results may correspond to the change in the mobility of As and Pb, since *Acinetobacter* are often studied for the detoxification of heavy metals and metalloids because they tend to be resistant to those elements via biosorption and/or extracellular transformation (Lan *et al.*, 2021). *Actinobacteria* play an important role in organic matter mineralization and C cycling, while increases in recalcitrant C may trigger a rise in *Actinobacteria* abundance (Mickan *et al.*, 2018). A molar H/C ratio lower than 0.7 is defined as a criterion to determine the aromaticity of biochar (International Biochar Initiative, 2015). In the current study, the H/C ratios of PBC (0.5) and FePBC (0.4) were both lower than 0.7 (Table 6-1), indicating a high aromaticity and stability of C in both biochars. It is likely that the increased *Actinobacteria* abundance could be explained by the higher aromaticity of FePBC (i.e., lower H/C ratio) under IF conditions, where the aromatic carbon could be concentrated due to the decomposition of labile organic carbon under oxidizing conditions (Yang *et al.*, 2022a). Similarly, Qu *et al.* (2022) reported that the addition of sulfur-iron functionalized biochar enhanced the abundance of *Actinobacteria* in soil. However, the lower relative abundance of *Actinobacteria* in the CF-PBC treatment might be attributed to the relative low

proportion of recalcitrant organic carbon under reducing conditions (Yang *et al.*, 2021). The inhibition effect of PBC on *Actinobacteria* indicated that biochar-induced effects are possibly biochar- or soil-specific. For instance, biochar with a higher capacity to sorb various organic molecules could inhibit bacterial activities through physical sorption and blocking reaction sites (Elzobair *et al.*, 2016), which might have occurred in the CF-PBC treatment, thereby causing a decline in *Actinobacteria* abundance.

Table 6-4 Relative abundance of bacterial phyla in soils as affected by biochar application and water regime.

Phyla	Continuously flooded			Intermittently flooded		
	CF-Control	CF-PBC	CF-FePBC	IF-Control	IF-PBC	IF-FePBC
<i>Acidobacteria</i>	8.4±3.0b	6.7±0.4bc	4.3±2.3c	14.8±2.3a	14.1±0.5a	4.1±0.3c
<i>Actinobacteria</i>	23.6±1.3ab	14.5±0.7c	23.1±5.1ab	17.3±5.7c	19.6±2.8bc	25.8±0.4a
<i>Bacteroidetes</i>	6.3±2.4ab	5.2±0.3b	6.1±4.2ab	6.6±1.2ab	6.4±1.2ab	8.8±0.5a
<i>Chloroflexi</i>	5.4±1.9bc	5.4±0.2bc	4.3±2.5c	7.5±0.9ab	9.4±0.6a	7.1±0.2b
<i>Firmicutes</i>	25.2±12.0a	31.1±2.2a	40.8±22.5a	2.7±1.0b	1.8±0.3b	2.9±0.1b
<i>Gemmatimonadetes</i>	1.9±0.4c	2.6±0.3b	1.3±0.5d	3.1±0.2b	4.1±0.1a	3.9±0.4a
<i>Patescibacteria</i>	0.7±0.3d	0.6±0.0d	1.7±0.7b	1.3±0.4bc	0.8±0.1cd	5.3±0.1a
<i>Planctomycetes</i>	4.1±1.4bc	6.3±1.7ab	2.4±1.9c	6.8±1.5a	5.7±0.7ab	3.7±0.2bc
<i>Proteobacteria</i>	17.5±1.2c	16.6±1.1c	10.6±4.0d	27.9±3.5b	26.6±1.2b	31.6±1.3a
<i>Verrucomicrobia</i>	3.4±1.1b	5.2±0.1a	2.0±1.2c	5.2±0.4a	5.9±0.2a	2.5±0.2bc
<i>Others</i>	3.5±1.6b	5.8±0.4ab	3.5±2.5b	7.0±2.3a	5.7±1.0ab	4.4±0.3b

Overall, the above results suggested that water management regime was a more important driver than biochar application in shaping the bacterial community composition in the paddy soil. In order to visualize the consequence of both factors, principal component analysis (PCA) was performed at the phylum level (Figure 6-6). The first two PCs explained approximately 84% of the total variation. It is clearly depicted that the CF and IF treatments separated across the first PC, suggesting that the change in water management regimes is a main source of variation to the bacterial communities at the phylum level. The biochar treatments separated across the second PC, revealing that biochar application played a secondary role in regulating the bacterial communities. Furthermore, PBC was more effective than FePBC in altering the bacterial communities under CF conditions, considering the larger deviation between the PBC treatment and control than that between the FePBC treatment and control. However, overlapping between clusters of the control and PBC treatment revealed that PBC had negligible influence on the bacterial communities under IF conditions, whereas FePBC remarkably shifted the bacterial communities relative to the control, since the brown star cluster stranded alone in the upper right of Figure 6-6.

Apart from PCA, the soil pH, organic carbon content, available nutrients, as well as bioavailable As and Pb were selected as predominant environmental factors for redundancy analysis (RDA), to evaluate the correlations between these environmental factors and the bacterial communities (Figure 6-7). For the CF group, RDA 1 explaining 76.33% of the variance was predominantly contributed by soil pH, available As and N due to the relatively small angles ($< 90^\circ$) between those arrows and RDA 1 axis. RDA 2 explaining 10.43% of the variance was mainly driven by organic carbon, available K, P and Pb. However, RDA1 explained 84.87% of the variance and RDA 2 explained 12.20% in the IF group. Except available Pb and N, which mostly contributed to the variation of RDA 1, the contributions of other factors were inconsistent. These results indicated that various environmental factors shaped the soil bacterial communities under different water management regimes in multiple and intricate ways (Xiao *et al.*, 2022). The interactions between soil bacterial communities and functionalized biochars were complex. For instance, increase of the relative abundances of *Gemmatimonadetes* and of *Verrucomicrobia* in the CF-PBC treatment relative to the control might be attributed to the PBC-induced increase of soil pH, because of their positive correlations (Figure 6-7). Conversely, the increase of *Gemmatimonadetes* abundance could partly explain the decline in available N, since some genera belonging to *Gemmatimonadetes* phylum were reported as N-reducing bacteria (Chen *et al.*, 2020b). Thus, it is likely that PBC application promoted the soil N loss under CF conditions by increasing the abundance of denitrification bacteria. Moreover, RDA results confirmed our assumption that biochar shifted the abundance of *Actinobacteria* through regulating the content and composition of organic carbon in the soil under IF conditions, as indicated by the positive correlation between the abundance of *Actinobacteria* and organic carbon content (Figure 6-7).

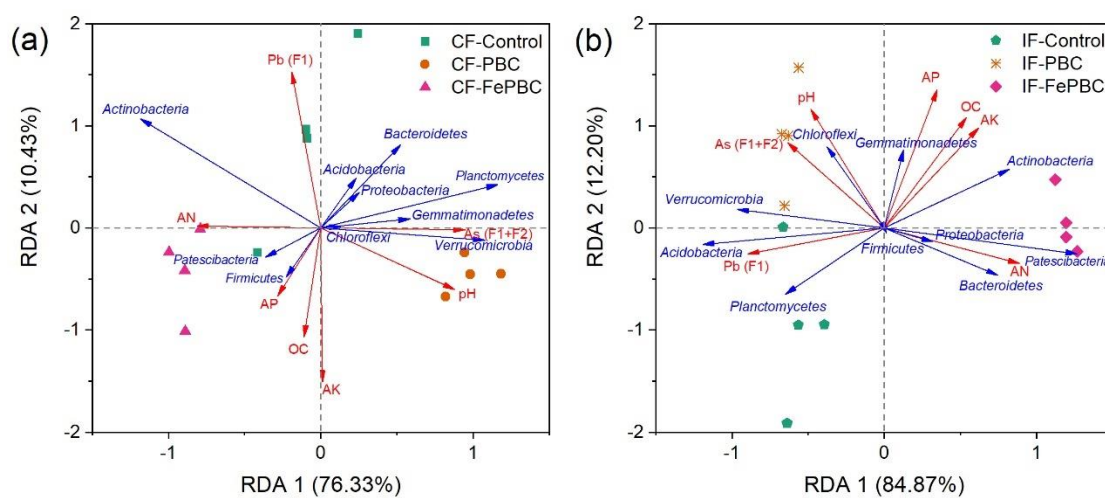


Figure 6-7 Redundancy analysis (RDA) between environmental factors and soil bacterial communities at the phyla level.

The genus *Bacillus* dominated in the CF-treated soils, comprising 26.6-34.1%, whereas the unclassified genera belonging to *Actinobacteria* (comprising 2.6-4.2%) and *Gaiellales* (comprising 2.1-4.8%) dominated in the IF-treated soils. Other genera including *Nocardioides*, *Marmoricola*, *Candidatus_Solibacter*, *Geobacter*, *Dyella*, *Anaeromyxobacter*, *Acidovorax*, *Sphingomonas*, *Fictibacillus*, *Gemmatimonas*, *Arthrobacter*, *Candidatus_Koribacter*, *Anaerolinea*, as well as several unclassified genera were commonly detected in all treatments (Figure 6-8). Although the application of PBC and FePBC exhibited limited effects on the bacterial phyla in paddy soils, more noticeable changes in the bacterial communities were found at the genus level (Table 6-5). Furthermore, hierarchical clustering dendrogram analysis depicted that the CF-Control and CF-FePBC treatments clustered together and away from the CF-PBC treatment, whereas the IF-Control and IF-PBC treatments clustered together and away from the IF-FePBC treatment (Figure 6-8). These observations further supported that PBC was more effective on shaping the bacterial communities under CF conditions, whereas FePBC was more effective under IF conditions. The tremendous shifts in these genera caused by water management regimes and application of functionalized biochars possibly altered the As and Pb biogeochemical behavior and soil nutrient cycling, thus affecting the resultant rice yield and the accumulation of As and Pb (see section 6.3.4). For example, the relative abundances of *Bacillus*, *Geobacter*, and *Anaeromyxobacter*, known as Fe(III)-reducing genera (Dong *et al.*, 2021), were higher in the CF-treated soils in comparison to the IF-treated ones (Figure 6-8, Table 6-5). The reduction of Fe(III) can plausibly promote the release of inorganic As from As-bearing Fe minerals (Yang *et al.*, 2022b). Wang *et al.* (2019) also noticed that the abundances of genera *Geobacter* and *Anaeromyxobacter* positively correlated with the concentrations of As and Fe. Conversely, the presence of genus *Acidovorax* belonging to phylum *Proteobacteria*, a facultative anaerobic Fe(II) and As(III) oxidizer (Zhang *et al.*, 2017), in the paddy soil (particularly under IF conditions) may enhance the immobilization of As. Teng *et al.* (2021) found that inoculation of the phosphate-mobilizing bacteria belonging to *Bacillus* caused a relatively high solubility of P, and in turn reduced the bioavailability of Pb through precipitation. Moreover, genera *Arthrobacter* and *Gemmatimonas* could be involved in C and N cycling, thus altering the soil fertility (Chen *et al.*, 2020b).

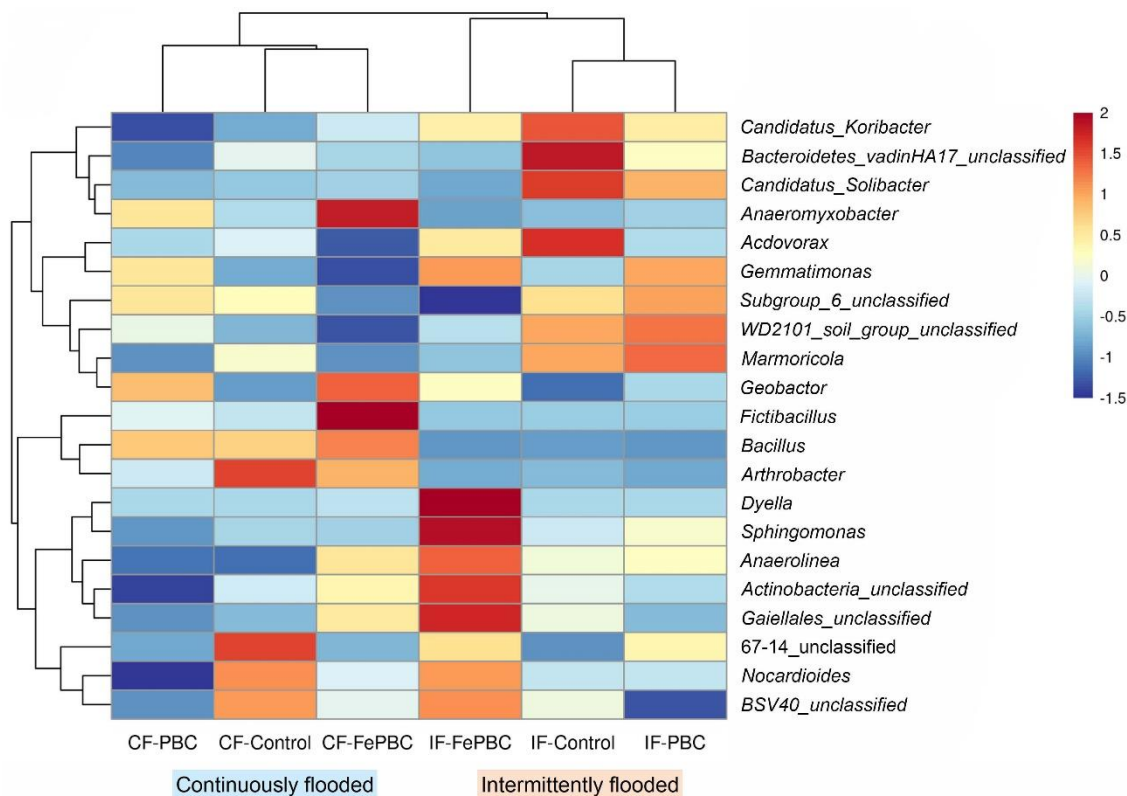


Figure 6-8 Hierarchical clustering dendrogram and heat map based on the relative abundance of bacterial communities at the genus level.

6.3.4 Rice yield and accumulation of As and Pb

It is noteworthy that the rice grain yield increased by 47.4% and 19.6% in the CF-FePBC and IF-FePBC treatments, respectively, compared to the controls (Figure 6-9). This could be interpreted as the improved soil fertility, which may enhance nutrient utilization efficiency by plants (Chen *et al.*, 2022; Wan *et al.*, 2022). As aforementioned (section 6.3.1), FePBC could more effectively improve the soil organic carbon content and nutrient availability than PBC, thus distinctively promoting plant growth and increasing rice yield. Furthermore, As and Pb are well-known to render negative effects on the plant growth due to their phytotoxicity (Wen *et al.*, 2021). Therefore, the increased rice yield might also be attributed to the alleviated bioavailability of As and Pb, in particular As (Figure 6-4). Pearson's correlation coefficient showed that grain yield was negatively correlated ($P < 0.01$) with As (F1+F2) and Pb (F1) in the control + FePBC group (Figure 6-5), which supported our above speculation. In addition, changes in bacterial communities could have played a potential role in enhancing plant growth and rice yield. For instance, *Bacillus* are ubiquitously found in soils and widely accepted as a series of bacteria that can promote plant growth and increase crop yield (Mickan *et al.*, 2018). In our study, the application of FePBC significantly increased the abundance of *Bacillus* under CF conditions (Table 6-5), indicating a probable role of *Bacillus* in

promoting rice growth. In addition to *Bacillus*, the shifts in abundances of genera *Arthrobacter* and *Gemmatimonas* in the FePBC-treated soils (Table 6-5) could promote plant growth by regulating the nutrient status in soil (Chen *et al.*, 2020b). Li *et al.* (2018) reported that *Arthrobacter* could promote plant growth through the production of phytohormone indole-3-acetic acid.

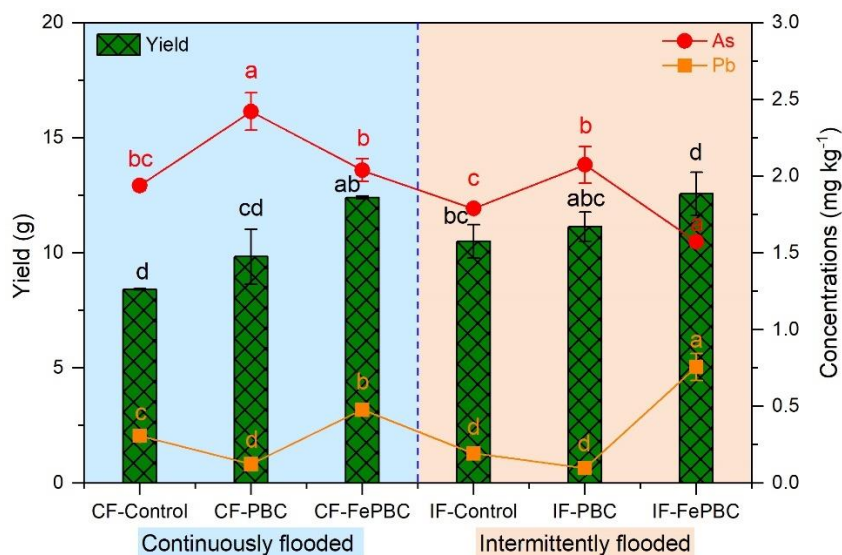


Figure 6-9 Rice grain yield and concentrations of As and Pb in rice grains as affected by biochar application and water management regime.

Interestingly, under CF conditions, PBC application significantly ($P < 0.05$) decreased the concentration of Pb in rice grain to 0.12 mg kg^{-1} (by 60.1%), which is below the permissible limit of Pb in brown rice regulated by the National Food Standard of China (GB 2762-2017, 0.20 mg kg^{-1}), and FePBC application significantly ($P < 0.05$) decreased the concentration of As (by 12.2%) in rice grain (Figure 6-9). However, the concentrations of Pb in the IF-Control (0.19 mg kg^{-1}) and IF-PBC (0.10 mg kg^{-1}) treatments were both lower than the permissible limit. Compared to the controls, the application of PBC significantly ($P < 0.05$) increased the concentration of As in rice grain by 24.9% and 15.8%, while FePBC increased the concentration of Pb by 2.9 and 6.6 times under CF and IF conditions, respectively (Figure 6-9). This could be linked to the changes in the redistribution of As and Pb, especially in the PBC treatment, since there were positive correlations between grain-As and As (F1+F2) and between grain-Pb and Pb (F1), respectively (Figure 6-5). Thus, the mechanisms of PBC application reducing the bioavailability of As and Pb illuminated in section 6.3.2 could also be employed for the interpretation of their accumulation in rice grain. Nonetheless, the concentration of As in rice grain was not correlated, while Pb was negatively correlated ($P < 0.01$) with their soil available concentrations in the control + FePBC treatments (Figure 6-5). These results suggested that compared to PBC, FePBC possibly affected the As and Pb accumulation in rice

grain in more complicated and complex ways. For As, it could be associated with microbiological activities and Fe chemistry under different redox conditions (Yang *et al.*, 2022b). Namely, As can be incorporated and/or co-precipitated by Fe oxides with eliciting of Fe-oxidizing bacteria (e.g., *Acidovorax*) under IF conditions, where oxygen interrupted temporarily and the abundance of *Acidovorax* was relatively high (Table 6-5). For Pb, it could be apparently attributed to the FePBC-induced decline of soil pH (Table 6-2), although no significant correlation was found between grain Pb and pH (Figure 6-5). Furthermore, the enhanced accumulation of Pb in rice grain (particularly under CF conditions) could be plausibly attributed to the change in the abundance of *Bacillus* (Table 6-5). As phosphate-mobilizing bacteria, *Bacillus* can solubilize inorganic Pb-bearing phosphates (Chen *et al.*, 2020b), thereby increasing the concentration of dissolved Pb during rice cultivation, and in turn elevating Pb uptake by rice plants.

Table 6-5 Relative abundance of bacterial genus in soils as affected by biochar application and water regime.

Genera	Continuously flooded			Intermittently flooded		
	CF-Control	CF-PBC	CF-FePBC	IF-Control	IF-PBC	IF-FePBC
<i>Bacillus</i>	26.0±5.5b	27.4±2.2b	34.1±4.0a	0.4±0.1c	0.4±0.1c	0.4±0.0c
<i>Actinobacteria_unclassified</i>	2.8±0.3b	1.7±0.2c	3.2±0.5b	2.9±0.7b	2.6±0.2b	4.2±0.3a
<i>Gaiellales_unclassified</i>	2.1±0.4c	1.8±0.2c	3.4±0.7b	2.9±0.4b	2.1±0.1c	4.8±0.3a
<i>Bacteroidetes_vadinHA17_unclassified</i>	1.7±0.4bc	1.1±0.1d	1.5±0.4bcd	2.9±0.5a	1.9±0.2b	1.4±0.0cd
<i>Nocardioides</i>	2.2±0.3a	0.8±0.0c	1.5±0.4b	1.5±0.2b	1.5±0.2b	2.1±0.1a
<i>Marmoricola</i>	1.8±0.3b	1.1±0.1c	1.1±0.2c	2.3±0.6a	2.6±0.3a	1.3±0.1c
<i>Candidatus_Solibacter</i>	0.8±0.3c	0.7±0.1cd	0.9±0.2c	3.8±0.3a	2.9±0.1b	0.5±0.0d
<i>WD2101_soil_group_unclassified</i>	1.0±0.2c	1.4±0.2b	0.7±0.1d	2.0±0.2a	2.1±0.1a	1.2±0.1bc
<i>Geobacter</i>	0.6±0.1e	2.4±0.3b	2.9±0.0a	0.4±0.1e	1.1±0.1d	1.8±0.4c
<i>Subgroup_6_unclassified</i>	1.6±0.2c	1.8±0.1bc	0.8±0.2d	1.8±0.1b	2.1±0.1a	0.4±0.0e
<i>Dyella</i>	0.0±0.0c	0.0±0.0c	0.5±0.1b	0.0±0.0c	0.0±0.0c	8.2±0.5a
<i>Anaeromyxobacter</i>	1.0±0.1c	1.6±0.1b	2.4±0.1a	0.8±0.3cd	0.9±0.1cd	0.7±0.1d
<i>Acidovorax</i>	1.1±0.2c	1.2±0.0bc	0.9±0.1d	1.1±0.1c	1.8±0.1a	1.4±0.1b
<i>67-14_unclassified</i>	1.6±0.8a	1.0±0.2a	1.1±0.7a	1.0±0.1a	1.3±0.1a	1.4±0.0a
<i>Sphingomonas</i>	0.8±0.2d	0.4±0.0e	0.8±0.1d	1.0±0.1c	1.4±0.1b	2.9±0.1a
<i>Fictibacillus</i>	0.7±0.2bc	1.3±0.0b	6.8±1.2a	0.0±0.0c	0.0±0.0c	0.0±0.0c
<i>BSV40_unclassified</i>	1.2±0.1a	0.6±0.0c	0.9±0.1b	0.9±0.2b	0.5±0.1c	1.2±0.0a
<i>Gemmatimonas</i>	0.8±0.1b	1.4±0.1a	0.5±0.1c	0.9±0.1b	1.6±0.1a	1.6±0.1a
<i>Arthrobacter</i>	1.0±0.1c	3.7±0.9a	2.7±0.4b	0.1±0.0d	0.3±0.0d	0.2±0.0d
<i>Candidatus_Koribacter</i>	0.7±0.2d	0.4±0.0e	1.0±0.1c	1.8±0.2a	1.3±0.1b	1.3±0.1b
<i>Anaerolinea</i>	0.5±0.1d	0.5±0.0d	1.5±0.2b	1.2±0.1c	1.3±0.1c	2.0±0.0a
<i>Others</i>	49.9±2.1c	47.7±2.8c	31.0±2.9d	70.1±2.3a	70.4±0.8a	61.0±0.6b

6.4 Conclusions

This study demonstrated that both water management strategy and functionalized biochar application can change soil pH and nutrient status including organic carbon content and availability of N, P and K, alter the geochemical redistribution of As and Pb, and shape the bacterial community structure in the paddy soil, thus regulating the rice yield and the accumulation of As and Pb in rice grain. Water management regime did not affect rice yield. Under continuously flooded condition, the accumulation of As in the rice grain was generally promoted in all treatments when compared with that under intermittently flooded conditions. However, the accumulation of Pb in the rice grain was reduced under intermittently flooded conditions, where Pb concentrations in the control (0.19 mg kg^{-1}) and PBC treatment (0.10 mg kg^{-1}) were lower than the permissible threshold value of Pb in brown rice regulated by the National Food Standard of China (GB 2762-2017, 0.20 mg kg^{-1}). The application of the raw P-rich biochar significantly reduced the accumulation of Pb in rice grain, to 0.12 mg kg^{-1} under continuously flooded conditions. However, the raw P-rich biochar application significantly promoted the accumulation of As in the rice grain under both continuously and intermittently flooded regimes. Although the application of the Fe-modified P-rich biochar noticeably raised the rice grain yield under both water management regimes and also significantly reduced the accumulation of As in the rice grain, it undesirably increased the concentration of Pb in the rice grain regardless of the water management regimes. Therefore, the multiple-functionalized biochar, Fe-modified P-rich biochar, is more promising for increasing the rice yield, compared to the mono-functionalized P-rich biochar. Also, it decreased As uptake by rice (particularly under intermittently flooded conditions), although the declined concentration of As (1.6 mg kg^{-1}) is still much higher than the threshold value of As in brown rice (GB 2762-2017, 0.20 mg kg^{-1}). As per the above remaining issues, more efforts on using functionalized biochar for sustainable remediation of As and Pb co-contaminated soils are still needed in the future, e.g., adjusting the application rate, changing the ratio of additive materials, optimizing modification techniques, and designing new functionalized materials.

6.5 Acknowledgments

This work was supported by the National Natural Science Foundation of China (21876027), the Key Scientific and Technological Project of Foshan City, China (2120001008392), and the Special Fund for the Science and Technology Innovation Team of Foshan City, China (1920001000083).

6.6 References

- Anawar, H.M., Rengel, Z., Damon, P., Tibbett, M., 2018. Arsenic-phosphorus interactions in the soil-plant-microbe system: Dynamics of uptake, suppression and toxicity to plants. *Environ. Pollut.* 233, 1003-1012. <https://doi.org/10.1016/j.envpol.2017.09.098>
- Bastida, F., Torres, I.F., Romero-Trigueros, C., Baldrian, P., Větrovský, T., Bayona, J.M., Alarcón, J.J., Hernández, T., García, C., Nicolás, E., 2017. Combined effects of reduced irrigation and water quality on the soil microbial community of a citrus orchard under semi-arid conditions. *Soil Biol. Biochem.* 104, 226-237. <https://doi.org/10.1016/j.soilbio.2016.10.024>
- Bolan, N. S., Adriano, D. C., Naidu, R., 2003. Role of phosphorus in (im)mobilization and bioavailability of heavy metals in the soil-plant system. *Rev. Environ. Contam. Toxicol.* 177, 1-44. https://doi.org/10.1007/0-387-21725-8_1
- Bolan, N., Mahimairaja, S., Kunhikrishnan, A., Seshadri, B., Thangarajan, R., 2015. Bioavailability and ecotoxicity of arsenic species in solution culture and soil system: implications to remediation. *Environ. Sci. Pollut. Res.* 22, 8866-8875. <https://doi.org/10.1007/s11356-013-1827-2>
- Chen, H., Feng, Y., Yang, X., Yang, B., Sarkar, B., Bolan, N., Meng, J., Wu, F., Wong, J.W.C., Chen, W., Wang, H., 2022. Assessing simultaneous immobilization of lead and improvement of phosphorus availability through application of phosphorus-rich biochar in a contaminated soil: A pot experiment. *Chemosphere* 296, 133891. <https://doi.org/10.1016/j.chemosphere.2022.133891>
- Chen, H., Yang, X., Wang, H., Sarkar, B., Shaheen, S.M., Gielen, G., Bolan, N., Guo, J., Che, L., Sun, H., Rinklebe, J., 2020a. Animal carcass- and wood-derived biochars improved nutrient bioavailability, enzyme activity, and plant growth in metal-phthalic acid ester co-contaminated soils: A trial for reclamation and improvement of degraded soils. *J. Environ. Manage.* 261, 110246. <https://doi.org/10.1016/j.jenvman.2020.110246>
- Chen, S., Qi, G., Ma, G., Zhao, X., 2020b. Biochar amendment controlled bacterial wilt through changing soil chemical properties and microbial community. *Microbiol. Res.* 231, 126373. <https://doi.org/10.1016/j.micres.2019.126373>
- Das, S., Chou, M.L., Jean, J.S., Liu, C.C., Yang, H.J., 2016. Water management impacts on arsenic behavior and rhizosphere bacterial communities and activities in a rice agro-ecosystem. *Sci. Total Environ.* 542, 642-652. <https://doi.org/10.1016/j.scitotenv.2015.10.122>
- Dong, G., Han, R., Pan, Y., Zhang, C., Liu, Y., Wang, H., Ji, X., Dahlgren, R.A., Shang, X., Chen, Z., Zhang, M., 2021. Role of MnO₂ in controlling iron and arsenic mobilization from illuminated flooded arsenic-enriched soils. *J. Hazard. Mater.* 401, 123362. <https://doi.org/10.1016/j.jhazmat.2020.123362>
- Elzobair, K.A., Stromberger, M.E., Ippolito, J.A., Lentz, R.D., 2016. Contrasting effects of biochar versus manure on soil microbial communities and enzyme activities in an Aridisol. *Chemosphere* 142, 145-152. <https://doi.org/10.1016/j.chemosphere.2015.06.044>
- Feng, Y., Yang, X., Singh, B.P., Mandal, S., Guo, J., Che, L., Wang, H., 2019. Effects of contrasting biochars on the leaching of inorganic nitrogen from soil. *J. Soils Sediments* 20, 3017-3026. <https://doi.org/10.1007/s11368-019-02369-5>
- Fulda, B., Voegelin, A., Ehlert, K., Kretzschmar, R., 2013. Redox transformation, solid phase speciation and solution dynamics of copper during soil reduction and reoxidation as affected by sulfate availability. *Geochim. Cosmochim. Acta* 123, 385-402. <https://doi.org/10.1016/j.gca.2013.07.017>
- Han, L., Sun, K., Yang, Y., Xia, X., Li, F., Yang, Z., Xing, B., 2020. Biochar's stability and effect on the content, composition and turnover of soil organic carbon. *Geoderma* 364, 114184. <https://doi.org/10.1016/j.geoderma.2020.114184>

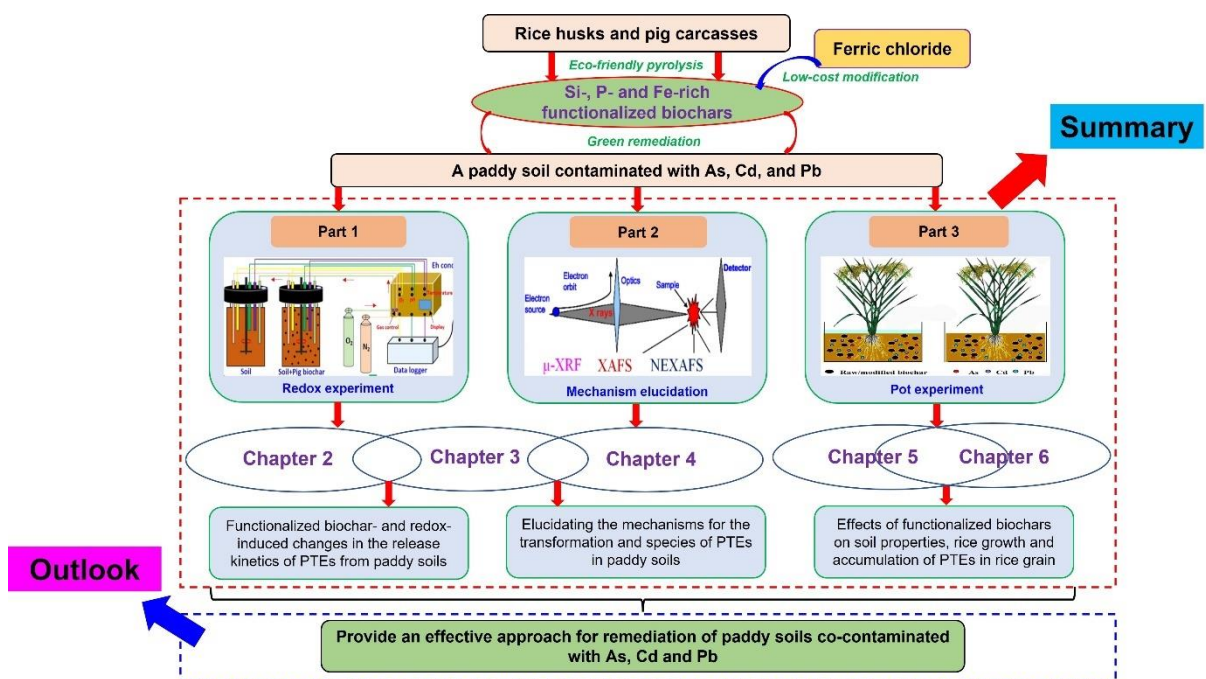
- Hartley, W., Dickinson, N.M., Riby, P., Lepp, N.W., 2009. Arsenic mobility in brownfield soils amended with green waste compost or biochar and planted with *Miscanthus*. *Environ. Pollut.* 157, 2654-2662. <https://doi.org/10.1016/j.envpol.2009.05.011>
- He, L., Shan, J., Zhao, X., Wang, S., Yan, X., 2019. Variable responses of nitrification and denitrification in a paddy soil to long-term biochar amendment and short-term biochar addition. *Chemosphere* 234, 558-567. <https://doi.org/10.1016/j.chemosphere.2019.06.038>
- International Biochar Initiative (IBI), 2015. Standardized product definition and product testing guidelines for biochar that is used in soil. pp. https://www.biochar-international.org/wp-content/uploads/2018/2004/IBI_Biochar_Standards_V2012.2011_Final.pdf.
- Kashif Irshad, M., Noman, A., Wang, Y., Yin, Y., Chen, C., Shang, J., 2022. Goethite modified biochar simultaneously mitigates the arsenic and cadmium accumulation in paddy rice (*Oryza sativa*) L. *Environ. Res.* 206, 112238. <https://doi.org/10.1016/j.envres.2021.112238>
- Kumarathilaka, P., Bundschuh, J., Seneweera, S., Ok, Y.S., 2021. An integrated approach of rice hull biochar-alternative water management as a promising tool to decrease inorganic arsenic levels and to sustain essential element contents in rice. *J. Hazard. Mater.* 405, 124188. <https://doi.org/10.1016/j.jhazmat.2020.124188>
- Lan, J., Zhang, S., Dong, Y., Li, J., Li, S., Feng, L., Hou, H., 2021. Stabilization and passivation of multiple heavy metals in soil facilitating by pinecone-based biochar: Mechanisms and microbial community evolution. *J. Hazard. Mater.* 420, 126588. <https://doi.org/10.1016/j.jhazmat.2021.126588>
- Lee, C.-H., Wu, C.-H., Syu, C.-H., Jiang, P.-Y., Huang, C.-C., Lee, D.-Y., 2016. Effects of phosphorous application on arsenic toxicity to and uptake by rice seedlings in As-contaminated paddy soils. *Geoderma* 270, 60-67. <https://doi.org/10.1016/j.geoderma.2016.01.003>
- Li, J., Li, K., Cave, M., Li, H.B., Ma, L.Q., 2015. Lead bioaccessibility in 12 contaminated soils from China: Correlation to lead relative bioavailability and lead in different fractions. *J. Hazard. Mater.* 295, 55-62. <https://doi.org/10.1016/j.jhazmat.2015.03.061>
- Li, M., Guo, R., Yu, F., Chen, X., Zhao, H., Li, H., Wu, J., 2018. Indole-3-Acetic Acid Biosynthesis Pathways in the Plant-Beneficial Bacterium *Arthrobacter pascens* ZZ21. *Int. J. Mol. Sci.* 19, 443. <https://doi.org/10.3390/ijms19020443>
- Liu, J., Hou, H., Sheng, R., Chen, Z., Zhu, Y., Qin, H., Wei, W., 2012. Denitrifying communities differentially respond to flooding drying cycles in paddy soils. *Appl. Soil Ecol.* 62, 155-162. <https://doi.org/10.1016/j.apsoil.2012.06.010>
- MEE, C., 2018. Soil Environmental Quality Risk Control Standard for Soil Contamination of Agricultural Land.
- MEE, C., MNR, C., 2014. The Report on the National Soil Contamination Survey. http://www.mlr.gov.cn/xwdt/jrxw/201404/t20140417_1312998.htm.
- Mickan, B.S., Abbott, L.K., Solaiman, Z.M., Mathes, F., Siddique, K.H.M., Jenkins, S.N., 2018. Soil disturbance and water stress interact to influence arbuscular mycorrhizal fungi, rhizosphere bacteria and potential for N and C cycling in an agricultural soil. *Biol. Fertil. Soils* 55, 53-66. <https://doi.org/10.1007/s00374-018-1328-z>
- Okkenhaug, G., Zhu, Y.G., He, J., Li, X., Luo, L., Mulder, J., 2012. Antimony (Sb) and arsenic (As) in Sb mining impacted paddy soil from Xikuangshan, China: differences in mechanisms controlling soil sequestration and uptake in rice. *Environ. Sci. Technol.* 46, 3155-3162. <https://doi.org/10.1021/es2022472>
- Palansooriya, K.N., Shaheen, S.M., Chen, S.S., Tsang, D.C.W., Hashimoto, Y., Hou, D., Bolan, N.S., Rinklebe, J., Ok, Y.S., 2020. Soil amendments for immobilization of potentially toxic elements in contaminated soils: A critical review. *Environ. Int.* 134, 105046. <https://doi.org/10.1016/j.envint.2019.105046>
- Pan, H., Yang, X., Chen, H., Sarkar, B., Bolan, N., Shaheen, S.M., Wu, F., Che, L., Ma, Y., Rinklebe, J., Wang,

- H., 2021. Pristine and iron-engineered animal- and plant-derived biochars enhanced bacterial abundance and immobilized arsenic and lead in a contaminated soil. *Sci. Total. Environ.* 763, 144218. <https://doi.org/10.1016/j.scitotenv.2020.144218>
- Patrick, W.H., Mikkelsen, D.S., Wells, B.R., 1985. Plant nutrient behavior in flooded soil. In: Engelstad, O.P. (Ed.), *Fertilizer Technology and Use*. Soil Science Society of America, USA.
- Pei, L., Yang, F., Xu, X., Nan, H., Gui, X., Zhao, L., Cao, X., 2021. Further reuse of phosphorus-laden biochar for lead sorption from aqueous solution: Isotherm, kinetics, and mechanism. *Sci. Total. Environ.* 792, 148550. <https://doi.org/10.1016/j.scitotenv.2021.148550>
- Philippot, L., Raaijmakers, J.M., Lemanceau, P., van der Putten, W.H., 2013. Going back to the roots: the microbial ecology of the rhizosphere. *Nat. Rev. Microbiol.* 11, 789-799. <https://doi.org/10.1038/nrmicro3109>
- Purakayastha, T.J., Bera, T., Bhaduri, D., Sarkar, B., Mandal, S., Wade, P., Kumari, S., Biswas, S., Menon, M., Pathak, H., Tsang, D.C.W., 2019. A review on biochar modulated soil condition improvements and nutrient dynamics concerning crop yields: Pathways to climate change mitigation and global food security. *Chemosphere* 227, 345-365. <https://doi.org/10.1016/j.chemosphere.2019.03.170>
- Qu, J., Yuan, Y., Zhang, X., Wang, L., Tao, Y., Jiang, Z., Yu, H., Dong, M., Zhang, Y., 2022. Stabilization of lead and cadmium in soil by sulfur-iron functionalized biochar: Performance, mechanisms and microbial community evolution. *J. Hazard. Mater.* 425, 127876. <https://doi.org/10.1016/j.jhazmat.2021.127876>
- Reddy, K.R., Patrick Jr., W.H., 1975. Effect of alternate aerobic and anaerobic conditions on redox potential organic matter decomposition and nitrogen loss in a flooded soil. *Soil Biol. Biochem.* 7, 87-94. [https://doi.org/10.1016/0038-0717\(75\)90004-8](https://doi.org/10.1016/0038-0717(75)90004-8)
- Rong, Q., Zhong, K., Li, F., Huang, H., Li, C., Nong, X., Zhang, C., 2019. Combined effect of ferrous ion and biochar on cadmium and arsenic accumulation in rice. *Appl. Sci.* 10, 300. <https://doi.org/10.3390/app10010300>
- Shaheen, S.M., Niazi, N.K., Hassan, N.E.E., Bibi, I., Wang, H., Tsang, Daniel C.W., Ok, Y.S., Bolan, N., Rinklebe, J., 2018. Wood-based biochar for the removal of potentially toxic elements in water and wastewater: a critical review. *Int. Mater. Rev.* 64, 216-247. <https://doi.org/10.1080/09506608.2018.1473096>
- Shaheen, S.M., Wang, J., Baumann, K., Ahmad, A.A., Hsu, L.-C., Liu, Y.-T., Wang, S.-L., Kühn, O., Leinweber, P., Rinklebe, J., 2022. Stepwise redox changes alter the speciation and mobilization of phosphorus in hydromorphic soils. *Chemosphere* 288, 132652. <https://doi.org/10.1016/j.chemosphere.2021.132652>
- Shetaya, W.H., Marzouk, E.R., Mohamed, E.F., Bailey, E.H., Young, S.D., 2019. Chemical and isotopic fractionation of lead in the surface soils of Egypt. *Appl. Geochem.* 106, 7-16. <https://doi.org/10.1016/j.apgeochem.2019.04.013>
- Smith, J.L., Collins, H.P., Bailey, V.L., 2010. The effect of young biochar on soil respiration. *Soil Biol. Biochem.* 42, 2345-2347. <https://doi.org/10.1016/j.soilbio.2010.09.013>
- Sun, Z., Zhang, Z., Zhu, K., Wang, Z., Zhao, X., Lin, Q., Li, G., 2020. Biochar altered native soil organic carbon by changing soil aggregate size distribution and native SOC in aggregates based on an 8-year field experiment. *Sci. Total Environ.* 708, 134829. <https://doi.org/10.1016/j.scitotenv.2019.134829>
- Tang, X., Shen, H., Chen, M., Yang, X., Yang, D., Wang, F., Chen, Z., Liu, X., Wang, H., Xu, J., 2020. Achieving the safe use of Cd- and As-contaminated agricultural land with an Fe-based biochar: A field study. *Sci. Total Environ.* 706, 135898. <https://doi.org/10.1016/j.scitotenv.2019.135898>
- Tang, X., Zou, L., Su, S., Lu, Y., Zhai, W., Manzoor, M., Liao, Y., Nie, J., Shi, J., Ma, L.Q., Xu, J., 2021. Long-term manure application changes bacterial communities in rice rhizosphere and arsenic speciation in rice grains. *Environ. Sci. Technol.* 55, 1555-1565. <https://doi.org/10.1021/acs.est.0c03924>
- Teng, Z., Zhao, X., Yuan, J., Li, M., Li, T., 2021. Phosphate functionalized iron based nanomaterials coupled with

- phosphate solubilizing bacteria as an efficient remediation system to enhance lead passivation in soil. *J. Hazard. Mater.* 419, 126433. <https://doi.org/10.1016/j.jhazmat.2021.126433>
- Ure, A.M., Quevauviller, P., Muntau, H., Griepink, B., 1993. Speciation of heavy metals in soils and sediments. An account of the improvement and harmonization of extraction techniques undertaken under the auspices of the BCR of the commission of the European communities. *J. Environ. Anal. Chem.* 51, 135-151. <https://doi.org/10.1080/03067319308027619>
- Wan, X., Li, C., Parikh, S.J., 2020. Simultaneous removal of arsenic, cadmium, and lead from soil by iron-modified magnetic biochar. *Environ. Pollut.* 261, 114157. <https://doi.org/10.1016/j.envpol.2020.114157>
- Wan, Y., Devereux, R., George, S.E., Chen, J., Gao, B., Noerpel, M., Scheckel, K., 2022. Interactive effects of biochar amendment and lead toxicity on soil microbial community. *J. Hazard. Mater.* 425, 127921. <https://doi.org/10.1016/j.envpol.2020.114157>
- Wang, M., Tang, Z., Chen, X.P., Wang, X., Zhou, W.X., Tang, Z., Zhang, J., Zhao, F.J., 2019. Water management impacts the soil microbial communities and total arsenic and methylated arsenicals in rice grains. *Environ. Pollut.* 247, 736-744. <https://doi.org/10.1016/j.envpol.2019.01.043>
- Wen, E., Yang, X., Chen, H., Shaheen, S.M., Sarkar, B., Xu, S., Song, H., Liang, Y., Rinklebe, J., Hou, D., Li, Y., Wu, F., Pohorely, M., Wong, J.W.C., Wang, H., 2021. Iron-modified biochar and water management regime-induced changes in plant growth, enzyme activities, and phytoavailability of arsenic, cadmium and lead in a paddy soil. *J. Hazard. Mater.* 407, 124344. <https://doi.org/10.1016/j.jhazmat.2020.124344>
- Wenzel, W.W., Kirchbaumer, N., Prohaska, T., Stingeder, G., Lombi, E., Adriano, D.C., 2001. Arsenic fractionation in soils using an improved sequential extraction procedure. *Anal. Chim. Acta* 436, 309-323. [https://doi.org/10.1016/S0003-2670\(01\)00924-2](https://doi.org/10.1016/S0003-2670(01)00924-2)
- Wu, Q., Mou, X., Wu, H., Tong, J., Sun, J., Gao, Y., Shi, J., 2021. Water management of alternate wetting and drying combined with phosphate application reduced lead and arsenic accumulation in rice. *Chemosphere* 283, 131043. <https://doi.org/10.1016/j.chemosphere.2021.131043>
- Xia, B., Qiu, H., Knorr, K.H., Blodau, C., Qiu, R., 2018. Occurrence and fate of colloids and colloid-associated metals in a mining-impacted agricultural soil upon prolonged flooding. *J. Hazard. Mater.* 348, 56-66. <https://doi.org/10.1016/j.jhazmat.2018.01.026>
- Xiao, W., Lin, G., He, X., Yang, Z., Wang, L., 2022. Interactions among heavy metal bioaccessibility, soil properties and microbial community in phyto-remediated soils nearby an abandoned realgar mine. *Chemosphere* 286, 131638. <https://doi.org/10.1016/j.chemosphere.2021.131638>
- Xiao, X., Chen, B., Chen, Z., Zhu, L., Schnoor, J.L., 2018. Insight into multiple and multilevel structures of biochars and their potential environmental applications: a critical review. *Environ. Sci. Technol.* 52, 5027-5047. <https://doi.org/10.1021/acs.est.7b06487>
- Yang, X., Hinzmann, M., Pan, H., Wang, J., Bolan, N., Tsang, D.C.W., Ok, Y.S., Wang, S.L., Shaheen, S.M., Wang, H., Rinklebe, J., 2022a. Pig carcass-derived biochar caused contradictory effects on arsenic mobilization in a contaminated paddy soil under fluctuating controlled redox conditions. *J. Hazard. Mater.* 421, 126647. <https://doi.org/10.1016/j.jhazmat.2021.126647>
- Yang, X., Lu, K., McGrouther, K., Che, L., Hu, G., Wang, Q., Liu, X., Shen, L., Huang, H., Ye, Z., Wang, H., 2017. Bioavailability of Cd and Zn in soils treated with biochars derived from tobacco stalk and dead pigs. *J. Soils Sediments* 17, 751-762. <https://doi.org/10.1007/s11368-015-1326-9>
- Yang, X., Pan, H., Shaheen, S.M., Wang, H., Rinklebe, J., 2021. Immobilization of cadmium and lead using phosphorus-rich animal-derived and iron-modified plant-derived biochars under dynamic redox conditions in a paddy soil. *Environ. Int.* 156, 106628. <https://doi.org/10.1016/j.envint.2021.106628>
- Yang, X., Shaheen, S.M., Wang, J., Hou, D., Ok, Y.S., Wang, S.L., Wang, H., Rinklebe, J., 2022b. Elucidating

- the redox-driven dynamic interactions between arsenic and iron-impregnated biochar in a paddy soil using geochemical and spectroscopic techniques. *J. Hazard. Mater.* 422, 126808. <https://doi.org/10.1016/j.jhazmat.2021.126808>
- Yu, M., Su, W., Parikh, S.J., Li, Y., Tang, C., Xu, J., 2021. Intact and washed biochar caused different patterns of nitrogen transformation and distribution in a flooded paddy soil. *J. Clean. Prod.* 293, 126259. <https://doi.org/10.1016/j.jclepro.2021.126259>
- Zama, E.F., Reid, B.J., Sun, G.-X., Yuan, H.-Y., Li, X.-M., Zhu, Y.-G., 2018. Silicon (Si) biochar for the mitigation of arsenic (As) bioaccumulation in spinach (*Spinacia oleracea*) and improvement in the plant growth. *J. Clean. Prod.* 189, 386-395. <https://doi.org/10.1016/j.jclepro.2018.04.056>
- Zemberyova, M., Bartekova, J., Hagarova, I., 2006. The utilization of modified BCR three-step sequential extraction procedure for the fractionation of Cd, Cr, Cu, Ni, Pb and Zn in soil reference materials of different origins. *Talanta* 70, 973-978. <https://doi.org/10.1016/j.talanta.2006.05.057>
- Zhang, H., Shao, J., Zhang, S., Zhang, X., Chen, H., 2020a. Effect of phosphorus-modified biochars on immobilization of Cu(II), Cd(II), and As(V) in paddy soil. *J. Hazard. Mater.* 390, 121349. <https://doi.org/10.1016/j.jhazmat.2019.121349>
- Zhang, J., Zhao, S., Xu, Y., Zhou, W., Huang, K., Tang, Z., Zhao, F.J., 2017. Nitrate stimulates anaerobic microbial arsenite oxidation in paddy soils. *Environ. Sci. Technol.* 51, 4377-4386. <https://doi.org/10.1021/acs.est.6b06255>
- Zhang, Q., Song, Y., Wu, Z., Yan, X., Gunina, A., Kuzyakov, Y., Xiong, Z., 2020b. Effects of six-year biochar amendment on soil aggregation, crop growth, and nitrogen and phosphorus use efficiencies in a rice-wheat rotation. *J. Clean. Prod.* 242, 118435. <https://doi.org/10.1016/j.jclepro.2019.118435>
- Zhang, R., Chen, L., Niu, Z., Song, S., Zhao, Y., 2019. Water stress affects the frequency of Firmicutes, Clostridiales and *Lysobacter* in rhizosphere soils of greenhouse grape. *Agric. Water Manag.* 226, 105776. <https://doi.org/10.1016/j.agwat.2019.105776>
- Zhang, S., Yang, X., Hsu, L.-C., Liu, Y.-T., Wang, S.-L., White, J.R., Shaheen, S.M., Chen, Q., Rinklebe, J., 2021. Soil acidification enhances the mobilization of phosphorus under anoxic conditions in an agricultural soil: Investigating the potential for loss of phosphorus to water and the associated environmental risk. *Sci. Total Environ.* 793. <https://doi.org/10.1016/j.scitotenv.2021.148531>
- Zhao, F.-J., Wang, P., 2019. Arsenic and cadmium accumulation in rice and mitigation strategies. *Plant Soil* 446, 1-21. <https://doi.org/10.1007/s11104-019-04374-6>
- Zhong, D., Jiang, Y., Zhao, Z., Wang, L., Chen, J., Ren, S., Liu, Z., Zhang, Y., Tsang, D.C.W., Crittenden, J.C., 2019. pH dependence of arsenic oxidation by rice-husk-derived biochar: roles of redox-active moieties. *Environ. Sci. Technol.* 53, 9034-9044. <https://doi.org/10.1021/acs.est.9b00756>

CHAPTER 7: Summary and Outlook



7.1 Summary

The general framework of the current thesis concerns using functionalized biochars for the remediation of soils contaminated with potentially toxic elements (PTEs) in both cationic (e.g., Cd and Pb) and anionic (e.g., As) forms. The various characteristics of different functionalized biochars determine their ability for PTE (im)mobilization. In this thesis, a suite of experiments, including incubation experiments and pot experiments were carried out to investigate (1) the effects of P-rich pig carcass-derived biochar on the mobilization and speciation of As in a contaminated paddy soil under systematic changed redox conditions (Chapter 2), (2) the impacts of the Fe-modified green waste-derived biochar and change in redox conditions on the biogeochemical behavior of As in the contaminated paddy soil and the underlying mechanisms (Chapter 3), (3) the interactions between P-rich pig carcass and Fe-rich modified biochars and cationic PTEs, Cd and Pb, in a contaminated paddy soil under a wide range of controlled redox conditions (Chapter 4), (4) the feasibility of different functionalized biochars, including the Si-rich, P-rich, and Fe-modified biochars for simultaneous immobilization of both cationic and anionic PTEs, i.e., As, Cd, and Pb, and in turn for the cleaner production of rice (Chapter 5), and (5) potential impacts of the raw and Fe-modified P-rich biochars on the geochemical transformation and redistribution of the PTEs (i.e., As and Pb), as well as the yield and quality of rice grain under different water management regimes (Chapter 6). The implementation of the whole study and the completion of this thesis have provided new understandings of using functionalized biochars for the alleviating the phytotoxicity of As, Cd, and Pb to rice growth, and thus human health, which is of great significance to the enhancement of the agricultural and environmental sustainability, and food security in China and all over the world. Chapters 2-4 answered the first two research questions: (1) *Can functionalized biochars affect the release dynamics and biogeochemical behaviors of As, Cd and Pb under dynamic redox conditions in paddy soil?* and (2) *How do functionalized biochars affect the biogeochemical processes and redox reactions while they are incorporated into the contaminated soils, and how do they affect the transformation and biogeochemical fractionation of As, Cd and Pb under fluctuating redox conditions?* Chapters 5-6 responded to the third research question: (3) *Are functionalized biochars able to regulate the physicochemical and microbial properties of paddy soils, growth of rice plants (*Oryza sativa*), as well as the biogeochemical behaviors of As, Cd, and Pb in the soil-plant interface and their uptake by rice plants and translocation from the roots to stems and leaves, and then edible grain under different irrigation regimes (simulation of different redox conditions)?* The main results and conclusions are as follows:

Chapter 2, indicated that the application of the P-rich pig carcass biochar caused a wider range of Eh, and an increase in soil pH. For the controlling factors, the application of pig carcass biochar immobilized Fe and Mn,

especially under moderately reducing conditions, but had no significant influence on the concentration of SO_4^{2-} . In addition, the application of the biochar could change the content and compositions of organic carbon in soil. Importantly, the application of the P-rich pig carcass biochar decreased the concentration of dissolved As by 38.7 and 35.4% under moderately reducing conditions with $E_h = +100$ and $+200$ mV, respectively, compared to the non-treated control, which could be mainly due to the co-precipitation of As with Fe-Mn (hydro)oxides and the complexation between As and the aromatic organic compounds generated by the biochar. Under strongly reducing conditions with $E_h = -300$ mV, the application of the P-rich pig carcass biochar increased the concentration of dissolved As by 13.5%, compared to the control, which could be attributed to the promoted reduction and decomposition of the As-bearing Fe minerals (e.g., Ferrihydrite and Fe-containing humic compounds) under reducing conditions. Under oxidizing conditions ($E_h = +250$ mV), the application of the P-rich pig carcass biochar accelerated the release of As, by 3.7 times, compared to the control, which could be due to the biochar-induced increase in soil pH. Overall, the application of the P-rich pig carcass biochar could cause a decrease in As mobilization and reduce the risk of As in paddy soils under moderately reducing conditions ($E_h = +100$ and $+200$ mV). However, this functionalized biochar cannot be appropriately used for immobilization of As in paddy soils under strongly reducing ($E_h < -300$ mV) and oxidizing ($E_h > +300$ mV) conditions.

Chapter 3 presented that the concentrations of dissolved As were relatively high under reducing conditions and low under oxidizing conditions, which indicate the high potential environmental and human health risk of As in flooded paddy soils and emphasize the need of remediating those contaminated paddy soils. The modification of green waste biochar with Fe materials has altered the surface and structural characteristics of the biochar, which could affect its capability on As (im)mobilization under different redox conditions. Results in this chapter also indicated that both biochars had a potential to affect the mobilization of As through changing soil pH and the redox reactions in the paddy soil. Under reducing conditions with $E_h = -300$ mV, the incorporation of the raw and Fe-modified biochars reduced the dissolved As by 41.3 and 71.8%, respectively, compared to the non-treated control, due to the decrease of pH caused by the application of the Fe-modified biochar. Under oxidizing conditions, the Fe-modified biochar was effective on decreasing the dissolved As, which could be due to the co-precipitation and complexation with exogenous Fe materials. An increase of dissolved As was found in the raw biochar treatment under strongly oxidizing condition ($E_h = +300$ mV), which could be associated with the indirectly increase of negative charges as a result of the increase of pH. The modification of RBC with Fe materials increased its effectiveness for As immobilization under reducing conditions, which could be mainly attributed to its abundant oxygen-containing functional groups and high aromaticity. The application of the raw biochar under

reducing conditions ($E_h < -100$ mV) could be due to the presence of the porous structure and oxygen-containing functional groups on the biochar. In conclusion, application of the Fe-impregnated biochar could decrease the concentration of dissolved As, in particular under reducing conditions, thus alleviating the environmental risks of As to be accumulated in the food chain and/or transported into groundwater.

Chapter 4 focused on using the P- and Fe-rich biochars for the immobilization of two cationic elements (Cd and Pb) in the paddy soil under dynamic redox conditions. Results showed that the concentrations of dissolved Cd increased up to $10.9 \mu\text{g L}^{-1}$ under reducing conditions, and decreased to a value below the detection limit of Cd (LDL = $2.7 \mu\text{g L}^{-1}$) in the raw and Fe-modified biochar treatments. Compared to the non-treated control, the application of the raw biochar decreased the concentrations of dissolved Cd by 43 to 59% under reducing conditions with $E_h < -100$ mV, while the application of the Fe-modified biochar and P-rich biochar decreased the concentrations of Cd by 31 to 59% and 8 to 19%, respectively, compared to the non-treated control. The immobilization of Cd under reducing conditions could be due to the formation of stable Cd-sulfides, whereas the immobilization of Cd under oxidizing conditions might be attributed to the increase of pH. Similar to Cd, the concentrations of dissolved Pb ranged from 29.4 to $198.2 \mu\text{g L}^{-1}$ under reducing conditions, whereas those under oxidizing conditions were all below the detection limit of Pb (LDL = $12.5 \mu\text{g L}^{-1}$). Compared to the raw and Fe-modified biochars, application of the P-rich biochar was more effective on immobilizing Pb, especially under reducing conditions with $E_h < 0$ mV, due to the formation of Pb-phosphates. The raw and Fe-modified biochars immobilized Pb under strongly reducing conditions with $E_h < -300$ mV; however, both biochars, in particular the Fe-modified one, mobilized Pb under moderately reducing and oxidizing conditions ($E_h > -200$ mV), especially under moderately reducing conditions with $E_h = +100$ mV, which could be mainly ascribed to the declined pH at this point. Overall, the Fe-modified biochar was more effective on immobilizing Cd than Pb, which was primarily due to the redox interactions between the applied Fe and Cd, including re-sorption and co-precipitation. The P-rich biochar had higher efficiency in immobilizing Pb than Cd, which might be due to its alkalinity and high ash content. In addition, the rich phosphate might contribute to immobilization Pb through precipitation. The application of both raw and Fe-rich biochars enable to immobilize Cd in paddy soils, particularly under strongly reducing conditions. We conclude that the amendment of P-rich pig carcass biochar could be a promising approach for mitigating the environmental and human health risk of Pb in paddy soils, whereas the raw and Fe-rich green waste-derived biochars can be used for immobilizing Cd under both reducing and oxidizing conditions and mitigate its potential risk in paddy soils.

Chapter 5 indicated that Si-, P-, and Fe-rich functionalized biochars exhibited various effects on soil nutrient

availability, enzyme activity and the phytoavailability of the PTEs (i.e., As, Cd, and Pb). The Si-rich biochar derived from rice husks decreased the concentrations of As in rice grain and straw by 59.4 and 61.4%, respectively, compared to the non-treated control, without compromising plant growth and grain yield. The application of the raw Si-rich biochar did not significantly change the concentrations of Cd and Pb in rice plants, whereas the Fe-modified Si-rich biochar significantly increased the concentrations of Cd and Pb in rice straw and grain, posing a relatively high environmental risk. The application of the P-rich biochar derived from pig carcasses enhanced the enzyme activities in soil (dehydrogenase, catalase, and urease), and reduced the concentrations of Pb in rice grain and straw by 49.3 and 43.2%, respectively, whereas it had non-significant effects on the concentrations of As and Cd in rice plants, plant growth parameters and rice grain yield. However, the application of the Fe-modified P-rich biochar decreased the concentrations of As in rice grain and straw by 12.2 and 51.2%, respectively, but increased those of Cd and Pb in both rice straw and grain, compared to the control. Overall, the Fe-modified rice husk-derived Si-rich and pig carcass-derived P-rich biochars could be employed as amendments for improving soil quality and increasing the yield and quality of rice when As is the only concern in soils. If Pb is a concern, however, application of pristine P-rich biochar could be a promising approach in limiting Pb accumulation in rice. However, the application of the Fe-modified biochars may induce an elevated accumulation of Cd and Pb in rice, thus posing a high risk of these elements to food security and human health. In this chapter, we found that none of the tested functionalized biochars could reach an appropriate effectiveness on a simultaneous alleviation of As, Cd and Pb in rice plants grown in the contaminated paddy soil.

Chapter 6 investigated the effects of the raw and Fe-modified pig carcass-derived P-rich biochars coupled with different water management regimes, i.e., continuously flooded and intermittently flooded, on the yield of rice grain, and the accumulation of As and Pb in the rice grain. We found that both functionalized biochar application and water management practice could (1) change soil properties and nutrient status including pH, organic carbon content, and availability of N, P and K, (2) alter the geochemical redistribution of As and Pb, (3) shape the bacterial community structure in the paddy soil, and eventually (4) regulate the rice yield and the accumulation of As and Pb in rice grain. Results in this chapter showed that the application of the Fe-modified P-rich biochar increased the rice yield by 47.4 and 19.6%, respectively, under continuously flooded and intermittently flooded conditions, due to the improved soil nutrient availability and the enhanced microbial activities, such as the abundance of genera *Bacillus*, *Arthrobacter* and *Gemmatimonas*. The application of both biochars altered the accumulation of As and Pb in rice grain, mainly through changing the geochemical fractions of the elements and the bacterial community structure in the soil, especially at the genus level. The concentrations of As in the rice grain were

higher under continuously flooded conditions (1.94-2.42 mg kg⁻¹) than under intermittently flooded conditions (1.56-2.31 mg kg⁻¹). Conversely, the concentrations of Pb in the rice grain were higher under intermittently flooded conditions (0.10-0.76 mg kg⁻¹) than under continuously flooded conditions (0.12-0.48 mg kg⁻¹). The application of the raw P-rich biochar decreased the concentration of Pb in the rice grain by 60.1% in the continuously flooded treatment, whilst the application of the Fe-modified P-rich biochar reduced the concentration of As in the rice grain by 12.2% in the intermittently flooded treatment, and meanwhile increased the concentrations of grain Pb by 2.9 and 6.6 times, respectively, in the continuously flooded and intermittently flooded treatments when compared with the non-treated controls. Importantly, the accumulation of Pb in the rice grain was reduced under intermittently flooded conditions, where Pb concentrations in the control (0.19 mg kg⁻¹) and PBC treatment (0.10 mg kg⁻¹) were lower than the permissible threshold value of Pb in brown rice regulated by the National Food Standard of China (GB 2762-2017, 0.20 mg kg⁻¹). The application of the raw P-rich biochar significantly reduced the accumulation of Pb in rice grain, to 0.12 mg kg⁻¹ under continuously flooded conditions. However, the application of the raw P-rich biochar significantly promoted the accumulation of As in the rice grain under both continuously and intermittently flooded regimes. Despite the application of the Fe-modified P-rich biochar noticeably raised the rice grain yield under both water management regimes and also significantly reduced the accumulation of As in the rice grain, it undesirably increased the concentration of Pb in the rice grain regardless of the water management regimes.

In summary, the application of the P-rich pig carcass-derived biochar could immobilize cationic elements, i.e., Cd and Pb, under both reducing and oxidizing conditions, primarily based on its high P content, cationic exchange capacity, and alkalinity, as well as the presence of porous structure and oxygen-containing functional groups. However, the application of the P-rich biochar could cause a contradictory impact on As (exists in anionic forms) mobilization under virous Eh conditions, as compared to Cd and Pb. Namely, the application of the P-rich biochar significantly decreased the concentration of dissolved As under moderately reducing conditions, whereas the concentration of dissolved As significantly elevated under both strongly reducing and oxidizing conditions. The loading of Fe materials enhanced the efficacy of the raw green waste biochar in As immobilization, but decreased the effectiveness of the raw biochar for Pb immobilization. In addition, the Fe-rich biochar was more effective on immobilizing As and Cd than Pb. The interactions between the Fe-rich biochar and Cd could be ascribed to the transformation of sulfur in soil, whereas the interactions between the Fe-rich biochar could be due to the redox-induced transformation of Fe (hydro)oxides and the changes in net charges on soil particles. From a perspective of practical application, the P-rich biochar could significantly increase the rice yield, whilst reducing the

accumulation of Pb, especially under continuously flooded water management regime. However, the application of the P-rich biochar enhanced the accumulation of As in the rice grain. The Fe-modified P-rich biochar could also cause a noticeable increase in rice yield, while its application elevated the risk of Pb exposure in rice grain. In addition, the application of the raw Si-rich rice husk-derived biochar could improve soil fertility and microbial activities, promote rice growth, thus increasing rice yield. In the meantime, the application of the raw Si-rich biochar could reduce the accumulation of As in rice grain, but had no significant impacts on the uptake of Cd and Pb by rice plants. Although the application of the Fe-modified Si-rich biochar could reduce the uptake of As by rice plants, it is unlikely to be used for the remediation of multi-PTE contaminated paddy soils since it dramatically promoted the uptake of Cd and Pb by rice plants and elevated their environmental risks. Overall, application of the P-rich pig carcass biochar could be a promising way for immobilizing Cd and Pb, in particular Pb in paddy soils; the raw and Fe-rich green waste biochars have higher ability in immobilizing Cd (under both reducing and oxidizing conditions) and As (particularly under reducing conditions); the Si-rich rice husk biochar could be a suitable amendment for improving soil quality and increasing the yield and quality of rice when As is the only concern in soils. However, none of the tested functionalized biochars could reach an appropriate effectiveness on the simultaneous immobilization of multiple potentially toxic elements in the paddy soil, or achieve a simultaneous alleviation of the accumulation of those elements in rice grain.

7.2 Outlook

Recently, different modification methods were employed for the production of functionalized biochars, to modulate the functions of biochar for remediation of soils contaminated with potentially toxic elements. Compared to chemical modification methods (e.g., acid and alkalinity modification, oxidizing agent modification, metal salt modification), physical modification may provide a low-cost way to produce functionalized biochars. For instance, selection and use of specialized low-cost biomass (e.g., P- or Si-rich feedstocks), as well as the production of hybrid composite of biochar and other materials (e.g., Fe materials) might be promising ways to produce functionalized biochars. Based on the findings in the thesis, none of the tested functional biochars could achieve an anticipated effect. Thus, more efforts on using effective functionalized biochar for sustainable remediation of soils co-contaminated with multiple potentially toxic elements, both cationic and anionic ones (e.g., As, Cd, and Pb), are still needed in the future.

For instance, future studies shall focus on selecting suitable feedstocks for functionalized biochar production,

optimizing practical techniques for biochar modification, and exploring appropriate application rates and manners of the obtained functionalized biochars based on different environmental purposes. Additionally, because different functionalized biochars have different properties, they showed various mechanisms on the immobilization of potentially toxic elements. Those underlying mechanisms need to be further clarified in the future, with integration of various advanced technologies, including chemical analyses, microbiological methods, and spectroscopic techniques. Moreover, functionalized biochars showed bright prospect in remediating soils contaminated with potentially toxic elements, whereas most of the relevant studies have been conducted under laboratory conditions. The natural environment is more complex than in the laboratory, which causes the uncertainty of the stability and environmental function of functionalized biochars. Therefore, future *in-situ* studies are urgently needed to investigate the effect of functionalized biochars on the immobilization of PTEs in soils under field conditions. In addition, functionalized biochars will undergo long-term aging and oxidizing via abiotic and biotic processes when applied into soils. However, little is known about the remediation efficacy of aged functionalized biochars. Further studies are warranted to examine the duration of remediation effect with aging process and mechanisms as affected by different modification techniques.

Appendix A

***Supplementary Material* for Chapter 2**

Effects of Pig Carcass-Derived Phosphorus-Rich Biochar on Arsenic Mobilization under Fluctuating Controlled Redox Conditions in Paddy Soil

A1. Additional materials and methods

A1.1 Sampling procedures and analytical methods for controlling factors

Briefly, eight MCs were used for the control soil and pig biochar-treated soil (four replicates for each). Eight glass vessels were filled with 210 g of air-dried soil and 1680 mL of tap water to reach a soil/water ratio of 1:8 and hermetically sealed with an air-tight lid. The slurry in each MC was continuously stirred to achieve homogeneity. The Eh levels of the soil suspension were reduced over a prolonged period by flushing the MCs with N₂. The values of Eh and pH for the MCs were recorded every 10 min in a data logger. Those data were used as measured by the calibrated sensors. The data were not calculated as a reference to the standard hydrogen electrode aiming to present the actual redox potential in relation to the solution. The total incubation period was approximately 24 days (574 h). The targeted Eh values ranged between -400 and +300 mV, allowing for the examination of eight pre-defined Eh windows (-400, -300, -200, -100, 0, +100, +200, and +300 mV, respectively). The pre-set Eh windows were achieved at least 48 h before sampling and automatically maintained with the flushing of N₂ and synthetic air/O₂. The Eh values 6 h before sampling for each Eh window are calculated for statistics. The initial sampling was collected after 2 h stirring the MCs. An 85 mL of the slurry was sampled from each MC approximately 48 or 72 h after reaching the Eh-window using syringes. The suspension was centrifuged for 15 min at 5000 rpm and the supernatant was filtered under anaerobic conditions (O₂ concentration within less than 0.2%) in a glove box (MK3 Anaerobic Work Station, Don Whitley Scientific, Shipley, UK). The concentration of dissolved As in addition to the controlling factors (Fe, Mn, Cl⁻, SO₄²⁻ and DOC) were gained separately. To collect the dissolved fraction, samples were filtered to pass through a 0.45-µm Millipore membrane (Whatman Inc., Maidstone, UK).

The dissolved concentrations of As, Fe and Mn were analyzed by an inductively coupled plasma optical spectroscopy (ICP-OES, Horiba Jobin Yvon, Uterhaching, Germany). The concentrations of SO₄²⁻ and Cl⁻ was analyzed by an ion chromatograph (Metrohm, Filderstadt, Germany). The DOC concentrations were measured using a C/N-analyzer (multi N/C 2100 S, Analytik Jena, Germany). The Specific UV absorbance (SUVA) was measured and calculated according to Weishaar *et al.* (2003).

A1.2 Biochar characterization

The pig biochar was examined under the scanning electron microscope (SEM) (Sirion-100, FEI, Poland) equipped with an energy-dispersive spectrometer at 20 kV (EDS, INCA X-sight, Oxford Instruments). X-ray diffraction (XRD) was carried out on a computer-controlled diffractometer (X'Pert PRO, PANalytical, Netherlands). The surface functional groups and structural features of the pig biochar were characterized using a Fourier transform

infrared spectroscopy (FTIR: Frontier, PerkinElmer, USA) at a resolution of 4 cm^{-1} and a Raman spectrometer (ARAMIS: Horiba Jobin, Japan) with a resolution better than 2 cm^{-1} at room temperature, respectively. The XPS spectrum of the biochar was obtained using a PHI Quantera spectrometer (USA). The binding energies were referenced to the C1s peak at 284.6 eV for calibration.

A1.3 Soil pre-incubation

Plastic beakers were filled with 800 g of pre-incubated contaminated paddy soil and added with 0 (control) and 3% (w/w) of pig biochar and mixed homogenously. The control and pig biochar treatments were incubated at around 25°C with steady flooding to simulate paddy field. Each treatment had 4 replicates. All beakers were irrigated with deionized water to maintain 2~3 cm water layer above the soil surface. After 30 days of incubation, the control and pig biochar-treated soils were retrieved from each beaker, air-dried, ground and passed through a 2-mm sieve before using in the automated biogeochemical microcosm experiment.

A2. Supporting results

A2.1 Properties of pig biochar

The pig biochar was alkaline with a pH of 10.6 and a surface alkalinity of 245.7 cmol/kg . The biochar had relatively low carbon content (30.8%) but high ash content (49.9%). As for other elements, 2.1% of nitrogen, 1.3% of hydrogen and 0.2% of sulfur were detected. The atomic ratio of H/C was 0.5, which was lower than the criteria value (0.7) as defined for a stable biochar suggested by the International Biochar Initiative (2015). Additionally, pig biochar had moderate surface area of $18.4\text{ m}^2/\text{g}$ (Table 2-1).

The typical SEM images of biochar were shown in Figure 1A, it was apparent that pig biochar had highly irregular porous structures coexisting with cellular and tubular shapes, the edges of pores were sharp and clear. However, some pores were occupied by weeny fragments, which were considered as some inorganic compounds formed during pyrolysis or attributed to the artificial physical crushing prior to the analysis. The EDS elemental mapping (Figure 1B) indicated that some elements, such as Na (0.6%), Mg (0.2%), Si (3.0%), P (3.9%), S (0.1%), K (1.5%), Ca (6.9) and Fe (5.4%) were detected in the pig biochar. (Table 2-1). The XRD pattern of pig biochar revealed the presence of different inorganic mineral such as sylvite (KCl), silicon chloride (SiCl_4), potassium oxide (K_2O) and potassium hydroxide (KOH) (Figure 1C). Generally, biochars contain a considerable amount of aromatic carbon and tend to form a series of functional groups (Vithanage *et al.*, 2017). In the FTIR profile of the pig biochar (Figure 1D), the adsorption peaks around 1100 cm^{-1} , 1350 cm^{-1} , 1590 cm^{-1} , 2900 cm^{-1} and 3400 cm^{-1} were detected, which were associated with C–OH/C–O–C/Si–O–Si groups, C=C groups, C=O groups, $-\text{CH}_3$ groups

and –OH groups, respectively (Yang *et al.*, 2018; Chen *et al.*, 2019). The high-resolution XPS C1s spectra were run for the further interpretation of the presence and composition of functional groups on the surface of pig biochar (Figure 1E). The XPS spectra could be deconvoluted as four major signals at 284.5 eV, 285.6 eV, 286.5 eV and 288.6 eV, which were designated for C=C (C–C/C–H) bonds, C-O (C–O–C/C–OH) bonds, C=O (O=C–O) bonds and –COOH bonds, respectively. Thereinto, the total abundance bonds of C-H and C=O were 56.67% and 12.48%. Raman spectroscopic analysis was performed for better understanding of the aromaticity of pig biochar. As shown in Figure 1F, two peaks around 1350 cm⁻¹ and 1590 cm⁻¹ were observed. The corresponding assignments were the D band associated with sp³ hybridization (disordered graphite ring structures) and the tangential G band induced by sp² carbon stretching vibrations (graphitic carbon structures) (Igalavithana *et al.*, 2018). Generally, the higher intensity ratio of D and G bands (I_D/I_G) indicates higher functionalities of biochar (Inyang *et al.*, 2014), while the lower ratio means greater carbonization degree and higher aromaticity (Yang *et al.*, 2018). In this study, the I_D/I_G ratio of 1.76 indicated relatively high functionalities, such as –OH, –COOH and –C=O on the surface of pig biochar. In addition, the higher intensity of D band than G band also illustrated more graphene like structures that could improve the pore structures and surface areas of biochar (Vithanage *et al.*, 2017). These characteristics of pig biochar presented above suggest a promising potential of it being used as a soil amendment for immobilization of toxic elements (Inyang *et al.*, 2014; Yang *et al.*, 2018; Shaheen *et al.*, 2019).

A2.2 Redistribution of As in soils after incubation

Figure S1 shows the different fractions of As in the control and pig biochar-treated soils after 30 days of pre-incubation. The predominant fractions of As in the two soils was bound with iron oxide, the sum of two iron oxide fractions accounted for 75.5 and 85.0%, respectively, in the control and pig biochar treatment. The sum of potentially mobile fractions (sum of soluble + exchangeable, carbonate, manganese oxide, organic matter, sulfide, amorphous and crystalline iron oxides fractions) was less than 5% in both soils. In addition, the proportion of potentially mobile fraction increased from 76.9 to 87.0%, while the proportion of residual fraction slightly decreased from 23.1 to 13.0% after pig biochar application.

A3. References

- Chen, H., Yang, X., Gielen, G., Mandal, S., Xu, S., Guo, J., Shaheen, S.M., Rinklebe, J., Che, L., Wang, H., 2019. Effect of biochars on the bioavailability of cadmium and di-(2-ethylhexyl) phthalate to *Brassica chinensis* L. in contaminated soils. *Sci. Total Environ.* 678, 43-52.
- Igalavithana, A.D., Yang, X., Zahra, H.R., Tack, F.M.G., Tsang, D.C.W., Kwon, E.E., Yong, S.O., 2018. Metal(loid)

- immobilization in soils with biochars pyrolyzed in N₂ and CO₂ environments. *Sci. Total Environ.* 630, 1103-1114.
- Inyang, M., Gao, B., Zimmerman, A., Zhang, M., Chen, H., 2014. Synthesis, characterization, and dye sorption ability of carbon nanotube–biochar nanocomposites. *Chem. Eng. J.* 236, 39-46.
- Shaheen, S.M., El-Naggar, A., Wang, J., Hassan, N.E.E., Niazi, N.K., Wang, H., Tsang, D.C.W., Ok, Y.S., Bolan, N., Rinklebe, J., 2019. Biochar as an (im)mobilizing agent for the potentially toxic elements in contaminated soils. In: Ok, Y.S., Tsang, D. (Eds.), *Biochar from Biomass and Waste*. Elsevier, New York, USA, pp. 256-274.
- Takeno, N., 2005. *Atlas of Eh-pH diagrams*. National Institute of Advanced Industrial Science and Technology.
- Vithanage, M., Herath, I., Joseph, S., Bundschuh, J., Bolan, N., Ok, Y.S., Kirkham, M.B., Rinklebe, J., 2017. Interaction of arsenic with biochar in soil and water: A critical review. *Carbon* 113, 219-230.
- Weishaar, J. L., Aiken, G. R., Bergamaschi, B. A., Fram, M. S., Fujii, R., Mopper, K., 2003. Evaluation of Specific Ultraviolet Absorbance as an Indicator of the Chemical Composition and Reactivity of Dissolved Organic Carbon. *Environ. Sci. Technol.* 37, 4702-4708.
- Yang, X., Igalavithana, A.D., Oh, S.E., Nam, H., Ming, Z., Wang, C.H., Kwon, E.E., Tsang, D.C.W., Yong, S.O., 2018. Characterization of bioenergy biochar and its utilization for metal/metalloid immobilization in contaminated soil. *Sci. Total Environ.* 640-641, 704.

Appendix B

***Supplementary Material* for Chapter 3**

Effects of Iron-Impregnated Green Waste Biochar on Arsenic Mobilization under Fluctuating Controlled Redox Conditions in Paddy Soil

B1. Supplemental methods

B1.1 Analysis of controlling factors

The dissolved concentrations of As, Fe were analyzed by an inductively coupled plasma optical spectroscopy (ICP-OES, Horiba Jobin Yvon, Uterhaching, Germany). The concentration of SO_4^{2-} was analyzed by an ion chromatograph (Metrohm, Filderstadt, Germany). The concentrations of Fe^{2+} were extracted and determined calorimetrically (CADAS 200, Dr. Lange, Germany) at 510 nm according to the method of Harvey *et al.* (1955). The DOC concentrations were measured using a C/N-analyzer (multi N/C 2100 S, Analytik Jena, Germany).

B1.2 Experimental conditions and sampling

Briefly, twelve MCs were used for the non-treated soil and biochar-treated soil (four replicates for each). Twelve glass vessel was filled with 210 g of air-dried soil and 1680 mL of tap water to reach a soil/water ratio of 1:8 and hermetically sealed with an air-tight lid. The slurry in each MC was continuously stirred to achieve homogeneity. The Eh levels of the soil suspension were reduced over a prolonged period by flushing the MCs with N_2 . The values of Eh and pH for the MCs were recorded every 10 min in a data logger. Those data were used as measured by the calibrated sensors. The data were not calculated as a reference to the standard hydrogen electrode aiming to present the actual redox potential in relation to the solution. The total incubation period was approximately 24 days (574 h). The targeted Eh values ranged between -400 and +300 mV, allowing for the examination of eight pre-defined Eh windows (-400, -300, -200, -100, 0, +100, +200, and +300 mV, respectively). The pre-set Eh windows were achieved at least 48 h before sampling and automatically maintained with the flushing of N_2 and synthetic air/ O_2 . The Eh values 6 h before sampling for each Eh window are calculated for statistics. The initial sampling was collected after 2 h stirring the MCs. An 85 mL of the slurry was sampled from each MC approximately 48 or 72 h after reaching the Eh-window using syringes. The suspension was centrifuged for 15 min at 5000 rpm and the supernatant was filtered under anaerobic conditions (O_2 concentration within less than 0.2%) in a glove box (MK3 Anaerobic Work Station, Don Whitley Scientific, Shipley, UK). The dissolved As in addition to the controlling factors (DOC, Fe, Fe^{2+} and SO_4^{2-}) were gained separately. To collect the dissolved fraction, samples were filtered to pass through a 0.45- μm Millipore membrane (Whatman Inc., Maidstone, UK).

B1.3 XANES data analysis

The energy scale was calibrated using gold foil for As and Fe foil for Fe as standards, respectively. All spectra were processed by background removal, and normalization. Principal component (PCA) analysis was subsequently performed to extract the major components in all spectra. Then, the target transformation (TT) was done to identify the possible As species in our soil samples. The previously

established As reference database, including As(III)- and As(V)-sorbed on goethite and ferrihydrite, humic, Fe-humic, Al arsenate ($\text{AlAsO}_4 \cdot 2\text{H}_2\text{O}$), scorodite ($\text{FeAsO}_4 \cdot 2\text{H}_2\text{O}$), beudantite ($\text{PbFe}_3(\text{OH})_6\text{SO}_4\text{AsO}_4$), and arsenopyrite (FeAsS), was used for TT. Thereafter, linear combination fitting (LCF) was performed to determine the species of As in the soil samples. Various LCF results were obtained through a function of fit all combinations in Athena. The best LCF result was selected based on the R-value ($\frac{\sum(\text{data-fit})^2}{\sum(\text{data})^2}$) and visual examination of fit (Ravel and Newville, 2005). Moreover, FeO and Alpha- Fe_2O_3 were respectively chosen as the Fe(II) and Fe(III) standard minerals to estimate the oxidation states of Fe in the soil samples.

B1.4 Quality assurance

The quality assurance for the determination of dissolved As was checked by analyzing certified references, standard solutions (Merck) and reagent blanks. In addition, a certified reference soil material (BRM12, TMC, and TML) was used for the quality assurance of the extraction efficiency of the total content of As to guarantee a high-quality measurement and the recovery rate of total As was 93.1–95.2%. For the values lower than the limit of quantification of As ($53 \mu\text{g L}^{-1}$), 1/8 of this limit ($6.625 \mu\text{g L}^{-1}$) was used for statistics.

B2. References

- Harvey, A.E., Smart, J.A., Amis, E.S., 1955. Simultaneous spectrophotometric determination of iron (II) and total iron with 1, 10-phenanthroline. *Analytical Chemistry* 27, 26-29.
- Ravel, B., Newville, M., 2005. ATHENA, ARTEMIS, HEPHAESTUS: data analysis for X-ray absorption spectroscopy using IFEFFIT, *J. Synchrotron Radiat.* 12, 537-541.

Appendix C

***Supplementary Material* for Chapter 4**

Effects of Phosphorus- and Iron-Rich Biochars on Cadmium and Lead Mobilization under Fluctuating Controlled Redox Conditions in Paddy Soil

C1. Supporting methods and materials

C1.1 Analysis of the pre-incubated soils

The organic carbon and available (Olsen) P were determined according to Lu (1999). The available Fe was extracted using a compound extractant (pH=7.3) consist of 0.005 M DTPA (diethylenetriaminepentaacetic acid), 0.1 M triethanolamine, and 0.01 M CaCl₂ (Lindsay and Norvell, 1978). A five-step sequential extraction method recommended by Tessier *et al.* (1979) was exploited to determine the bonding forms of Cd and Pb in the pre-incubated soils. The extracted fractions were exchangeable Cd and Pb, carbonate bound Cd and Pb, Fe/Mn oxide bound Cd and Pb, organic bound Cd and Pb, and residual Cd and Pb.

C2. Supporting results and discussion

C2.1 Effect of biochar application on the content of organic carbon, Olsen phosphorus and DTPA-extractable Fe in the pre-incubated soils

The organic carbon contents, and the concentrations of Olsen phosphorus (P) and DTPA-extractable Fe in soils were determined after 30 days of pre-incubation (Figure S7) to explore how different biochars would influence the soil C, P and Fe levels. Compared to the control, the organic carbon content increased by 50, 166 and 171% with the incorporation of the P-rich, raw and Fe-rich biochars, respectively. For the Olsen P, the highest increase was achieved with incorporation of the P-rich biochar, which had a content approximately 3 times that of the control. Application of the raw and Fe-rich biochars also elevated the concentration of Olsen P in soils, by 32 and 86%, respectively. Apparently, the P-rich biochar had distinct advantage in enhancing the soil P availability compared to the other two biochars. Interestingly, application of biochars, including the Fe-rich biochar, decreased the concentration of DTPA-extractable Fe by 15%~48%.

Two green waste derived (raw and Fe-rich) biochars were more effective in increasing soil organic carbon, compared to the P-rich biochar. This might be mainly attributed to the higher carbon content of the raw biochar and the Fe-rich biochar compared to the P-rich biochar (69.3, 59.9 and 30.8%, respectively). Approximately 80~97% of the organic carbon derived from biochar exists in stable forms, which are not mineralized even for a quite long time (over hundreds of years) (Han *et al.* (2020). Therefore, the content of organic carbon in soil could be directly elevated once the carbon-rich biochar is added. A similar interpretation also supports the results of Olsen P, as following the application of P-rich biochar, the amount and fraction of P in soil would be changed because of the biochar-derived P. In addition, biochar might indirectly influence the biogeochemical processes by regulating the

turnover of C and P in soil. For instance, Sun *et al.* (2020) found that a mixed biomass-derived biochar indirectly changed the soil organic carbon through altering the soil aggregation and wheat residue generated organic carbon. The lower availability of Fe in soils treated with the P-rich and raw biochars was found as compared to the control. This might be mainly due to the liming effect of these two biochars. A sharp decrease of DTPA-extractable Fe was observed in the Fe-rich biochar-treated soil as compared to the control, which might be explained as the inhibition of iron-reducing bacteria with the decrease of soil pH (Figure S3). As Liu *et al.* (2020) reported, application of the composite of red mud and nanoscale zero-valent iron caused a lower bacterial activity, which was attributed to the change in soil pH. The above findings preliminarily showed the feasibility of using the defined “P-rich biochar” to increase P availability and organic carbon content in soil. However, the defined “Fe-rich” biochar contributed little to the soil Fe availability during the pre-incubation.

C2.2 Effect of biochar application on the binding forms of Cd and Pb in the pre-incubated soil

The results obtained from the five-steps sequential extraction showed that application of the Fe-rich biochar decreased the exchangeable and organic fraction of Cd from 26.9 and 19.1 to 23.7 and 14.3%, while increased the Fe-Mn oxide fraction of Cd from 18.6 to 22.8%; however, application of the P-rich and raw biochars significantly ($P < 0.05$) decreased the Fe-Mn oxide fraction of Cd from 18.6 to 12.8 and 13.4%, respectively, but increased the organic fraction Cd from 19.1 to 22.6 and 22.7%, respectively, compared to the control (Figure S5). The predominant fraction of Pb in the control and biochar-treated soils was associated with the residual, which accounted from 45.4 to 58.1%. Compared to the control, application of all three biochars significantly ($P < 0.05$) decreased the exchangeable, while it increased the organic fraction of Pb. In addition, application of the P-rich biochar decreased the carbonate fraction of Pb from 7.8 to 3.9%, and a higher proportion of the Fe-Mn oxide fraction was observed in the Fe-rich biochar treatment, compared to the control.

Generally, the exchangeable fraction of toxic metal(loid)s is the most soluble fraction and easily absorbed by plants (Kashif Irshad *et al.*, 2020). The fractions bound to Fe-Mn oxides, organic and the residual are more stable and considered low bioavailability (Rajendran *et al.*, 2019). Application of different biochars triggered the transformation of Cd and Pb from the exchangeable fraction to the other fractions in the pre-incubated soil, which is considered as the basic mechanism of metal(loid)s immobilizing by amendments (Kashif Irshad *et al.*, 2020). The enhancement of Pb immobilization caused by the P-rich biochar application could be mainly attributed to its high ash content, rich P and the abundance of O-containing fraction groups (Table 4-1). He *et al.* (2019) indicated that the released P from sewage sludge biochar could precipitate with cationic metal ions to form stable phosphates.

Lu *et al.* (2017) reported that the presence of mineral elements such as Ca, K and Mg in rice straw biochar highly contributed to Pb immobilization. Additionally, the O-containing functional groups on biochar might contribute to the stabilization of toxic metal(loid)s through formation of the stable complexes (Oustriere *et al.*, 2017; Kashif Irshad *et al.*, 2020). Immobilization of Cd and Pb by the raw biochar was likely due to its liming effect, as well as the high organic carbon content and large surface area (Table 4-1). As reported by previous studies, the shift of metals from relatively labile fractions to stable ones was mainly ascribed to the increase of soil pH (Oustriere *et al.*, 2017; He *et al.*, 2019). In addition, the biochar-derived organic matter could either directly adsorb metal(loid)s or indirectly increase the soil pH through releasing protons, thereby promoting the immobilization of metal(loid)s (Hamid *et al.*, 2020). Moreover, the raw biochar had a relatively high specific surface area, implying the stronger electrostatic interactions between the biochar and cationic metals as mentioned by Lu *et al.* (2017). For the Fe-rich biochar, we assume that the predominant mechanism might be the cycling of Fe, which may respectively cause the dissolution of Fe under reducing conditions, and the re-precipitation under oxidizing conditions. Although our pre-incubation experiment was conducted under flooding condition throughout the entire period, some oxidation reactions might have occurred while milling and drying the soil samples. Our assumption could be supported by Mehmood *et al.* (2018), who also found that the decrease of dissolved Cd and Pb was attributed to the formation of stable Fe-oxides. The above observations provide a clear sign that both P-rich and Fe-rich biochars could convert the fractions of Cd and Pb from relatively labile forms to stable ones, thereby decreasing their mobilization in soil.

C3. References

- Hamid, Y., Tang, L., Hussain, B., Usman, M., Gurajala, H.K., Rashid, M.S., He, Z., Yang, X., 2020. Efficiency of lime, biochar, Fe containing biochar and composite amendments for Cd and Pb immobilization in a co-contaminated alluvial soil. *Environ. Pollut.* 257, 113609. <https://doi.org/10.1016/j.envpol.2019.113609>
- Han, L., Sun, K., Yang, Y., Xia, X., Li, F., Yang, Z., Xing, B., 2020. Biochar's stability and effect on the content, composition and turnover of soil organic carbon. *Geoderma* 364, 114184. <https://doi.org/10.1016/j.geoderma.2020.114184>
- He, E., Yang, Y., Xu, Z., Qiu, H., Yang, F., Peijnenburg, W., Zhang, W., Qiu, R., Wang, S., 2019. Two years of aging influences the distribution and lability of metal(loid)s in a contaminated soil amended with different biochars. *The Sci. Total Environ.* 673, 245-253. <https://doi.org/10.1016/j.scitotenv.2019.04.037>
- Kashif Irshad, M., Chen, C., Noman, A., Ibrahim, M., Adeel, M., Shang, J., 2020. Goethite-modified biochar restricts the mobility and transfer of cadmium in soil-rice system. *Chemosphere* 242, 125152. <https://doi.org/10.1016/j.chemosphere.2019.125152>
- Lindsay, W.L., Norvell, W.A., 1978. Development of a DTPA Soil Test for Zinc, Iron, Manganese, and Copper. *Soil Sci. Soc. Am. J.* 42, 421-428. <https://doi.org/10.2136/sssaj1978.03615995004200030009x>
- Liu, Q., Sheng, Y., Wang, W., Li, C., Zhao, G., 2020. Remediation and its biological responses of Cd contaminated sediments using biochar and minerals with nanoscale zero-valent iron loading. *Sci. Total Environ.* 713, 136650. <https://doi.org/10.1016/j.scitotenv.2020.136650>
- Lu, R., 1999. Analytical methods for soil agrochemistry. Chinese Agricultural Science and Technology Publishing House, Beijing.
- Lu, K., Yang, X., Gielen, G., Bolan, N., Ok, Y.S., Niazi, N.K., Xu, S., Yuan, G., Chen, X., Zhang, X., Liu, D., Song, Z., Liu, X., Wang, H., 2017. Effect of bamboo and rice straw biochars on the mobility and redistribution of heavy metals (Cd, Cu, Pb and Zn) in contaminated soil. *J. Environ. Manage.* 186, 285-292. <https://doi.org/10.1016/j.jenvman.2016.05.068>
- Mehmood, S., Rizwan, M., Bashir, S., Ditta, A., Aziz, O., Yong, L.Z., Dai, Z., Akmal, M., Ahmed, W., Adeel, M., Imtiaz, M., Tu, S., 2018. Comparative Effects of Biochar, Slag and Ferrous-Mn Ore on Lead and Cadmium Immobilization in Soil. *B. Environ. Contam. Tox.* 100, 286-292. <https://doi.org/10.1007/s00128-017-2222-3>
- Oustriere, N., Marchand, L., Rosette, G., Friesl-Hanl, W., Mench, M., 2017. Wood-derived-biochar combined with compost or iron grit for in situ stabilization of Cd, Pb, and Zn in a contaminated soil. *Environ. Sci. Pollut. Res.* 24, 7468-7481. <https://doi.org/10.1007/s11356-017-8361-6>
- Rajendran, M., Shi, L., Wu, C., Li, W., An, W., Liu, Z., Xue, S., 2019. Effect of sulfur and sulfur-iron modified biochar on cadmium availability and transfer in the soil-rice system. *Chemosphere* 222, 314-322. <https://doi.org/10.1016/j.chemosphere.2019.01.149>
- Sun, Z., Zhang, Z., Zhu, K., Wang, Z., Zhao, X., Lin, Q., Li, G., 2020. Biochar altered native soil organic carbon by changing soil aggregate size distribution and native SOC in aggregates based on an 8-year field experiment. *Sci. Total Environ.* 708, 134829. <https://doi.org/10.1016/j.scitotenv.2019.134829>
- Tessier A., Campbell, P.G.C., Bisson, M., 1979. Sequential extraction procedure for the speciation of particulate trace metals. *Anal. Chem.* 51, 844-851. <https://doi.org/10.1021/ac50043a017>

Appendix D

***Supplementary Material* for Chapter 5**

Influences of Iron-Modified Phosphorus- and Silicon-Rich Biochars on Arsenic, Cadmium, and Lead Accumulation in Rice and Microbial Activities in Paddy Soil

D1. Properties of the used soil

The soil was contaminated with 141 mg kg⁻¹ of As, 0.5 mg kg⁻¹ of Cd, and 736 mg kg⁻¹ of Pb, measured by ICP-OES after completely digestion with HF-HClO₄-HNO₃, according to the method reported by Carignan and Tessier (Carignan R. and A., 1988). Based on the Soil Environmental Quality Risk Control Standard for Soil Contamination of Agricultural Land (GB15618-2018) (Ministry of Ecology and Environment of China, 2018), the total content of As and Cd exceeded the risk screening value of As (30 mg kg⁻¹) and Cd (0.4 mg kg⁻¹), respectively, while the total content even exceeded the risk intervention value of Pb (100 mg kg⁻¹) for acidic wetland soils (5.5 < pH ≤ 6.5). A detailed explanation of the soil properties was published in the previous studies (Pan *et al.*, 2021; Wen *et al.*, 2021) and is briefly provided here: pH (H₂O) = 5.8, cationic exchange capacity = 13.4 cmol kg⁻¹, electrical conductivity = 0.05 dS m⁻¹, organic carbon content = 1.3 %, Olsen P = 10.1 mg kg⁻¹, available Si = 22.7 mg kg⁻¹.

D2. Analytical methods for biochar properties

Biochar pH was measured on a 1:20 (w/v) water suspension of the biochar samples after stirring for 1 h. The concentrations of As, Cd, and Pb in biochars were measured using HNO₃-HF-HClO₄ digestion method, and quantified by ICP-OES (Lu, 2000). The specific surface area (SSA) of the biochar was determined by Brunauer-Emmett-Teller (BET) N₂ adsorption analysis at 77 K on a surface area analyzer (TristarII3020, Micromeritics Instrument Corporation, USA) after degassing (Lu *et al.*, 2014). The functional groups of the biochars were analyzed by Fourier transform infrared (FTIR) spectrometer (Nicolet iS10, ThermoFisher, USA) following KBr disc sample preparation method. The total C, H, N, and S contents were measured by an elemental analyzer (Flash EA1112, Thermo Finnigan, Italy). Ash content of biochar was determined according to the ASTM D1762-84 method. A scanning electron microscope (SEM, Siron-100, FEI, Poland) was used for the analysis of biochar structural and morphological characteristics. The surface elemental components of biochars were analyzed using an energy dispersive X-ray spectroscopy (EDX) (Hitachi S-4800 with ISIS 310, Japan). The presence of functional groups on biochars was determined by a Fourier transform infrared spectrometer (FTIR, Nicolet iS10, ThermoFisher, USA)

D3. Quality assurance and quality control

The ultra-pure Milli-Q water was used for all analyses, and all devices used in the current study were calibrated to ensure the accuracy of environmental data. The accuracy of analytical methods for available nutrients and PTEs was valued through analyzing blanks and standard solutions with known spiked concentrations of elements.

Triplicates were run for each standard solution and the relative standard deviation was < 5%. The quality control for the determination of total PTE content in the soil and plant was implemented by analyzing the certified reference materials (GBW-07405 for soil and GBW-07603 for plant, respectively). The recovery percentage of As, Cd, and Pb ranged between 87.5 and 99.5%.

D4. Soil pH, organic carbon content and nutrient availability

Application of P-BC increased soil pH by approximately 1.0 unit, whereas the addition of Si-BC made no significant difference in soil pH as compared to the control (Figure 5-7). However, the addition of Fe-Si-BC had no significant effects on soil pH, whereas the application of Fe-P-BC significantly ($P<0.05$) decreased soil pH from 6.0 to 5.2 (Figure 5-7). Application of all smart biochars significantly ($P<0.05$) increased soil organic carbon content, by 30.9%, 41.4%, 25.1%, and 31.9% for Si-BC, Fe-Si-BC, P-BC, and Fe-P-BC, respectively as compared to the control (Figure 5-6). Both Fe-modified biochar were more effective in elevating soil organic carbon content than the pristine biochars, although modification process led to a converse consequence of the organic carbon content of biochars (Table 5-1, Figure 5-6).

Notable differences were found in the availability of soil nutrients, inclusive of nitrogen (N), potassium (K), phosphorus (P), iron (Fe), and silicon (Si) (Figure 5-2). Compared to the control, the addition of both pristine biochars caused a slight decrease of available N, whereas the amendment of both Fe-modified biochars increased soil available N by 22.3% and 25.2%, respectively, compared to the control. The concentrations of available K and P increased by 78.6% and 71.4% after P-BC application, and increased by 83.2% and 71.0% after Fe-P-BC application, respectively. The addition of Si-BC and Fe-Si-BC actually increased available K by 55.0% and 64.8%, respectively, relative to the control, but did not affect available P in soil. It is noteworthy that, in all biochar-treated soils, the concentrations of available Fe significantly ($P<0.05$) decreased as compared to the non-amended control. In contrast to available N, application of both pristine biochars led to a significant ($P<0.05$) increase of available Si (by 39.8% for Si-BC and 28.0% for P-BC, respectively), whereas a slight decrease of available Si was observed after the addition of both Fe-modified biochars.

D5 References

- Carignan R., A., T., 1988. The co-diagenesis of sulfur and iron in acid lake sediments of southwestern Québec. *Geochim. Cosmochim. Acta* 52, 1179-1188.
- Casida, L.E., Klein, D.A., Santoro, T., 1964. Soil dehydrogenase activity. *Soil Sci.* 98, 371-376.
- Eivazi, F., Tabatabai, M.A., 1988. Glucosidases and galactosidases in soils. *Soil Biol. Biochem.* 20, 601-606.

- Johnson, J.L., Temple, L., 1964. Some variables affecting the measurement of “catalase activity” in soil. *Soil Sci. Soc. Am. J.* 28, 207-209.
- Kandeler, E., Gerber, H., 1988. Short-term assay of soil urease activity using colorimetric determination of ammonium. *Biol. Fertil. Soil.* 8, 199-202.
- Pan, H., Yang, X., Chen, H., Sarkar, B., Bolan, N., Shaheen, S.M., Wu, F., Che, L., Ma, Y., Rinklebe, J., Wang, H., 2021. Pristine and iron-engineered animal- and plant-derived biochars enhanced bacterial abundance and immobilized arsenic and lead in a contaminated soil. *Sci. Total Environ.* 763, 144218.
- Tabatabai, M.A., Bremner, J.M., 1969. Use of p-nitrophenyl phosphate for assay of soil phosphatase activity. *Soil Biol. Biochem.* 1, 301-307.
- Wen, E., Yang, X., Chen, H., Shaheen, S.M., Sarkar, B., Xu, S., Song, H., Liang, Y., Rinklebe, J., Hou, D., Li, Y., Wu, F., Pohořelý, M., Wong, J.W.C., Wang, H., 2021. Iron-modified biochar and water management regime-induced changes in plant growth, enzyme activities, and phytoavailability of arsenic, cadmium and lead in a paddy soil. *J. Hazard. Mater.* 407, 124344.

Appendix E

***Supplementary Material* for Chapter 6**

Influences of the iron-modified phosphorus-rich biochar on rice yield, arsenic and lead redistribution, and bacterial community structure in paddy soil

E1. Properties of the used soil

The soil was contaminated with 141 mg kg⁻¹ of As, 0.5 mg kg⁻¹ of Cd, and 736 mg kg⁻¹ of Pb, respectively, measured by ICP-OES after completely digestion with HF-HClO₄-HNO₃, according to the method reported by Carignan and Tessier (Carignan R. and A., 1988). Based on the Soil Environmental Quality Risk Control Standard for Soil Contamination of Agricultural Land (GB15618-2018) (Ministry of Ecology and Environment of China, 2018), the total content of As and Cd exceeded the risk screening value of As (30 mg kg⁻¹) and Cd (0.4 mg kg⁻¹), respectively, while the total content even exceeded the risk intervention value of Pb (100 mg kg⁻¹) for acidic wetland soils (5.5 < pH ≤ 6.5). A detailed explanation of the soil properties was published in the previous studies (Pan *et al.*, 2021; Wen *et al.*, 2021) and is briefly provided here: pH (H₂O) = 5.8, cationic exchange capacity = 13.4 cmol kg⁻¹, electrical conductivity = 0.05 dS m⁻¹, organic carbon content = 1.3 %, Olsen P = 10.1 mg kg⁻¹, available Si = 22.7 mg kg⁻¹.

E2. Analytical method for biochar properties

The pH was measured on a 1:20 (w/v) water suspension of the biochar samples after stirring for 1 h. The concentrations of As, Cd, and Pb in biochars were measured using HNO₃-HF-HClO₄ digestion method, and quantified by ICP-OES (Lu, 2000). The specific surface area (SSA) of the biochar was determined by Brunauer-Emmett-Teller (BET) N₂ adsorption analysis at 77 K on a surface area analyzer (TristarII3020, Micromeritics Instrument Corporation, USA) after degassing (Lu *et al.*, 2014). The functional groups of the biochars were analyzed by Fourier transform infrared (FTIR) spectrometer (Nicolet iS10, ThermoFisher, USA) following KBr disc sample preparation method. The total C, H, N, and S contents were measured by an elemental analyzer (Flash EA1112, Thermo Finnigan, Italy). Ash content of biochar was determined according to the ASTM D1762-84 method. A scanning electron microscope (SEM, Siron-100, FEI, Poland) was used for the analysis of biochar structural and morphological characteristics. The surface elemental components of biochars were analyzed using an energy dispersive X-ray spectroscopy (EDX) (Hitachi S-4800 with ISIS 310, Japan). The presence of functional groups on biochars was determined by a Fourier transform infrared spectrometer (FTIR, Nicolet iS10, ThermoFisher, USA).

E3. Soil pH, organic carbon content and nutrient availability

Sub-samples of the air-dried one were collected and passed through a 2-mm sieve before analyses. Soil pH, organic carbon, and available nutrient (N, P, and K) were determined according to the standard methods presented

in Lu, (2000). In brief, soil pH was measured in a soil/water slurry at a 1:2.5 (w/v) ratio. Organic carbon content was determined using Walkley–Black method. The concentration of available N was extracted using a micro-diffusion technique after alkaline-hydrolysis method. The available P was extracted using sodium bicarbonate (NaHCO₃) and measured by spectrophotometric method (UVA 132122, Thermo Electron Corporation, England) at 700 nm wavelength. Soil available K was extracted using ammonium acetate, and analyzed by a flame photometer (FP640, Xinyi Instrument, China).

E4. Sequential extraction of As and Pb

E4.1 Arsenic

Briefly, 1) 1 g of air-dried soil sample (< 2 mm) was weighed into an acid-washed 50-mL centrifuge tube and was extracted sequentially with 40 mL of 0.05 M ammonium sulfate corresponding to nonspecifically absorbed As (F1); 2) 40 mL of 0.05 M ammonium dihydrogen phosphate corresponding to specifically absorbed As (F2); 3) 40 mL of 0.2 M ammonium oxalate corresponding to As associated with amorphous hydrous oxides (F3); 4) 40 mL of a mixture of 0.2 M ammonium oxalate and 0.1 M ascorbic acid corresponding to As associated with crystalline hydrous oxides (F4); and 5) finally digested by aqua regia corresponding to residual As (F5). In the current study, all extractions were performed in triplicates, and the extracts were filtered through 0.45- μ m filter membranes anterior to As determination using ICP-OES.

E4.2 Lead

According to the protocol (Zemberyova *et al.*, 2006), four sequential extractions were done as follows. 1) 0.11 M acetic acid to extract the acid extractable fraction; 2) 0.1 M hydroxylamine hydrochloride (pH 2) to extract the fraction bound to Fe/Mn oxides; 3) 30% m/v H₂O₂ and 1 M NH₄OAc (pH 2) to extract the fraction bound to organic matter; and the mixture of HNO₃- HF-HClO₄ (volume ratio = 5: 7: 1) to extract the residual fraction of Pb. The concentrations of Pb in each step were determined using ICP-OES.

E5. Quality assurance and quality control

The ultra-pure Milli-Q water was used for all analyses, and all devices used in the current study were calibrated to ensure the accuracy of environmental data. The accuracy of analytical methods for available nutrients and PTEs was valued through analyzing blanks and standard solutions with known spiked concentrations of elements. Triplicates were run for each standard solution and the relative standard deviation was < 5%. The quality control for the determination of total PTE content in the soil and plant was implemented by analyzing the certified

reference materials (GBW-07405 for soil and GBW-07603 for plant, respectively). The recovery percentage of As and Pb ranged between 87.5% and 99.5%.

E6. References

- Carignan R., A., T., 1988. The co-diagenesis of sulfur and iron in acid lake sediments of southwestern Québec. *Geochim. Cosmochim. Ac* 52, 1179-1188.
- Pan, H., Yang, X., Chen, H., Sarkar, B., Bolan, N., Shaheen, S.M., Wu, F., Che, L., Ma, Y., Rinklebe, J., Wang, H., 2021. Pristine and iron-engineered animal- and plant-derived biochars enhanced bacterial abundance and immobilized arsenic and lead in a contaminated soil. *Sci. Total Environ.* 763, 144218.
- Wen, E., Yang, X., Chen, H., Shaheen, S.M., Sarkar, B., Xu, S., Song, H., Liang, Y., Rinklebe, J., Hou, D., Li, Y., Wu, F., Pohořelý, M., Wong, J.W.C., Wang, H., 2021. Iron-modified biochar and water management regime-induced changes in plant growth, enzyme activities, and phytoavailability of arsenic, cadmium and lead in a paddy soil. *J. Hazard. Mater.* 407, 124344.
- Wenzel, W.W., Kirchbaumer, N., Prohaska, T., Stingeder, G., Lombi, E., Adriano, D.C., 2001. Arsenic fractionation in soils using an improved sequential extraction procedure. *Anal. Chim. Acta* 436, 309-323
- Zemberyova, M., Bartekova, J., Hagarova, I., 2006. The utilization of modified BCR three-step sequential extraction procedure for the fractionation of Cd, Cr, Cu, Ni, Pb and Zn in soil reference materials of different origins. *Talanta* 70, 973-978.

List of Publications (During Ph.D. Study)

1. International peer-reviewed journals

- Yang, X.**, Shaheen, S.M., Wang, J., Hou, D., Ok, Y.S., Wang, S.L., Wang, H., Rinklebe, J., 2022. Elucidating the redox-driven dynamic interactions between arsenic and iron-impregnated biochar in a paddy soil using geochemical and spectroscopic techniques. *Journal of Hazardous Materials* 422, 126808. <https://doi.org/10.1016/j.jhazmat.2021.126808>
- Yang, X.**, Hinzmann, M., Pan, H., Wang, J., Bolan, N., Tsang, D.C.W., Ok, Y.S., Wang, S.-L., Shaheen, S.M., Wang, H., Rinklebe, J., 2022. Pig carcass-derived biochar caused contradictory effects on arsenic mobilization in a contaminated paddy soil under fluctuating controlled redox conditions. *Journal of Hazardous Materials*, 421, 126647. <https://doi.org/10.1016/j.jhazmat.2021.126647>
- Yang, X.**, Pan, H., Shaheen, S.M., Wang, H., Rinklebe, J., 2021. Immobilization of cadmium and lead using phosphorus-rich animal-derived and iron-modified plant-derived biochars under dynamic redox conditions in a paddy soil. *Environment International* 156, 106628. <https://doi.org/10.1016/j.envint.2021.106628>
- Wen, E.[#], **Yang, X.**[#] (co-first author), Chen, H., Shaheen, S.M., Sarkar, B., Xu, S., Song, H., Liang, Y., Rinklebe, J., Hou, D., Li, Y., Wu, F., Pohorely, M., Wong, J.W.C., Wang, H., 2021. Iron-modified biochar and water management regime-induced changes in plant growth, enzyme activities, and phytoavailability of arsenic, cadmium and lead in a paddy soil. *Journal of Hazardous Materials* 407, 124344. <https://doi.org/10.1016/j.jhazmat.2020.124344> (ESI highly cited)
- Pan, H.[#], **Yang, X.**[#] (co-first author), Chen, H., Sarkar, B., Bolan, N., Shaheen, S.M., Wu, F., Che, L., Ma, Y., Rinklebe, J., Wang, H., 2021. Pristine and iron-engineered animal- and plant-derived biochars enhanced bacterial abundance and immobilized arsenic and lead in a contaminated soil. *Science of the Total Environment* 763, 144218. <https://doi.org/10.1016/j.scitotenv.2020.144218>
- Nie, T.[#], **Yang, X.**[#] (co-first author), Chen, H., Müller, K., Shaheen, S.M., Rinklebe, J., Song, H., Xu, S., Wu, F., Wang, H., 2021. Effect of biochar aging and co-existence of diethyl phthalate on the mono-sorption of cadmium and zinc to biochar-treated soils. *Journal of Hazardous Materials* 408, 124850. <https://doi.org/10.1016/j.jhazmat.2020.124850>
- Al-Solaimani, S.G., Abohassan, R.A., Alamri, D.A., **Yang, X.**, Rinklebe, J., Shaheen, S.M., 2022. Assessing the risk of toxic metals contamination and phytoremediation potential of mangrove in three coastal sites along the Red Sea. *Marine Pollution Bulletin* 176, 113412. <https://doi.org/10.1016/j.marpolbul.2022.113412>
- Lashen, Z.,M., Shams, M.S., El-Sheshtawy, H.S., Slaný, M., Antoniadis, V., **Yang, X.**, Rinklebe, J., Shaheen, S.M., Elmahdy, S.M., 2022. Remediation of Cd and Cu contaminated water and soil using novel nanomaterials derived from sugar beet processing- and clay brick factory-solid wastes. *Journal of Hazardous Materials* 428, 128205. <https://doi.org/10.1016/j.jhazmat.2021.128205>
- Chen, H., Feng, Y., **Yang, X.**, Yang, Sarkar, B., Bolan, Meng, J., Wu, F., Wong, J.W.C., Chen, W., Wang, H., 2022. Assessing simultaneous immobilization of lead and improvement of phosphorus availability through application of phosphorus-rich biochar in a contaminated soil: A pot experiment. *Chemosphere* 296, 133891. <https://doi.org/10.1016/j.chemosphere.2022.133891>
- Chen, H., Gao, Y., El-Naggar, A., Niazi, N.K., Sun, C., Shaheen, S.M., Hou, D., **Yang, X.**, Tang, Z., Liu, Z., Hou, H., Chen, W., Rinklebe, J., Pohořelý, M., Wang, H., 2022. Enhanced sorption of trivalent antimony by chitosan-loaded biochar in aqueous solutions: Characterization, performance and mechanisms. *Journal of Hazardous Materials* 425, 127971. <https://doi.org/10.1016/j.jhazmat.2021.127971>

- Farid, I.M., Siam, H.S., Abbas, M.H.H., Mohamed, I., Mahound, S.A., Tolba, M., Abbas, H.H., **Yang, X.**, Antoniadis, V., Rinklebe, J., Shaheen, S.M., 2022. Co-composted biochar derived from rice straw and sugarcane bagasse improved soil properties, carbon balance, and zucchini growth in a sandy soil: A trial for enhancing the health of low fertile arid soils. *Chemosphere* 292, 133389. <https://doi.org/10.1016/j.chemosphere.2021.133389>
- Zhang, S., **Yang, X.**, Hsu, L.C., Liu, Y.T., Wang, S.L., White, J.R., Shaheen, S.M., Chen, Q., Rinklebe, J., 2021. Soil acidification enhances the mobilization of phosphorus under anoxic conditions in an agricultural soil: Investigating the potential for loss of phosphorus to water and the associated environmental risk. *Science of the Total Environment* 793, 148531. <https://doi.org/10.1016/j.scitotenv.2021.148531>
- Chen, H., Qin, P., **Yang, X.**, Bhatnagar, A., Shaheen, S.M., Rinklebe, J., Wu, F., Xu, S., Che, L., Wang, H., 2021. Sorption of diethyl phthalate and cadmium by pig carcass and green waste-derived biochars under single and binary systems. *Environmental Research* 193, 110594. <https://doi.org/10.1016/j.envres.2020.110594>
- Tang, X., Shen, H., Chen, M., **Yang, X.**, Yang, D., Wang, F., Chen, Z., Liu, X., Wang, H., Xu, J., 2020. Achieving the safe use of Cd- and As-contaminated agricultural land with an Fe-based biochar: A field study. *Science of the Total Environment* 706, 135898. <https://doi.org/10.1016/j.scitotenv.2019.135898>
- Chen, H., **Yang, X.**, Wang, H., Sarkar, B., Shaheen, S.M., Gielen, G., Bolan, N., Guo, J., Che, L., Sun, H., Rinklebe, J. Animal carcass- and wood-derived biochars improved nutrient bioavailability, enzyme activity, and plant growth in metal-phthalic acid ester co-contaminated soils: A trial for reclamation and improvement of degraded soils. *Journal of Environmental Management* 261, 110246. <https://doi.org/10.1016/j.jenvman.2020.110246>
- Feng, Y., **Yang, X.**, Singh, B.P., Mandal, S., Guo, J., Che, L., Wang, H., 2020. Effects of contrasting biochars on the leaching of inorganic nitrogen from soil. *Journal of Soil and Sediments* 20, 3017-3026. <https://doi.org/10.1007/s11368-019-02369-5>
- Chen H., **Yang, X.**, Gielen, G., Mandal, S., Xu, S., Guo, J., Shaheen, S.M., Rinklebe, J., Che, L., Wang H., 2019. Effect of biochars on the bioavailability of cadmium and di-(2-ethylhexyl) phthalate to Brassica chinensis L. in contaminated soils. *Science of the Total Environment*, 678: 43-52. <https://doi.org/10.1016/j.scitotenv.2019.04.417>

2. Chinese peer-reviewed journals

- Dai, Z., Yang, X., Chen, H., Chen, J., Zhang, Y., Wang, H., 2022. Effect of raw and iron-modified biochars on the bioavailability of As and Pb and functional diversity of the microbial community in soils. *Acta Scientiae Circumstantiae*, in press. doi: 10.13671/j.hjkxxb.2021.0527 (In Chinese with English `)
- Yang, B., Chen, H., **Yang, X.**, Wu, X., Chen, J., Wang, H., 2022. Effects of different soil amendments on soil nutrient transformation and bioavailability of arsenic and lead in contaminated soil. *Journal of Soil and Water Conservation* 36(1), 332-339, 345. doi: 10.13870/j.cnki.stbcbx.2022.01.042 (In Chinese with English abstract)
- Dai, Z., Wen, E., Chen, H., **Yang, X.**, Chen, J., Guo, J., Wang, H., 2021. Effect of raw and iron-modified biochar on the sorption of As(V) by soils. *Journal of Zhejiang A & F University* 38(2), 346-354. doi: 10.11833/j.issn.2095-0756.20200392 (In Chinese with English abstract)
- Nie, T., **Yang, X.**, Li, Y., Wang, H., 2020. Research progress of polymer materials in soil physical properties improvement. *Chinese Journal of Soil Science* 51(5), 1-9. doi: 10.19336/j.cnki.trtb.2020.06.33 (In Chinese with English abstract)

- Qian, Q., **Yang, X.**, Guo, M., Qin, P., Xu, S., Wang, H., 2019. Adsorption of Zn^{2+} from a Zn^{2+} -DEP (diethyl phthalate) composite solution using biochars in soil. *Journal of Zhejiang A&F University* 36(6), 1051-1061. doi: 10.11833/j.issn.2095-0756.2019.06.001 (In Chinese with English abstract)
- Zhu, G., He, L., Qin, P., **Yang, X.**, Lu, K., Liu, X., Wang, H., 2019. Dead pig-derived biochar treatments and soil adsorption of Pb^{2+} . *Journal of Zhejiang A&F University* 36(3), 573-580. doi: 10.11833/j.issn.2095-0756.2019.03.019 (In Chinese with English abstract)
- Wen, E., Zhao, W., **Yang, X.**, Guo, J., Wang, H., 2019. Effect of biochars derived from *Platanus Orientalis* branches and leaves on the adsorption of Pb^{2+} in aqueous solution. *Journal of Soil and Water Conservation* 33(2), 309-316. doi: 10.13870/j.cnki.stbcbx.2019.02.047 (In Chinese with English abstract)
- Zhao, W., **Yang, X.**, He, L., Guo, J., Wang, H., 2018. Effect of pyrolysis temperature on physicochemical properties of biochars derived from typical urban woody green wastes in southern China. *Journal of Zhejiang A & F University* 35(6): 1007-1016. doi: 10.11833/j.issn.2095-0756.2018.06.003 (In Chinese with English abstract)

3. Research articles under review or ready for submission

- Yang, X.**, Wen, E., Ge, C., El-Naggar, A., Wang, S., Kwon, E.E., Song, H., Shaheen, S.M., Wang, H., Rinklebe, J., 2022. Iron-modified phosphorus- and silicon-based biochars exhibited various influences on arsenic, cadmium and lead accumulation in rice and enzyme activities in a paddy soil. Ready for being submitted to *Journal of Cleaner Production*.
- Yang, X.**, Dai, Z., Ge, C., Bolan, N., Tsang, D.C.W., Song, H., Hou, D., Shaheen, S.M., Wang, H., Rinklebe, J., 2022. Multiple-functionalized biochar enhances rice yield via regulating arsenic and lead redistribution and bacterial community structure in soils under different hydrological conditions. Ready for being submitted to *Environment International*.
- Xing, Y., Wang, J., Kinder, C.E.S, **Yang, X.**, Slaný, M., Wang, B., Shaheen, S.M., Leinweber, P., Rinklebe, J., 2022. Rice hull biochar enhances the mobilization and methylation of mercury via changing the composition of organic matter in an anthropogenic-polluted rice paddy soil under dynamic redox conditions. Ready for being submitted to *Journal of Hazardous Materials*.
- Zheng, X., Han, G., Song, Z., Liang, B., **Yang, X.**, Yu, C., Guan, D., 2022. Copper isotope fractionation and biogeochemical cycling in plant–soil systems. *Earth Science Reviews*. (Under review)
- Chen, H., Gao, Y., Li, J., Fang, Z., Bolan, N., Bhatnagar, A., Gao, B., Hou, D., Wang, S., Song, H., **Yang, X.**, Shaheen, S.M., Meng, J., Chen, W., Rinklebe, J., Wang, H. Engineered biochar for environmental decontamination in aquatic and soil systems: A critical review. *Carbon Research*. (Under review)
- Chen, H., Gao, Y., Li, J., Sun, C., Sarkar, B., Bhatnagar, A., Bolan, N., **Yang, X.**, Meng, J., Liu, Z., Hou, H., Wong, J.W.C., Hou, D., Chen, W., Wang, H. Insight into simultaneous adsorption and oxidation of antimonite [Sb(III)] by crawfish shell-derived biochar: Spectroscopic investigation and theoretical calculations. *Biochar*. (Under review)

4. Book chapters

- Yang, X.**, Shaheen, S.M., Wang, H., Rinklebe, J., 2022. Functionalized biochars for the (im)mobilization of potentially toxic elements in paddy soils under dynamic redox conditions: A case study. In: Tsang, D.C.W., Ok, Y.S. (eds.), *Biochar in Agriculture for Achieving Sustainable Development Goals*. Elsevier Publishers.
- Hussain, M.M., Mohy-Ud-Din, W., Younas, F., Niazi, N.K., Bibi, I., **Yang, X.**, Rasheed, F., Farooqi, Z.U.R., 2021. Biochar: A Game Changer for Sustainable Agriculture. pp: 143-157. In: Bandh S.A (ed.), *Sustainable Agriculture Technical Progressions and Transitions*. Springer.

Curriculum Vitae

Personal information:			
First Name	Xing	Family Name	Yang
Gender	Male	Date of Birth	August 18, 1988
Place of Birth	Anyang, China	Nationality	Chinese
Education:			
Since 11/2018	Ph.D., Institute of Foundation Engineering, Water- and Waste-Management, Faculty of Architecture and Civil Engineering, University of Wuppertal, Germany		
09/2012--06/2015	M.Sc., College of Environmental and Resource Sciences, Zhejiang A & F University, China		
09/2008--06/2012	B.Sc., Faculty of Resource and Environmental Sciences, Pingdingshang University, China		
07/2007--06/2008	Anyang County No. 1 High School		
09/2004--06/2007	Anyang Experimental High School		
09/2001--06/2004	Anyang No. 34 Intermediate School		
09/1995--06/2001	Anyang Qiukou Central Primary School (Huangfutun Primary School)		
Working experiences:			
06/2015--11/2018	Research assistant, Key Laboratory of Soil Contamination Bioremediation of Zhejiang Province, Zhejiang A & F University, China		
Scientific Community Services:			
<ul style="list-style-type: none"> ● Have been invited to be reviewer of international peer-reviewed journals, including <i>Chemical Engineering Journal</i>, <i>Global Change Biology</i>, <i>Journal of Cleaner Production</i>, <i>Geoderma</i>, <i>Agriculture, Ecosystems and Environment</i>, <i>GCB-Bioenergy</i>, <i>Biochar</i>, <i>Environmental Pollution</i>, <i>Science of the Total Environment</i>, <i>Chemosphere</i>, <i>Environmental Research</i>, <i>Ecotoxicology and Environmental Safety</i>, <i>CLEAN - Soil, Air, Water</i>, <i>Environmental Geochemistry and Health</i>, <i>Archives of Agronomy and Soil Science</i>, etc. ● Registered as a member of the German Soil Science Society (Deutsche Bodenkundliche Gesellschaft) 			